Employing patient-derived iPSC-technology and hepatocyte-like cells to investigate liver diseases

Inauguraldissertation

Zur Erlangung des Doktorgrades
der Mathematisch-Naturwissenschaftlichen Fakultät
der Heinrich-Heine-Universität Düsseldorf

vorgelegt von

Christiane Lörch

aus Köln

Düsseldorf, August 2025

Aus dem Institut für Stammzellforschung und Regenerative Medizin
der Heinrich-Heine-Universität Düsseldorf

Gedruckt mit der Genehmigung der
Mathematisch-Naturwissenschaftlichen Fakultät der
Heinrich-Heine-Universität Düsseldorf

Berichterstatterinnen:

1. PD Dr. rer. nat. Nina Graffmann
2. Prof. Dr. Henrike Heise

Tag der mündlichen Prüfung: 23.10.2025

Die vorliegende Arbeit ist eine kumulative Dissertation
gemäß § 6 (3) der Promotionsordnung der
Mathematisch-Naturwissenschaftlichen Fakultät
der Heinrich-Heine-Universität Düsseldorf vom 15.08.2018
zur Verleihung des Grades “Doctor rerum naturalium”

Acknowledgements

Für mich war die Zeit des PhDs eine spannende, prägende und herausfordernde Zeit, voll von neuen Erkenntnissen. Gerade in herausfordernden Phasen war es für mich als junge Wissenschaftlerin sehr wichtig, gut betreut zu sein: Rat einholen zu können, aus Fehlern lernen zu dürfen und gelegentlich auch motiviert zu werden. Ich hatte das große Glück, von gleich zwei Mentor*innen betreut worden zu sein, denen die Förderung von jungen Wissenschaftler*innen sehr wichtig ist.

Zunächst möchte ich mich bei meiner Betreuerin und Erstgutachterin PD Dr. rer. nat. Nina Graffmann bedanken. Für dein Training der Labortechniken und experimenteller Planung, Schreibarbeiten und beim Publizieren. Dein Feedback, das immer schnell, detailliert und konstruktiv war, war immer sehr wertvoll. Deine wertschätzende Kommunikation und deine Unterstützung in Bezug auf meine wissenschaftliche Laufbahn waren nicht nur eine Bereicherung für die Zeit des PhDs, sondern werden mich auch weiterhin begleiten. Vielen lieben Dank dafür!

I would also like to express my gratitude to my supervisor and mentor Prof. Dr. James Adjaye. Thank you for your open-door policy, and taking the time, for your encouragement and your dedicated support. Especially when the project didn't go smoothly, you always had constructive advice. Throughout, you thoughtfully and kindly supported my studies and career path. Thank you very much for that!

Ich möchte mich außerdem bei meiner Zweitgutachterin Prof. Dr. Henrike Heise bedanken für die Begutachtung dieser Dissertation. Weiterhin möchte ich mich bei Dr. Stephanie Simon für ihre Ratschläge und die Möglichkeit, Einsicht in die industrielle Forschung zu erlangen, bedanken.

Ich danke allen aktuellen und ehemaligen Institutsmitgliedern, die eine tolle Arbeitsatmosphäre geschaffen haben. Danke für die kurzen Dienstwege, die schönen Mittagspausen und die gute Zusammenarbeit. Es war mir immer eine Freude, an das Institut zu kommen. Besonders bedanken möchte ich mich bei denen, die das Labor zusammenhalten und ihre jahrelange Erfahrung mit uns geteilt haben: Martina Bohndorf und Silke Wehrmeyer. Vielen Dank für

euren wichtigen Beitrag, eure aufmunternden Worte, eure Motivation und eure allgegenwärtige Hilfe im gesamten Institut!

Biologie ist ein kompliziertes Fach und ich bin sehr dankbar, dass manche von den tollen Kolleg*innen zu Freund*innen geworden sind. In zehrenden wie auch in entspannteren Zeiten haben wir zusammen auf Ergebnisse gehofft und uns gegenseitig angefeuert. Vielen lieben Dank Lisa, Abida, Vanessa und Alessia für all den Spaß, eure Aufmunterungen und euer Verständnis – ich weiß es zu schätzen!

Ich bin dankbar für mein ultimatives Unterstützerteam, meine Eltern Ulli und Uwe Lörch, meine Schwester Stefanie und meinen Partner Dominik Klang. Ihr habt die schwierigen Zeiten sehr nah miterlebt und mich immer wieder aufgemuntert und motiviert. Ich bin außerdem dankbar für meine Freund*innen, die nichts mit Biologie zu tun haben. Ihr habt mich immer daran erinnert, das Labor auch mal im Labor bleiben zu lassen. Trotz all eurer Anfeuerungen ist mir in den letzten 4,5 Jahren einmal mehr bewusst geworden, was wirklich zählt. Ihr habt mein Herz!

Abstract

Liver diseases contribute extensively to the global health burden. Multifactorial and monogenic liver diseases such as metabolism dysfunction-associated fatty liver disease (MAFLD) and alpha$_1$-antitrypsin deficiency (AATD) can cause liver fibrosis, cirrhosis and hepatocellular carcinoma. Despite extensive pre-clinical research, progress in understanding liver diseases and drug development remains limited by the inability of conventional models to adequately recapitulate physiologically relevant hepatocytes. Hence, the underlying pathomechanisms and additional driving factors causing the distinct onset and variable symptoms of MAFLD or AATD remain uncertain. iPSC-derived hepatocyte-like cells (HLCs) can be reproduced indefinitely while providing the genetic background of interest. In the first study, urine-derived somatic cells from adult and pediatric AATD patients carrying the most severe genotype were successfully reprogrammed into iPSCs, providing a platform to help close the knowledge gap regarding AATD onset in children. To overcome the well-known limitation of restricted maturation and functionality of HLCs, several aspects of an established protocol were re-evaluated and optimized in the second study. A key finding of this study was that forskolin induced the expression of farnesoid X receptor, an essential regulator of hepatic functions *in vivo*. Forskolin significantly enhanced hepatic gene and protein expression as well as the inducibility and activity of the cytochrome P450 3A4, a clinically relevant metabolizer of xenobiotics. The establishment of this optimized, time- and cost-efficient differentiation protocol contributes to the scientific understanding of hepatic differentiation and provides relevant platforms for liver disease modeling and toxicological assessment of liver safety. In the third study, MAFLD was modeled in functional HLCs, derived from diseased and healthy individuals, by induction of intrahepatic lipid accumulation (steatosis) for seven days. Steatotic HLCs successfully recapitulated relevant hits on the progressive axis from steatosis to steatohepatitis. Dysregulation of genes involved in AMP activated protein kinase (AMPK)- and peroxisome proliferator-activated receptor (PPAR)-signaling as well as insulin resistance and glutathione metabolism indicated metabolic alterations and cell stress. Furthermore, inflammatory signaling was detected by elevated expression of genes involved in NFkB-, TNF-, and cytokine-cytokine signaling pathways. Key findings included the elevated secretion of dipeptidyl peptidase 4 (DPP4) and corresponding activity upon steatosis. DPP4 is a ubiquitously expressed protease, involved in a plethora of inflammatory and metabolic pathways and is associated with MAFLD, however its concrete role in steatotic hepatocytes remains elusive. Inhibition of DPP4 resulted in the downregulation of inflammatory pathways

such as inflammatory bowel disease and type 1 diabetes mellitus. Simultaneously, expression of genes involved in metabolism associated pathways were upregulated. The presented study is the first in this format and confirms pre- and clinical data, proposing a modulating role of DPP4 at the interface between metabolism and inflammation. The novel perspective based on a relevant human *in vitro* hepatic steatosis model reveals potential pathomechanisms of the hepatocyte-specific contribution mediated by hepatic DPP4 activity in the context of MAFLD.

Zusammenfassung

Die globale Gesundheitsbelastung durch Lebererkrankungen steigt durch die drastisch steigende Prävalenz der multifaktoriell-bedingten metabolischen Dysfunktion-assoziierten Fettleber (MAFLD) stark an. Jedoch nicht nur MAFLD, sondern ebenfalls monogene Erkrankungen wie die Alpha$_1$-Antitrypsin-Defizienz können Leberfibrosen, lebensbedrohliche Leberzirrhosen und hepatozelluläre Karzinome auslösen. Trotz umfangreicher präklinischer *in vitro* und *in vivo* Studien, sind die zugrundeliegenden Pathomechanismen beider Erkrankungen nicht vollständig bekannt und die höchst unterschiedlichen Symptome und Verläufe erschweren die Entwicklung von Medikamenten.

Lebermodelle basierend auf Nagern, Primärzellen oder immortalisierten Zelllinien können natürliche Hepatozyten nur begrenzt widerspiegeln und limitieren dadurch die Translation von Ergebnissen aus dem Labor in klinische Studien. Patientenbasierte induzierte pluripotente Stammzellen (iPSCs) und differenzierte Hepatozyten-ähnliche Zellen (HLCs) bieten hier zwei Vorteile: Sie sind unbegrenzt reproduzierbar, während sie einen gesunden oder patientenspezifischen genetischen Hintergrund aufweisen.

In der ersten Studie wurden somatische Zellen von adulten und pädiatrischen AATD-Patienten aus Urin gewonnen und erfolgreich zu iPSCs reprogrammiert. Besonders iPSCs von pädiatrischen Patienten bieten eine wichtige Plattform, um den aktuell eingeschränkten Kenntnisstand über Ausbruch und Verlauf der AATD-Erkrankung bei Kindern zu erweitern. Eine Limitation der Nutzung von iPSCs für die Modellierung von Lebererkrankungen ist jedoch die begrenzte Reife von differenzierten HLCs. In der zweiten Studie wurde ein etabliertes Differenzierungsprotokoll evaluiert und optimiert, um die Reife der HLCs zu erhöhen. Eine zentrale Erkenntnis dieser Analyse war, dass Forskolin, ein Aktivator von zyklischem AMP (cAMP), die Expression des Farnesoid-X-Rezeptors (FXR) induzierte. Dieser Kernrezeptor wird natürlicherweise von Gallensäure aktiviert und ist essenziell für hepatische Funktionen. Hepatische Gen- und Proteinexpression sowie die Induzierbarkeit und Aktivität von Cytochrom P450 3A4 wurden signifikant erhöht. Dieses optimierte, zeit- und kosteneffiziente Differenzierungsprotokoll trägt somit nicht nur zum aktuellen Wissensstand der HLC-Differenzierung bei, sondern bietet darüber hinaus eine Plattform für hepatozytenspezifische Studien. In der dritten Studie wurde der hepatozytenspezifische Beitrag zum Verlauf von MAFLD untersucht. Funktionale HLCs von vier Individuen wurden mithilfe des optimierten Protokolls generiert und intrahepatische Fetteinlagerung (Steatose) induziert. Die globale Transkriptionsanalyse zeigte, dass steatoseinduzierte HLCs erfolgreich relevante Schritte des

Erkrankungsverlaufs reproduzierten. Die Dysregulierung von Genen, die in AMPK- und PPAR-Signalwegen involviert sind, sowie die Hochregulierung von Genen, die an Insulin Resistenz und Glutathion-Stoffwechsel beteiligt sind, deuteten auf metabolische Veränderungen und Zellstress hin. Weiterhin waren Gene, die an NFkB-, TNF- sowie Zytokin-Zytokin-Signalwegen beteiligt sind, hochreguliert, welche einen Fortschritt der Erkrankung zu Steatohepatitis andeuteten. Eine weitere zentrale Erkenntnis war die Steatose-induzierte Sekretion und Aktivität von hepatischer Dipeptidyl Peptidase 4 (DPP4). DPP4 ist ein ubiquitär vorkommender Regulator von Stoffwechsel und Entzündungsreaktionen und bekannterweise im Blutplasma von MAFLD-Patienten erhöht. Der konkrete Ursprung und Mechanismus von DPP4 ist jedoch bislang unbekannt. Inhibierung von DPP4-Aktivität führte zu einer Reduktion der Expression von Genen involviert in entzündungsassoziierte Signalwege, wie zum Beispiel die chronisch-entzündliche Darmerkrankung und Typ-1 Diabetes mellitus. Hingegen waren stoffwechselassoziierte Signalwege wie Lipidbiosynthese und Purinstoffwechsel hochreguliert. Die vorgelegte Studie ist die erste in diesem Format und bestätigt die Assoziationen von DPP4 und MAFLD aus anderen prä- und klinischen Studien in einem relevanten humanen Steatosis hepatis Modell. Diese neue Perspektive beleuchtet die steatoseinduzierte, hepatozytenspezifische DPP4-Aktivität und suggeriert eine modulatorische Rolle im Kontext des Verlaufs von MAFLD.

Contents

List of figures

Abbreviations

Symbol	Full name
2D	two-dimensional
3D	three-dimensional
AATD	alpha1 antitrypsin deficiency
ACC	acetyl-CoA carboxylase 1
ACTA	alpha actin 2
ADA	adenosine deaminase
AFP	alphafetoprotein
AGPAT2	1-acylglcerol-3-phosphate O-acyltransferase 2
ALB	albumin
AMPK	adenosine monophosphate-activated protein kinase
ASCs	adult stem cells
βIII-tubulin	beta-3-tubulin
BMI	body mass index
c-MYC	cellular myelocytomatosis oncogene
cAMP	cyclic adenosine monophosphate (AMP)
CEBPA	CCAAT(enhancer binding prptein alpha
CK18	cytokeratin 18
CK19	cytokeratin 19
CKD	chronic kidney disease
CMRFs	cardiometabolic risk factors
COPD	chronic obstructive pulmonary disease
CPT1A	cartinin-palmitoyltransferase 1 A
CRISPR/Cas9	clustered regularly interspaced short palindromic repeats/ CRISPR associated protein 9
CVD	cardiovascular disease
CYP2D6	cytochrome P450 2D6
CYP3A4	cytochrome P450 3A4
DAG	diacylglycerol
DGAT	diacylglycerol-O-acyltransferases
DEX	dexamethasone
DMEM	Dulbecco’s modified eagle medium
DMSO	dimethyl sulfoxid
DPP4	dipeptidyl peptidase 4
DSB	double strand break
E-CAD	e-cadherin
ECM	extracellular matrix
EMA	European medicines agency
EPAC2	exchange protein activated by cAMP2
ER	endoplasmic reticulum

ESCs	embryonic stem cells
FAs	fatty acyls
FDA	food and drug administration
FGF2	fibroblast growth factor 2
FOXA2	forkhead box A2
FXR	farnesoid X receptor
GI-tract	gastrointestinal tract
GIP	glucose-dependent insulinotropic protein 1
GLP-1	glucagon like protein 1
GSK3β	glycogen synthase kinase 3 beta
HCC	hepatocellular carcinoma
Hep-Par-1	hepatocyte paraffin 1/hepatocyte specific antigen
HGF	hepatocyte growth factor
HLCs	hepatocyte-like cells
HLX	H2.0 like homeobox
HMGCR	3-hydroxy-3-methylglutaryl-CoA reductase
HNF4α	hepatocyte nuclear factor 4alpha
hPSC	human pluripotent stem cells
HSCs	hematopoietic stem cells
HSL	hormone-sensitive lipase
Ins	insulin
iPSCs	induced pluripotent stem cells
IRS2	insulin receptor 2
KLF4	krüppel like factor 4
L-15	Leibovitz-15 medium
LDL-C	low density lipoprotein cholesterol
LESCs	liver epithelial sinusoidal cells
LIN28	lin-28 homologue A
LKB1	liver kinase B1
LPCs	lymphoid progenitor cells
MAFLD	metabolic dysfunction-associated fatty liver disease
MASH	metabolic dysfunction-associated steatohepatitis
MASLD	metabolic dysfunction-associated steatotic liver disease
MEK	mitogen activated protein kinase kinase (MAP2K)
metALD	metabolic dysfunction and alcohol-related liver disease
MSCs	mesenchymal stem cells
mTOR	mammalian target of rapamycin
NAFLD	non-alcoholic fatty liver disease
NANOG	nanog homeobox
NASH	non-alcoholic steatohepatitis
NFkB	nuclear factor kappa B
NLRP3	NOD like receptor protein 3
NGS	next generation sequencing

NT5C2	5'-nucleotidase, cytosolic 2
OA	oleic acid
OCT3/4	octamer binding transcription factor 3/4
OSM	oncostatin M
PA	palmitic acid
PAX6	paired box 6
PCG-1α	PPAR coactivator 1-alpha
PHH	primary human hepatocytes
Pi*ZZ	protease inhibitor, homologous Z alleles
PKC	protein kinase C
PLIN2	perilipin 2
PLIN3	perilipin 3
PNPLA3	patatin like domain 3, 1-acylglycerol-3-phosphate O-acyltransferase
PPAR	peroxisome proliferator-activated receptor
PXR	pregnane X receptor
RPMI	Roswell Park Memorial Institute Medium
ROS	reactive oxygen species
SERPINA1	serpin peptidase inhibitor clade A, member 1
SFA	saturated fatty acid
SIX2	sine oculis homeobox homolog 2
SMAD	small mothers against decapentaplegic
SNP	single nucleotide polymorphism
SOX17	SRY (sex determining region Y)-box 17
SOX2	SRY (sex determining region Y)-box 2
SOX9	SRY (sex determining region Y)-box 9
SSEA-4	stage-specific embryonic antigen 4
T1DM	type 1 diabetes mellitus
T2DM	type 2 diabetes mellitus
TGFβ	transforming growth factor beta
TGFβR2	tranforming growth factor beta receptor 2
THRb	thyroid hormone receptor beta
TKFC3	triokinase/FMN cyclase
TNF	tumor necrotic factor
TNFα	tumor necrosis factor alpha
TRA-1-60	tumor related antigen 1-60
TRA-1-81	tumor related antigen 1-81
UdRPCs	urine derived renal progenitor cells
VLDL	very low density lipoprotein
wt	wild type
WT1	Wilms tumor protein 1
YAP	yes associated protein
ZAAT	Z alpha-1 antitrypsin

1. Introduction

1.1. Stem cells

Stem cells are defined as undifferentiated cells, capable to either self-renew or differentiate into a specific cell type (Till & McCulloch, 1961). One of the first observations of cells that possess these abilities were made in transplantable ovarian tumors in mice by Jackson and Brues in 1941 (Jackson & Brues, 1941). They observed a variety of well-differentiated tissues next to rapidly dividing embryonal cells which seemed to either mature to specialized cells or retain the ability to grow indefinitely (Jackson & Brues, 1941). Early studies have already mentioned the term pluripotent, as a spontaneous and wide-range differentiation potential seen in ovarian cancers in mice (Stevens & Little, 1954). Yet, the concept of categorizing the differentiation potential of distinct stem cell populations was recognized during studies of hematopoietic stem cells (Metcalf, 1974; Till & McCulloch, 1961).

During mammalian embryonic development, totipotent cells include the diploid zygote, and cells resulting from zygote cleavage (Zakrzewski et al., 2019). The morula is a 16plus cell state, consisting of totipotent cells, enveloped in extracellular matrix (Zakrzewski et al., 2019). Upon further cell division, on day 5 - 6 of human embryonic development, the blastocyst derives. It consists of trophectodermal cells, representing the outer cell mass and pluripotent embryonic stem cells (ESCs), representing the inner cell mass (Figure 1). Trophectodermal cells derive the extraembryonic tissue, while ESCs undergo gastrulation. Upon gastrulation the three germ layers ectoderm, mesoderm and endoderm are established, generating all cell types of the embryo (Thomson et al., 1998). Isolation and cultivation of mouse ESCs from the inner blastocyst were performed by Evans and Kaufman in 1981 for the first time (Evans & Kaufman, 1981). They proved that pluripotent stem cells could be cultured *in vitro* while keeping the potency to differentiate and self-renew (Evans & Kaufman, 1981; Martin & Evans, 1975). Less than 20 years later, the first isolation of human ESCs by Thomson et al. in 1998 marked a milestone for developmental research and launched the field of regenerative medicine (Thomson et al., 1998).

In comparison to ESCs, adult stem cells (ASCs) reside in the postnatal human body in specialized stem cell niches, to regenerate tissues over the entire lifespan (Figure 1)

(Chowdhury & Ghosh, 2021). The first observation of adult stem cells was made by James A. Till and Ernest A. McCulloch in 1961 in the bone marrow of mice (Till & McCulloch, 1961). They discovered hematopoietic stem cells (HSCs) and defined the term of 'multipotency' as the potential to produce cell progeny of different lineages (Till & McCulloch, 1961). An example of such a stem cell niche is the bone marrow which represents a finely orchestrated 3D microenvironment for the HSCs (Chowdhury & Ghosh, 2021). Mesenchymal stem/stromal cells (MSCs) are another example for multipotent stem cells, however they reside in several tissues, giving rise to different cell lineages such as adipocytes, osteocytes and chondrocytes, among others (Tonk et al., 2020). The physical, chemical and biochemical cues such as mechanical forces from the extracellular matrix (ECM), oxygen concentration and pH, as well as signals from the surrounding cells control stem cell self-renewal, differentiation and migration (Chowdhury & Ghosh, 2021; Huang et al., 2024). HSCs can differentiate into lymphoid and myeloid cell lineage progenitors (LPCs and MPCs), regenerating the entire blood system (Yusoff et al., 2025). LPCs and MPCs are oligopotent stem cells and give rise to different cell types of each cell lineage, while unipotent stem cells such as epidermal stem cells are only capable of regenerating the same cell type (Chowdhury & Ghosh, 2021; Zakrzewski et al., 2019). A brief schematic of the differentiation potencies is provided in Figure 1.

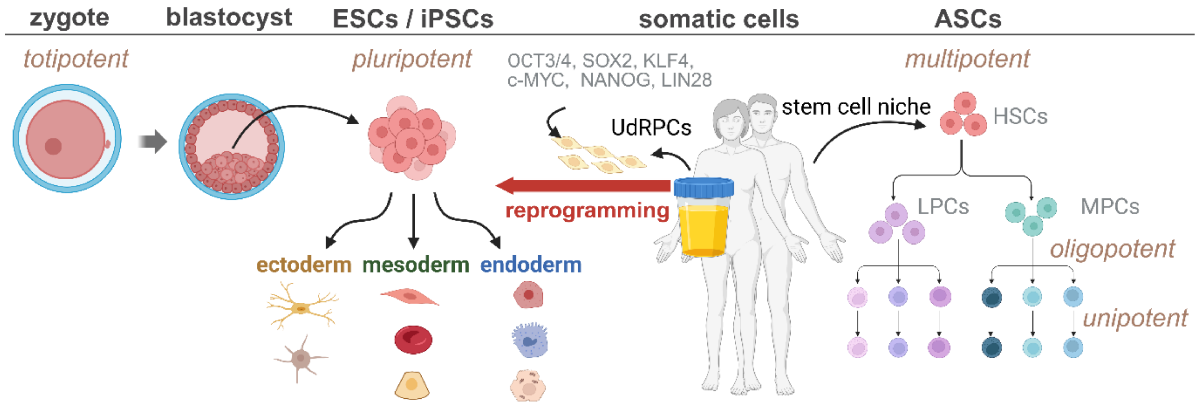

Figure 1 Schematic of stem cells and differentiation capacities.[1]

The zygote displays a totipotent cell, developing into the blastocyst which contains the outer cell mass building extraembryonic tissue and the inner cell mass consisting of pluripotent embryonic stem cells (ESCs). ESCs are capable to differentiate to all cells of the three germ layers ectoderm, mesoderm and endoderm, building the human embryo. Somatic human cells of different sources can be reprogrammed, exemplarily urine derived renal progenitor cells are shown (UdRPCs). By episomal-based

[1] Created in BioRender. (2025) https:// BioRender.com/40phe6f

overexpression of the Yamanaka and Thomson factors OCT3/4, SOX2, KLF4, c-MYC, NANOG and LIN28 they are reprogrammed to induced pluripotent stem cells (iPSCs). Adult stem cells (ASCs) remain in stem cell niches of the adult human body. Exemplarily, multipotent hematopoietic stem cells (HSCs) are shown, capable to differentiate to distinct cell lineages displayed in lymphoid progenitor cells (LPCs) and myeloid progenitor cells (MPCs). LPCs and MPCs can self-renew and differentiate to distinct cell types of the respective cell lineage. Cells of each lineage are unipotent, capable to restore one specific cell type.

1.2. Induced pluripotent stem cells (iPSCs)

Human ESCs, isolated from donated embryos, provide insightful knowledge for the study of developmental processes and disease mechanisms. However, especially in Germany, the use of human embryos opened up ethical debates as the embryo's life needs to be terminated for ESC isolation (Tuffs, 2001; Vazin & Freed, 2010). The potential of reprogramming terminally differentiated cells to an unspecialized stage was first published by Gurdon et al. in 1958. They observed that a somatic nucleus, transferred into an enucleated frog oocyte could develop into a normal tadpole (Gurdon et al., 1958). The results implied firstly, that somatic frog nuclei possess the complete genetic information to develop a normal tadpole (Gurdon et al., 1958). Secondly, the environmental factors of an oocyte are able to reprogram these to an embryonic-like state (Gurdon et al., 1958). In 2006, Yamanaka and his colleagues narrowed down five reprogramming factors, namely octamer binding transcription factor 3/4 (OCT3/4), SRY-box transcription factor 2 (SOX2), krüppel-like factor 4 (KLF4), nanog homeobox (NANOG) and myc proto-oncogene protein (c-MYC) which reprogrammed murine somatic cells into 'induced' pluripotent stem cells (iPSCs) (Takahashi & Yamanaka, 2006). In 2007, Yamanaka and Thomson independently proved that it is possible to also reprogram human somatic cells to iPSCs by combination of OCT3/4, SOX2, KLF4, NANOG and either c-MYC or lin-28 homologous (LIN28) (Takahashi et al., 2007; Yu et al., 2007). Gurdon and Yamanaka enabled the study of early developmental processes without ethical concerns and their seminal discoveries were rewarded with the Nobel prize in 2012 (Karagiannis et al., 2019; Nobel Assembly at Karolinska Insitutet, 2012).

The generation of iPSCs from somatic cells was established by retroviral overexpression of the pluripotency factors (Takahashi et al., 2007; Yu et al., 2007). However, the integration of the DNA results in genetically modified cells and might induce tumorigenic mutations, which restrict their clinical application. Furthermore, such tumorigenic mutations can further restrict the functionality of reprogrammed cells. There are several approaches to overcome these

limitations by reprogramming footprint free. Overexpression of the transcription factors through mRNA, Sendai virus or episomal-based are non-integrating methods (Schlaeger et al., 2015). Episomal-based reprogramming is highly reliable and specifically efficient when combined with small molecules (Yu et al., 2011). The possibility to reprogram any somatic cell into an iPSC has enabled unprecedented opportunities for developmental studies and disease modeling. Since the first attempts, various reprogramming protocols and commercial iPS cell lines were established. Despite differences in the reprogramming efficiencies and durations, which are method- and vector-dependent, today iPSCs are a relatively easy-to-use platform to study almost any cell type of the human body (Schlaeger et al., 2015). Nevertheless, several factors can affect the reprogramming efficiency and differentiation success. The source cell type, its exposure to environmental hazards, the method of reprogramming, and incomplete erasure of the source cells' epigenetic memory can interfere with reprogramming and differentiation (Yu & Thomson, 2014).

In order to maintain the pluripotent state of reprogrammed cells, the transforming growth factor β (TGFβ) pathway, downstream of fibroblast growth factor 2 (FGF2) signaling, plays an essential role. If the TGFβ/activin/nodal signaling branch is activated, suppressor of mothers against decapentaplegic (SMAD) 2/3/4 translocate to the nucleus and promote the expression of *OCT3/4*, which positively regulates downstream expression of stem cell regulators like *NANOG* and *SOX2* (Babaie et al., 2007; Greber et al., 2007). On the other hand, the bone morphogenic protein (BMP) induced branch of the TGFβ pathway has to be suppressed, since SMAD1/5/8 induce differentiation of iPSCs (Greber et al., 2007). The fundamental studies on the mechanisms underlying pluripotency are the basis for the efficient reprogramming and cultivation of iPSCs.

The possibility to recreate the genetic background of healthy and diseased individuals in iPSCs is particularly advantageous. Immortalized or tumor-derived cell lines, such as HepG2, Huh-7 or HepB3 cells have acquired mutations and karyotypic abnormalities and can only limitedly mimic physiological functions (Kasai et al., 2018; Simon et al., 1982). The unlimited proliferation of iPSCs is furthermore advantageous in comparison to primary cell cultures, which tend to show senescence, loss of function and dedifferentiation upon cultivation *in vitro* (Godoy et al., 2016; Kim, 1973; Striedter, 2022). However, iPSC culture basics such as media, coating matrices and their differentiation are costly, compared to tumor-derived cell line culture, and can pose difficulties. Additionally, because of the individual genetic background

of each iPS cell line it is important to include several iPS cell lines to enhance the reproducibility and significance of produced data (Volpato & Webber, 2020).

1.2.1. Urine-derived cells as a source for iPSCs

Urine provides a non-invasive, mostly age- and disease- independent and easily accessible source of cells. Humans shed approximately $6x10^4$ living and dead cells per day within the urine, consisting of different cell types (Lang et al., 2013). A fraction of this mixture of cells is rice-grain shaped and able to grow on a plastic surface. Because these cells exhibit renal progenitor properties like sine oculis homeobox homolog 2 (SIX2) and Wilms tumor protein 1 (WT1) expression, additionally to stem cell marker expression such as stage specific embryonic antigen 4 (SSEA4), T cell receptor alpha locus (TRA) -1-60 and TRA-1-81, they are designated urine-derived renal progenitor cells (UdRPCs) (Rahman et al., 2020). Besides their feasible acquisition, UdRPCs show higher reprogramming efficiencies for non-integrative reprogramming methods, compared to terminally differentiated fibroblasts. This might be due to their progenitor cell or mesenchymal stem/stromal cell (MSC) identity, which is discussed within the field (Benda et al., 2013; Y. Z. Huang et al., 2022; Rahman et al., 2020). By episomal expression of the Yamanaka and Thomson transcription factors *OCT3/4*, *NANOG*, *KLF4*, *c-MYC* and *LIN28* in UdRPCs with or without inhibition of TGFβ, mitogen-activated protein kinase kinase (MEK) and glycogen synthase kinase 3β (GSK3β), iPSCs can be generated integration-free within weeks (Bohndorf et al., 2017; Yu et al., 2011). Their accessibility, relatively low exposure to environmental hazards, and their reprogramming efficiency make them an efficient resource to receive patient-derived iPSCs for differentiation to organ-specific cells. By registering a patient-derived reprogrammed hPSC line, this enables other scientists to use the cell line for their respective studies (*hPSCreg – The Human Pluripotent Stem Cell Registry*, 2025).

1.2.2. Application of iPSCs

Since the discovery of the reprogramming factors almost two decades ago, research in the field has provided an extensive portfolio of protocols for reprogramming somatic cells into iPSCs. It seems that all cells of the human body, independent of their differentiation status, can be reprogrammed to iPSCs (Cerneckis et al., 2024; Karagiannis et al., 2019). Multipotent hematopoietic stem cells, UdRPCs as well as terminally differentiated T-cells have been reprogrammed successfully (Bohndorf et al., 2017; Loh et al., 2009; Seki et al., 2010). A far-

reaching implementation of the iPSC technology is gene editing to study disease mechanisms. An example is the clustered regularly interspaced short palindromic repeats associated protein 9 (CRISPR/Cas9) system. The technology is based on the Cas9 enzyme, which is directed to a specific DNA sequence by a guide RNA and introduces a double-strand break (DSB). The endogenous DNA DSB repair mechanism will introduce random sequence deletions or insertions to knock out the gene (Xue & Greene, 2021). A repair template harboring the desired gene mutation ensures the implementation of the genetic variant of interest (Xue & Greene, 2021). Gene editing approaches for iPSCs promote the generation of isogenic cell lines harboring the corrected or disease-relevant mutation within the individual genetic background. Upon differentiation, the cell type specific effect of the genetic variant can be studied to understand its contribution to the disease development (Reinhardt et al., 2013; Schwank et al., 2013). The individual genetic background is essential for the study of disease mechanisms, especially considering complex phenotypes caused by the interplay of different genetic variants.

This is specifically interesting for the study of human diseases which are not easily reproduced in other models. For example, rodent models have been used extensively to study liver fibrosis, however due to metabolic differences, inbred mice do not naturally develop liver fibrosis upon a high-fat/glucose diet (Febbraio et al., 2019; Vacca et al., 2024). This also accounts for genetic variants, which do not naturally occur in rodents, as the monogenic disease alpha$_1$-antitrypsin deficiency (AATD). The human genetic variant within the *SERPINA1* locus, has to be artificially introduced (Carlson et al., 1989; Sifers et al., 1987). This artificial induction of the disease phenotype potentially accounts for the poor transferability of results from animal-studies to humans (Marshall et al., 2023). With human iPSCs based on patients of respective diseases, the cell type specific pathomechanisms and additional driving factors deriving from the genetic background can be analyzed.

Beyond disease modeling, iPSC-derived cells, for example cardiomyocytes, can be applied in toxicological studies to limit animal studies and enhance the relevance of generated data in comparison to data established from immortalized cell lines (C. Y. Huang et al., 2022). Thereby iPSCs can contribute to the 3R-principle, published by Russel and Burch in 1960 (Karagiannis et al., 2019; O'Connor, 2013; W. M. S. Russell, 1960). The **3R**-Principle stands for **R**eplacement and **R**eduction of animal experiments and the **R**efinement of animal handling to reduce animal suffering to an absolute minimum, displaying the basis for animal experiment

policies (Burch 1959). iPSCs also offer the possibility to test drug toxicity in a population-based, or personal manner (C. Y. Huang et al., 2022; Paik et al., 2020).

Besides *in vitro* applications of iPSCs, several clinical studies are ongoing, focusing on the use of autologous iPSC-derived cell products to treat diseases (Kobold et al., 2020). There are several successful case reports, such as the transplantation of iPSC-derived retinal epithelial sheets, cardiomyocytes or dopaminergic neurons to treat macular degeneration, cardiomyopathy or Parkinson's disease, respectively (Araki et al., 2019; Miyagawa et al., 2022; Schweitzer et al., 2020). In 2024, the first treatment of type-1-diabetes mellitus (T1DM) showed promising results and clinical trials are ongoing to decipher autologous iPSC-treatment for several diseases (Kirkeby et al., 2025; Wang et al., 2024). However, providing autologous cell therapy is extremely time- and cost-intensive.
More efficient might be the use of allogenic iPSCs or derived cell products, albeit the hosts immune response to foreign donor cells can cause rejection. Human leukocyte antigen (HLA)-homozygous iPSC-banks are a future direction, to provide recipients with HLA-matching donor cells, when a transplantation is needed (Escribá et al., 2024). However, the extensive geographical distribution of HLA frequencies makes cross-border iPSC banks difficult and requires national iPSC banks to cover the respective populations (Arrieta-Bolaños et al., 2023; Kuebler et al., 2023; Yoshida et al., 2023). In summary, the application of iPSCs and iPSC-derived cell products offers great potential for the treatment of diseases in the future.

Albeit the steady progression of iPSC application, there are still challenges in the field, such as the differentiation efficiency. Not only for clinical approaches, but also for disease modeling and drug testing, the differentiated cells need to show all features of the desired cell type. Although differentiation protocols are established for a plethora of organ-specific cell types, iPSC-derived tissue-specific cells lack maturity and resemble rather a fetal state (Cerneckis et al., 2024; Karagiannis et al., 2019). Different approaches have been developed to enhance maturation, but these are inherently more complex and costly, which limits their applicability. This indicates the necessity for further research, to provide useful and relevant iPSC-derived models. Because of genetic background of iPSCs, their use harbors the risk of bias caused by donor-to-donor variability. Thus, it is indispensable to include iPSCs from several donors to obtain relevant and reproducible data. Global human pluripotent stem cell (hPSC) registries facilitate the exchange of genetically integer and pluripotent cell lines between scientists (Seltmann et al., 2015).

1.3. The liver

The liver is a highly functional and complex gatekeeper of the human body, processing blood from the gastrointestinal (GI-) tract, pancreas and spleen, providing macronutrient homeostasis, production of bile and hormones, as well as xenobiotic metabolism (Trefts et al., 2017). In order to perform these energy demanding tasks, the liver is capable of anabolic and catabolic macronutrient metabolism. Glucose is degraded for glycolysis, stored as glycogen, or assembled upon fasting via the gluconeogenic pathway (Han et al., 2016). Fatty acids are built upon excess glucose and oxidized upon fasting to produce energy. Furthermore, fatty acids are assembled to triacylglycerol (TG) and stored or exported to adipose tissue (Chiang, 2014). Finally, the liver builds the majority of plasma proteins and processes amino acids for gluconeogenesis, or energy production, deamination and waste disposal of nitrogen via the urea metabolism (Charlton, 1996; Paulusma et al., 2022).

1.3.1. Microstructure of the liver

Additionally to macronutrient metabolism, hepatocytes produce bile and hormones and perform xenobiotic clearance, to ensure blood homeostasis. To perform these numerous functions, they are supported by four other cell types and organized in functional units called liver lobules. In Figure 2, a schematic of the liver lobule organization is given. At the outer rim of each liver lobule, blood and bile vessels build portal triads, additionally to the central vein, localized in the center. Oxygen- and nutrient-rich blood enters the liver lobule and travels from the portal triad through the sinusoids towards the central vein. Specialized endothelial cells with big fenestrae and no subendothelial matrix line the sinusoids and are called liver sinusoidal endothelial cells (LSECs) (Kanel, 2009; Wisse, 1970). LSECs ensure complete submergence of the hepatic basolateral membranes in blood plasma to allow blood processing before draining through the central vein back into circulation (Trefts et al., 2017). On the apical side, hepatocytes produce bile, which is drained through the bile canaliculi towards the bile duct in the opposite direction (Kanel, 2009). The bile ducts are lined with heterogenous epithelial cholangiocytes which perform secretory and absorptive functions to modify the produced bile for further transport (Tabibian et al., 2013). Kupffer cells are sinusoidal resident macrophages adherent to the LSECs, clearing pathogens, antigens, dead or dying cells and other waste products by mononuclear phagocytotic mechanisms (Nguyen-Lefebvre & Horuzsko, 2015). Furthermore, they are tolerogenic, keeping immune homeostasis (Nguyen-Lefebvre & Horuzsko, 2015). Hepatic stellate cells (SCs) are found in the space of Disse between the

LSECs and the hepatocytes. During physiological conditions, SCs remain inactive, storing retinoids and possibly functioning as liver-specific pericytes. Furthermore, SCs are known for their fibrogenic potential upon activation, however also their regenerative potential has been discussed (Friedman, 2008; Kordes et al., 2013; Kordes et al., 2014).

1.3.2. Hepatic zonation

The diverse hepatic functions are organized throughout each liver lobule. Wnt- and Hedgehog (Hh)-signaling are key regulators of hepatic zonation, dominating distinct lobular regions and suppressing each other (Benhamouche et al., 2006; Kolbe et al., 2019). Hh-signaling regulates, among others, protein and cholesterol synthesis, and fatty acid metabolism (Dutta et al., 2023). In comparison; Wnt dependent β-catenin mediates xenobiotic metabolism, bile and fatty acid synthesis (Goel et al., 2022). Finely orchestrated gradients of oxygen, nutrients, and hormones are additional important determinants of hepatic functions (Chiang, 2014).

Higher levels of oxygen and Hh-signaling determine the periportal zone (zone I) around the portal triad. The mid-lobular zone (zone II) displays an unspecialized transit zone between zone I and zone II, the pericentral zone. In the pericentral zone, located around the central vein, higher levels of Wnt-signaling are found (Benhamouche et al., 2006; Kolbe et al., 2019). Figure **2** provides an overview of the main functions segregated throughout the zones of the liver lobule. Energy-demanding tasks such as β-oxidation of fatty acids (FAs), gluconeogenesis, cholesterol and urea synthesis are mainly performed by periportal hepatocytes (Martini et al., 2023; Trefts et al., 2017). In comparison, pericentral hepatocytes use the synthesized cholesterol for bile production, perform xenobiotic metabolism, synthesize triglycerides from FAs or recycle waste products to keep the acid/base equilibrium (Martini et al., 2023; Panday et al., 2022; Trefts et al., 2017). Hepatocytes of zone II seem to display an intermediate phenotype, as they are capable to take over functions of zone I or III if needed (Martini et al., 2023).

Besides spatial compartmentalization also temporal and circadian stimuli influence the hepatic functional activities (Reinke & Asher, 2016). As indicated, the tightly orchestrated spatiotemporal regulation of the diverse hepatic functions is complex, and pathologies inflicting with homeostasis of lobule zonation result in serious consequences for liver function (Martini et al., 2023). Dysregulation of Hh-signaling, for example, can induce hepatic steatosis, and aberrant activation of Hh and Wnt-signaling are associated with hepatocellular carcinoma (HCC) (Dutta et al., 2023; Zhao et al., 2024).

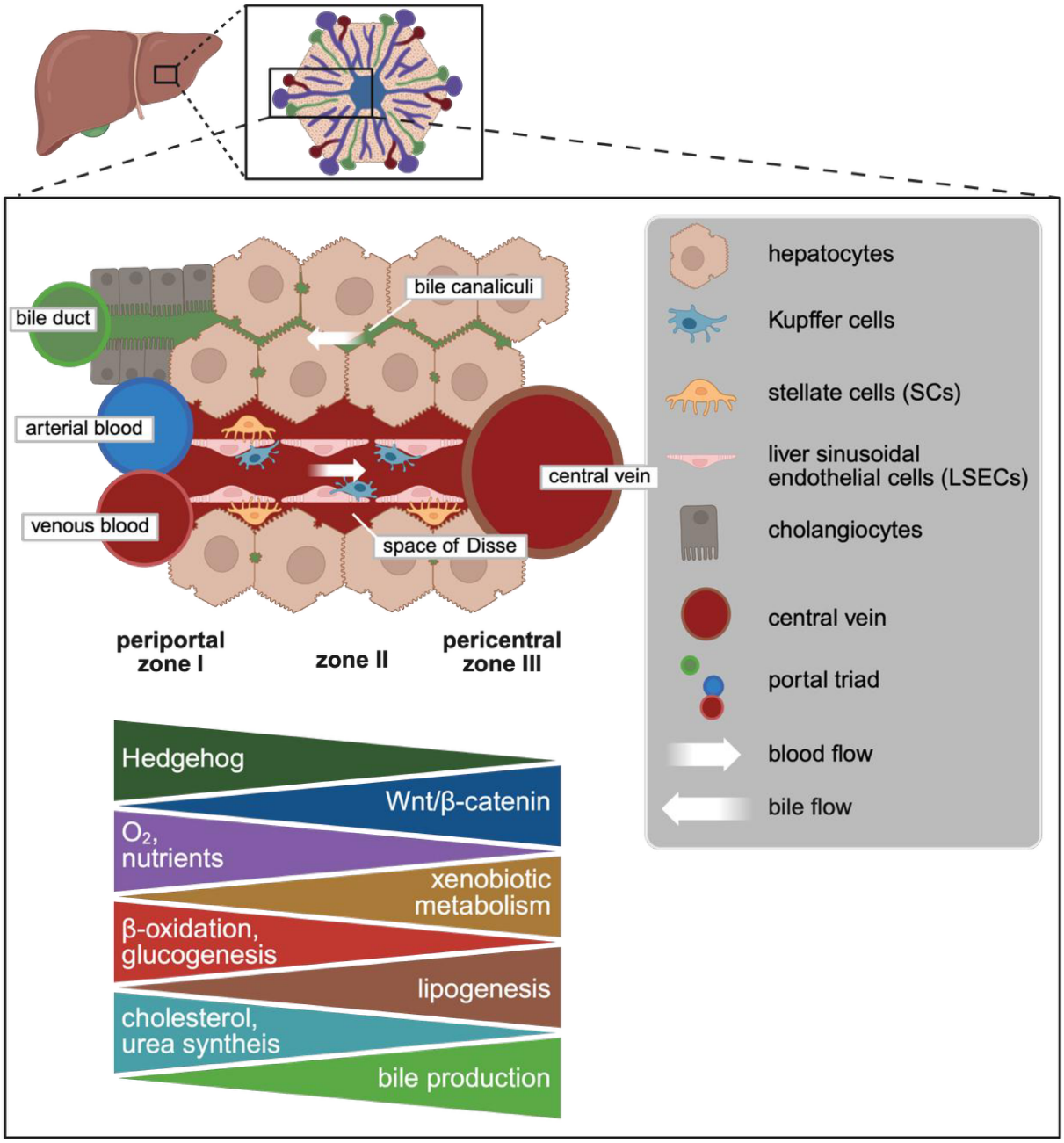

Figure 2 Schematic of the liver lobule. [2]

Indicated are the different cell types, the flow of blood and bile and the zone-specific functions. Arterial blood from the lung and venous blood from the gastrointestinal tract flow through sinusoids towards the central vein to re-enter the circulation. Liver sinusoidal endothelial cells (LSECs) with big fenestrae line the sinusoids and provide submergence of hepatocytes in blood plasma on the basal side. Liver resident LSECs associated macrophages (Kupffer cells) clear pathogens, antigens, dead or dying cells. In the space of Disse, between LSECs and hepatocytes, stellate cells (SCs) reside. On the apical side, hepatocytes build the bile canaliculi, which drain produced bile into bile ducts, lined by cholangiocytes

[2] Created in BioRender. (2025) https://BioRender.com/0x5pnd9

for transport to the gall bladder. The concentration gradients Hedgehog (Hh) and Wnt/β-catenin signaling, oxygen and nutrients determine the zonation of hepatocytes, promoting β-oxidation, gluconeogenesis, cholesterol and urea synthesis in the periportal zone I. In the pericentral zone III, xenobiotic metabolism, lipogenesis and bile production take place. The intermediate zone II connects zone I and zone III.

1.3.3. **Embryonic development of the liver**

During gastrulation, definitive endoderm is induced by a complex array of extracellular signals, released in a spatiotemporal manner, including high levels of activin A and Wnt/β-catenin signaling (Sumi et al., 2008; Trefts et al., 2017). From the definitive primitive gut tube, liver budding is initiated by FGF signaling from the cardiac mesoderm and BMP signaling from septum transversum, respectively (Lemaigre, 2007; Sumi et al., 2008; Trefts et al., 2017). Hepatoblast invasion and liver bud expansion is regulated by external signals including FGF, BMP, hepatocyte growth factor (HGF), tumor necrosis factor (TNF) and Wnt; secreted from neighboring mesenchymal and endothelial cells (Lammert et al., 2003; Lemaigre, 2007). The complex orchestration of external signals stimulates the expression of endogenous signals regulating apoptosis, proliferation and cell adhesion of the bipotent hepatoblasts (Tachmatzidi et al., 2021).

The exact mechanism of the cell fate decision towards hepatocyte or cholangiocyte remains elusive, however spatiotemporal gradients of multiple classical signaling cascades such as Wnt, TGFβ, yes-associated protein (YAP) / hippo- and notch-signaling seem to be essential (Sahoo 2022, boulter 2013, Zong 2009 and Yimlamai 2014). Indeed, during fetal development, hepatocytes and cholangiocytes share expression of transcription factors like hepatocyte nuclear factor (HNF) 3α/β and HNF6 (Limaye et al., 2008). However, in normal adult liver, HNF4α, HNF6 and hepatocyte specific antigen (Hep-Par1) are expressed exclusively in hepatocytes, while HNF1β, HNF3α/β and cytokeratin (CK) 19 are only expressed in cholangiocytes (Limaye et al., 2008). Furthermore, recent findings indicate, that increased gene levels of CCAAT enhancer binding protein α (*CEBPα*) and inhibited gene expression of SRY box transcription factor 9 (*SOX9*) and TGFβ receptor 2 (*TGFβR2*) are deterministic for hepatocyte fate along the TGFβ signaling axis (Sahoo et al., 2022). After cell fate decision, hepatocytes mature their functions dependent on their organization within the liver lobule (as described in detail in sections 1.3.1 and 1.3.2).

1.3.4. *In vitro* differentiation of iPSCs to hepatocyte-like cells

Various protocols have been established to differentiate ESCs or iPSCs towards hepatocyte-like cells (HLCs) *in vitro* (Jozefczuk et al., 2011). The initial protocols, developed beginning in 2008, form the foundation; and the majority of current protocols are based on their findings (Agarwal et al., 2008; Cai et al., 2007; Hay et al., 2008b; Touboul et al., 2010). While *in vivo* the complex interplay of signaling cascades is orchestrated by finely tuned gradients of signals, *in vitro* three to four main differentiation steps are induced. A brief overview on one of the main differentiation approaches by chemical induction is given in Figure 3A. Definitive endoderm (DE) differentiation can be initiated by the induction of Wnt- and activin/nodal-signaling. This is achieved either by direct or indirect induction of the canonical Wnt pathway. Wnt3A is a direct inducer of the pathway, while CHIR99021 (CHIR) prevents GSK3-dependent degradation of β-catenin and thereby induces Wnt indirectly (Hay et al., 2008a; MacDonald et al., 2009). Supplementation of a plain basal medium such as Roswell Park Memorial Institute Medium (RPMI) with CHIR or Wnt3A and activin A, a member of the TGFβ superfamily, for the first three days induces DE cells (Graffmann et al., 2022; Hay et al., 2008b; Kubo et al., 2004). Hepatic endoderm formation can be induced by supplementing low concentrations of dimethyl sulfoxid (DMSO) to a nutrient depleted medium such as Dulbecco's modified eagle medium (DMEM) knockout medium for five days and results in bipotent hepatic endodermal cells. HLC induction can be performed in Leibovitz 15 (L15) basal medium, supplemented with HGF, oncostatin M (OSM), dexamethasone (DEX) and insulin (Ins) for approximately 15 days. The resulting HLCs show, among others, gene and protein expression of albumin (ALB), HNF4α and alpha$_1$-antitrypsin (AAT), as well as urea secretion, glycogen storage and activity of cytochrome P450 3A4 (CYP3A4) (Graffmann et al., 2016; Matz et al., 2017).

Although the resulting HLCs show key hepatic marker expression and functionality, the gene expression levels are significantly lower compared to primary human hepatocytes (PHHs) and resemble rather a fetal hepatic phenotype (Baxter et al., 2015; Graffmann et al., 2022; Yuan et al., 2023). This is noticed by high levels of alphafetoprotein (AFP) expression, a fetal version of ALB. Next to differentiation by chemical induction as described above, it is also possible to overexpress genes regulating the hepatic development (Figure 3B) (Inamura et al., 2011; Tomaz et al., 2022). The overexpression of relevant transcription factors—called 'forward programming'—seems to generate mature HLCs efficiently and enables transdifferentiation of somatic cells (Tomaz et al., 2022). Nevertheless, generating genetically modified cell lines is

time- and cost-intensive, and challenges the use for therapeutic approaches, due to the integrated DNA and potential off-target effects of, harboring the risk for tumorigenicity.

Besides 2D cell culture, various approaches are used to induce HLC maturation by 3D cell culture in spheroids, organoids or on tissue engineered scaffolds (Figure 3C-D). Spheroids are often referred to as single cell type aggregates while organoids typically consist of several cell types with structural organization. In order to form spheroids or organoids, iPSCs or progenitor cells are seeded in an environment preventing cellular attachment, resulting in spherical cell aggregates. As organoids consist of several cell types, this can be achieved by initially seeding the respective cell types together. Nevertheless, also only seeding iPSCs initially before start of differentiation will result in cells of different developmental stages within one organoid (Pranty et al., 2023; Szepanowski et al., 2024). While cell-cell interaction mimics natural development better, organoids are often referred to as less directed, implying less control of the cells' development, compared to single-cell type spheroids (Moro et al., 2024). Another approach is to seed iPSCs or progenitor cells into synthetic or natural scaffolds e.g. electrospun polycaprolactone or decellularized extracellular matrix or tissue (Cameron et al., 2015; Heydari et al., 2020; Lu et al., 2013; Weber et al., 2023). Considering multi-cell-type cultures, the cell-cell interaction of other liver cell types has been shown to advance maturation in multicellular liver organoids, assembloids or organ on a chip approaches (Andersen et al., 2020; Huh et al., 2011; Lekkala et al., 2025; Mills & Hudson, 2020; Takebe et al., 2014; Yuan et al., 2023). Furthermore, the 3D environment provides mechanical forces which mimic the physiological environment better and enable prolonged cultivation, enhancing the maturation (Rashidi et al., 2018).

Although these methods provide more complex models which recapitulate the physiological state of the cells more precisely, a major limitation is the handling. Not only seeding these cells can be complicated but harvesting the cells from the aggregates for flow cytometric analyses or immunocytochemistry poses challenges. Furthermore, necrotic cores are often recognized in spheroids and organoids challenging the isolation of sufficient quantity of high-quality RNA and protein.

Human HLCs are physiologically relevant tools needed for basic (disease modeling) and translational (drug development) liver research in line with the 3R-principle (section 1.2.2). Therefore simple, reproducible, cost- and time-efficient differentiation protocols are needed,

yielding HLCs which express hepatic genes and proteins and show relevant functionality. In order to meet these criteria, it is necessary to constantly re-evaluate and optimize established methods and techniques. Optimized HLC protocols can then further be adapted to provide tools for the study of liver diseases and development of drugs.

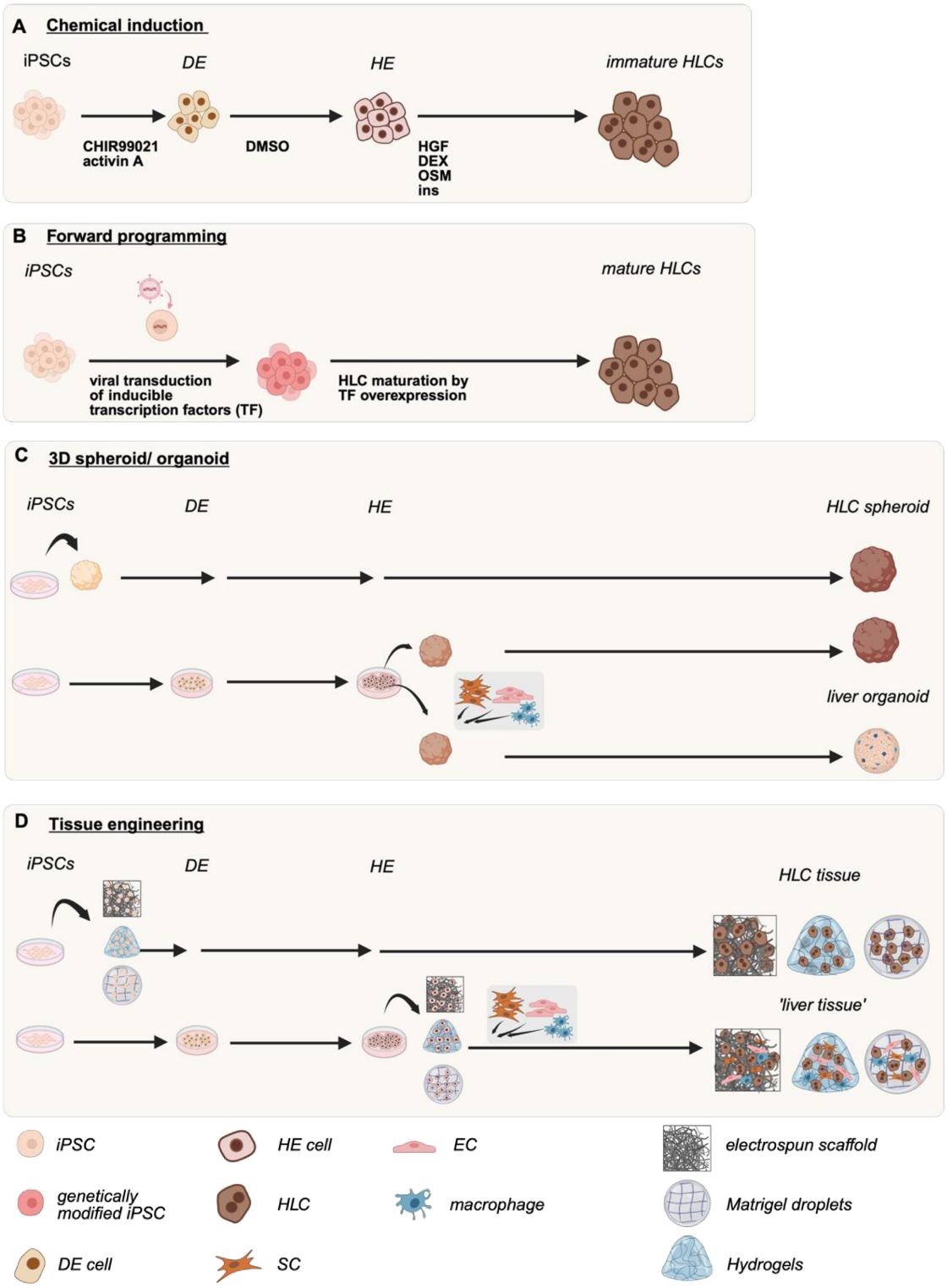

Figure 3 Brief schematic of different approaches for HLC differentiation.[3]

(A) *Exemplary schematic of a three-step HLC differentiation protocol (Graffmann et al., 2016; Matz et al., 2017). Chemical induction of definitive endoderm (DE) by treatment with CHIR99021 and activin*

[3] Created in BioRender. (2025) https:// BioRender.com/8cgrue1

A in the first three days. Hepatic endoderm (HE) is introduced by DMSO treatment for four days and hepatocyte-like cells (HLCs) are differentiated by addition of hepatocyte growth factor (HGF), dexamethasone (DEX), oncostatin M (OSM) and insulin (Ins) for 15 days. As indicated, the resulting HLCs are rather immature/fetal. ***(B)*** *Forward programming is established by transfection of effective and inducible hepatic transcription factors. Upon induction for several days in HLC medium, iPSCs will differentiate to mature HLCs.* ***(C)*** *Spheroid or organoid cell culture can either be induced in the iPSC-state (upper part) or in the hepatic endoderm state (lower part). Cells are re-seeded from 2D to 3D environment and other cell types such as endothelial and stellate cells (ECs and SCs) as well as macrophages can be included to result in liver organoids.* ***(D)*** *For tissue engineering approaches, iPSCs are either seeded directly on scaffolds, (example: electrospun scaffold), hydrogels or embedded in matrices (example: matrigel droplet) (upper part) or first differentiated to HE cells and then re-seeded from 2D to 3D (lower part). Pure HLC culture or incorporation of other cell types result either in 'HLC tissues' or 'liver tissues'.*

1.4. Health burden of liver diseases

Liver diseases are a tremendous global health burden, which has caused 2 million deaths in 2023, representing the 11th leading cause of death (Devarbhavi et al., 2023). There are several etiologies causing liver diseases such as infections, auto-immune diseases, inherited genetic disorders, other co-morbidities as well as the lifestyle. The prevalences of these etiologies vary from region to region. An example is hepatitis B virus (HBV) infection, which is still the leading cause for liver mortality in China, India and Nigeria. In Asia, 75% of all liver cancers are caused by HBV and hepatitis C virus (HCV) infections (Devarbhavi et al., 2023). On the other hand, genetical disorders such as alpha$_1$-antitrypsin deficiency (AATD) and auto-immune diseases of the liver are more prominent in the USA, Europe and other high-income countries (de Serres & Blanco, 2014; Devarbhavi et al., 2023). Reasons are the geographic distribution of genetic variants, however, potentially also result from better recognition and awareness.

The 'modern' lifestyle with inadequate movement and a high-caloric, highly processed diet, has caused the pandemic of obesity and is responsible for the drastic increase of fatty liver diseases. Indeed, in the past 30 years the prevalence of non-alcoholic fatty liver disease (NAFLD) has drastically increased and is estimated to affect one-third of the global population (Riazi et al., 2022; Teng et al., 2023). Together with increasing alcohol and drug consumption globally, these factors will likely even enhance the health burden of liver diseases in the future (Devarbhavi et al., 2023).

Independently of the underlying etiologies for liver diseases, they cause liver damage and can lead to cirrhosis. Since to date there is no treatment for liver cirrhosis, the only option for

decompensated cirrhosis is liver transplantation along with life-long medication and lifestyle adjustment (Singh & Watt, 2012). The socio-economic status, education, donor availability but also cultural and religious differences influence the number of liver transplantation and their outcome (Devarbhavi et al., 2023). Conclusively, global lifestyle changes, together with higher rates of alcohol and drug use indicate a probable increase of liver disease associated mortality globally. Due to the aforementioned lacking therapeutics and differences in liver transplantations, this will likely especially affect countries of lower socio-economic status.

1.4.1. Alpha$_1$-antitrypsin deficiency (AATD)

AATD is an inherited genetic disorder resulting from distinct mutations within the *SERPINA1* gene locus (Strnad et al., 2020). Alpha$_1$-antitrypsin (AAT) is a serine protease inhibitor and is expressed in several cell types, however predominantly in hepatocytes (de Serres & Blanco, 2014). AAT is an acute phase protein, and its expression increases during inflammation, infection or injury (de Serres & Blanco, 2014). Distinct mutations, such as the so called 'Z mutation', can lead to misfolding of AAT, resulting in the retention of the protein within the hepatocytes and correspondingly lower levels in the circulation. As it regulates anti-inflammatory responses and inhibits neutrophil elastases, lacking AAT can cause damage of the lung parenchyma and emphysema (de Serres & Blanco, 2014; Stoller JK et al., 2006, updated 2023). Furthermore, misfolded AAT is retained in the hepatic endoplasmic reticulum (ER), which causes hepatic stress and can promote chronic liver disease.
Nevertheless, the symptoms of AATD vary as over 100 distinct mutations cause different levels of AAT misfolding, retention and different levels of AAT in the circulation. The most severe phenotype is caused by the aforementioned homogenous Z allele of the proteinase inhibitor (Pi), designated Pi*ZZ genotype (Katzer et al., 2021; Ruiz et al., 2023). The homogenous missense mutation of G→A at position rs28929474 results in the substitution of glutamate to lysine at position 342 (Stoller JK et al., 2006, updated 2023). This substitution leads to the formation of insoluble AAT polymers, called 'ZAAT' and causes a drastic decrease of wildtype (wt) AAT serum levels. Furthermore, circulating ZAAT itself has proinflammatory properties, enhancing an inflammatory environment (Strnad et al., 2020).

Interestingly, the onset of symptoms varies drastically between AATD patients carrying the Pi*ZZ genotype (Ruiz et al., 2023). The disease typically manifests either in infants (<4 years) or in middle-aged adults (>50 years). 10% of Pi*ZZ infants exhibit a severe liver phenotype, resulting in cirrhosis and the requirement for liver transplantation, life-long medication and the

adjustment of the lifestyle (Ruiz et al., 2023). Due to limitedly available studies focusing on AATD in children, the underlying mechanisms, additional driving factors and predictors of the disease are yet to be determined (Lemke et al., 2024). Another factor is that there are only limited *in vitro* studies focusing on AATD in children, with no or very limited iPSCs derived from pediatric AATD patients under 16 (Kaserman et al., 2020).

In middle-aged adults, the lung phenotype is more prevalent, typically showing a gradual deterioration over the years resulting in lung emphysema or chronic obstructive pulmonary disease (COPD). Additionally, adults can also develop a liver phenotype but usually more gradually, often remaining undiagnosed. Therapeutic options are currently only available for the lung phenotype by supplementation of human wt AAT. The only option to treat the liver phenotype is to slow down fibrosis and prevent cirrhosis development (Ruiz et al., 2023). Low awareness and limited genotypic screenings, together with varying symptoms typically result in late diagnosis of the AATD genotype and indicates a probably high number of unreported cases. The distinct symptoms and onset of the disease indicate additional driving factors to be involved in the disease progression, however the underlying mechanisms remain elusive.

1.4.2. Hepatic steatosis

Hepatic steatosis describes the storage of fatty acids (FAs) packed as triacylglycerol (TAG) or cholesterol esters organized in lipid droplets in hepatocytes, representing >5% of the liver mass (Idilman et al., 2016). Enhanced levels of lipids and insulin in the blood (hyperinsulinemia and hyperlipidemia), can induce hepatic steatosis by disbalancing lipid accumulation and lipid disposal (Angulo, 2007; Deng et al., 2022). Additionally, upon excess glucose, it is converted to FAs during *de novo* lipogenesis, which can contribute to hepatic steatosis (Adeva-Andany et al., 2016; Sanders et al., 2018). In a multistep reaction, fatty acyls are converted to TAGs or cholesterol esters and assembled in lipid droplets which bud from the ER and are coated with associated proteins, such a perilipins (PLIN), and diacylglycerol-O-acyltransferases (DGAT) (Chiang, 2014; Dempsey et al., 2023; Rui, 2014). Lipid droplets are dynamic organelles, storing neutral FAs, protecting cells from acute lipotoxicity and serving as substrate for very low density lipoprotein (VLDL) packaging, for lipid export (Dempsey et al., 2023). Upon chronic steatosis and increasing metabolic stress, FAs can convert over saturated fatty acids (SFAs) into lipotoxic ceramides or palmitates. Furthermore, due to the hampered lipid metabolism, metabolic intermediates such as diacylglycerol (DAG) or cholesterol accumulate (Deng et al., 2022). Cholesterol crystals activate the hepatic inflammasome via the NOD like receptor protein 3 (NLRP3), increase interleukin (IL) -1b and hepatic caspase expression, and

subsequently recruit Kupffer cells (Deng et al., 2022). DAG on the other hand was shown to promote insulin resistance by activating protein kinase C (PKC) and downstream inhibition of the insulin receptor 2 (IRS2) (Kumashiro et al., 2011).
Hepatic steatosis induction due to hyperinsulinemia and hyperlipidemia underline the strong association between fatty liver diseases, obesity and insulin resistance. Hence, the epidemic of obesity caused by Western diet and sedentary lifestyle has led to a drastic increase in metabolic fatty liver disease (FLD) worldwide (Asrani et al., 2019; Clemente-Suárez et al., 2023; Jiang et al., 2023; Teng et al., 2023). Particularly FLD and insulin resistance form a vicious circle as they accelerate each other (Angulo, 2007; Barrera et al., 2024).

1.4.3. Metabolism dysfunction-associated fatty liver disease (MAFLD)

The estimated prevalence of metabolism-derived FLD was 32% in all adults and 75% in obese individuals in 2023 (Teng et al., 2023). Chronic inflammation upon lipotoxicity can result in fibrosis, which represents aberrant ECM accumulation and a pro-inflammatory environment and hepatocytes undergoing apoptosis (Bataller & Brenner, 2005). Fibrosis can progress to life-threatening liver cirrhosis and HCC. In 2019, 2.4% of global deaths were caused by liver cirrhosis (Asrani et al., 2019; Huang et al., 2023). Considering its serious consequences, metabolism-associated FLD is predicted to be the leading cause of liver transplantation in 2030 displaying a tremendous global health burden (Jiang et al., 2023).

MAFLD is a relatively new diagnosis, established in 2020 to replace non-alcoholic fatty liver disease (NAFLD). The term NAFLD was established to discriminate the disease from other etiologies, such as alcohol consumption, drug abuse, or infections (Lonardo et al., 2020). The term NAFLD, however, was shown to be quite nebulous to medical staff outside the gastroenterological field and contributed to limited monitoring, low visibility and unnoticed progression of the disease (Bergqvist et al., 2013).

In order to better monitor the patients, several symptoms are included in the diagnosis of MAFLD: hepatic steatosis plus either overweight, type 2 diabetes mellitus (T2DM) or 2 out of 7 cardiometabolic risk factors (CMRFs) (Eslam et al., 2020). CMRFs include obesity, raised blood pressure, elevated plasma triglycerides, pre-diabetes, insulin resistance and high plasma c-reactive protein (Gofton et al., 2023). These criteria reflect the huge contribution of metabolic risk factors for the disease and indicate the complexity of symptoms and disease progression (Eslam et al., 2020; Gofton et al., 2023). However, there are also other causes such as single

nucleotide polymorphisms (SNPs) and genetic variants which promote the development or progression of MAFLD. An example is a mutation changing cytosine to guanine at the locus rs738409 encoding patatin like domain 3, 1-acylglycerol-3-phosphate O-acyltransferase (PNPLA3), which is involved in the degradation of unsaturated fatty acids (Johnson et al., 2024; Romeo et al., 2008). This SNP and the respective substitution from isoleucine to methionine (I148M) drive the development of fatty liver (Romeo et al., 2008; Tilson et al., 2021). Upon progression of MAFLD, an inflammatory state of the disease develops, called metabolic dysfunction-associated steatohepatitis (MASH). MASH can progress to fibrosis, cirrhosis and HCC. Patients show highly variable disease onset, progression and symptoms, which has caused underestimation of the prevalence and severity in the past, and challenges the understanding of the disease mechanisms.

To advance the understanding of the complex pathology, Day and James established a two-hit model (Day & James, 1998). The 'first hit' described hepatic steatosis triggered by T2DM, insulin resistance or elevated FA flux from adipose tissue or a high fat diet. The 'second hit' was represented by the production of reactive oxygen species (ROS) and lipotoxicity resulting in hepatic injury and ER stress (Fang et al., 2022; Masarone et al., 2018). It was assumed, that the power of the second hit was highly dependent on predispositions and co-pathologies and explained progression differences between patients.
Recent theories imply rather a several hit model. Such multiple events may happen simultaneously, causing either mild steatosis or rapid progression towards steatohepatitis (Tilg & Moschen, 2010).

AMP activated protein kinase (AMPK) is an essential energy sensor, which is activated upon high ratios of AMP/ATP, promoting fatty acid degradation for ATP production and inhibiting lipogenesis. Upon activation by liver kinase B1 (LKB1), AMPK phosphorylates PPAR coactivator 1-alpha (PCG-1α), CPT1 and hormone-sensitive lipase (HSL) to enhance fatty acid β-oxidation and lipolysis. On the other hand, 3-hydroxy-3-methylglutaryl-CoA reductase (HSL) and acetyl-CoA carboxylase 1 (ACC) are inhibited to prevent lipogenesis and cholesterol synthesis (Fang et al., 2022). Additionally, AMPK regulates mammalian target of rapamycin (mTOR) to promote autophagy (Vergara Nieto Á et al., 2025). In steatosis patients, AMPK is typically downregulated, indicating inadequate compensatory effects and imbalanced metabolic homeostasis (Fang et al., 2022). Inflammatory signaling via TNFα, nuclear factor light chain enhancer (NFkB) and cytokine signaling, results in the recruitment of immune cells and the

progression to steatohepatitis (Catrysse & van Loo, 2017; Fang et al., 2022; Heida et al., 2021; Vachliotis & Polyzos, 2023). Furthermore, a recent study dissected different stages of HCC, and found pathways involved in gluconeogenesis differentially regulated, strengthening the importance of metabolic remodeling for end-stage liver diseases (Yu et al., 2024). The findings indicate that although earlier hits likely represent metabolic changes there is not an exact sequence of events.

Progressive MAFLD is an independent risk factor for other diseases. The aforementioned association with insulin resistance provides a proinflammatory, profibrogenic and procoagulant systemic environment (Pipitone et al., 2023) This environment increases the risk for T2DM, cardiovascular disease (CVD), chronic kidney disease (CKD), and cancer (Pipitone et al., 2023). Considering the epidemic of obesity and related diseases, MAFLD is a leading contributor to the global health burden of liver diseases underlining the importance for the development of treatments and prevention measures.

Due to the above-mentioned renaming from NAFLD and non-alcoholic steatohepatitis (NASH) to MAFLD/MASH in 2020 both terms are used in the present dissertation, according to the terminology employed in the referenced literature.

1.4.4. The role of dipeptidyl peptidase 4 (DPP4) in MAFLD

DPP4 (or CD26) is a ubiquitously expressed transmembrane serine protease. It consists of relatively small intracellular and transmembrane domains, and a large extracellular domain with catalytical activity (Misumi et al., 1992). Upon shedding, the catalytic activity remains and soluble DPP4 circulates in the blood (Misumi et al., 1992). The type 2 serine protease has cleaving potential on a variety of proteins such as incretins, chemokines, cytokines and extracellular matrix proteins (Deacon, 2019).

Glucose-dependent insulinotropic protein 1 (GIP1) and glucagon-like protein 1 (GLP-1) are small proteins with incretin function, facilitating glucose dependent release of insulin from the pancreatic β-cells (Baggio & Drucker, 2007). Beyond insulin release, both incretins have shared and distinct functions on several organs such as the GI-tract, the pancreas, brain, heart, bones and also adipose tissue (Seino et al., 2010).

Upon carbohydrate containing meals, GIP-1 and GLP-1 are secreted from the K cells of the upper small intestine and L cells of the lower intestine and colon, respectively (Baggio &

Drucker, 2007; Seino et al., 2010). Circulating GIP-1 and GLP-1 reach the pancreas and bind to their respective receptors GIPR and GLP-1R, on β-cells activating adenylate cyclase which leads to enhanced intracellular cyclic AMP (cAMP) (Baggio & Drucker, 2007; Seino et al., 2010). Elevated cAMP activates protein kinase A (PKA) and exchange protein activated by cAMP2 (EPAC2). Activation of PKA regulates Ca^2-dependent mitochondrial membrane depolarization and EPAC2 facilitates the fusion of insulin-containing granules with the cell membrane and corresponding release of insulin (Seino et al., 2010).
The incretin function of GLP-1 and GIP-1 is, among others, regulated by DPP4, which rapidly cleaves off dipeptides on the amino terminus and inactivates them. Indeed, 85-90% of secreted functional GIP-1 and GLP-1 are cleaved by the ubiquitously expressed DPP4 before entering circulation (Seino et al., 2010). Additionally to the mentioned indirect effects of DPP4 on incretin regulation, it was also found to directly reduce insulin sensitivity in HepG2 and primary mouse hepatocytes (Baumeier et al., 2017b). Correspondingly, DPP4 secretion from adipocytes correlates with the metabolic syndrome (Lamers et al., 2011). Besides regulating insulin sensitivity, DPP4 can induce T-cell activation and proliferation by binding adenosine deaminase or caeveolin-1, among others (Klemann et al., 2016). Soluble DPP4 was shown to induce inflammation and stress signaling in smooth muscle cells by phosphorylation of NFkB-pathway members and enhanced the secretion of interleukins (IL) (Wronkowitz et al., 2014). Accordingly, inhibition of DPP4 activity reduced inflammation by suppressing the secretion of IL-1β, IL-6 and IL-8 as well as NFkB- and TNFα-pathway (Wang et al., 2021; Wicinski et al., 2020; Wronkowitz et al., 2014).

Due to its various functions and complex entanglements in metabolism and immune regulation, DPP4 is suggested a moonlighting protein, with context-dependent functions (Barchetta et al., 2022). A brief overview on some of the associations of DPP4 is given in Figure 4. Epigenetic regulation probably plays a role in the modulation of DPP4 expression (Baumeier et al., 2016; Saussenthaler et al., 2019). In obese patients, DPP4 expression was increased upon hepatic steatosis, while DPP4 DNA methylation was decreased (Hyun & Jung, 2020). In line with these findings, glucose-induced DPP4 expression was promoted by de-methylation events in mice (Baumeier et al., 2016).

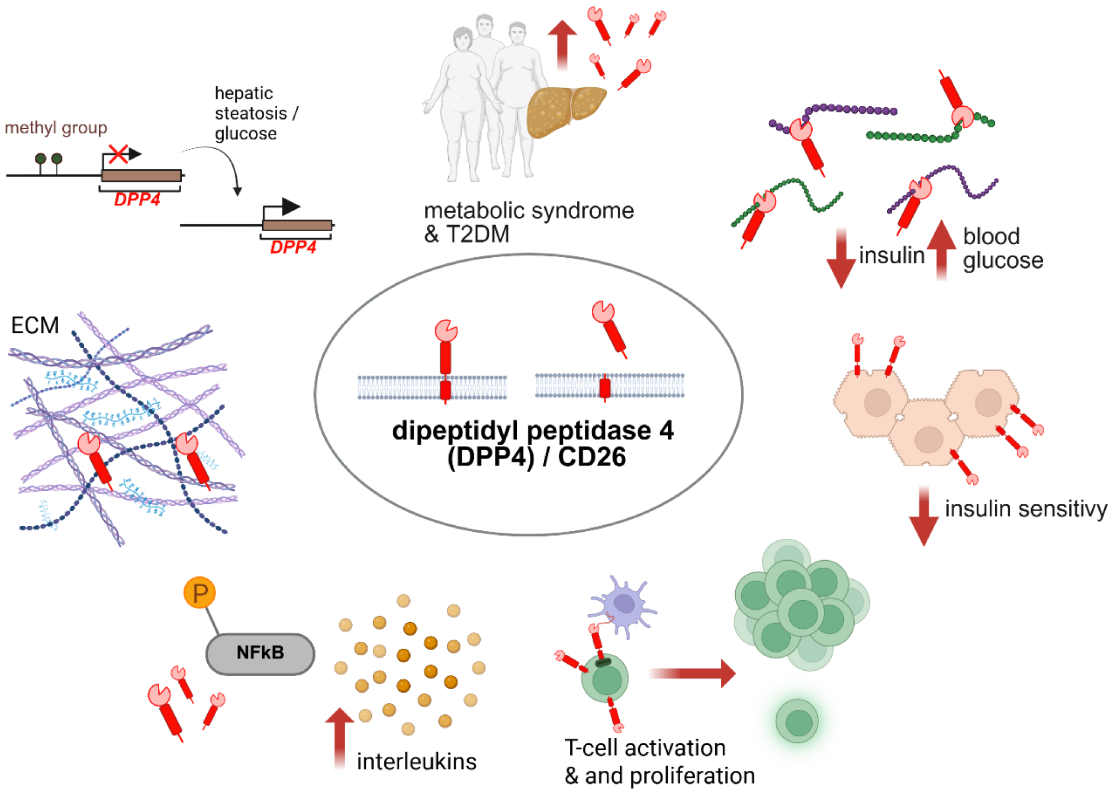

Figure 4 Associations of DPP4/CD26.[4]

Hepatic steatosis and glucose can induce demethylation of the DPP4 promoter and enhance DPP4 expression. In NAFLD, metabolic syndrome and T2DM patients elevated DPP4 concentrations were found in blood plasma which links DPP4 to obesity (Barchetta et al., 2021; Lamers et al., 2011). A prominent function of DPP4 is the degradation of incretins such as GLP-1 and GIP-1 and thereby indirectly regulating postprandial insulin release and glycemia (Ahrén et al., 2007). DPP4 was found to impair insulin sensitivity in primary hepatocytes and HepG2 cells (Baumeier et al., 2017b). DPP4 promotes T-cell activity and proliferation (Klemann et al., 2016) and was found to modulate NFkB, resulting in enhanced interleukin secretion (Wronkowitz et al., 2014). Furthermore, DPP4 cleaves extracellular matrix (ECM) proteins, potentially linking it to fibrosis (Deacon, 2019).

Considering the aforementioned relations of DPP4, it not surprising that DPP4 activity is enhanced in plasma of NAFLD patients (Baumeier et al., 2017b; Dawood et al., 2018; Niu et al., 2019). Indeed, DPP4 is associated with NAFLD/NASH severity independently of obesity or other metabolic diseases and was proposed a new potential target in NAFLD pathogenesis (Barchetta et al., 2021; Dawood et al., 2018). Recent findings indicate a mediating role between

[4] Created in BioRender. (2025) https:// BioRender.com/5ipfz3y

metabolism and inflammation (Gorrell et al., 2001; Trzaskalski et al., 2020). Although a potential role of DPP4 for MAFLD modulation is suggested, its ubiquitous expression poses difficulties to decipher the concrete source and mechanism. Considering that DPP4 regulates hepatic insulin sensitivity, further studies are required, employing relevant, human based hepatocyte models to decipher hepatic DPP4 mechanisms in the context of MAFLD.

1.4.5. Vildagliptin

Vildagliptin belongs to the drug class of gliptins, potent DPP4 inhibitors, preventing the degradation of GIP-1 and GLP-1, hence prolonging the incretin answer which results in improved blood glucose clearance (Ahrén et al., 2004; Baggio & Drucker, 2007; Deacon, 2019). Additionally, vildagliptin significantly reduced the mean fasting liver triglycerides and plasma glucose in a time-dependent manner, without changing the body mass index (BMI) and peripheral insulin sensitivity (Macauley et al., 2015). Another study found indeed reduction of the body weight and BMI together with improvements of the general lipid profile, aminotransferase levels and fatty liver grading (Hussain et al., 2016).
Genetic ablation of DPP4 also improved insulin sensitivity and liver functions in rats (Mitani et al., 2002). Vildagliptin seems to further inhibit inflammatory signaling by interfering with the TNF4α, NFkB and the TGFβ pathway and to promote insulin sensitivity in several species (Hendawy et al., 2022; Khalil et al., 2020; Wicinski et al., 2020). The findings indicate a role of DPP4 activity beyond glycemic control *in vivo* and *in vitro*, however further studies are needed to dissect the exact mechanism of vildagliptin in the context of MAFLD. Since fatty acid dysregulation, insulin resistance and progression to inflammation are hallmarks of MAFLD progression, vildagliptin might be an interesting therapeutic candidate. Nevertheless, to date investigations on the direct effect of vildagliptin on steatotic human hepatocytes are lacking.

1.5. Drug development for fatty liver disease

Considering the multifactorial and multisystemic character of MAFLD, there is an urgent need for therapeutic measurements. Indeed, liver fibrosis is a determinant for liver-related mortality (Ekstedt et al., 2015). Currently, lifestyle interventions, physical activity and dietary adaptations are measurements, proven to reverse all features of MASH (Friedman et al., 2018; Lara-Romero & Romero-Gómez, 2024). However, the strong associations with diseases such as obesity, T2DM, metabolic syndrome, and correlated hormonal dysregulation frequently

interfere with the outcome of these measures, underlining the need for additional pharmacotherapy (Lara-Romero & Romero-Gómez, 2024; Tincopa et al., 2024).

1.5.1. Challenges of drug development

Although there are various potential candidates for the treatment of fatty liver disease, to date only resmetirom, an agonist of thyroid hormone receptor β (THRβ), has been conditionally approved for the treatment of non-cirrhotic NASH by the food and drug administration (FDA) (Harrison et al., 2024). Several aspects challenge the development of efficient MAFLD therapeutics:

The aim of pharmacotherapy is to confer significant and defined clinical benefits for the patients (Anania et al., 2021). For chronic liver diseases, an endpoint for full approval of a therapeutic would be a significant reduction of cirrhosis and its complications (Anania et al., 2021). However, the typically gradual and slow progression of MAFLD and the low incidence of these outcomes challenges the fulfilment of the recommended endpoints. Therefore, surrogate endpoints are defined, which should be met in the course of a 12-18 months clinical trial. Nevertheless, for histological improvements and fibrosis resolution, this period might also be too short and two years might need to be considered to meet such endpoints for accelerated conditional approval (Anania et al., 2021; U.S. Food and Drug Administration, 2018). This would be in line with the European guidelines for interim studies (Loomba et al., 2022). However, to date, there are no non-invasive biomarkers which reliably and consistently work as surrogate efficacy endpoints for accelerated approval (Anania et al., 2021). The gold standard for surrogate efficacy endpoints is histologic improvement validated in liver biopsies. Potential misclassification due to differences in the sample quality, however, can influence the interpretation by pathologists and implies the need for at least two independent analyses (Anania et al., 2021; Davison et al., 2020). The recruitment of study participants can pose additional challenges as the prospect of undergoing liver biopsy might be deterrent and many screened patients fail to show definitive features qualifying them for enrolment (Ampuero & Romero-Gomez, 2020). Furthermore, placebo effects have been observed, possibly caused by lifestyle interventions upon study enrolment (Ampuero & Romero-Gomez, 2020; Anania et al., 2021).

Despite the mentioned challenges for MAFLD drug development, accelerated conditional approval was conferred for resmetirom by the FDA, and is currently under revision at the European medicines agency (EMA) (European Medicines Agency (EMA), 2024; Harrison et

al., 2024). The agonistic mode of action of resmetirom on the liver-selective nuclear THRβ increases the gene expression of carnitine palmitoyltransferase 1 (*CPTA1*), resulting in increased fatty acid β-oxidation. The use of resmetirom together with dietary and lifestyle interventions resulted in NASH resolution and fibrosis improvement, which defined the surrogate endpoints (Harrison et al., 2024). Furthermore, the treatment significantly lowered low-density lipoprotein cholesterol (LDL-C) levels. The approval of resmetirom is an important step in the development of therapeutics for MAFLD (Xue & Wei, 2024). Nevertheless, long-term effects, treatment response in multimorbid patients and drug-drug interactions remain to be detected in the post-market phase to gain definitive approval (Anania et al., 2021; Xue & Wei, 2024).

In 2024, various therapeutic agents or compounds were under clinical investigation for their potential to modulate different stages of the disease progression. The approaches target a variety of components of metabolic, inflammatory, or fibrotic pathways in the liver (Tincopa et al., 2024). Metabolic targets are typically involved in the regulation of insulin sensitivity and fatty acid metabolism within the liver but also on the gut-liver-axis (Ciardullo et al., 2024). Anti-inflammatories target immune cell trafficking to prevent infiltration and antifibrotics interfere with collagen deposition of stellate cells (Tincopa et al., 2024). Although numerous agents are tested in pre-clinical and phase-1 and -2 clinical trials, only few of them progress to phase-3. At the moment, regulators of fatty acid metabolism (PPAR agonists) and the incretin pathway (GLP-1-agonists) are promising phase-3 candidates (Tincopa et al., 2024). As described, there are several aspects challenging the outcome of a clinical trial. One of the underlying reasons for the limited translatability of pre-clinical studies might also arise from limited *in vitro* liver disease models, not capable to sufficiently recapitulate the physiological state.

1.6. Modeling MAFLD with iPSC-derived steatotic HLCs

Numerous healthy, patient-derived or genetically edited iPSC-based models have been developed for NAFLD or MAFLD modeling (Graffmann et al., 2021; Gurevich et al., 2020; Jozefczuk et al., 2012; Park et al., 2023; Park et al., 2021; Reinhardt et al., 2013; Varghese et al., 2022). To induce the phenotype of NAFLD or MAFLD in iPSC-derived HLCs, different agents are being used. A common method is the combination of the most abundant fatty acids (FAs) in the human body, the saturated palmitic acid (PA) and the unsaturated oleic acid (OA) in a ratio of 1:2 (Hodson et al., 2008; Ramos et al., 2022). In addition, also combinations with linoleic acid, and other inducers such as lactate, pyruvate or glucose are applied (Collin de

l'Hortet et al., 2019; Gurevich et al., 2020; Sinton et al., 2021). HLCs store FAs as triglycerides within 24 h of exposure, however, the response seems to depend on the inducing agent. PA is suggested to be more damaging for hepatocytes and induces a progressive MAFLD phenotype in shorter time, while OA is more steatogenic and less apoptotic (Ricchi et al., 2009). Besides distinct agents used to induce the phenotype, the time of induction also varies between one and several days. Confirmation of MAFLD is typically performed by detection of the incorporated triglycerides within the hepatocytes and lipid metabolism associated gene and protein expression like perilipin-2 (PLIN2) (Scorletti et al., 2024; Wruck et al., 2015). Moreover, research groups have shown elevated gene expression of inflammation or fibrosis associated genes (*TGFB*, alpha-actin-2 (*ACTA)*, *TNFA*) (Ramos et al., 2022).

Currently, there is no standardized method to verify the phenotype, which is also due to the distinct treatment agents and times. Distinct phenotypes are observed depending on the time of fatty acid exposure. After 24-48 h of exposure, expression of genes involved in lipid metabolism might be upregulated. However, upon several days of exposure, the fatty acid metabolism might be overloaded, and expression of respective genes may be downregulated. Furthermore, the genetic background influences the metabolic response, resulting in heterogeneity when focusing on specific pathways (Graffmann et al., 2021; Wruck et al., 2015). On the other hand, the heterogeneity of models probably best reflects the MAFLD/NAFLD patient stratification observed in the clinical setting (Gatzios et al., 2022). The individual background, the origin of the cells and distinct inducers allow tailoring models to the specific requirements, by including the population diversity, dietary habits, previous disorders and gut dysbiosis among others (Gatzios et al., 2022). The use of distinct time points and inducers, allows to investigate different stages of the disease. Beyond that, biomarkers, which have been validated in different settings, may be more valuable compared to those developed during only one standardized treatment.

The plethora of treatments provides distinct perspectives on the pathomechanisms of the disease. Global approaches such as omics analyses allow the comparison of metabolic responses with other *in vitro* models as well as with clinical data (Ramos et al., 2022). Conclusively, iPSC-derived hepatocyte-like cells offer a great potential to develop disease models for MAFLD. Simple and time- and cost-efficient models, representing later stages of steatosis, will help to understand the hepatocyte-specific contribution to MAFLD.

2. Aims and objectives

Considering the globally alarming numbers of liver diseases, there is an urgent need for relevant hepatocyte models to unravel pathomechanisms and develop therapeutics. Liver models relying on primary cells, animals or immortalized cell lines are limited due to their availability or insufficient recapitulation of the human physiology, representing a bottleneck for the translation of basic discoveries. The iPSC-technology offers great potential for liver models, due to the patient-derived genetic background and indefinite proliferation. The genetic background is important for the study of both monogenic, inherited diseases such as AATD as well as multifactorial diseases such as MAFLD.

The overall aim of this study was to establish and employ a relevant hepatic steatosis model and use patient-derived iPSCs as platforms for future liver disease studies. Both approaches aimed to strengthen the understanding of underlying pathomechanisms of liver diseases.

To address the overarching aim, the first objective (i) was the generation of AATD patient-derived iPSCs from adult and pediatric individuals with a severe liver phenotype, carrying the Pi*ZZ genotype. Comprehensively characterized iPSCs carrying a respective genotype, will provide a platform for future analyses of potential factors modulating the onset of AATD.

A well-known challenge in the field of liver modeling is the limited maturation of iPSC-derived differentiated HLCs. Although protocols have been developed to overcome this, these are typically complicated, time- and cost-intensive. Thus, the second objective (ii) was to optimize an established HLC-differentiation protocol to significantly enhance HLC functionality and hepatic gene and protein expression in a time- and cost-efficient manner. The third objective (iii) was to study the hepatocyte-specific contribution of MAFLD, by inducing hepatic steatosis and recapitulating the complicated expressional changes, representing clinical features of MAFLD. Furthermore, the fourth objective (iv) was to analyze pathomechanisms of hepatic steatosis and test a potential drug to unravel molecular mechanisms of the disease. Conclusively, this thesis aimed to provide and apply state-of-the-art iPSC technology in the field of hepatocyte differentiation and enhance the understanding of hepatic steatosis pathomechanisms in the context of MAFLD.

3. Structure of this thesis

In this thesis, four publications are presented, addressing the application of iPSC-technology for the study of AATD and MAFLD:

- **Christiane Loerch**, Rabea Hokamp, Wasco Wruck, David Katzer, Alexander Weigert, Alexander Machui, Nina Graffmann, Rainer Ganschow, James Adjaye '**Generation of an induced pluripotent stem cell line HHUUKDi013-A (ISRM-AATD-iPSC-3) from a pediatric patient of Alpha-I Antitrypsin Deficiency (AATD)**' Under revision at *Stem Cell Research*, 87: 103762.

- Audrey Ncube, Lisa Bewersdorf, Lucas-Sebastian Spitzhorn, **Christiane Loerch**, Martina Bohndorf, Nina Graffmann, Lea May, Samira Amzou, Malin Fromme, Wasco Wruck, Pavel Strnad, James Adjaye. 2023. '**Generation of two Alpha-I antitrypsin deficiency patient-derived induced pluripotent stem cell lines ISRM-AATD-iPSC-1 (HHUUKDi011-A) and ISRM-AATD-iPSC-2 (HHUUKDi012-A)**', *Stem Cell Research*, 71: 103171.

- **Christiane Loerch**, Leon-Phillip Szepanowski, Julian Reiss, James Adjaye, Nina Graffmann. 2024. '**Forskolin induces FXR expression and enhances maturation of iPSC-derived hepatocyte-like cells**', *Frontiers in Cell and Developmental Biology*, 12.

- **Christiane Loerch**, Wasco Wruck, Reiss Julian, James Adjaye, Nina Graffmann. 2024. '**Inhibiting DPP4 activity protects hiPSC-derived steatotic HLCs by supporting fatty acid and purine metabolism and dampening inflammation**'. Under revision at *Disease Modeling and Mechanisms*.

The introduction gave an overview on stem cells, current applications of the iPSC-technology, liver development and HLC-differentiation. Furthermore, MAFLD was highlighted as well as current limitations considering drug development and liver disease modeling. In the following results section, a deeper understanding is presented by original research articles focusing on the establishment of patient-derived iPS cell lines and the optimization of the differentiation from iPSCs towards HLCs. Finally, a model of hepatic steatosis was established and employed to analyze potential hepatic pathomechanisms modulating the disease progression in the context of MAFLD. In the discussion, the different parts are comprehensively discussed, integrating

the generated findings with current literature. The conclusion focusses on the overall insights, with regards to the aims and objectives of this thesis.

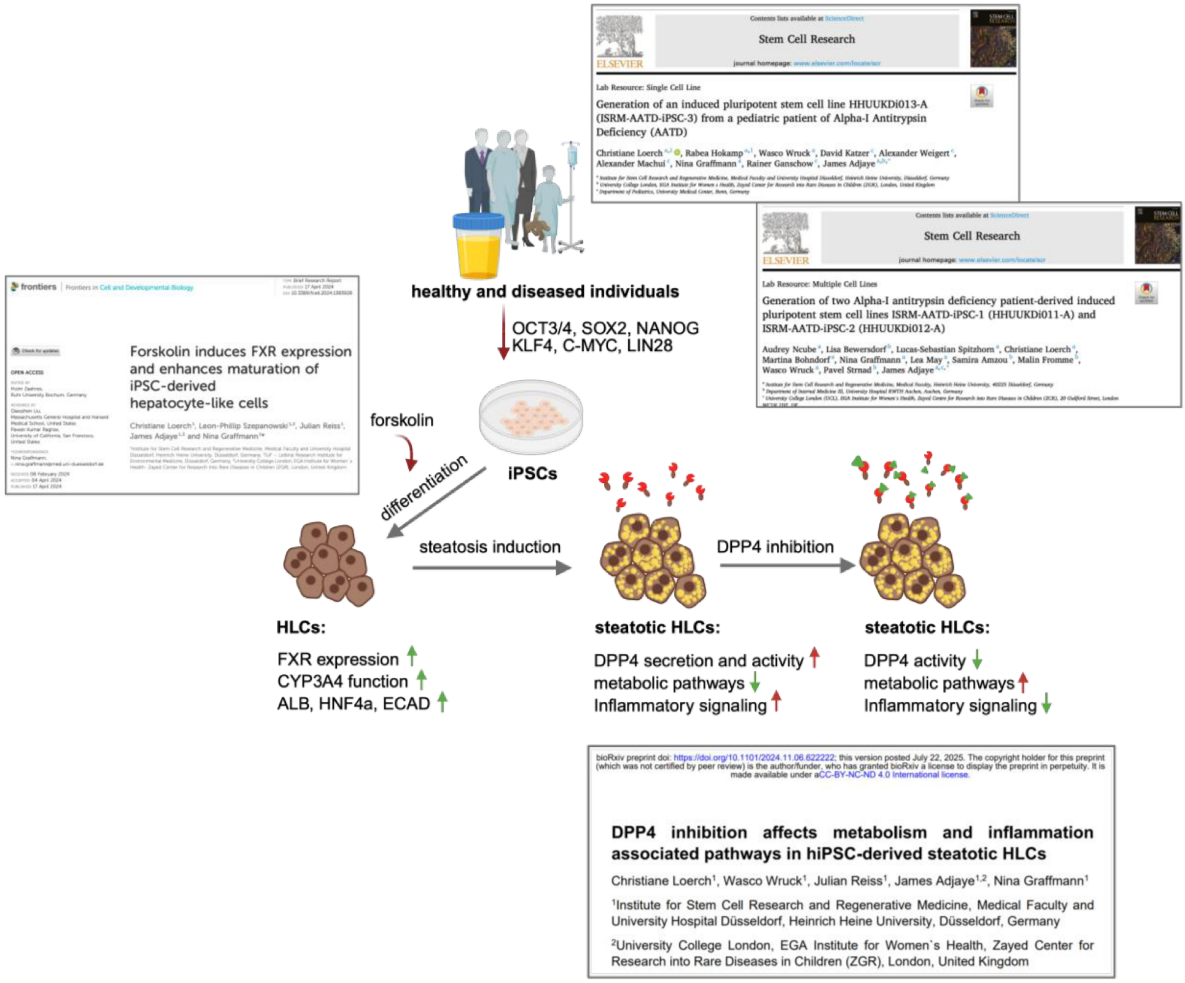

Figure 5: Synopsis of the presented publications and key findings.[5]

Urine was collected from adult and pediatric alpha$_1$-antitrypsin (AATD) patients and isolated somatic cells were reprogrammed to iPSCs, providing prospective platforms for the study of AATD. iPSC differentiation to hepatocyte-like cells (HLCs) was re-evaluated and optimized. Forskolin was found to enhance HLC maturation by induction of farnesoid-X-receptor (FXR) gene and protein expression. HLC gene and protein expression, as well as cytochrome P450 3A4 (CYP3A4) functionality (inducibility and activity) was enhanced. In order to analyze the hepatocyte-specific contribution to fatty liver disease, fat accumulation (steatosis) was induced in HLCs derived from four individuals. Global transcriptomic analyses revealed alterations in metabolic pathways as well as elevated inflammatory signaling.

[5] Created in BioRender. (2025) https://BioRender.com/7eyer6x

Dipeptidyl peptidase 4 (DPP4) secretion and activity was enhanced upon steatosis induction. Inhibition of DPP4 activity induced modulation of metabolism- and inflammatory-associated pathways.

4. Scientific publications

4.1. Generation of an induced pluripotent stem cell line HHUUKDi013-A (ISRM-AATD-iPSC-3) from a pediatric patient of Alpha-I Antitrypsin Deficiency (AATD)

Christiane Loerch, Rabea Hokamp, Wasco Wruck, David Katzer, Alexander Weigert, Alexander Machui, Nina Graffmann, Rainer Ganschow, James Adjaye

Stem Cell Research, Volume 87, Article number 103762

Abstract:

Renal progenitor cells were isolated from urine from a male, pediatric AATD-patient, harboring the homologous Pi*ZZ genotype. SIX2-positive urine derived renal progenitor cells (UdRPCs) were reprogrammed to iPSCs by integration-free nucleofection of episomal-based plasmids expressing OCT4, KLF4, C-MYC, SOX2, NANOG and LIN28. ISRM-AATD-iPSC-3 show pluripotent gene and protein expression, are capable of forming embryoid bodies and carry the parental Pi*ZZ genotype. Global transcriptome analyses revealed a correlation co-efficient of 0.9091 between the human embryonic stem cell line H9 and ISRM-AATD-iPSC-3.

Author contributions (50-60%) of C.L. included:

- Acquisition of the samples together with N.G. and A.M.
- Cultivation of isolated cells before reprogramming together with N.G.
- Training of R.H. in the methodology
- Conceptualization of experiments together with N.G. and J.A.
- Analysis of data together with R.H. and N.G
- Curation of the data
- Writing the original draft
- Reviewing and editing the manuscript together with N.G., J.A. and D.K.

Status: Published online in June 2025 as open access article under the CC BY license. **DOI:** 10.1016/j.scr.2025.103762

Parts of the published and herein discussed data are part of the Master Thesis of Rabea Hokamp.

Stem Cell Research 87 (2025) 103762

Contents lists available at ScienceDirect

Stem Cell Research

journal homepage: www.elsevier.com/locate/scr

Lab Resource: Single Cell Line

Generation of an induced pluripotent stem cell line HHUUKDi013-A (ISRM-AATD-iPSC-3) from a pediatric patient of Alpha-I Antitrypsin Deficiency (AATD)

Christiane Loerch [a,1], Rabea Hokamp [a,1], Wasco Wruck [a], David Katzer [c], Alexander Weigert [c], Alexander Machui [c], Nina Graffmann [a], Rainer Ganschow [c], James Adjaye [a,b,*]

[a] Institute for Stem Cell Research and Regenerative Medicine, Medical Faculty and University Hospital Düsseldorf, Heinrich Heine University, Düsseldorf, Germany
[b] University College London, EGA Institute for Women s Health, Zayed Center for Research into Rare Diseases in Children (ZGR), London, United Kingdom
[c] Department of Pediatrics, University Medical Center, Bonn, Germany

A B S T R A C T

Renal progenitor cells were isolated from urine from a male, pediatric AATD-patient, harboring the homologous Pi*ZZ genotype. SIX2-positive urine derived renal progenitor cells (UdRPCs) were reprogrammed to iPSCs by integration-free nucleofection of episomal-based plasmids expressing *OCT4, KLF4*, *c-MYC*, *SOX2*, *NANOG* and *LIN28*. ISRM-AATD-iPSC-3 show pluripotent gene and protein expression, are capable of forming embryoid bodies and carry the parental Pi*ZZ genotype. Global transcriptome analyses revealed a correlation coefficient 0.9091 between the human embryonic stem cell line H9 and ISRM-AATD-iPSC-3.

Resource Table:

Unique stem cell lines identifier	HHUUKDi013-A
Alternative name(s) of stem cell lines	ISRM-AATD-iPSC-3
Institution	Institute for Stem Cell Research and Regenerative Medicine, Medical Faculty, Heinrich-Heine University Düsseldorf
Contact information of distributor	Prof. Dr. James Adjaye James.adjaye@med.uni-duesseldorf.de
Type of cell lines	iPSCs
Origin	Human
Additional origin info required	Age: 11 years Sex: Male Ethnicity: Unknown
Cell Source	Urine derived renal progenitor cells (UdRPCs)
Clonality	Clonal
Method of reprogramming	Episomal expression of *OCT4*, *c-MYC*, *KLF4*, *SOX2*, *NANOG*, *LIN28*
Genetic Modification	Yes
Type of Genetic Modification	Hereditary
Evidence of the reprogramming transgene loss	PCR
Cell culture system	N/A

(*continued on next column*)

(*continued*)

Unique stem cell lines identifier	HHUUKDi013-A
Associated disease	Alpha-1 Antitrypsin deficiency
Gene/locus	*SERPINA*1rs28929474
Date archived/stock date	06.06.2024
Cell line repository/bank	https://hpscreg.eu/cell-line/HHUUKDi013-A
Ethical approval	Ethical committee of the medical faculty of Heinrich Heine University Düsseldorf, Germany Approval number: 2021-1627_1

1. Resource Utility

Alpha-1 Antitrypsin Deficiency (AATD) is caused by a mutation in the *SERPINA*1rs28929474 locus resulting in misfolded AAT-polymers. AATD liver disease mainly manifests biphasic during early childhood or later adulthood, however the underlying mechanisms remain unclear. Therefore, AATD-iPSCs from pediatric patients may serve as a tool for studying the etiology at the molecular and cellular levels. A summary of the characterization can be found in Table 1.

* Corresponding author.
E-mail address: James.adjaye@med.uni-duesseldorf.de (J. Adjaye).
[1] These authors contributed equally.

https://doi.org/10.1016/j.scr.2025.103762
Received 27 May 2025; Received in revised form 26 June 2025; Accepted 27 June 2025
Available online 28 June 2025

2. Resource details

Alpha-1 Antitrypsin Deficiency (AATD) is a hereditary disease caused by a missense mutation of G > A in the *SERPINA*1rs28929474 locus resulting in Glu342Lys switch (called PI*Z genotype) and misfolding of the AAT protein, causing retention in the hepatocytes (Greene et al., 2016). The disease manifests typically by pulmonary symptoms in adults and or liver cirrhosis in pediatric (<4 years) or adult (>50 years) patients (Strnad et al., 2020; Katzer et al., 2021). Inclusions of AAT-polymers within the hepatocytes are the histological hallmark of the Pi*ZZ liver phenotype, and can lead to chronic inflammation and liver fibrosis (Strnad et al., 2013). Furthermore retention of AAT-polymers results in a reduction of serum AAT and decreased inhibitory effect on proteases, which can cause a pulmonary phenotype due to degradation of lung parenchyma (Strnad et al., 2020). Although there is a relatively high prevalence of AATD within Europe the undiagnosed proportion of patients remains high and further research is necessary to elucidate the underlying molecular mechanisms (Horváth et al., 2019). In addition to our previously published AATD-iPSCs from adults (Ncube et al., 2023), we have now generated an AATD-iPSC line from a pediatric patient (male, 11 years) with compensated liver cirrhosis, carrying the homozygous Pi*ZZ genotype. The cells were nucleofected and episomal-based reprogramming was induced by the ectopic expression of *OCT4*, *KLF4*, *SOX2*, *c-MYC*, *NANOG* and *LIN28* as described in our previous publication (Bohndorf et al., 2017). Reprogrammed cells showed the typical iPSC morphology with a high nucleus/cytoplasm ratio in comparison to the rice-grain shaped UdRPCs (Fig. 1A). Vector dilution of AATD-iPSC-3 (p12) was confirmed (Fig. 1B). Chromosomal analysis from 20 metaphase spreads revealed a normal karyotype (46, XY) (Fig. 1C). The expression of OCT4, SOX2, NANOG, SSEA4, TRA-60 and TRA1-81 was confirmed by immunocytochemistry (Fig. 1D). Reprogramming resulted in 96.8% OCT4+ and 95.9% SSEA4+ cells (p13) (Fig. 1E). Global transcriptome analysis revealed a correlation coefficient of 0.91 between the hESC line H9 and AATD-iPSC-3 (Fig. 1F). Sanger Sequencing confirmed the mis-sense mutation within the locus *SERPINA*1rs28929474 of G to A (Fig. 1G) Immunocytochemistry of spontaneous differentiation to the three germ layers by the embryoid body (EB) assay is shown in Fig. 1H. SRY-box transcription factor-17 (SOX17) and forkhead box A2 (FOXA2) were stained to identify endoderm, alpha smooth muscle actin (aSMA) and Brachyury for mesoderm. Paired box 6 (PAX6) and beta-3-tubulin (βIII-Tubulin) were stained to identify ectoderm (Fig. 1H). Table 2 displays the used reagents.

3. Materials and methods

3.1. Cell culture

SIX2-positive UdRPCs were isolated from urine samples and expanded as previously described (Bohndorf et al., 2017; Rahman et al., 2020). iPSCs were cultivated on Matrigel (Corning) coated wells, using StemMACs iPS Brew (Miltenyi). At 80–90% confluency, iPSCs were detached by incubation with PBS w/o Mg^{2+} and Ca^{2+} and colony-split in a ratio of 1:6.

3.2. Derivation of iPSCs

AATD-UdRPCs were nucleofected with 3 μg of the plasmids pEP4EO2SCK2MEN2L and pEP4EO2SET2K, respectively, as described in our previous publication (Bohndorf et al., 2017; Yu et al., 2011). To activate WNT-signalling 3 μM CHIR99021 was added. TGFβ-, MEK-, and Rock-signaling were inhibited with 0.5 μm A83-01, 0.5 μM PD0325901, 10 μM Y-27632, respectively. After clones attained typical pluripotency-associated morphology they were picked and further cultivated as iPSCs.

3.3. PCR

Vector dilution and endogenous *OCT4* expression was confirmed by PCR using the GoTaq DNA Polymerase kit (Promega). Genomic DNA was isolated from iPSCs using the Tissue DNA Purification Kit (EurX). Supernatants were collected from dense cultures to confirm the absence of mycoplasma contamination. To confirm genetic relationship of AATD-iPSC-3 to the parental AATD-UdRPCs, DNA fingerprinting analysis, short tandem repeats (STR) of 9 distinct loci were amplified by PCR and compared with the parental line.

3.4. Embryoid body (EB) formation

EB formation was performed by seeding single cell iPSCs into a 6 cm petri-dish, coated with anti-adherence-solution (Stem cell technologies) in StemMACS w 10 μM ROCK inhibitor for 24 h. Aggregates were cultivated shaking, in StemMACS w/o ROCK inhibitor for 6 days to form EBs. EBs were plated onto Matrigel coated plates, in DMEM containing 10% FBS, 1% Glutamax and 1% NEEA (all Gibco), for 4 days until immunocytochemistry.

Table 1
Characterization and validation.

Classification	Test	Result	Data
Morphology	Microphotography Bright field	Normal	Fig. 1 panel A
Phenotype	Immunocytochemistry	Expression of pluripotency associated markers: OCT4, SOX2, NANOG, SSEA-4 TRA-1–60, TRA-1–81,	Fig. 1 panel D
	Flow Cytometry	Assess of 96.8% OCT4 positive cells: Assess of 95.9% SSEA4 positive cells	Fig. 1 panel E
Genotype	Karyotype (G-banding) and resolution	46XY 200–400 Bd	Fig. 1 panel C, Supplementary figure 2
Identity	Microsatellite PCR (mPCR) OR STR analysis	STR analysis by PCR of 6 loci, matched.	Supplementary file 2
Mutation analysis	Sanger sequencing	missense mutation at SERPINA1rs28929474locus, of G to A	Fig. 1 panel G
	Southern Blot OR WGS	Not performed	N/A
Microbiology and virology	Mycoplasma	Mycoplasma testing by PCR: Negative	Supplementary Fig. 1
Differentiation potential	Embryoid body formation	Expression of germ layer specific proteins. Mesoderm: alpha smooth muscle actin (aSMA), Brachyury; Ectoderm: βIII-tubulin, Paired box 6 (PAX6) Endoderm: SRY-box transcription factor 17, Forkhead Box A2 (FOXA2)	Fig. 1 panel H
Donor screening	HIV 1 + 2 Hepatitis B, Hepatitis C	Not performed	N/A
Genotype additional info	Blood group genotyping	Not performed	N/A
	HLA tissue typing	Not performed	N/A

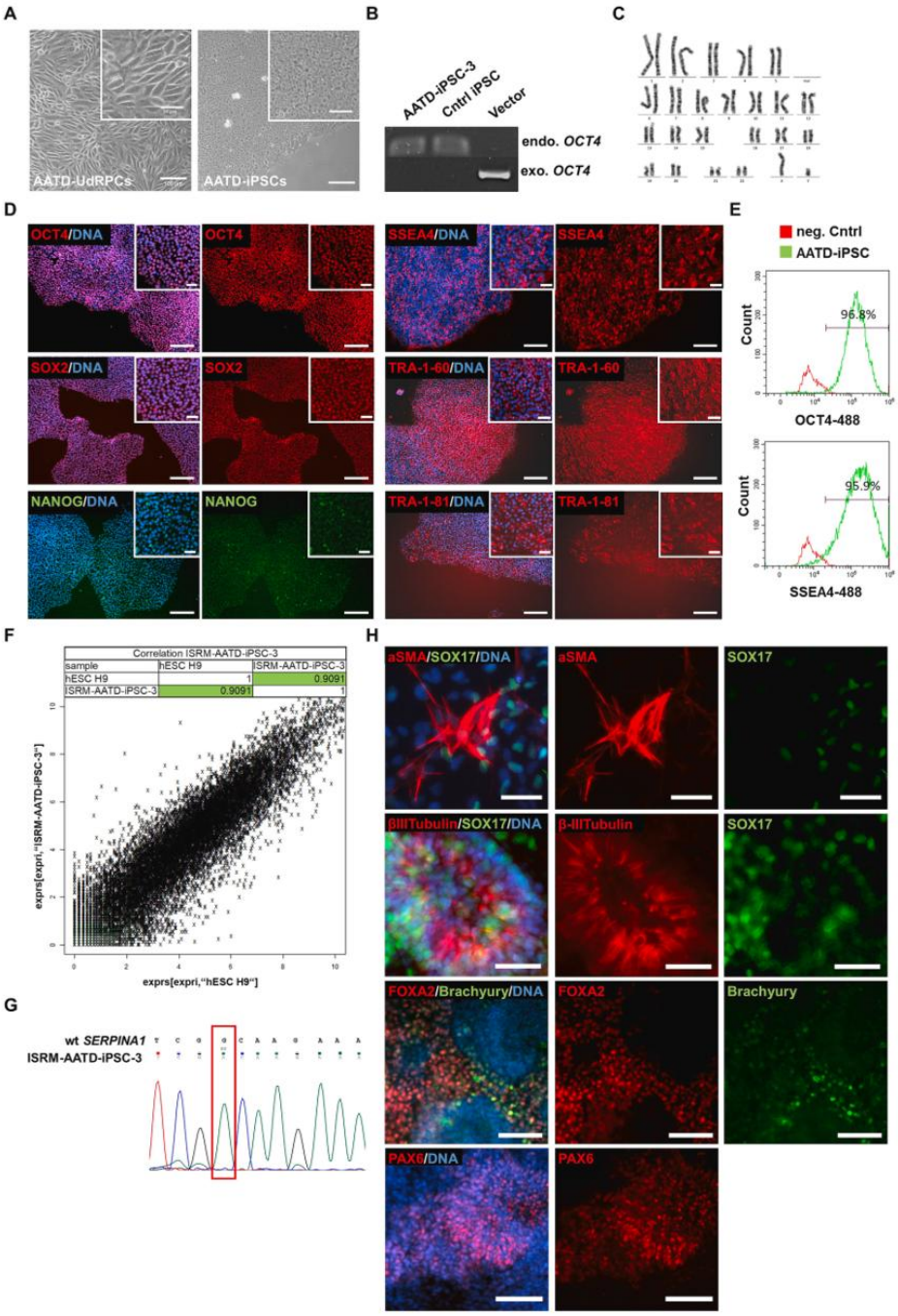

Fig. 1. Characterization of iPSC-line HHUUKDi013-A / ISRM-AATD-iPSC-3.

Table 2
Reagents details.

	Antibodies used for immunocytochemistry/flow-cytometry			
	Antibody	**Dilution**	**Company Cat #**	**RRID**
Flow Cytometry	Rabbit anti-OCT4	1:50	Cell Signaling Technologies #2840S	AB_2167691
Flow Cytometry	Mouse anti-SSEA4	1:50	Cell Signaling Technology	AB_1264259
Pluripotency Marker	Rabbit anti-OCT4	1:400	Cell Signaling Technologies #2840S	AB_2167691
Pluripotency Marker	Rabbit anti-SOX2	1:400	Cell Signaling Technologies #3579S	AB_2195767
Pluripotency Marker	Rabbit anti-NANOG	1:200	Cell Signaling Technologies #4903S	AB_10559205
Pluripotency Marker	Mouse anti-SSEA4	1:1000	Cell Signaling Technology	AB_1264259
Pluripotency Marker	Mouse anti-Tra-1-60	1:1000	Cell Signaling Technologies #4746S	AB_2119059
Pluripotency Marker	Mouse anti-Tra-1-81	1:1000	Cell Signaling Technologies #4745S	AB_2119060
Differentiation Marker	anti-aSMA	1:1000	Dako; # M0851	AB_2223500
Differentiation Marker	Mouse anti- SOX17	1:50	R and D Systems Cat# AF1924	AB_355060
Differentiation Marker	anti-BIII Tubulin	1:250	Cell Signaling Technologies #4466S	AB_1904176
Differentiation Marker	anti-PAX6	1:200	Synaptic Systems # 153 011	AB_887758
Secondary Antibody	anti-mouse- Alexa555	1:500	Thermo Fisher Scientific Cat# A10521	AB_2534030
Secondary Antibody	anti-rabbit- Alexa488	1:500	Thermo Fisher Scientific Cat# A27034	AB_2536097
Secondary Antibody	anti-rabbit- Alexa647	1:500	Thermo Fisher Scientific Cat# A-31573	AB_2536183
Nuclear Co– Staining	Hoechst33258	1:5000	Thermo Fisher Scientific Cat# H3569	AB_2651133
	Primers			
	Target	**Size of band**	**Forward/Reverse primer (5′-3′)**	
Endogenous OCT4	OCT4	113 bp	AGTTTGTGCCAGGGTTTTTG ACTTCACCTTCCCTCCAACC	
Episomal Plasmids (exo)	OCT4	657 bp	AGTGAGAGGCAACCTGGAGA AGGAACTGCTTCCTTCACGA	
Mycoplasma PCR	mycoplasma-specific 16S rRNA gene	265 – 278 bp	GGGAGCAAACAGGATTAGATACCCT TGCACCATCTGTCACTCTGTTAACCTC	
PiZ genotyping by Sanger Sequencing	SERPINA1	N/A	AGCGCTTCCTGGGAGGTGT	
STR-PCR	D16S539	N/A	GGGGGTCTAAGAGCTTGTAAAAAG GTTTGTGTGTGCATCTGTAAGCATGTATC	
	D13S317	N/A	ACAGAAGTCTGGGATGTGGAGGA GGCAGCCCAAAAAGACAGA	
	D7S820	N/A	ATGTTGGTCAGGCTGACTATG GATTCCACATTTATCCTCATTGAC	
	TH01	N/A	ATTCAAAGGGTATCTGGGCTCTGG GTGGGCTGAAAAGCTCCCGATTAT	
	vWA	N/A	CTAGTGGATGATAAGAATAATCAGTAT GTG GGACAGATGATAAATACATAGGATGGATGG	
	Amel	N/A	ACCTCATCCTGGGCACCCTGGTT AGGCTTGAGGCCAACCATCAG	
	CSF1PO	N/A	AACCTGAGTCTGCCAAGGACTAGC TTCCACACACCACTGGCCATCTTC	
	TPOX	N/A	ACTGGCACAGAACAGGCACTTAGG GGAGGAACTGGGAACCACACAGGTTA	
	D5S818	N/A	GGTGATTTTCCTCTTTGGTATCC AGCCACAGTTTACAACATTTGTATCT	

3.5. Immunofluorescence

Cells were fixed with 4% PFA for 10 min at RT, and permeabilized for 10 min with 0.5% Triton-x-100 (Sigma). For extracellular staining the permeabilization step was skipped. Cells were blocked for 1 h at RT with 3% BSA and incubated with respective primary antibodies overnight at 4 °C. Fluorophore-coupled antibodies against the host IgG were incubated for 1 h at RT in the dark and DNA was counterstained with 4 μM Hoechst33342. Fluorescence microscopy was performed using the LSM700 (Zeiss) microscope and ZEN2012 (blue edition) software, version 6.1.7601.

3.6. Flow cytometry

Cells were detached to single cells, centrifuged and fixed in 4% PFA for 10 min at RT. After 3x wash with PBS-/-, cells were permeabilized for 10 min with 0.5 % Triton-x-100. For extracellular staining this step was skipped. Cells were blocked in 0.5% BSA and 2 mM EDTA for 1 h at RT and primary antibodies were incubated overnight, at 4 °C. Fluorophore-coupled antibodies against the host IgG were incubated for 1 h at RT in the dark. Cells were washed and resuspended in blocking buffer. Fluorescence was measured using the CytoFLEX S Flow Cytometer (Beckman Coulter) and analyzed with the CytExpert software version 2.6.0.105 (Beckman Coulter).

3.7. Karyotype analysis

Karyotype analysis was performed and evaluated at the Institute of Human Genetics and Anthropology, Heinrich-Heine-University, Düsseldorf.

3.8. Sanger sequencing and global transcriptome analysis

Sanger sequencing and 3'RNA-Seq were performed at the core facility BMFZ-GTL of Heinrich-Heine-University Düsseldorf.

CRediT authorship contribution statement

Christiane Loerch: Writing – review & editing, Writing – original draft, Visualization, Methodology, Investigation, Formal analysis, Data curation, Conceptualization. **Rabea Hokamp:** Writing – review & editing, Visualization, Methodology, Investigation, Formal analysis, Data curation. **Wasco Wruck:** Writing – review & editing, Methodology, Investigation, Formal analysis, Data curation. **David Katzer:** Writing – review & editing, Writing – original draft, Resources, Project administration, Investigation. **Alexander Weigert:** Writing – review & editing,

Resources. **Alexander Machui:** Writing – review & editing, Resources, Methodology, Investigation. **Nina Graffmann:** Writing – review & editing, Writing – original draft, Supervision, Resources, Project administration, Methodology, Investigation, Funding acquisition, Data curation, Conceptualization. **Rainer Ganschow:** Writing – review & editing, Supervision, Resources, Project administration, Conceptualization. **James Adjaye:** Writing – review & editing, Writing – original draft, Supervision, Resources, Project administration, Methodology, Investigation, Funding acquisition, Conceptualization.

Declaration of competing interest

The authors declare the following financial interests/personal relationships which may be considered as potential competing interests: Christiane Loerch reports financial support was provided by Else Kroner-Fresenius Foundation. Nina Graffmann reports financial support was provided by Else Kroner-Fresenius Foundation. If there are other authors, they declare that they have no known competing financial interests or personal relationships that could have appeared to influence the work reported in this paper.

Acknowledgements

J.A. acknowledges support from the Medical faculty of Heinrich-Heine University Düsseldorf C.L. and N.G. are funded by the Else Kröner-Fresenius Stiftung – 2020_EKEA.64.

Appendix A. Supplementary data

Supplementary data to this article can be found online at https://doi.org/10.1016/j.scr.2025.103762.

Data availability

Data will be made available on request.

References

Greene, C.M., Marciniak, S.J., Teckman, J., Ferrarotti, I., Brantly, M.L., Lomas, D.A., Stoller, J.K., et al., 2016. α1-Antitrypsin deficiency. Nat. Rev. Dis. Primers 2, 16051.
Strnad, P., McElvaney, N.G., Lomas, D.A., 2020. Alpha(1)-Antitrypsin Deficiency. N. Engl. J. Med. 382, 1443–1455.
Katzer, D., Ganschow, R., Strnad, P., Hamesch, K., 2021. Pi*ZZ-related liver disease in children and adults—narrative review of the typical presentation and management of alpha-1 antitrypsin deficiency. Digestive Medicine Research.
Strnad, P., Nuraldeen, R., Guldiken, N., Hartmann, D., Mahajan, V., Denk, H., Haybaeck, J., 2013. Broad spectrum of hepatocyte inclusions in humans, animals, and experimental models. Compr. Physiol. 3, 1393–1436.
Horváth, I., Canotilho, M., Chlumský, J., Chorostowska-Wynimko, J., Corda, L., Derom, E., Ficker, J.H., et al., 2019. Diagnosis and management of α(1)-antitrypsin deficiency in Europe: an expert survey. ERJ Open Res 5.
Ncube, A., Bewersdorf, L., Spitzhorn, L.S., Loerch, C., Bohndorf, M., Graffmann, N., May, L., et al., 2023. Generation of two Alpha-I antitrypsin deficiency patient-derived induced pluripotent stem cell lines ISRM-AATD-iPSC-1 (HHUUKDi011-a) and ISRM-AATD-iPSC-2 (HHUUKDi012-a). Stem Cell Res. 71, 103171.
Bohndorf, M., Ncube, A., Spitzhorn, L.S., Enczmann, J., Wruck, W., Adjaye, J., 2017. Derivation and characterization of integration-free iPSC line ISRM-UM51 derived from SIX2-positive renal cells isolated from urine of an african male expressing the CYP2D6 *4/*17 variant which confers intermediate drug metabolizing activity. Stem Cell Res. 25, 18–21.
Rahman, M.S., Wruck, W., Spitzhorn, L.S., Nguyen, L., Bohndorf, M., Martins, S., Asar, F., et al., 2020. The FGF, TGFβ and WNT axis Modulate Self-renewal of Human SIX2(+) Urine Derived Renal Progenitor Cells. Sci. Rep. 10, 739.
Yu, J., Chau, K.F., Vodyanik, M.A., Jiang, J., Jiang, Y., 2011. Efficient feeder-free episomal reprogramming with small molecules. PLoS One 6, e17557.

4.2. Generation of two Alpha-I antitrypsin deficiency patient-derived induced pluripotent stem cell lines ISRM-AATD-iPSC-1 (HHUUKDi011-A) and ISRM-AATD-iPSC-2 (HHUUKDi012-A)

Audrey Ncube, Lisa Bewersdorf, Lucas-Sebastian Spitzhorn, **Christiane Loerch**, Martina Bohndorf, Nina Graffmann, Lea May, Samira Amzou, Malin Fromme, Wasco Wruck, Pavel Strnad, James Adjaye

Stem Cell Research, Volume 71, Article number 103171

Abstract:

SIX2-positive urine derived renal progenitor cells were isolated from a male and female alpha1-antitrypsin deficiency (AATD) patients both harboring the homozygous PiZZ genotype. The cells were reprogrammed to generate two integration-free induced pluripotent stem cell (iPSC) lines by transfecting episomal-based plasmids expressing OCT4, SOX2, NANOG, c-MYC, KLF4 and LIN28. Pluripotency was confirmed by immunocytochemistry for associated markers and embryoid body-based differentiation into the three germ layers. The iPSC lines carried the parental PiZZ genotype. Comparative transcriptome analyses with human embryonic stem cell line H9 revealed a Pearson correlation of 0.945 for ISRM-AATD-iPSC-1 and 0.939 for ISRM-AATD-iPSC-2 respectively.

Author contributions (20%) of C.L. included:

- Curation and visualization of the data
- Writing the original draft together with A.N., N.G. and J.A.
- Reviewing and editing of the manuscript together with A.N., N.G. and J.A.

Status: Published online in July 2023 under open access article under the CC BY-NC-ND license. **DOI:** 10.1016/j.scr.2023.103171

Stem Cell Research 71 (2023) 103171

Contents lists available at ScienceDirect

Stem Cell Research

journal homepage: www.elsevier.com/locate/scr

Lab Resource: Multiple Cell Lines

Generation of two Alpha-I antitrypsin deficiency patient-derived induced pluripotent stem cell lines ISRM-AATD-iPSC-1 (HHUUKDi011-A) and ISRM-AATD-iPSC-2 (HHUUKDi012-A)

Audrey Ncube [a], Lisa Bewersdorf [b], Lucas-Sebastian Spitzhorn [a], Christiane Loerch [a], Martina Bohndorf [a], Nina Graffmann [a], Lea May [a], Samira Amzou [b], Malin Fromme [b], Wasco Wruck [a], Pavel Strnad [b], James Adjaye [a,c,*]

[a] Institute for Stem Cell Research and Regenerative Medicine, Medical Faculty, Heinrich Heine University, 40225 Düsseldorf, Germany
[b] Department of Internal Medicine III, University Hospital RWTH Aachen, Aachen, Germany
[c] University College London (UCL), EGA Institute for Women's Health, Zayed Centre for Research into Rare Diseases in Children (ZCR), 20 Guilford Street, London WC1N 1DZ, UK

A B S T R A C T

SIX2-positive urine derived renal progenitor cells were isolated from a male and female alpha1-antitrypsin deficiency (AATD) patients both harboring the homozygous PiZZ genotype. The cells were reprogrammed to generate two integration-free induced pluripotent stem cell (iPSC) lines by transfecting episomal-based plasmids expressing OCT4, SOX2, NANOG, c-MYC, KLF4 and LIN28. Pluripotency was confirmed by immunocytochemistry for associated markers and embryoid body-based differentiation into the three germ layers. The iPSC lines carried the parental PiZZ genotype. Comparative transcriptome analyses with human embryonic stem cell line H9 revealed a Pearson correlation of 0.945 for ISRM-AATD-iPSC-1 and 0.939 for ISRM-AATD-iPSC-2 respectively.

Resource Table:

Unique stem cell lines identifier	1. HHUUKDi011-A 2. HHUUKDi012-A
Alternative name(s) of stem cell lines	1. ISRM-AATD-iPSC-1, AATD-iPSC-1 2. ISRM-AATD-iPSC-2, AATD-iPSC-2
Institution	Institute for Stem Cell Research and Regenerative Medicine
Contact information of distributor	James Adjaye, James.Adjaye@med.uni-duesseldorf.de
Type of cell lines	iPSC
Origin	Human
Additional origin info required	Age: 1.: 57, 2.: 63; Sex: 1.: Male 2.: Female; Ethnicity if known: white
Cell source	Urine derived renal progenitor cells (UdRPCs)
Clonality	Clonal
Method of reprogramming	Episomal expression of OCT4, SOX2, NANOG, LIN28, c-MYC, KLF-4
Genetic modification	Yes
Type of genetic modification	Hereditary
Evidence of the reprogramming transgene loss	PCR
Cell culture system	N/A
Associated disease	Alpha-1 Antitrypsin deficiency
Gene/locus	SERPINA1rs28929474
Date archived/stock date	27.01.2022
Cell line repository/bank	1. https://hpscreg.eu/cell-line/HHUUKDi011-A 2. https://hpscreg.eu/cell-line/HHUUKDi012-A
Ethical approval	Ethical approval was provided by the ethical committee of the medical faculty at Heinrich-Heine university Düsseldorf, Approval number: 2021–1627

(continued on next column)

(continued)

1. Resource utility

Alpha1-antitrypsin (AAT) is a major protease inhibitor produced primarily in the liver and secreted into the bloodstream. AAT deficiency is caused by mutations in the SERPINA1 gene and the characteristic PiZ variant results in hepatic AAT accumulation. Therefore, these iPSC lines represent cellular tools for studying the pathomechanisms of AATD. Table 1 displays the results of the characterization and validation.

* Corresponding author.
E-mail address: james.adjaye@med.uni-duesseldorf.de (J. Adjaye).

https://doi.org/10.1016/j.scr.2023.103171
Received 28 April 2023; Received in revised form 17 July 2023; Accepted 21 July 2023
Available online 23 July 2023

Table 1
Characterization and validation.

Classification	Test	Result	Data
Morphology	Photography Bright field	Normal	Fig. 1 panel A
Phenotype	Immunocytochemistry	Expression of pluripotency associated markers: OCT4, SOX2, NANOG, TRA-1–60, TRA-1–81, SSEA-4	Fig. 1 panel C
	Flow Cytometry	1. Assess 91.41% OCT4 positive cells 2. Assess 79.85% OCT4 positive cells	Fig. 1 panel D
Genotype	Karyotype (G-banding) and resolution	1. ISRM-AATD-iPSC-1, 46XY 2. ISRM-AATD-iPSC-2, 46XX Resolution 450–500	Fig. 1 panel H, Supplementary Fig. 2
Identity	Microsatellite PCR (mPCR) OR	Not performed	N/A
	STR analysis	21 STR System	Supplementary file 2
Mutation analysis	RFLP	PiZZ genotype	Fig. 1 panel F
	Southern Blot OR WGS	Not performed	N/A
Microbiology and virology	Mycoplasma	Mycoplasma testing by RT-PCR Negative	Supplementary Fig. 1
Differentiation potential	Embryoid body formation	Expression of germ layer specific proteins: Mesoderm - smooth muscle actin (SMA), Ectoderm - βIII-tubulin Endoderm - SOX17.	Fig. 1 panel E
Donor screening	HIV 1 + 2 Hepatitis B, Hepatitis C	Not performed	N/A
Genotype additional info	Blood group genotyping	Not performed	N/A
	HLA tissue typing	Not performed	N/A

2. Resource details

Alpha1-antitrypsin deficiency (AATD) is an autosomal recessive disorder with a frequency of approximately 1:3000 in Caucasians (Strnad et al., 2020). The disorder is caused by a mutation in the *SERPINA1* gene and is an inherited metabolic disease of the liver. Individuals with this deficiency are predisposed to developing liver (due to gain of function proteotoxicity) and lung (loss of function phenotype) disease. Whereas the wild-type M−allele is the most common, the homozygous PiZ mutation known as the PiZZ genotype is rare, but the predominant cause of severe AATD conferring a strong risk for development of end-stage liver disease. (Segeritz et al., 2018; Tafaleng et al., 2015).

We generated two iPSC lines, one male (ISRM-AATD-iPSC-1) and one female (ISRM-AATD-iPSC-2), from AATD patients both carrying the homozygous PiZ mutation. Urine derived renal progenitor cells (UdRPCs) were first isolated from both patients and used to generate the described iPSC lines. The cells were reprogrammed by nucleofection of the episomal plasmids pEP4EO2SCK2MEN2L and pEP4EO2SET2K (7F1) expressing OCT4, SOX2, NANOG, LIN28, c-MYC and KLF-4, using the T-13PC3 (ATCC) program and epithelial cells nucleofection kit. The resulting iPSC lines have the typical iPSC morphology (Fig. 1A) and vector dilution was confirmed by the absence of exogenous (vector expressed) *OCT4* and the presence of endogenous *OCT4* (Fig. 1B). Pluripotency was confirmed by immunocytochemistry for the pluripotency-regulating transcription factors OCT4, NANOG, SOX2 and cell surface markers SSEA-4, TRA-1–60 and TRA-1–81 (Fig. 1C and not shown) and flow cytometry-based detection of OCT4 expression (Fig. 1D). Pluripotency was further demonstrated *in vitro* by embryoid body (EB)-based differentiation into cell types representative of the three germ layers - endoderm (SOX17), ectoderm (βIII-Tubulin) and mesoderm (SMA – smooth muscle actin) (Fig. 1E). The mutation was confirmed by a RFLP (Restriction Fragment Length Polymorphism) assay (Fig. 1F). Comparative transcriptome and cluster analysis with the human embryonic stem cell line H9 revealed a Pearson correlation of 0.945 for ISRM-AATD-iPSC-1 (p8) and 0.939 for ISRM-AATD-iPSC-2 (p5) respectively (Fig. 1G). Chromosomal content analysis counting 20 metaphase spreads revealed normal karyotypes for both lines: ISRM-AATD-iPSC-1 (p9) − 46, XY and ISRM-AATD-iPSC-2 (p7) − 46, XX (Fig. 1H & Supplementary Fig. 2). DNA fingerprinting confirmed the identity of ISRM-AATD-iPSC-1 (p8) and ISRM-AATD-iPSC-2 (p5) with the respective parental UdRPCs (Supplementary file 2). A PCR-based Mycoplasma contamination test was negative (Supplementary Fig. 1).

3. Materials and methods

3.1. Cell culture

UdRPCs were isolated from urine samples and expanded as previously described (Bohndorf et al., 2017; Rahman et al., 2020).

3.2. Derivation of iPSCs

SIX2-positive AATD-1 and AATD-2 UdRPCs were reprogrammed into iPSCs (Bohndorf et al., 2017; Yu et al., 2011) using the T-13PC3 (ATCC) program (Amaxa nucleofector II, Amaxa Inc.,) and epithelial cells nucleofection kit (LONZA): 3 μg pEP4EO2SCK2MEN2L and pEP4EO2-SET2K (7F1) were introduced and 0.5 μm A83-01, 0.5 μM PD0325901, 10 μM Y-27632, and 3 μM CHIR99021 were added to inhibit TGFß-, MEK-, and Rock-signaling and activate WNT-signaling pathway, respectively. Cells were cultured with mTeSR™1 medium on Matrigel® at 37 °C and 5% CO_2 with daily medium changes. Well-defined iPSC colonies were picked and detached using PBS without Mg^{2+} and Ca^{2+} and distributed at a 1:3 – 1:10 ratio into new Matrigel coated plates.

3.3. PCR

Vector dilution were confirmed by PCR using the GoTaq DNA Polymerase kit (Promega). Genomic DNA was extracted using the DNeasy Blood and Tissue kit (QIAGEN). Supernatants from dense cultures were collected and PCR run to confirm the absence of mycoplasma contamination.

3.4. DNA fingerprint analysis

STR analysis was performed and evaluated at the Institute of Forensic Medicine, University Hospital Düsseldorf.

3.5. Embryoid body (EB) formation

Sub-confluent iPSCs were scrapped off, transferred into a T25 flask and cultured for one week in high glucose DMEM, containing 1% NEAA to form EBs. Afterwards, EBs were settled for 3 – 4 days on a gelatin-coated 12-well plate.

3.6. Immunofluorescence

Cells were fixed with 4% paraformaldehyde for 15 min at room

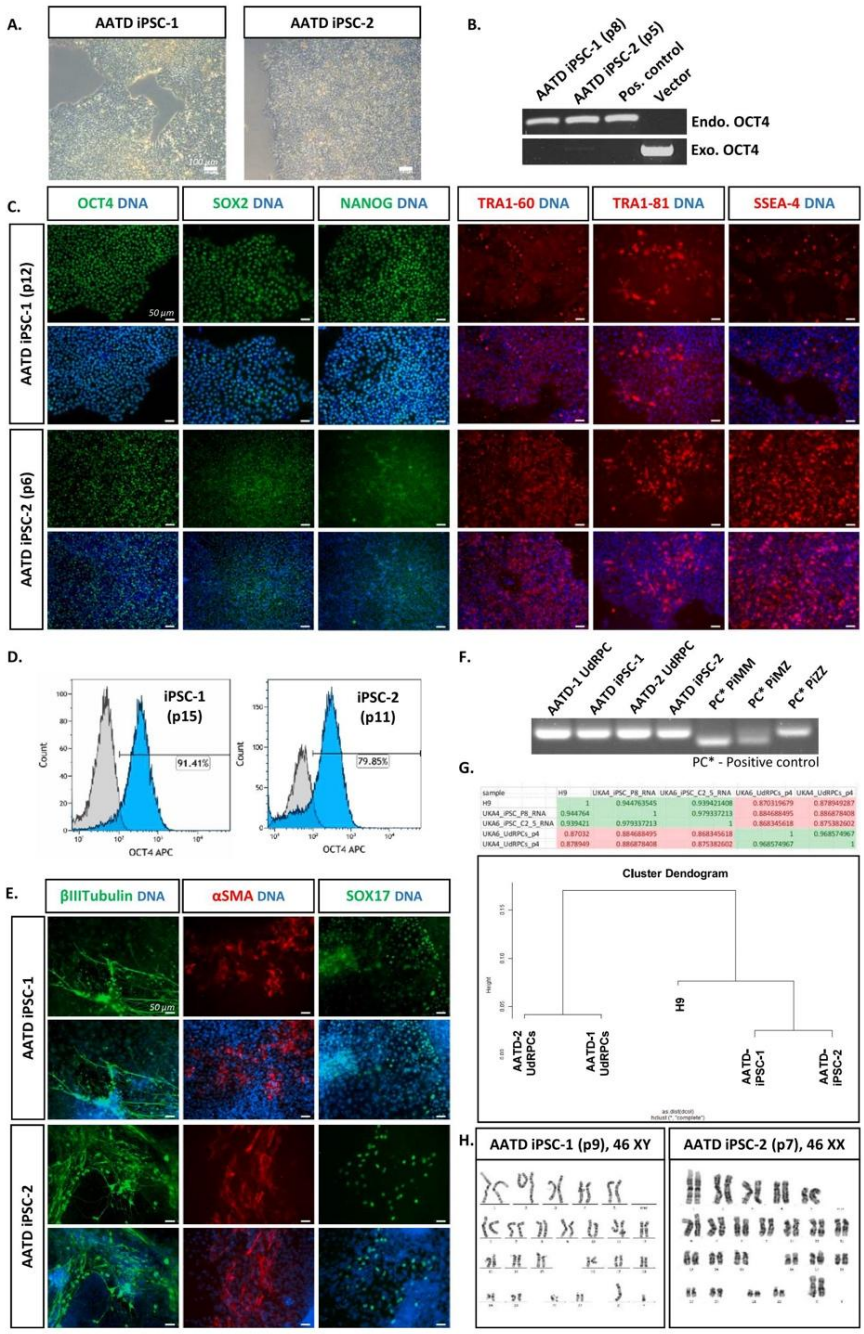

Fig. 1. Characterization of iPSC lines ISRM-AATD-iPSC-1 and ISRM-AATD-iPSC-2.

temperature (RT). Cells were blocked with 5% BSA in 0.5% Triton-X100/PBS and incubated with respective primary antibodies (Table 2) overnight at 4 °C. Cells were incubated for 2 h with Alexa488 or Alexa555-conjugated secondary antibodies and nuclear Hoechst at RT. Fluorescence images were captured by a LSM700 microscope (Carl Zeiss).

Table 2
Reagents details.

	Antibodies used for immunocytochemistry/flow-cytometry			
	Antibody	Dilution	Company Cat #	RRID
Flow Cytometry	Anti-OCT3/4- APC	1:100	Miltenyi Biotec Cat# 130–109- 764	AB_2653082
Pluripotency Marker	Rabbit anti-OCT4	1:400	Cell Signaling Technologies #2840S	AB_2167691
Pluripotency Marker	Rabbit anti-SOX2	1:400	Cell Signaling Technologies #3579S	AB_2195767
Pluripotency Marker	Rabbit anti-NANOG	1:400	Cell Signaling Technologies #4903S	AB_10559205
Pluripotency Marker	Mouse anti-Tra-1–60	1:1000	Cell Signaling Technologies #4746S	AB_2119059
Pluripotency Marker	Mouse anti-Tra-1–81	1:1000	Cell Signaling Technologies #4745S	AB_2119060
Differentiation Marker	anti-aSMA	1:1000	Dako # M0851	AB_2223500
Differentiation Marker	Mouse anti- SOX17	1:50	R and D Systems Cat# AF1924	AB_355060
Differentiation Marker	anti-BIII Tubulin	1:1000	Abcam Cat# ab52623	AB_869991
Secondary Antibody	anti-mouse- Alexa555	1:2000	Thermo Fisher Scientific Cat# A10521	AB_2534030
Secondary Antibody	anti-rabbit- Alexa488	1:2000	Thermo Fisher Scientific Cat# A27034	AB_2536097
Nuclear Co– Staining	Hoechst	1:5000	Thermo Fisher Scientific Cat# H3569	AB_2651133
	Primers			
	Target	Size of band	Forward/Reverse primer (5′-3′)	
Endogenous OCT4	OCT4	113 bp	GTGGAGGAAGCTGACAACAA/ ATTCTCCAGGTTGCCTCTCA	
Episomal Plasmids (exo)	OCT4	657 bp	GTGGAGGAAGCTGACAACAA/ ATTCTCCAGGTTGCCTCTCA	
Mycoplasma ITW Reagents #A3744	mycoplasma-specific 16S rRNA gene	270 bp	Negative samples show a 270 bp band only	
		357 bp	Positive ones have two bands 270 bp & 357 bp	
PiZ genotyping	SERPINA1	M: 250 bp Z: 300 bp	GTGCATAAGGCTGTGCTGACCATCGTC/ GCAGGGACCAGCTCAACCCTTCTTTAATG	

3.7. Flow-cytometry

Flow-cytometry analysis was carried out using an APC-coupled OCT4 antibody and isotype control (Miltenyi). After fixation for 20 min at RT in fixation buffer and permeabilization in 1x intracellular staining perm wash buffer (Biolegend), cells were stained for 30 min at 4 °C and washed. Fluorescence was measured using the CyAn ADP Flow Cytometer (Dako). Analysis was performed with the Kaluza software (Beckman Coulter).

3.8. Karyotype analysis

Karyotype analysis was performed and evaluated at the Institute of Human Genetics and Anthropology, Heinrich-Heine-University, Düsseldorf.

3.9. Mutation analysis by Restriction Fragment Length Polymorphism

The donor underwent a routine AATD diagnostics at the German reference center in the Marburg university hospital. This one consists of (i) measuring AAT serum levels; (ii) isoelectric focusing for protein phenotyping (Bals et al., 2007); (iii) multiplex PCR-based genotyping for the 14 most frequent AATD variants that relies hybridization with allel-specific probes (Veith et al., 2019). Mutations were confirmed at the Department of Internal Medicine III, University Hospital RWTH Aachen. Isolated genomic DNA from parental UdRPCs and iPSCs was used for RFLP (Restriction Fragment Length Polymorphism) assay to distinguish between M and Z alleles. PCR with *my*-Budget 5x PCR-Mastermix and respective primers (Table 2) was followed by *Taq*I enzymatic digestion at 65 °C for 1 h. Gel electrophoresis differentiated between M−allele (250 bp) and Z-allele (300 bp). Previously sequenced human DNA samples served as controls.

3.10. Microarray-based transcriptome analysis

Global transcriptome analysis was carried out on the Human-Clariom-S Affymetrix microarray platform. 1 μg total RNA was hybridized by the Biologisch-medizinisches Forschungszentrum, Heinrich-Heine University, Düsseldorf. The dendrogram was calculated using the package affy of the R/Bioconductor software.

Declaration of Competing Interest

The authors declare that they have no known competing financial interests or personal relationships that could have appeared to influence the work reported in this paper.

Acknowledgements

J.A. acknowledges support from the Medical faculty of Heinrich-Heine University Düsseldorf and the Federal Ministry for economic affairs and climate action as well as the European Social Fund (EXIST Transfer of Research, grant number 03EFNNW217). P.S. is supported by the Deutsche Forschungsgemeinschaft (DFG) consortium SFB 1382 “Gut-Liver Axis” (ID 403224013) the DFG grant STR1095/6-1 and an unrestricted research grant from CSL Behring. C.L. and N.G. are funded by the Else Kröner-Fresenius Stiftung – 2020_EKEA.64.

Appendix A. Supplementary data

Supplementary data to this article can be found online at https://doi.org/10.1016/j.scr.2023.103171.

References

Bals, R., Koczulla, R., Kotke, V., Andress, J., Blackert, K., Vogelmeier, C., 2007. Identification of individuals with alpha-1-antitrypsin deficiency by a targeted screening program. Respir. Med. 101, 1708–1714. https://doi.org/10.1016/j.rmed.2007.02.024.

Bohndorf, M., Ncube, A., Spitzhorn, L.-S., Enczmann, J., Wruck, W., Adjaye, J., 2017. Derivation and characterization of integration-free iPSC line ISRM-UM51 derived from SIX2-positive renal cells isolated from urine of an African male expressing the CYP2D6 *4/*17 variant which confers intermediate drug metabolizing activity. Stem Cell Res. 25, 18–21. https://doi.org/10.1016/j.scr.2017.10.004.

Rahman, M.S., Wruck, W., Spitzhorn, L.S., Nguyen, L., Bohndorf, M., Martins, S., Asar, F., Ncube, A., Erichsen, L., Graffmann, N., Adjaye, J., 2020. The FGF, TGFβ and WNT axis Modulate Self-renewal of Human SIX2+ Urine Derived Renal Progenitor Cells. Sci. Rep. 10 https://doi.org/10.1038/s41598-020-57723-2.

Segeritz, C.-P., Rashid, S.T., De Brito, M.C., Serra, M.P., Ordonez, A., Morell, C.M., Kaserman, J.E., Madrigal, P., Hannan, N.R.F., Gatto, L., Tan, L., Wilson, A.A., Lilley, K., Marciniak, S.J., Gooptu, B., Lomas, D.A., Vallier, L., 2018. hiPSC hepatocyte model demonstrates the role of unfolded protein response and inflammatory networks in α1-antitrypsin deficiency. J. Hepatol. 69, 851–860. https://doi.org/10.1016/j.jhep.2018.05.028.

Strnad, P., McElvaney, N.G., Lomas, D.A., 2020. Alpha$_1$ -Antitrypsin Deficiency. N. Engl. J. Med. 382 (15), 1443–1455.

Tafaleng, E.N., Chakraborty, S., Han, B., Hale, P., Wu, W., Soto-Gutierrez, A., Feghali-Bostwick, C.A., Wilson, A.A., Kotton, D.N., Nagaya, M., Strom, S.C., Roy-Chowdhury, J., Stolz, D.B., Perlmutter, D.H., Fox, I.J., 2015. Induced pluripotent stem cells model personalized variations in liver disease resulting from α1-antitrypsin deficiency. Hepatology 62, 147–157. https://doi.org/10.1002/hep.27753.

Veith, M., Klemmer, A., Anton, I., El Hamss, R., Rapun, N., Janciauskiene, S., Kotke, V., Herr, C., Bals, R., Vogelmeier, C.F., Greulich, T., 2019. Diagnosing Alpha-1-Antitrypsin Deficiency Using A PCR/Luminescence-Based Technology. Int. J. Chron. Obstruct. Pulmon. Dis. 14, 2535–2542. https://doi.org/10.2147/COPD.S224221.

Yu, J., Chau, K.F., Vodyanik, M.A., Jiang, J., Jiang, Y., Pera, M., 2011. Efficient Feeder-Free Episomal Reprogramming with Small Molecules. PLoS One 6 (3), e17557. https://doi.org/10.1371/journal.pone.0017557.

4.3. Forskolin induces FXR expression and enhances maturation of iPSC-derived hepatocyte-like cells

Christiane Loerch, Leon-Phillip Szepanowski, Julian Reiss, James Adjaye, Nina Graffmann.

Frontiers in Cell and Developmental Biology, Volume 12

Abstract:

The generation of iPSC-derived hepatocyte-like cells (HLCs) is a powerful tool for studying liver diseases, their therapy as well as drug development. iPSC-derived disease models benefit from their diverse origin of patients, enabling the study of disease-associated mutations and, when considering more than one iPSC line to reflect a more diverse genetic background compared to immortalized cell lines. Unfortunately, the use of iPSC-derived HLCs is limited due to their lack of maturity and a rather fetal phenotype. Commercial kits and complicated 3D-protocols are cost- and time-intensive and hardly useable for smaller working groups. In this study, we optimized our previously published protocol by fine- tuning the initial cell number, exchanging antibiotics and basal medium composition and introducing the small molecule forskolin during the HLC maturation step. We thereby contribute to the liver research field by providing a simple, cost- and time-effective 2D differentiation protocol. We generate functional HLCs with significantly increased HLC hallmark gene (ALB, HNF4α, and CYP3A4) and protein (ALB) expression, as well as significantly elevated inducible CYP3A4 activity.

Author contributions (75%) of C.L. included:

- Conceptualization of experiments together with N.G. and J.A.
- Investigation and methodology together with N.G.
- Conduction and analysis of experiments together with N.G (hepatocyte-like cell differentiation, cell culture, Immunofluorescence, PCR, qRT-PCR, Western blot, ICG uptake/release, Cytochrome P450 assays, Urea assay)
- Curation and visualization of data
- Writing the original draft together with N.G. and L-P.S.
- Reviewing and editing of the manuscript together with N.G. and J.A.
- Modifications of the manuscript during revision process together with N.G.
- Response to the reviewers together with N.G. and J.A.

Status: Published online in April 2024 as open access article under the CC BY license.
DOI: 10.3389/fcell.2024.1383928

frontiers | Frontiers in Cell and Developmental Biology

TYPE Brief Research Report
PUBLISHED 17 April 2024
DOI 10.3389/fcell.2024.1383928

OPEN ACCESS

EDITED BY
Holm Zaehres,
Ruhr University Bochum, Germany

REVIEWED BY
Qiaozhen Liu,
Massachusetts General Hospital and Harvard Medical School, United States
Pawan Kumar Raghav,
University of California, San Francisco, United States

*CORRESPONDENCE
Nina Graffmann,
nina.graffmann@med.uni-duesseldorf.de

RECEIVED 08 February 2024
ACCEPTED 04 April 2024
PUBLISHED 17 April 2024

CITATION
Loerch C, Szepanowski L-P, Reiss J, Adjaye J and Graffmann N (2024), Forskolin induces FXR expression and enhances maturation of iPSC-derived hepatocyte-like cells.
Front. Cell Dev. Biol. 12:1383928.
doi: 10.3389/fcell.2024.1383928

Forskolin induces FXR expression and enhances maturation of iPSC-derived hepatocyte-like cells

Christiane Loerch[1], Leon-Phillip Szepanowski[1,2], Julian Reiss[1], James Adjaye[1,3] and Nina Graffmann[1]*

[1]Institute for Stem Cell Research and Regenerative Medicine, Medical Faculty and University Hospital Düsseldorf, Heinrich Heine University, Düsseldorf, Germany, [2]IUF – Leibniz Research Institute for Environmental Medicine, Düsseldorf, Germany, [3]University College London, EGA Institute for Women`s Health- Zayed Center for Research Into Rare Diseases in Children (ZGR), London, United Kingdom

The generation of iPSC-derived hepatocyte-like cells (HLCs) is a powerful tool for studying liver diseases, their therapy as well as drug development. iPSC-derived disease models benefit from their diverse origin of patients, enabling the study of disease-associated mutations and, when considering more than one iPSC line to reflect a more diverse genetic background compared to immortalized cell lines. Unfortunately, the use of iPSC-derived HLCs is limited due to their lack of maturity and a rather fetal phenotype. Commercial kits and complicated 3D-protocols are cost- and time-intensive and hardly useable for smaller working groups. In this study, we optimized our previously published protocol by fine-tuning the initial cell number, exchanging antibiotics and basal medium composition and introducing the small molecule forskolin during the HLC maturation step. We thereby contribute to the liver research field by providing a simple, cost- and time-effective 2D differentiation protocol. We generate functional HLCs with significantly increased HLC hallmark gene (*ALB, HNF4α*, and *CYP3A4*) and protein (*ALB*) expression, as well as significantly elevated inducible CYP3A4 activity.

KEYWORDS

induced pluripotent stem cells (iPSCs), hepatocyte-like cells (HLCs), Forskolin, cytochrome P450 activity, *in vitro* Differentiation

1 Introduction

Precise liver (-disease) models are indispensable considering society's burden of emerging liver diseases (Asrani et al., 2019). However, to date, none of the available models is able to recapitulate human liver physiology accurately. Rodents show differences in the basal metabolic rate and cytochrome P450 activity compared to humans, implying an insufficient translation of rodent models to humans (Demetrius, 2004; 2005; Martignoni et al., 2006). Besides available tumor-derived cell lines such as HepaRG and HepG2, primary human hepatocytes (PHHs) are currently the gold standard for hepatocyte research. However, apart from their relatively high costs and ethical limitations, cultivation of the cells results in dedifferentiation within 24 h, thus attenuating their utility for disease modeling or analyses involving longer incubation (Godoy et al., 2016). In addition, donor-to-donor variation in their CYP genotype limits the reproducibility of results obtained with these cells.

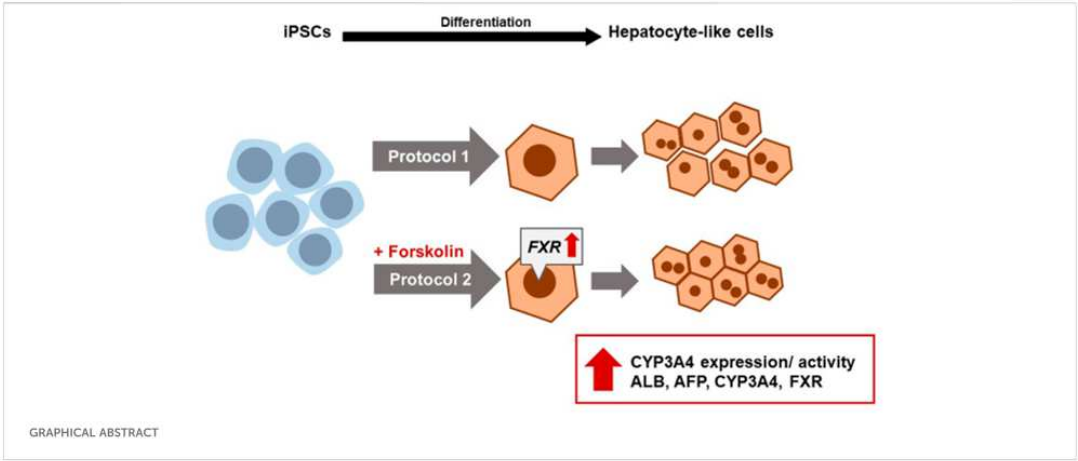

GRAPHICAL ABSTRACT

Human induced pluripotent stem cells (iPSCs) and their differentiation potential to various cell types represent the future source for disease models. Patient-derived iPSC lines allow the consideration of specific genetic background. On the other hand, including several iPSC lines into a study, represents human genetic diversity more accurately and thus provides higher quality data compared to tumor-derived cell lines. Working with more than one iPSC line enables researchers to detect disease-associated factors, which span the genetic variance between patients.

Protocols differentiating iPSCs into hepatocyte-like cells (HLCs) were first established in 2007–2008 (Cai et al., 2007; Agarwal et al., 2008; Hay et al., 2008a; Hay et al., 2008b), and scientists have so far established various HLC differentiation protocols adapted to their needs. The 2D differentiation process takes about 3 weeks and provides a feasible tool to generate i) a HLC model for studying basic liver functions as well as ii) models to study the hepatocytes' specific contribution to inherited and acquired diseases and iii) to test drugs. However, so far, the 2D HLC differentiation mostly results in rather immature HLCs resembling fetal hepatocytes (Baxter et al., 2015; Graffmann et al., 2022). As HLCs are mainly used for the study of diseases and drug development, HLC publications rather focus on a specific disease phenotype rather than the differentiation outcome itself. However, improving the differentiation protocols to consistently generate more mature iPSC-derived HLCs is indispensable for liver research.

In this study, we present our simple, cost- and time-efficient 2D differentiation protocol, optimizing our previously published protocols (Jozefczuk et al., 2011; Graffmann et al., 2016; Matz et al., 2017; Graffmann et al., 2021). By i) fine-tuning the cell number, ii) replacing penicillin/streptomycin with doxycycline, iii) using DMEM/F12 instead of L15 as a medium basis in the last step, as well as iv) adding the small molecule forskolin during the HLC maturation stage, we considerably increased stability of the process as well as maturation of the derived cells. This improved method provides a feasible protocol generating iPSC-derived HLCs within 18–20 days, showing a significant increase of HLC-hallmark gene and protein expression, enhanced functionality and improved uniformity of cell morphology. Since the generated HLCs show inducible activity of the adult enzyme CYP3A4, our model provides an interesting tool for drug development or disease modelling.

2 Methods

2.1 Ethical approval and human iPSC-Cultivation

The use of the human iPSC lines was approved by the Ethical Committee of the medical faculty of Heinrich Heine University, Düsseldorf, Germany, approval number: 5,704 and 5,013. Cell lines 2, 3 were kindly provided by Andrea Rossi, IUF–Leibnitz Institute für umweltmedizinische Forschung GmbH.

Urine-derived human iPSCs from a 51-year old healthy African male (Bohndorf et al., 2017), were cultivated on Matrigel (Corning) coated cell culture dishes with mTesR Plus (Stemcell Technologies) and penicillin/streptomycin (P/S) (Gibco). They were sub-cultivated in clusters by incubating with PBS w/o Ca^{2+}, Mg^{2+} for 3–5 min at RT before mechanical detachment with a cell spatula and centrifugation at 40 *g* for 3 min. Before differentiation, the cells were sub-cultivated as single cells by incubating them with StemPro Accutase Cell Dissociation Reagent (Life Technologies) for 4 min at 37°C and subsequent centrifugation at 110 *g* for 4 min.

To show improvement of a protocol you need more than a single line-this is a major weakness!

2.2 HLC-differentiation

Human iPSCs were differentiated according to two distinct protocols, in the following referred to as protocol 1 (original) and protocol 2 (optimized), respectively. Protocol 1 is based on the protocol by Matz and Graffmann (Graffmann et al., 2016; Matz et al., 2017; Graffmann et al., 2021) with minor changes: Approximately 0.521×10^5 iPSCs/cm^2 were seeded onto Matrigel (Corning) coated plates. The medium was changed to Definitive Endoderm (DE) medium containing 96% RPMI supplemented with

2% B27 (w/o retinoic acid) 1% GlutaMAX (Glx) and P/S (all Gibco) and refreshed daily for the following 3 days. On the first day, 100 ng/mL Activin A (Peprotech) and 2.5 µM CHIR99021 (Stemgent) were added. For the next 2 days, the DE medium was supplemented only with 100 ng/mL Activin A. The medium was changed for hepatic endoderm (HE) induction to 77.5% DMEM/F12 supplemented with 20% Knockout Serum Replacement (KOSR), 0.5% Glx, 0.01% 2-Mercaptoethanol and 1% P/S (all Gibco). The medium was changed daily and 1% DMSO (Sigma-Aldrich) was freshly added for each medium change. After 4 days of HE medium, HLC medium was fed for 12–15 days, with medium changes every other day, consisting of 82% Leibovitz´s L-15 medium (Life Technologies), 8% FBS, 8% Tryptose Phosphate Broth (TPB), 1% Glx, 1% P/S (all Gibco). 1 µM insulin (Sigma-Aldrich), 10 ng/mL hepatocyte growth factor (HGF) (Peprotech), 25 ng/mL dexamethasone (Dex) (Sigma-Aldrich), and 20 ng/mL recombinant human Oncostatin M (rhOSM209a.a) (Immunotools) were freshly added to the medium.

In order to optimize the protocol, we adapted the original to generate protocol 2 as follows. We seeded 1.04×10^5 iPSCs/cm^2 onto Matrigel coated dishes. DE- and HE-induction were carried out as previously mentioned, but instead of P/S, 2 µM doxycycline was used. For the HLC medium we used DMEM/F12 as basal medium instead of Leibovitz´s L-15 (L-15) and 2 µM doxycycline instead of P/S. Insulin and growth factors remained, however, 20 µM forskolin (Tocris) was added freshly to the medium for every feeding.

2.3 Immunocytochemistry

Immunocytochemistry was performed on 4% PFA fixed cells after 10 min permeabilization with 0.5% Triton-X-100 (Sigma-Aldrich) in PBS. The cells were blocked with 3% BSA/PBS and subsequently incubated with primary antibodies against AFP, Albumin (both Sigma-Aldrich), HNF4α (Abcam) and E-CAD (Cell Signaling Technologies) overnight at 4 °C. Afterwards the cells were washed 3x with 0.5% Triton-X-100/PBS and incubated with fluorescence labeled secondary antibody against respective host species IgG (Life technologies) for 2 h at RT. DNA was stained with Hoechst 33258. Photomicrographs were taken with a LSM 700 microscope (Zeiss) and processed with ZEN software (Zeiss). Antibodies with their corresponding catalogue numbers and dilutions in Supplementary Table S1.

2.4 Western blot

Cells were lysed for 20 min on ice in RIPA-buffer containing protease- and phosphatase inhibitor (Sigma-Aldrich). Remaining cellular debris was centrifuged at 20,000 xg for 20 min at 4°C, and the supernatant was stored at −80 °C. Pierce BCA Protein Assay (Life Technologies) was performed to determine protein concentration as described by the manufacturer. 20 µg of protein was resolved on a NuPAGE™ 4%–12%, Bis-Tris protein gel (Life Technologies). Proteins were wet-blotted onto a 0.45 µm nitrocellulose membrane (GE healthcare, Solingen, Germany) and blocked in 5% Milk (ROTH) in TBS-T buffer. Afterwards primary antibodies against AFP and Albumin and Beta-actin (Cell Signaling Technologies) as housekeeping protein were incubated for 2 h at RT. After 3x washing with TBS-T, Horseradish peroxidase (HRP)-coupled secondary antibodies against respective host IgG (Cell Signaling Technologies) were incubated for 1 h at RT and non-bound antibody was washed off 3x with TBS-T. HRP chemiluminescence was detected using the 1x Pierce ECL Western blotting Substrate (Life Technologies) on a Fusion FX instrument (PeqLab). Corresponding band sizes were detected using the PageRuler pre-stained protein ladder (Life Technologies). Quantification was performed using Fusion Capt Advance software (PeqLab) and rolling ball background correction (Image Studio light 5.2).

2.5 Real-time quantitative PCR

RNA was isolated from HLCs, using the direct-zol RNA isolation kit (Zymo Research), following the manufacturer's instructions. 500 ng of RNA were reversely transcribed to cDNA using the TaqMan reverse transcription kit (Life technologies). RT qPCR was performed in technical triplicates, using the Power Sybr Green Mastermix (Life technologies) and the VIIA7 machine (Life technologies). Primers were ordered from Eurofins. The mRNA expression was calculated as the log2-fold change relative to the housekeeping gene RPL0. Experiments were carried out in biological triplicates and two-tailed unpaired Student's t-test was performed to calculate significances (please find primer sequences in the Supplementary Table S1). A 1% agarose gel (1x TBS buffer) was stained with GeldRed Nucleid Acid Gel Stain (Hoezel) and qPCR products were resolved at 100 V for 45 min.

2.6 Urea production

Urea Assay (QuantiChrom) was performed following the manufacturer`s instructions for low urea-samples. In brief, supernatant was collected from 3 independent differentiations and stored at −20°C. Urea standard was prepared in a 1: 10 dilution, and 50 µL of samples were incubated with 200 µL of the reaction solution for 50 min at RT in the dark. Afterwards, emission was measured at a wavelength of 430 nm using the Epoch2 microplate reader (BioTek) and the concentration was calculated from the standard curve. Two-tailed unpaired Student's t-test was performed to calculate significance.

2.7 Cytochrome P450 activity

CYP3A4-activity was measured using the P450-Glo™ kit (Promega), following the manufacturer's instructions. In brief, cells were incubated with 1:1000 luciferin-IPA in Williams' E medium (Sigma-Aldrich) for 1 h at 37°C. An equal volume of detection reagent was added and incubated for 20 min at RT in the dark, before measuring the luminescence using a luminometer (Lumat LB 9507, Berthold Technologies). Two-tailed unpaired Student's t-test was performed to calculate significance.

2.8 Glycogen-storage

Glycogen storage was analysed using periodic acid-schiff (PAS)-reaction (Sigma-Aldrich) on PFA-fixated cells. The cells were

10.3389/fcell.2024.1383928

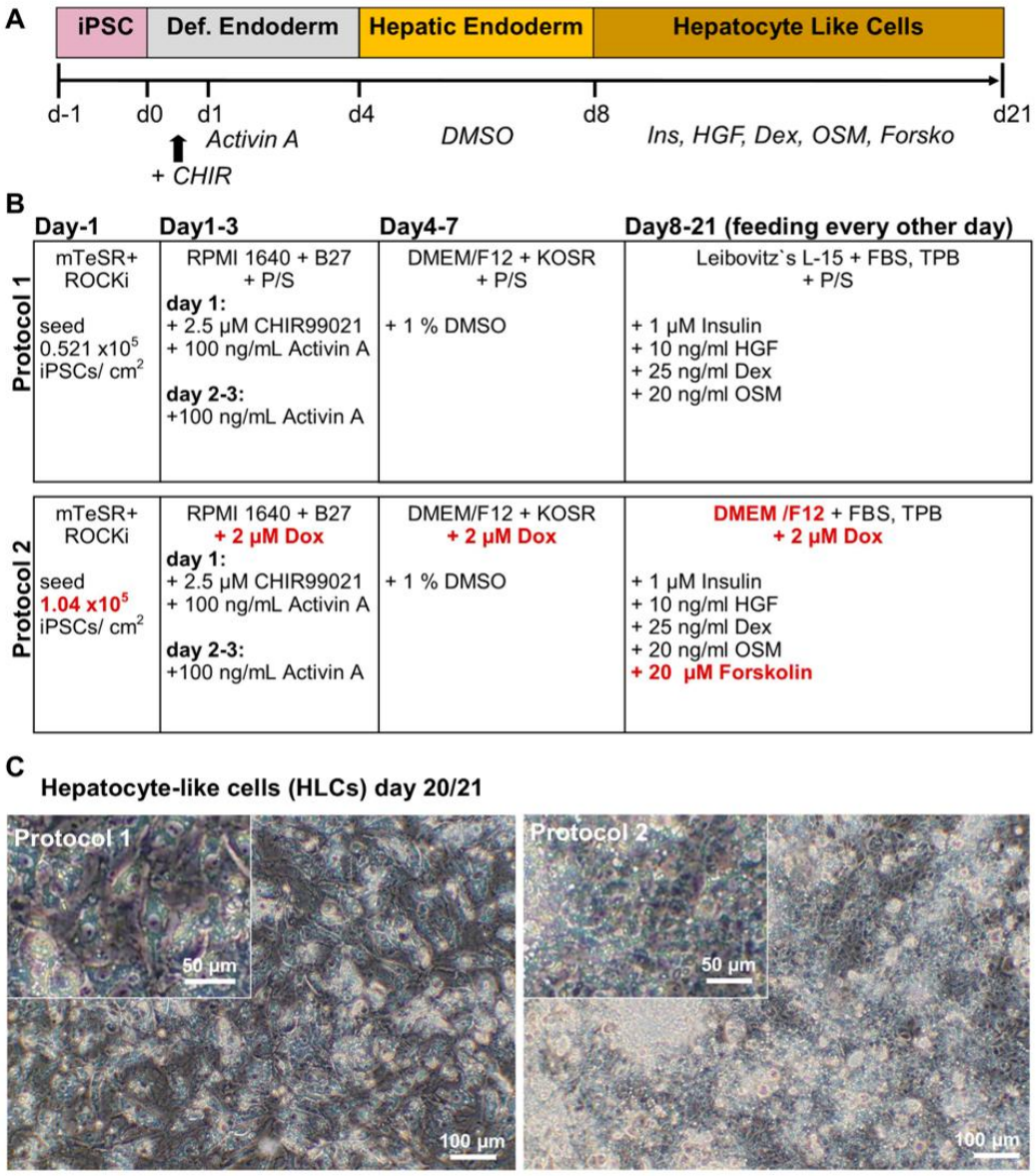

FIGURE 1
Generation of iPSC-derived hepatocyte-like cells (HLCs). **(A)** Time line for differentiation of iPSCs over 21 days, indicating Definitive Endoderm induction by CHIR99021 on d1, and Activin A treatment on d1-d3. Hepatic Endoderm was induced by adding DMSO on d4-d8. Maturation of HLCs was induced by insulin, hepatocyte growth factor (HGF), dexamethasone (Dex), oncostatin M (OSM) and forskolin (Forsko) treatment on d8-d21. **(B)** Comparison of protocol 1 and 2, changes in the media composition are marked in red. **(C)** Morphology of HLCs on day 20/21 generated with protocol 1 or 2.

incubated with periodic acid solution for 5 min at RT before washing 3x with dH_2O. Afterwards the cells were incubated with Schiff`s reagent for 15 min at RT and washed 3x with tap water. Hematoxylin solution, Gill No 3 was incubated for 90 s to counterstain the nuclei. Glycogen storage was documented using brightfield microscopy with the IX50 Olympus Microscope (Olympus).

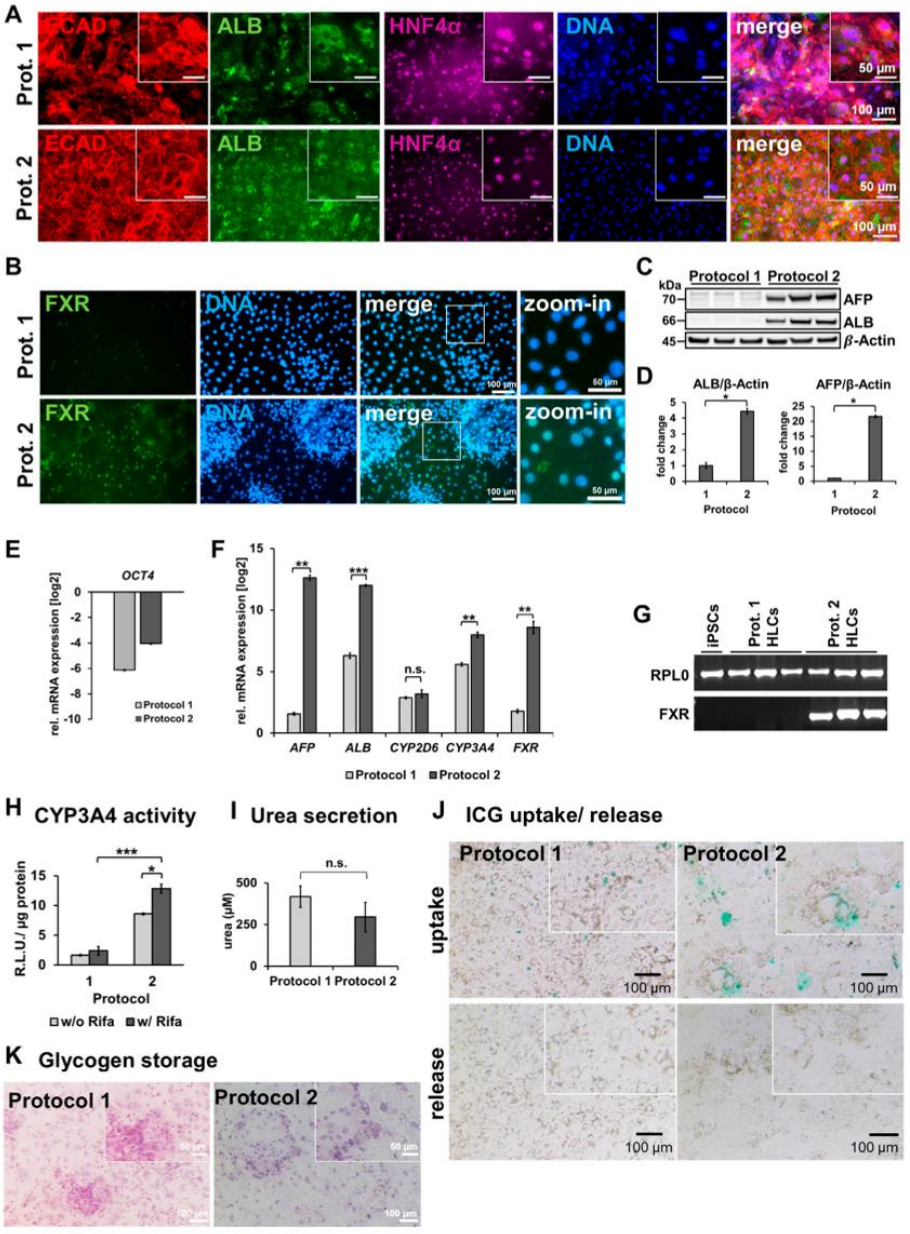

FIGURE 2
Characterization of HLCs generated with protocol 1 or protocol 2. **(A)** Representative immunofluorescence images of ECAD (red), ALB (green), HNF4α (purple) in HLCs differentiated with protocol 1 or two respectively. DNA was stained with Hoechst 33258. **(B)** Representative immunofluorescence images of FXR (green). DNA was stained with Hoechst 33258. **(C)** Western blots of AFP and ALB for 3 biological replicates of HLCs generated with protocol 1 or two respectively. **(D)** Fold change of protein expression (mean±SD) of three biological replicates of HLCs generated with protocol 1 or 2, normalized to housekeeping protein β-actin, relative to protocol 1. Two-tailed Student's t-test was performed to calculate significances (*$p < 0.05$, **$p < 0.01$). Relative mRNA expression of **(E)** *OCT4* **(F)** *AFP*, *ALB*, *CYP2D6*, *CYP3A4* and *FXR* normalized to the housekeeping gene *RPL0* of HLCs generated with protocol 1 or two relative to iPSCs, respectively. Bar plots show mean± SE from three biological replicates. Two-tailed Student's t-test was performed to calculate significances (*$p < 0.05$, **$p < 0.01$, ***$p < 0.001$). **(G)** Agarose gel electrophoresis showing bands of corresponding sizes indicating amplicons of housekeeping gene *RPL0* and *FXR* after RT-qPCR for iPSCs, and HLCs generated with protocol 1 or 2, respectively. **(H)** CYP3A4 activity determined by

(*Continued*)

FIGURE 2 (Continued)
metabolization of luciferin-IPA as relative light units (R.L.U) normalized to total protein in HLCs generated by protocol 1 or 2 with and without rifampicin (Rifa) treatment for 24 h. Bar plots show mean±SD and significances were calculated by using two-tailed Student's t-test (*$p < 0.05$, ***$p < 0.001$). **(I)** Secreted urea into the supernatant within 24 h. **(J)** Uptake and release after 6 h of indocyanine green (ICG) of HLCs generated with protocol 1 or 2. **(K)** Glycogen storage shown via Periodic Acid–Schiff (PAS) reaction on fixated HLCs generated with protocol 1 or 2 respectively.

2.9 Indocyanine green (ICG) uptake

To test for ICG uptake and release capacity, HLCs were washed 1x with HBSS (Sigma-Aldrich) and incubated for 20 min at 37°C with 0.5 mg/mL ICG (Sigma) in HLC basal medium. Cells were washed 1x with HBSS and ICG uptake was documented via brightfield microscopy using the IX50 Olympus Microscope (Olympus). To release ICG, HLCs were incubated with HLC basal medium for 5–6 h at 37°C. After washing 1x with HBSS, ICG-release was documented with brightfield microscopy.

3 Results

3.1 Morphology and protein expression

iPSCs from a healthy 51-year-old African male were differentiated to hepatocyte-like cells (HLCs) using protocol 1 (original) or protocol 2 (optimized), resulting in cells showing different morphology and HLC properties (Figures 1A–C). Protocol 1 generated relatively large HLCs, while protocol 2 resulted in smaller, tightly packed HLCs showing more prominent borders (Figure 1C). Immunofluorescence staining shows the expression of the epithelial marker protein E-cadherin (E-CAD), and the hepatocyte markers hepatocyte nuclear factor 4alpha (HNF4α), and albumin (ALB) of resulting HLCs (Figure 2A). We detected all three markers in HLCs generated with both protocols, however a tendency towards a higher number of HNF4α-positive HLCs was visible in cells generated with protocol 2. ALB was expressed in HLCs generated with both media, and no significant difference could be detected in the immunofluorescence. However, Western blot analysis (Figure 2C) of HLCs and corresponding quantification (Figure 2D) detected significantly more AFP and ALB in HLCs generated with protocol 2 compared to protocol 1. Furthermore, we detected farnesoid X receptor (FXR) solely under optimized conditions. ICC confirmed its location to the nucleus of HLCs while in protocol 1 only unspecific background staining was detected (Figure 2B). FXR is a nuclear hormone receptor, involved in liver metabolism (Repa and Mangelsdorf, 2000; Sinal et al., 2000). Expression of FXR in iPSC-derived HLCs was recently found *in vitro* to be associated with increased maturity as observed in PHHs (Nell et al., 2022).

3.2 Gene expression and functionality

To confirm successful differentiation of iPSCs into HLCs, we measured relative mRNA expression of selected markers (Figure 2F). We observed a drastic decrease in *OCT4* levels compared to undifferentiated iPSCs (Figure 2E), indicating the loss of pluripotency in HLCs. Differentiation with protocol 2 resulted in a significant increase of gene expression of HLC markers *AFP*, *ALB*, and *CYP3A4* compared to protocol 1 (Figure 2F). Interestingly, we could show for *ALB* and *AFP* that this increase is directly linked to forskolin treatment, as HLCs differentiated according to protocol 2 but without forskolin, had a much lower expression of both factors (Supplementary Figure S1A). While AFP is considered an immature, fetal marker and ALB is also an early marker for HLCs, CYP3A4 is considered a late marker for adult hepatocytes, indicating mature HLCs (Martínez-Jiménez et al., 2007; Ang et al., 2018). We detected FXR expression only under optimized conditions (Figures 2F,G).

With regards to functionality, we could measure a significant increase of CYP3A4 activity in cells derived with protocol 2 compared to protocol 1 (Figure 2H). Importantly, CYP3A4 was inducible upon rifampicin treatment in protocol 2 cells, confirming their higher level of maturity. Again, this effect was linked to the forskolin treatment, as CYP3A4 as well as CYP2D6 activity was drastically reduced when culturing cells according to protocol 2 but without forskolin (Supplementary Figure S1B). We further investigated the effects of the optimized protocol with regards to urea secretion (Figure 2I), uptake and release of indocyanine green dye (ICG) (Figure 2J), and glycogen storage (Figure 2K). All HLCs secreted urea into the medium indicating key features of functional hepatocytes, however, we could not detect a significant increase with the optimized medium. ICG uptake was visible for both conditions, however only HLCs generated by the optimized medium were able to release ICG after 6 h of incubation. HLCs generated from both protocols stored glycogen. Furthermore, we noticed less cell death at the DE stage as well as through the transition from DE to HE stage. This might have also contributed to the enhanced maturation and homogeneity, which we observed at the HLC stage. However, as we did not test cell viability, our observation are based on a subjective impression.

4 Discussion

4.1 Fine-tuning of cell number and use of doxycycline improves HLC differentiation outcome

Differentiation of iPSCs to various cell types is only possible to a limited level since *in vitro* conditions cannot yet meet the delicately orchestrated balance of chemical and mechanical stimuli which are provided during the development *in vivo* (Ang et al., 2018). Differentiation of cells towards DE primes them for further HLC differentiation. In order to induce Activin/Nodal signaling, we use high concentrations of Activin A to activate the SMAD2/3 branch of the TGFβ pathway, which is essential for successful DE induction

(Brown et al., 2011; Lee et al., 2011). Furthermore, WNT-signaling is needed to express SRY-box transcription factor 17 (SOX17) which upregulates several genes of the DE lineage. We use CHIR99021 to inhibit Glycogensynthase-Kinase 3 (GSK-3) and prevent β-catenin degradation, leading to the induction of SOX17 expression (Engert et al., 2013).

Especially during the first day of CHIR99021-and Activin A treatment, a lot of cell death has been observed, probably due to the drastic change in medium and Activin A and CHIR concentration (Peaslee et al., 2021). Nonetheless, after the first wave of cell death, massive cell proliferation takes place, demanding fine-tuning of the initial cell number. When the cell density is too low at the end of DE-stage, HE cells transit to an endothelial derived epithelial cell type, which is incapable of differentiating to HLCs (Graffmann et al., 2018). Therefore, we recommend testing the initial cell number for each cell line, as the DE outcome is indispensable for successful further differentiation. Peaslee et al. found that doxycycline can help to prevent apoptosis during the first Activin A incubation (Peaslee et al., 2021). Even though there was no direct effect on HLC-marker expression, they saw a general improvement in their HLC-culture with a more defined monolayer and better viability. This is consistent with our observation of lower cell death during DE-stage and enhanced HLC marker gene expression and functionality, when using doxycycline throughout the whole differentiation. However, we could not observe any direct effect on the DE-stage development.

During the HE-stage, numerous groups use 1% DMSO in a relatively plain basal medium to initiate hepatic endoderm development, though the direct mechanism of DMSO-induced differentiation is not yet completely resolved (Graffmann et al., 2022). In the past, we occasionally encountered a lot of cell death during the transition from DE to HE stage, leading to insufficient cell confluence and interference with the differentiation process. Although we did not analyze the direct impact of doxycycline on cell viability, we observed a lot less cell death during the transition from DE to HE. After 4 days of HE medium, we observed cobblestone shaped, tightly packed, polygonal HE-cells, expressing HNF4α and AFP.

4.2 Replacing L-15 medium with DMEM/F12 improves the maturation step

Many early hepatocyte differentiation protocols, including our protocol 1, used L-15 medium as a base for the maturation medium. It was introduced by Hay and others in 2008 (Hay et al., 2008a; Hay et al., 2008b) who based their maturation medium on a primary rat hepatocyte medium (Mitchell et al., 1984). L-15 medium is a phosphate and amino acid-buffered formulation, optimized for CO_2-free culture conditions. In contrast, the media used in preceding steps of HLC differentiation (RPMI1640, DMEM), are sodium bicarbonate-buffered formulations, requiring 5%–10% CO_2 for physiological pH of the culture medium. Cultivating cells in the L-15 based maturation medium in the same incubator utilized for the first steps of hepatocyte differentiation, results in a strong reduction of pH in the culture medium by exceeding the buffer capacity. This impairs cell survival, maturation, and function. Today, L-15 medium has been replaced by many groups with other media such as HepatoZYME from Gibco (Cameron et al., 2015) or hepatocyte basal medium from Lonza (Hannan et al., 2013). In our hands, DMEM/F12 (Sauer et al., 2016) turned out to be a reliable and cost-effective basal medium for successful HLC maturation.

4.3 Forskolin possibly induces HLC maturation via FXR and PXR pathway

The maturation phase of the differentiation is based on HLC promoting growth factors and the hormone insulin. Hepatocyte growth factor (HGF) is one of the essentials on the way towards HLC-differentiation since it is a morphogen and governs the development and regeneration of liver tissue via tyrosine kinase activity on its receptor C-MET (Bottaro et al., 1991; Graffmann et al., 2022). Oncostatin M, a cytokine which belongs to the interleukin six family and secreted by hematopoietic cells during embryonic liver development *in vivo*, is controversially discussed in the field. While some research groups found that it helps in the maturation of HLCs, it was also observed that it dedifferentiates HLCs, and is associated with cancers of several organs (Kamiya et al., 2001; Danoy et al., 2020; Graffmann et al., 2022). In our hands, the addition of OSM did not seem crucial for HLC development in the 2D culture, however, it mitigated the formation of cysts and prevented cell death in 3D (own unpublished data).

Using 1 μM of insulin for the HLC maturation has worked well for us. However, the concentrations vary throughout published protocols, and the exact function of insulin during hepatic differentiation is yet to be fully characterized. In fact, working groups have shown that manipulating energy metabolism of hepatic cells via insulin signaling might affect the differentiation outcome (Rodrigues et al., 2022).

Forskolin is a diterpene, found in the root of Coleus forskohlii (Dubey et al., 1981). The compound has been used in traditional medicine to treat hypertension, obesity, and respiratory diseases and its relevance for modern medicine is emerging (Lindner et al., 1978; Baumann et al., 1990; Jagtap et al., 2011; Sapio et al., 2017). On the biochemical level, it is known to upregulate adenylate cyclase which synthesizes cAMP from ATP (Seamon et al., 1981). cAMP promotes hepatocyte specific gene expression (Ogawa et al., 2013) and increases polarization of HepaRG cells via activation of farnesoid X receptor (FXR) and pregnane X receptor (PXR) (Mayati et al., 2018). This is in accordance with our detection of FXR-expression solely in the forskolin-containing protocol 2. Moreover, using protocol 2 without forskolin resulted in reduced levels of *ALB* and *AFP* expression as well as lower levels of CYP3A4 and CYP2D6 activity (Supplementary Figure S1A,B), demonstrating the important, yet elusive role of forskolin during HLC development.

FXR is a nuclear hormone receptor whose natural ligands are liver metabolites such as bile acids. While under physiological conditions it is involved in the clearance of bile acids and liver metabolism, its *in vitro* induction by using potent ligands leads to upregulation of HLC specific genes (Ali et al., 2015; Godoy et al., 2016; Stofan and Guo, 2020). Recently, Nell et al. demonstrated that FXR expression is essential for fostering hepatocyte fate while simultaneously inhibiting intestinal fate during HLC differentiation (Nell et al., 2022).

PXR is another nuclear hormone receptor, which is an environmental sensor of xenobiotics as well as endogenous ligands such as bile acids. Similar to FXR, it builds a heterodimer to activate transcription factor activity. As it is a chemical sensor for

the liver environment it plays a pivotal role in diseases affecting the bile acid (BA) metabolism such as cholestatic disease, where it downregulates the BA synthesis and upregulates its export (Sayaf et al., 2021). Furthermore, recent studies also found an association with metabolic, inflammatory and lipid metabolism disorders, thus indicating a role for the metabolism of hepatocytes (Lehmann et al., 1998; Moreau et al., 2008; Godoy et al., 2016; Hakkola et al., 2016).

With FXR and PXR functioning as nuclear receptors with transcriptional activity on the metabolism of hepatocytes, it is plausible that activation of FXR and PXR via forskolin mediated cAMP-signaling promotes liver specification during differentiation *in vitro* (Godoy et al., 2016; Nell et al., 2022).

In conclusion, our data show a drastic increase in liver specific gene and protein expression such as AFP, HNF4α, ALB, CYP3A4 as well as the induction of FXR expression. Notably, protein and gene expression of AFP and ALB were highly increased in protocol 2 compared to protocol 1. However, as both are early markers of HLC development, they can only be considered as part of the HLC confirmation. Next to other functionality tests such as urea secretion, glycogen storage and ICG uptake and release, we could detect improved CYPP3A4 activity as well as rifampicin inducibility. Together with the increased levels of AFP and ALB, we could show a drastic optimization of our previous protocol. Furthermore, we could observe less cell death during the early steps of differentiation and enhanced viability and homogeneity of the monolayer at the HLC stage with the optimized differentiation protocol 2. However, more research is needed to further improve the efficiency of HLC differentiation. In particular, the fact that cells from both protocols still expressed residual *OCT4*, albeit with no significant differences between the protocols and on low levels, requires our attention, at least when aiming to generate HLCs for transplantation. Further analyses are necessary, to determine if this expression can be tracked down to single cells that could be removed by FACS sorting or if *OCT4* is still present in the majority of HLCs, which would require further optimization of the protocol. Nevertheless, especially the high and inducible level of CYP3A4 activity in cells derived with protocol 2 indicates an improvement in functionality, which is essential for using these cells for drug development and toxicological test.

Besides the addition of small molecules, the composition of the basal medium might also need further consideration. Replacing fetal bovine serum (FBS) with knock-out serum might be an aspect to consider, to move the protocol towards a xenofree setting which is essential for potential HLC transplantation and to reduce variability resulting from lot-to-lot variation. Similarly, Matrigel, a heterogenous matrix can be replaced with standardized and xenofree laminins as has been shown before (Cameron et al., 2015). Furthermore, using relatively high levels of insulin should be avoided as it manipulates the energy metabolism and might interfere with the differentiation efficiency (Hakkola et al., 2016). Differentiation in 3D enhances HLC culture stability compared to 2D which enables researchers to improve maturity and as well as to perform long-term experiments (Rashidi et al., 2018). This development suggests improvement for HLC differentiation in the future. To enhance reproducible maturity throughout the scientific community, it is indispensable to constantly update on the latest differentiation protocol. We therefore provide our current differentiation protocol, which robustly improved HLC hallmark gene expression and functionality.

5 Summary and outlook

The use of human iPSC-derived HLCs provides an urgently needed tool for future *in vitro* studies of liver diseases and therapy development. However, the established differentiation protocols are limited, because the resulting HLCs lack maturity (Graffmann et al., 2022). Companies offer differentiation kits which provide high levels of reproducibility and maturity, but are relatively expensive and thus not affordable for smaller laboratories. This underlines the need for protocols enhancing the maturation of HLCs available at reasonable costs. In this study, we introduce our optimized, simple and cost-efficient differentiation protocol, enhancing reproducibility and maturity of HLCs by adapting the initial cell number, addition of doxycycline to prevent cell death and the use of forskolin, an indirect cAMP agonist, in a DMEM/F12 based maturation medium.

Data availability statement

The original contributions presented in the study are included in the article/Supplementary Material, further inquiries can be directed to the corresponding author.

Ethics statement

The studies involving humans were approved by Ethical Committee of the medical faculty of Heinrich Heine University, Düsseldorf, Germany, approval number: 5704 and 5013. The studies were conducted in accordance with the local legislation and institutional requirements. The participants provided their written informed consent to participate in this study.

Author contributions

CL: Conceptualization, Data curation, Investigation, Methodology, Visualization, Writing–original draft, Writing–review and editing. L-PS: Investigation, Methodology, Writing–original draft, Writing–review and editing. JR: Investigation, Methodology, Writing–original draft, Writing–review and editing. JA: Conceptualization, Project administration, Resources, Supervision, Writing–original draft, Writing–review and editing. NG: Conceptualization, Formal Analysis, Funding acquisition, Investigation, Methodology, Project administration, Resources, Supervision, Visualization, Writing–original draft, Writing–review and editing.

Funding

The author(s) declare that financial support was received for the research, authorship, and/or publication of this article. CL, NG, and JR are funded by the Else Kröner-Fresenius-Stiftung—2020_EKEA.64. NG acknowledges funding from Ministerium für Kultur und Wissenschaft NRW (Ministry of Culture and Sciences NRW)–005-2305-0038, "iPSC-AATD." JA is funded by the Medical faculty of Heinrich-Heine University Düsseldorf. JA and L-PS acknowledge funding by the Leibniz Association (project-number K246/2019). This work is partly

funded by the Deutsche Forschungsgemeinschaft (DFG, German Research Foundation) –417677437/GRK2578 "Impact of genotoxins on the differentiation efficacy of murine and human stem and progenitor cells and functional competence of thereof derived differentiated progeny"; Sub-project: 1a, PI: JA.

Acknowledgments

We are thankful to Andrea Rossi from the Leibniz-Institut für umweltmedizinische Forschung GmbH for the provision of cell lines 2,3.

Conflict of interest

The authors declare that the research was conducted in the absence of any commercial or financial relationships that could be construed as a potential conflict of interest.

The author(s) declared that they were an editorial board member of Frontiers, at the time of submission. This had no impact on the peer review process and the final decision.

Publisher's note

All claims expressed in this article are solely those of the authors and do not necessarily represent those of their affiliated organizations, or those of the publisher, the editors and the reviewers. Any product that may be evaluated in this article, or claim that may be made by its manufacturer, is not guaranteed or endorsed by the publisher.

Supplementary material

The Supplementary Material for this article can be found online at: https://www.frontiersin.org/articles/10.3389/fcell.2024.1383928/full#supplementary-material

References

Agarwal, S., Holton, K. L., and Lanza, R. (2008). Efficient differentiation of functional hepatocytes from human embryonic stem cells. *Stem Cells* 26 (5), 1117–1127. doi:10.1634/stemcells.2007-1102

Ali, A. H., Carey, E. J., and Lindor, K. D. (2015). Recent advances in the development of farnesoid X receptor agonists. *Ann. Transl. Med.* 3 (1), 5. doi:10.3978/j.issn.2305-5839.2014.12.06

Ang, L. T., Tan, A. K. Y., Autio, M. I., Goh, S. H., Choo, S. H., Lee, K. L., et al. (2018). A roadmap for human liver differentiation from pluripotent stem cells. *Cell Rep.* 22 (8), 2190–2205. doi:10.1016/j.celrep.2018.01.087

Asrani, S. K., Devarbhavi, H., Eaton, J., and Kamath, P. S. (2019). Burden of liver diseases in the world. *J. Hepatol.* 70 (1), 151–171. doi:10.1016/j.jhep.2018.09.014

Baumann, G., Felix, S., Sattelberger, U., and Klein, G. (1990). Cardiovascular effects of forskolin (HL 362) in patients with idiopathic congestive cardiomyopathy--a comparative study with dobutamine and sodium nitroprusside. *J. Cardiovasc Pharmacol.* 16 (1), 93–100. doi:10.1097/00005344-199007000-00013

Baxter, M., Withey, S., Harrison, S., Segeritz, C. P., Zhang, F., Atkinson-Dell, R., et al. (2015). Phenotypic and functional analyses show stem cell-derived hepatocyte-like cells better mimic fetal rather than adult hepatocytes. *J. Hepatol.* 62 (3), 581–589. doi:10.1016/j.jhep.2014.10.016

Bohndorf, M., Ncube, A., Spitzhorn, L. S., Enczmann, J., Wruck, W., and Adjaye, J. (2017). Derivation and characterization of integration-free iPSC line ISRM-UM51 derived from SIX2-positive renal cells isolated from urine of an African male expressing the CYP2D6 *4/*17 variant which confers intermediate drug metabolizing activity. *Stem Cell Res.* 25, 18–21. doi:10.1016/j.scr.2017.10.004

Bottaro, D. P., Rubin, J. S., Faletto, D. L., Chan, A.M.-L., Kmiecik, T. E., Vande Woude, G. F., et al. (1991). Identification of the hepatocyte growth factor receptor as the c-*met* proto-oncogene product. *Science* 251 (4995), 802–804. doi:10.1126/science.1846706

Brown, S., Teo, A., Pauklin, S., Hannan, N., Cho, C. H., Lim, B., et al. (2011). Activin/Nodal signaling controls divergent transcriptional networks in human embryonic stem cells and in endoderm progenitors. *Stem Cells* 29 (8), 1176–1185. doi:10.1002/stem.666

Cai, J., Zhao, Y., Liu, Y., Ye, F., Song, Z., Qin, H., et al. (2007). Directed differentiation of human embryonic stem cells into functional hepatic cells. *Hepatology* 45 (5), 1229–1239. doi:10.1002/hep.21582

Cameron, K., Tan, R., Schmidt-Heck, W., Campos, G., Lyall, M. J., Wang, Y., et al. (2015). Recombinant laminins drive the differentiation and self-organization of hESC-derived hepatocytes. *Stem Cell Rep.* 5 (6), 1250–1262. doi:10.1016/j.stemcr.2015.10.016

Danoy, M., Tauran, Y., Poulain, S., Arakawa, H., Mori, D., Araya, K., et al. (2020). Analysis of hiPSCs differentiation toward hepatocyte-like cells upon extended exposition to oncostatin. *Differentiation* 114, 36–48. doi:10.1016/j.diff.2020.05.006

Demetrius, L. (2004). Caloric restriction, metabolic rate, and entropy. *J. Gerontol. A Biol. Sci. Med. Sci.* 59 (9), B902–B915. doi:10.1093/gerona/59.9.b902

Demetrius, L. (2005). Of mice and men. When it comes to studying ageing and the means to slow it down, mice are not just small humans. *EMBO Rep.* 6, S39–S44. doi:10.1038/sj.embor.7400422

Dubey, M. P., Srimal, R. C., Nityanand, S., and Dhawan, B. N. (1981). Pharmacological studies on coleonol, a hypotensive diterpene from Coleus forskohlii. *J. Ethnopharmacol.* 3 (1), 1–13. doi:10.1016/0378-8741(81)90010-6

Engert, S., Burtscher, I., Liao, W. P., Dulev, S., Schotta, G., and Lickert, H. (2013). Wnt/β-catenin signalling regulates Sox17 expression and is essential for organizer and endoderm formation in the mouse. *Development* 140 (15), 3128–3138. doi:10.1242/dev.088765

Godoy, P., Widera, A., Schmidt-Heck, W., Campos, G., Meyer, C., Cadenas, C., et al. (2016). Gene network activity in cultivated primary hepatocytes is highly similar to diseased mammalian liver tissue. *Arch. Toxicol.* 90 (10), 2513–2529. doi:10.1007/s00204-016-1761-4

Graffmann, N., Ncube, A., Martins, S., Fiszl, A. R., Reuther, P., Bohndorf, M., et al. (2021). A stem cell based *in vitro* model of NAFLD enables the analysis of patient specific individual metabolic adaptations in response to a high fat diet and AdipoRon interference. *Biol. Open* 10 (1), bio054189. doi:10.1242/bio.054189

Graffmann, N., Ncube, A., Wruck, W., and Adjaye, J. (2018). Cell fate decisions of human iPSC-derived bipotential hepatoblasts depend on cell density. *PLoS One* 13 (7), e0200416. doi:10.1371/journal.pone.0200416

Graffmann, N., Ring, S., Kawala, M. A., Wruck, W., Ncube, A., Trompeter, H. I., et al. (2016). Modeling nonalcoholic fatty liver disease with human pluripotent stem cell-derived immature hepatocyte-like cells reveals activation of PLIN2 and confirms regulatory functions of peroxisome proliferator-activated receptor alpha. *Stem Cells Dev.* 25 (15), 1119–1133. doi:10.1089/scd.2015.0383

Graffmann, N., Scherer, B., and Adjaye, J. (2022). *In vitro* differentiation of pluripotent stem cells into hepatocyte like cells - basic principles and current progress. *Stem Cell Res.* 61, 102763. doi:10.1016/j.scr.2022.102763

Hakkola, J., Rysä, J., and Hukkanen, J. (2016). Regulation of hepatic energy metabolism by the nuclear receptor PXR. *Biochim. Biophys. Acta* 1859 (9), 1072–1082. doi:10.1016/j.bbagrm.2016.03.012

Hannan, N. R., Segeritz, C. P., Touboul, T., and Vallier, L. (2013). Production of hepatocyte-like cells from human pluripotent stem cells. *Nat. Protoc.* 8 (2), 430–437. doi:10.1038/nprot.2012.153

Hay, D. C., Fletcher, J., Payne, C., Terrace, J. D., Gallagher, R. C., Snoeys, J., et al. (2008a). Highly efficient differentiation of hESCs to functional hepatic endoderm requires ActivinA and Wnt3a signaling. *Proc. Natl. Acad. Sci. U. S. A.* 105 (34), 12301–12306. doi:10.1073/pnas.0806522105

Hay, D. C., Zhao, D., Fletcher, J., Hewitt, Z. A., McLean, D., Urruticoechea-Uriguen, A., et al. (2008b). Efficient differentiation of hepatocytes from human embryonic stem cells exhibiting markers recapitulating liver development *in vivo*. *Stem Cells* 26 (4), 894–902. doi:10.1634/stemcells.2007-0718

Jagtap, M., Chandola, H. M., and Ravishankar, B. (2011). Clinical efficacy of Coleus forskohlii (Willd.) Briq. (Makandi) in hypertension of geriatric population. *Ayu* 32 (1), 59–65. doi:10.4103/0974-8520.85729

Jozefczuk, J., Prigione, A., Chavez, L., and Adjaye, J. (2011). Comparative analysis of human embryonic stem cell and induced pluripotent stem cell-derived hepatocyte-like

cells reveals current drawbacks and possible strategies for improved differentiation. *Stem Cells Dev.* 20 (7), 1259–1275. doi:10.1089/scd.2010.0361

Kamiya, A., Kinoshita, T., and Miyajima, A. (2001). Oncostatin M and hepatocyte growth factor induce hepatic maturation via distinct signaling pathways. *FEBS Lett.* 492 (1-2), 90–94. doi:10.1016/s0014-5793(01)02140-8

Lee, K. L., Lim, S. K., Orlov, Y. L., Yit le, Y., Yang, H., Ang, L. T., et al. (2011). Graded Nodal/Activin signaling titrates conversion of quantitative phospho-Smad2 levels into qualitative embryonic stem cell fate decisions. *PLoS Genet.* 7 (6), e1002130. doi:10.1371/journal.pgen.1002130

Lehmann, J. M., McKee, D. D., Watson, M. A., Willson, T. M., Moore, J. T., and Kliewer, S. A. (1998). The human orphan nuclear receptor PXR is activated by compounds that regulate CYP3A4 gene expression and cause drug interactions. *J. Clin. Invest.* 102 (5), 1016–1023. doi:10.1172/jci3703

Lindner, E., Dohadwalla, A. N., and Bhattacharya, B. K. (1978). Positive inotropic and blood pressure lowering activity of a diterpene derivative isolated from Coleus forskohli: forskolin. *Arzneimittelforschung* 28 (2), 284–289.

Martignoni, M., Groothuis, G. M., and de Kanter, R. (2006). Species differences between mouse, rat, dog, monkey and human CYP-mediated drug metabolism, inhibition and induction. *Expert Opin. Drug Metab. Toxicol.* 2 (6), 875–894. doi:10.1517/17425255.2.6.875

Martínez-Jiménez, C. P., Jover, R., Donato, M. T., Castell, J. V., and Gómez-Lechón, M. J. (2007). Transcriptional regulation and expression of CYP3A4 in hepatocytes. *Curr. Drug Metab.* 8 (2), 185–194. doi:10.2174/138920007779815986

Matz, P., Wruck, W., Fauler, B., Herebian, D., Mielke, T., and Adjaye, J. (2017). Footprint-free human fetal foreskin derived iPSCs: a tool for modeling hepatogenesis associated gene regulatory networks. *Sci. Rep.* 7 (1), 6294. doi:10.1038/s41598-017-06546-9

Mayati, A., Moreau, A., Le Vée, M., Bruyère, A., Jouan, E., Denizot, C., et al. (2018). Functional polarization of human hepatoma HepaRG cells in response to forskolin. *Sci. Rep.* 8 (1), 16115. doi:10.1038/s41598-018-34421-8

Mitchell, A. M., Bridges, J. W., and Elcombe, C. R. (1984). Factors influencing peroxisome proliferation in cultured rat hepatocytes. *Arch. Toxicol.* 55 (4), 239–246. doi:10.1007/bf00341018

Moreau, A., Vilarem, M. J., Maurel, P., and Pascussi, J. M. (2008). Xenoreceptors CAR and PXR activation and consequences on lipid metabolism, glucose homeostasis, and inflammatory response. *Mol. Pharm.* 5 (1), 35–41. doi:10.1021/mp700103m

Nell, P., Kattler, K., Feuerborn, D., Hellwig, B., Rieck, A., Salhab, A., et al. (2022). Identification of an FXR-modulated liver-intestine hybrid state in iPSC-derived hepatocyte-like cells. *J. Hepatol.* 77 (5), 1386–1398. doi:10.1016/j.jhep.2022.07.009

Ogawa, S., Surapisitchat, J., Virtanen, C., Ogawa, M., Niapour, M., Sugamori, K. S., et al. (2013). Three-dimensional culture and cAMP signaling promote the maturation of human pluripotent stem cell-derived hepatocytes. *Development* 140 (15), 3285–3296. doi:10.1242/dev.090266

Peaslee, C., Esteva-Font, C., Su, T., Munoz-Howell, A., Duwaerts, C. C., Liu, Z., et al. (2021). Doxycycline significantly enhances induction of induced pluripotent stem cells to endoderm by enhancing survival through protein kinase B phosphorylation. *Hepatology* 74 (4), 2102–2117. doi:10.1002/hep.31898

Rashidi, H., Luu, N. T., Alwahsh, S. M., Ginai, M., Alhaque, S., Dong, H., et al. (2018). 3D human liver tissue from pluripotent stem cells displays stable phenotype *in vitro* and supports compromised liver function *in vivo*. *Arch. Toxicol.* 92 (10), 3117–3129. doi:10.1007/s00204-018-2280-2

Repa, J. J., and Mangelsdorf, D. J. (2000). The role of orphan nuclear receptors in the regulation of cholesterol homeostasis. *Annu. Rev. Cell Dev. Biol.* 16, 459–481. doi:10.1146/annurev.cellbio.16.1.459

Rodrigues, J. S., Faria-Pereira, A., Camões, S. P., Serras, A. S., Morais, V. A., Ruas, J. L., et al. (2022). Improving human mesenchymal stem cell-derived hepatic cell energy metabolism by manipulating glucose homeostasis and glucocorticoid signaling. *Front. Endocrinol. (Lausanne)* 13, 1043543. doi:10.3389/fendo.2022.1043543

Sapio, L., Gallo, M., Illiano, M., Chiosi, E., Naviglio, D., Spina, A., et al. (2017). The natural cAMP elevating compound forskolin in cancer therapy: is it time? *J. Cell Physiol.* 232 (5), 922–927. doi:10.1002/jcp.25650

Sauer, V., Tchaikovskaya, T., Wang, X., Li, Y., Zhang, W., Tar, K., et al. (2016). Human urinary epithelial cells as a source of engraftable hepatocyte-like cells using stem cell technology. *Cell Transpl.* 25 (12), 2221–2243. doi:10.3727/096368916x692014

Sayaf, K., Zanotto, I., Russo, F. P., Gabbia, D., and De Martin, S. (2021). The nuclear receptor PXR in chronic liver disease. *Cells* 11 (1), 61. doi:10.3390/cells11010061

Seamon, K. B., Padgett, W., and Daly, J. W. (1981). Forskolin: unique diterpene activator of adenylate cyclase in membranes and in intact cells. *Proc. Natl. Acad. Sci. U. S. A.* 78 (6), 3363–3367. doi:10.1073/pnas.78.6.3363

Sinal, C. J., Tohkin, M., Miyata, M., Ward, J. M., Lambert, G., and Gonzalez, F. J. (2000). Targeted disruption of the nuclear receptor FXR/BAR impairs bile acid and lipid homeostasis. *Cell* 102 (6), 731–744. doi:10.1016/s0092-8674(00)00062-3

Stofan, M., and Guo, G. L. (2020). Bile acids and FXR: novel targets for liver diseases. *Front. Med.* 7, 544. doi:10.3389/fmed.2020.00544

Glossary

h	hour
ALB	Albumin
AFP	Alpha-Fetoprotein
DE	Definitive endoderm
Dex	Dexamethasone
ECAD	E Cadherin
FXR	Farnesoid X receptor
Fig	Figure
Forsko	Forskolin
GSK-3	Glycogen synthase kinase 3
HBSS	Hanks buffered salt solution
HE	Hepatic endoderm
HGF	Hepatocyte growth factor
HLCs	Hepatocyte-like cells
HNF4a	Hepatocyte nuclear factor 4alpha
IgG	Immunoglobulin G
ICG	Indocyanine Green
iPSCs	induced pluripotent stem cells
kDa	kilo Dalton
min	minutes
OCT4	octamer-binding transcription factor 4
OSM	Oncostatin M
PFA	Paraformaldehyde
P/S	Penicillin/Streptomycin
PAS	reaction periodic acid-schiff reaction
PBS −/−	Phosphate buffered saline without calcium and magnesium
PXR	pregnane X receptor
prot	protocol
R.L.U	Relative light units
RPL0	Ribosomal Protein Lateral Stalk Subunit P0
SOX	SRY-related HMG-box genes
TBS-T	Tris-buffered saline with Tween20
TPB	Tryptose phosphate broth
WNT	Wingless-related integration site

4.4. DPP4 inhibition affects metabolism and inflammation associated pathways in hiPSC-derived steatotic HLCs

Christiane Loerch, Wasco Wruck, Julian Reiss, James Adjaye, Nina Graffmann

BioRxiv, Article number 2024.11.06.622222

Abstract:

Background: Metabolic dysfunction-associated steatotic liver disease (MAFLD) has a high prevalence and high co-morbidity for other diseases. Due to the complexity of this multifactorial disease, therapy options are still rather limited. We employed an *in vitro* pluripotent stem cell-based model to decipher potential disease-associated molecular pathways and to study the mode of action of prospective drugs. Dipeptidyl peptidase 4 (DPP4) or Cluster of differentiation 26 (CD26) is involved in inflammation, infections, immune disorders, type 2 diabetes, kidney disease and cancer. **Methods:** We induced the steatosis phenotype in human induced pluripotent stem cell (iPSC) derived hepatocyte-like cells (HLCs) by oleic acid (OA)-feeding and confirmed regulation of clinically relevant pathways by NGS-based global transcriptomic analyses. Analysis of the secretome of steatotic HLCs revealed DPP4 as a potential key mediator of the disease. To further elucidate its role in the development of MAFLD, we inhibited DPP4 activity with Vildagliptin (VILDA) and analyzed the global transcriptome changes as well as specific gene and protein expression of steatosis-associated genes with and without DPP4 inhibition. **Results:** MAFLD-associated pathways such as PPAR- and TNF signaling were differentially regulated in hiPSC-derived steatotic HLCs. We found increased hepatic DPP4 activity and secretion upon OA. Gene expression of fatty acid and purine metabolism and inflammation-associated pathways were regulated upon DPP4 inhibition. **Conclusions:** Our HLC-model confirmed association of DPP4 with metabolism and inflammation which foster the development of MAFLD. Inhibiting DPP4 with VILDA partially relieved the steatotic phenotype on a global transcriptomic level.

Author contribution: (80%) of C.L. included:

- Conceptualization of the project together with N.G. and J.A.
- Investigation and methodology together with N.G.
- Conduction of experiments (cell culture, hepatocyte-like cell differentiation and characterization, steatosis induction, drug treatment, molecular biological and biochemical analyses)

- Analysis of transcriptome data together with W.W., N.G. and J.A.
- Data curation and visualization
- Writing the original draft together with N.G.
- Reviewing and editing of the manuscript together with N.G. and J.A.
- Modifications of the manuscript during revision process together with N.G. and J.A.
- Response to the reviewers together with N.G. and J.A.

Status: Under revision at Frontiers in Cell and Developmental Biology, to be published as open access article under open access CC BY license. Available as Preprint on BioRxiv. **DOI:** 10.1101/2024.11.06.622222

DPP4 inhibition affects metabolism and inflammation associated pathways in hiPSC-derived steatotic HLCs

Christiane Loerch[1], Wasco Wruck[1], Julian Reiss[1], James Adjaye[1,2], Nina Graffmann[1]

[1]Institute for Stem Cell Research and Regenerative Medicine, Medical Faculty and University Hospital Düsseldorf, Heinrich Heine University, Düsseldorf, Germany

[2]University College London, EGA Institute for Women`s Health, Zayed Center for Research into Rare Diseases in Children (ZGR), London, United Kingdom

*** Correspondence:**

PD Dr. Nina Graffmann

Institute for Stem Cell Research and Regenerative Medicine

University Hospital Düsseldorf

Gebäude 14.80

Moorenstr. 5, 40225 Düsseldorf, Germany

Telephone: 0049211 8119835, Telefax: 0049211 8117858

e-mail: nina.graffmann@med.uni-duesseldorf.de

Keywords: human induced pluripotent stem cells, Hepatocyte-like cells, Dipeptidyl peptidase 4 (DPP4), Cluster of Differentiation 26 (CD26), MAFLD, MASLD, NAFLD, Steatosis, Diabetes, Vildagliptin

Abstract

Background: Metabolic dysfunction-associated steatotic liver disease (MAFLD) has a high prevalence and high co-morbidity for other diseases. Due to the complexity of this multifactorial disease, therapy options are still rather limited. We employed an *in vitro* pluripotent stem cell-based model to decipher potential disease-associated molecular pathways and to study the mode of action of prospective drugs. Dipeptidyl peptidase 4 (DPP4) or Cluster of differentiation 26 (CD26) is involved in inflammation, infections, immune disorders, type 2 diabetes, kidney disease and cancer.

Methods: We induced the steatosis phenotype in human induced pluripotent stem cell (iPSC) derived hepatocyte-like cells (HLCs) by oleic acid (OA)-feeding and confirmed regulation of clinically relevant pathways by NGS-based global transcriptomic analyses. Analysis of the secretome of steatotic HLCs revealed DPP4 as a potential key mediator of the disease. To further elucidate its role in the development of MAFLD, we inhibited DPP4 activity with Vildagliptin (VILDA) and analyzed the global transcriptome changes as well as specific gene and protein expression of steatosis-associated genes with and without DPP4 inhibition.

Results: MAFLD-associated pathways such as PPAR- and TNF signaling were differentially regulated in hiPSC-derived steatotic HLCs. We found increased hepatic DPP4 activity and secretion upon OA. Gene expression of fatty acid and purine metabolism and inflammation-associated pathways were regulated upon DPP4 inhibition.

Conclusions: Our HLC-model confirmed association of DPP4 with metabolism and inflammation which foster the development of MAFLD. Inhibiting DPP4 with VILDA partially relieved the steatotic phenotype on a global transcriptomic level.

Impact and implications:

Given the difficulties of identifying suitable anti-MAFLD drugs, novel model systems are urgently needed. Our *in vitro* HLC-model reproduced DPP4-dependent aspects of the disease and responded positively to Vildagliptin treatment. Further elucidation of the role of DPP4 in the etiology of MAFLD and other diseases is warranted.

Background

Steatotic liver diseases are an increasing health burden for industrialized countries all over the globe(1-4). Early, reversible stages involve steatosis and steatohepatitis, resulting in fibrosis, while nascent cirrhosis and hepatocellular carcinoma are non-reversible and life-threatening. Primary causes for steatosis are elevated fatty acid flux from adipose tissue, a high-fat diet, or elevated blood glucose levels. Thus, obesity and Type 2 diabetes mellitus (T2DM) are direct diagnostic criteria for Metabolic dysfunction-associated fatty/steatotic liver disease (MAFLD/MASLD)(2) . MAFLD is a complex, multisystem disease, with serious implications on the whole body, including cardiovascular disease and chronic kidney diseases(5, 6). Moreover, its multifactorial character and tissue heterogeneity is not only found in the clinic but is also shown in the molecular response to steatosis(7-9). These factors complicate research and to date resmetirom is the only FDA approved drug for treating MASLD(6, 10, 11).

Dipeptidyl peptidase 4 (DPP4) is a serine protease with catalytic activity for various substrates(12). The most prominent ones are the incretins- Glucagon like peptide 1 (GLP-1) and Glucose-dependent insulinotropic polypeptide (GIP1). However, DPP4 not only interferes with incretin signaling, but also cleaves chemotactic peptides with implications for the inflammatory response(12, 13). It is therefore considered a hepatokine, upregulated in metabolic liver disease and a driver of inflammation(13). Furthermore, DPP4 is known to be involved in various etiologies, such as immune disorders, fibrosis and cancer(14). Gliptins -potent DPP4 inhibitors- are used for the treatment of T2DM, prolonging the postprandial incretin answer(13, 15-17). Vildagliptin (VILDA) shows additional protective effects on hepatocytes by reducing hepatic triglyceride load as well as aminotransferase levels(18). Since the inflammatory

response was reduced, it might interfere with the traits towards steatohepatitis, thus indicating a beneficial effect on the progression of the disease(19, 20).

In this study, we differentiated human patient-derived induced pluripotent stem cells (iPSCs) to hepatocyte-like cells (HLCs) by using our previously published, efficient 2D differentiation protocol(21). We induced the steatosis phenotype and provide insights into the hepatocyte-specific contribution to the disease and the potential role of DPP4 for the interplay between metabolism and inflammation.

Methods

Human induced pluripotent stem cell (iPSC) culture and hepatocyte-like cell (HLC) differentiation:

The use of iPSC lines for this study was approved by the ethics committee of the medical faculty of Heinrich-Heine University under the numbers 5013 and 5704. iPSCs were cultivated on Matrigel (Corning) coated 6-well plates with daily changes of StemMACs medium (Miltenyi). Once iPSCs attained 90% confluency, they were colony-split by addition of PBS w/o magnesium or calcium (PBS-/-) (Gibco) and incubated for approximately 3 min at room temperature (RT). Colonies were detached from the surface with a cell scraper and centrifuged at 40 *xg* for 3 min. The pellet was carefully resuspended and clumps of colonies were seeded in a ratio of 1:6.

iPSCs were differentiated according to our previously published protocol(21). In brief, 1.04 x10^5 iPSCs/ cm^2 were seeded onto Matrigel-coated dishes. Definitive endoderm (DE) was induced by 1-3 days of 2.5 µM CHIR99021 (Stemgent) and 3-5 days of 100 ng/ml Activin A (Peprotech) in RPMI medium. Hepatic endoderm (HE) medium was fed for 4 days, and 1% DMSO was added with medium changes every day. HLC medium was fed for 12-15 days, with medium changes every other day. 1 µM insulin

(Sigma-Aldrich), 10 ng/mL hepatocyte growth factor (HGF) (Peprotech), 25 ng/ml dexamethasone (Dex) (Sigma-Aldrich), and 20 ng/mL recombinant human Oncostatin M (rhOSM209a.a) (Immunotools) were freshly added to the medium.

Table 1: iPSC lines used in this study.

iPSC line	Sex	Age (years)	Disease	Source	Ref.
Cntrl 1	male	50	healthy	urine derived renal progenitor cells	(22)
Cntrl 2	female	19	healthy	dermal fibroblasts	(23)
Stea 1	male	61	high grade steatosis	dermal fibroblasts	(24)
Stea 2	female	58	high grade steatosis	dermal fibroblasts	(25)

Immunocytochemistry:

Cells were washed with PBS-/-, fixed with 4% PFA for 10 min at RT, and washed 3x with PBS-/-. For intracellular staining, the cells were permeabilized with 0.5% Triton-X-100 (Sigma-Aldrich) in PBS-/- for 10 min at RT, and blocked with 3% BSA in PBS-/- for 1 h at RT. After incubation with primary antibodies (Supplementary material) at respective dilutions (table S2) overnight at 4°C, unbound antibodies were washed off 3x with PBS-/-. Secondary antibodies against the respective host IgG were incubated for 1 h at RT and washed 3x with PBS-/-. (Confocal) microscopy was performed, using a LSM 700 microscope (Zeiss) and images were processed with ZEN software (Zeiss).

Quantitative reverse transcription PCR (qRT-PCR) :

RNA was isolated using the Direct-zol RNA isolation kit (Zymo Research), following the manufacturer's instructions. 500 ng of RNA was reverse transcribed to cDNA using the TaqMan reverse transcription kit (Life technologies). qRT-PCR was performed using the VIIA7 machine and the power SYBR green master mix (all Life technologies). Expression of mRNA was presented as log2-fold-change in comparison to the housekeeping gene and the control condition (primer sequences are found in the supplementary material table S1).

Western Blot:

Cells were lysed in RIPA buffer containing protease and phosphatase inhibitors (all Sigma-Aldrich). 15 - 30 µg proteins were separated on NuPAGE 4 to 12% Bis-Tris protein gels (Life Technologies) and wet-blotted onto 0.45 µm nitrocellulose membranes (Amersham). After blocking with 5% non-fat milk (ROTH) in TBS-T buffer, the membranes were incubated with the respective primary antibodies (Supplementary material, table S2) overnight at 4 °C. After 3x washing with TBS-T buffer, fluorescence labeled secondary antibodies (Licor) against the host IgG were incubated for 1 h at RT at a 1:10000 dilution. Unbound antibodies were washed off with TBS-T buffer and the fluorescence signal was detected at 680 nm and 800 nm by using the ChemiDoc MP Imaging system (Bio-Rad). Quantification was performed using the Image Lab 6.0.1 software with lane background subtraction using disk size 1.

Cytochrome P450 activity measurement:

P450-Glo™ CYP3A4 and CYP2D6 assays (Promega) were used to measure Cytochrome P450 activity. Cells were incubated with 3 µM Luciferin-IPA or 10 µM

Luciferin-ME EGE, respectively, in William`s E Medium (Gibco) for 1 h at 37 °C. After incubation with the detection reagent, luminescence was measured in technical triplicates with a luminometer (Lumat LB 9507, Berthold Technologies).

Steatosis induction by OA-feeding and Vildagliptin (VILDA) treatment:

Oleic acid (Calbiochem) was bound to 14% (w/v) fatty acid free BSA (ROTH) in 0.1 M TRIS pH 8.0 for 1 h at 37 °C, and stored at 4 °C. After testing different concentrations and time periods of OA treatment, we selected 400 µM OA for 7 days to induce steatosis. From day 15-17 of HLC differentiation on, the cells were fed with complete HLC medium, supplemented with 400 µM OA or the respective volume of TRIS-BSA as mock-treatment. The medium was changed every other day for 7 days. A final concentration of 30µM VILDA (Sigma-Aldrich) dissolved in DMSO was fed to the cells after 48 h OA-/mock-induction for 5 days with medium changes every other day.

Next generation sequencing and analysis of deep sequencing data:

3`RNA-Seq was performed on a NextSeq2000 sequencing system (Ilumina) at the core facility Biomedizinisches Forschungszentrum Genomics and Transcriptomics laboratory (BMFZ-GTL) of Heinrich-Heine University Duesseldorf. The HISAT2 (version 2.1.0) software(26) was employed to align the fastq files received from the BMFZ-GTL core facility against the GRCh38 genome. For detailed description of the integration of the data please refer to the supplementary material, methods section.

GO and pathway analysis:

Subsets of genes expressed exclusively in one condition in the Venn diagram analysis and up- and down-regulated genes according to the criteria for differentially expressed genes (limma test, p-value <0.05 and fold change >1.5) (were subjected to over-representation analysis of gene ontologies (GOs) and KEGG (Kyoto Encyclopedia of Genes and Genomes) pathways(27). The hypergeometric test built-in in the R base package was used for over-representation analysis of KEGG pathways, which had been downloaded from the KEGG database in February 2023. The GOstats R package(28) was employed to determine over-represented GO terms. The most significant GO terms and KEGG pathways were displayed in dotplots via the R package ggplot2(29).

Enzyme-linked Immunosorbent assay (ELISA):

Secreted DPP4 was detected from supernatants 48 h after feeding using the human DPP4/CD26 DuoSet ELISA (R&D Systems) as described by the manufacturer. Optical density was measured using the EPOCH2 spectrophotometer (BioTek) at 450 nm with wavelength correction at 540 nm. 4-PL curve fitting was performed to calculate concentrations.

Enzyme activity assay:

DPP4 activity was measured in OA-/ VILDA-treated HLCs, using the Dipeptidyl peptidase IV (DPP4) Activity Assay Kit (Fluorometric) (Abcam), following the manufacturer's instructions. Fluorescence signal was measured on a Spectrophotometer (Tecan) at Ex/Em = 360/460 nm.

Cytokine array:

Supernatants of three biological replicates were harvested 24 h after medium change and Proteome Profiler Human XL Cytokine array (R&D Systems) analysis was performed following the manufacturer's protocol and signals were detected, using the Fusion FX instrument (PeqLab). Analysis and quantification was performed using the FIJI/ImageJ software(30) and the Microarray Profile plugin by Bob Dougherty and Wayne Rasband (https://www.optinav.info/MicroArray_Profile.htm, accessed on 21 December 2022). For details of the image analysis and follow-up normalization in the R/Bioconductor environment(31) we refer to the description in our previous publication(32). Cytokines were considered differentially expressed satisfying the criteria: detection p-value < 0.05 in at least one condition, fold change > 1.2 and limma-p-value < 0.05. The function heatmap.2 from the gplots package(33) and the R-builtin function barplot were applied for heatmap and bar plots.

Statistics:

Student's unpaired two-tailed t-test or ordinary one- or two-way ANOVA followed by Tukey's, Dunnet's, or Sidak's multiple comparison test were conducted to calculate significances using GraphPad Prism 8.0.2 software.

Results

iPSCs-derived hepatocyte-like cell (HLC) differentiation from four individuals

Induced pluripotent stem cells (iPSCs) derived from four individuals, two healthy controls (Cntrl 1, Cntrl 2)(22, 23) and two steatosis patients (Stea 1, Stea 2)(24,

25)(Table 1), were differentiated into HLCs following our recently published protocol(21). Representative immunocytochemistry of Cntrl 2 shows the expression of Octamer binding transcription factor 4 (OCT4) in iPSCs, SRY-box transcription factor 17 (SOX17) in definitive endoderm (DE), and Alpha-fetoprotein (AFP) in hepatic endoderm (HE) (Fig. 1A). HLCs were stained for the epithelial marker E-Cadherin (E-CAD), Hepatocyte nuclear factor 4 alpha (HNF4a) and Albumin (ALB) (Fig.1A). Representative pictures of the other cell lines are provided in the supplementary material section (Fig. S1 and S2A-C). HLCs showed significant increase of gene expression of the HLC-markers *ALB* and Cytochrome P450 family members *CYP3A4* and *CYP2D6* in comparison to the iPSC-stage (Fig. 1B). Representative gene expression of *OCT4* and *SOX17* in DE, as well as *AFP* in HE stage is provided in Fig. S2D. Protein expression of AFP and ALB is shown in comparison to the housekeeping protein beta-Actin (bActin) in HLCs derived from Cntrl 1 and Cntrl 2 (Fig. 1C). HLCs' functionality was confirmed by measuring CYP3A4 and CYP2D6 activity for the four cell lines (Fig. 1D).

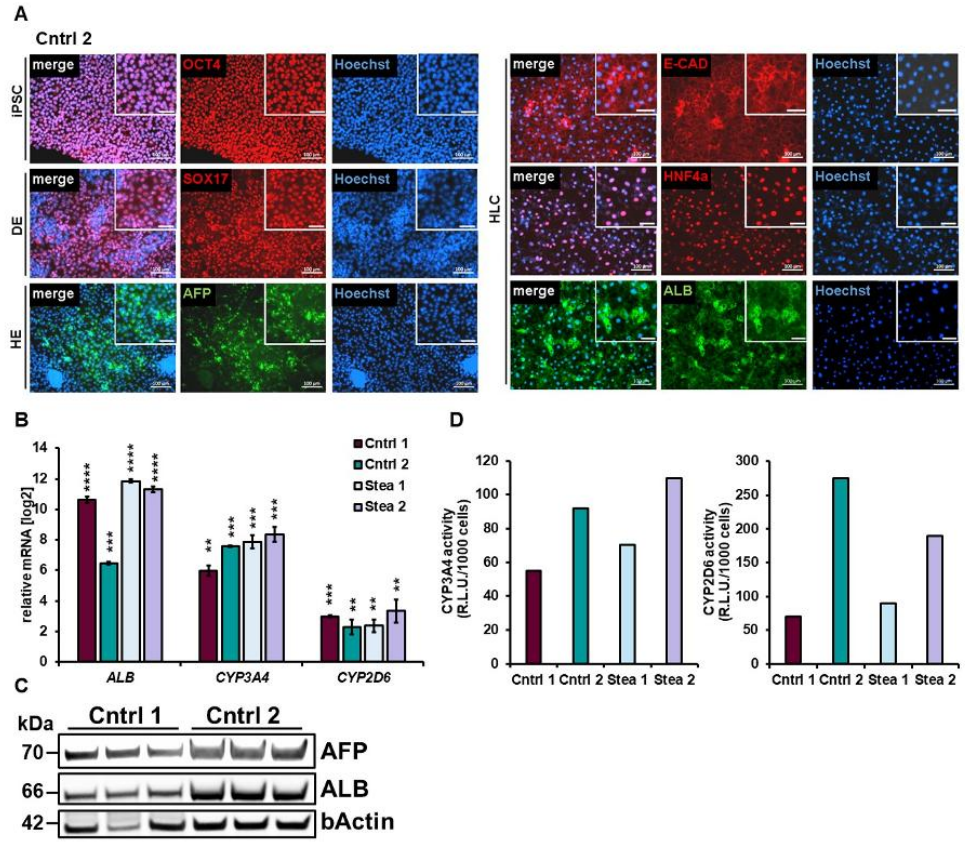

Fig. 1 Characterization of HLCs. (A) Representative immunocytochemistry of cell line Cntrl 2 during differentiation showing respective markers OCT4 in iPSCs, SOX17 in definitive endoderm (DE), and AFP in hepatic endoderm (HE). For hepatocyte-like cells (HLCs), the epithelial marker E-CAD, HNF4a and ALB are shown. Scale bars = 100 µm. **(B)** Gene expression of *ALB* and Cytochrome P450 family members *CYP3A4* and *CYP2D6* in HLCs (n=3) derived from four cell lines in comparison to iPSC-stage (n=2), shown in means of two or three biological replicates ±SE respectively, normalized to the housekeeping gene *RPLP0*. Two-tailed unpaired students' T-test was performed to calculate significances (*p < 0.05, **p < 0.01, ***p < 0.001). **(C)** Cropped WB of AFP, ALB and bActin in HLCs derived from Cntrl 1 and Cntrl 2 (n=3). Uncropped full-length blots can be found in the supplementary Fig. S9. **(D)** Representative cytochrome P450 activity of HLCs is for CYP3A4 and CYP2D6 in relative light units (R.L.U.) per 1000 cells in technical triplicates (n=3).

Oleic acid (OA) induces steatosis phenotype in HLCs

To induce the steatosis phenotype in iPSC-derived HLCs, we treated HLCs of all four cell lines on day 15-17 of differentiation with 400 µM oleic acid (OA) for 7 days. After OA induction, we detected the formation of Perilipin-2 (PLIN2) coated lipid droplets by immunocytochemistry in all cell lines (Fig. 2A/B and Fig. S3). Interestingly, from a visual impression, it seemed that Cntrl 1 showed less lipid droplets than Cntrl 2, indicating a cell line specific difference in the build-up of lipid droplets. In accordance with previous findings, we did not detect a disease specific difference in the lipid load w or wo OA, but rather a cell line specific effect(7). Previous findings indicated distinct gene expression profiles in response to OA-treatment related to the steatosis background of HLCs. To put these observations in perspective, we analyzed the global transcriptomic changes upon OA induction.

RNA-seq was performed and revealed gene expression clustering according to the treatment and based on the genetic background of each cell line (Fig. 2C). However, two samples of HLCs derived from cell line Stea 2, clustered ambiguously, (Fig. 2C, red asterisks). To prevent biases due to the genetic background of this cell line, we excluded Stea 2 in subsequent analysis. We identified 15,705 genes expressed in common in both conditions in cell lines Cntrl 1, Cntrl 2 and Stea 1, while 437 genes were exclusively expressed under OA in comparison to 393 genes solely expressed genes under mock treatment. Combining the exclusively expressed genes and genes expressed in common, we found 1,147 genes significantly upregulated and 884 genes significantly downregulated (Fig. 2D) after OA treatment. KEGG-associated pathway analysis revealed, among others, genes of the glutathione pathway and metabolic pathways significantly downregulated upon OA-treatment throughout Cntrl 1, Cntrl 2 and Stea 1 cell lines (Fig. 2E). Confirming results from a previous study(7), we found

genes associated with KEGG pathways of Peroxisome proliferator activated-receptor (PPAR)-, Adenosine monophosphate-activated protein kinase (AMPK)-signaling and fatty acid metabolism significantly upregulated (Fig. 2F). Furthermore, we detected genes belonging to inflammation-related pathways significantly upregulated upon OA, such as Tumor necrosis factor (TNF) signaling and NF-kappa-B pathway. Interestingly, also genes of the inflammatory bowel disease and insulin resistance pathways were upregulated upon OA (Fig. 2F). This KEGG-associated pathway analysis confirmed the induction of the steatosis phenotype by OA supplementation in the three cell lines Cntrl 1, Cntrl 2 and Stea 1. We performed Pearson's correlation heatmap analysis of genes associated with relevant KEGG-pathways (Fig. 3A). Notably, this revealed a change of clustering according to the treatment and independent of the genotype, indicating the relevance of these genes for the phenotype. Taken together, global transcriptomic analyses of Cntrl1, Cntrl2, and Stea1 cell lines confirmed successful steatosis induction but did not reveal an altered susceptibility of the patient derived cells.

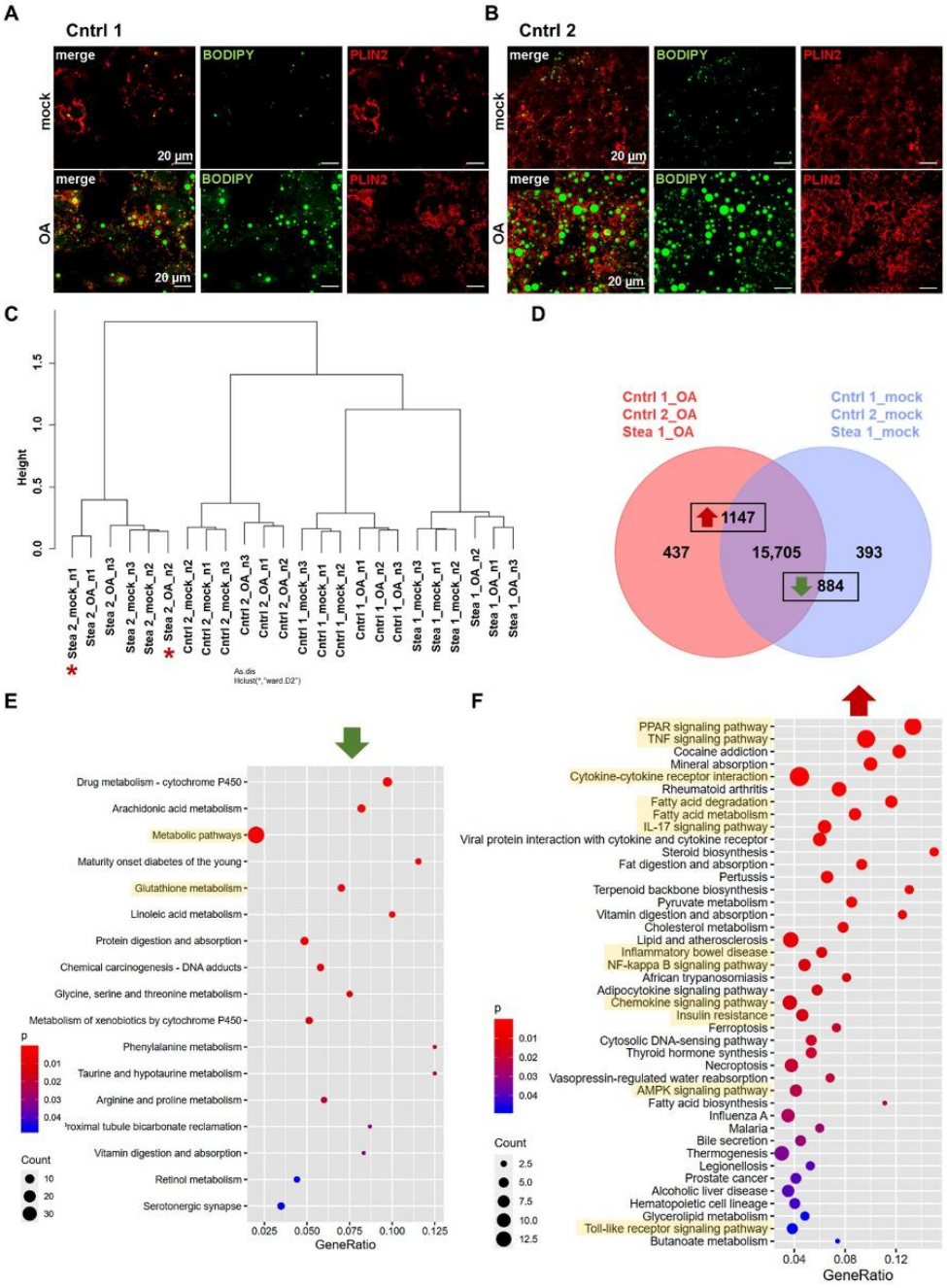

Fig. 2 Confirmation of steatosis phenotype in HLCs. (A/B) Representative immunofluorescence and BODIPY 493/503 staining of HLCs derived from Cntrl 1 and

Cntrl 2 treated with 400 µM OA and respective control (mock) for 7 days, PLIN2 is shown in red, fatty acids are stained in green. Scale bars = 20 µm. **(C)** Hierarchical cluster dendrogram of global transcriptomic changes upon OA treatment of HLCs derived from cell lines Cntrl 1, Cntrl 2, Stea 1, Stea 2 in three biological replicates (n=3). Ambiguous clustering of gene expression in Stea 2 is marked by red asterisks (correlation in supplementary material table 1). **(D)** Venn diagram of gene expression from OA treated HLCs derived from cell lines Cntrl 1, Cntrl 2, Stea 1 indicating 437 solely expressed genes upon OA, and 393 solely expressed genes upon mock treatment and 15,705 genes expressed in common. Among exclusively and commonly expressed genes 1,147 and 834 genes were significantly up- and down-regulated, respectively. **(E/F)** Dot plots of KEGG-associated pathway analysis of significantly down **(E)**- and up **(F)**-regulated genes (gene lists in supplementary table S3).

To confirm the global gene expression changes, we performed qRT-PCR for genes associated with relevant pathways (Fig. 3B). We found significant increases of PPAR-pathway associated genes, *PLIN2* and fatty acid binding protein-1 (*FABP1)* upon OA-treatment in at least 2 out of our 3 cell lines. Regarding insulin signaling associated genes, phosphoenolpyruvate carboxykinase-1 (*PCK1*) was significantly upregulated in Cntrl 2, and a non-significant trend towards upregulation was detectable in Cntrl 1 and Stea 1. Carnitine palmitoyltransferase-1A (*CPT1A*) was significantly upregulated in Cntrl 1 and 2. Interestingly, in contrast to the RNA-seq results, insulin-like growth factor binding protein-1 (*IGFBP1)* showed a tendency to upregulation upon OA, however not significantly. Considering genes associated with inflammation, a significant upregulation of CC-chemokine ligand 4 (*CCL4*) and interleukin 1beta (*IL1B)* expression was detected in Cntrl 1 and Stea 1, while in Cntrl 2 the increase was not significant. We found a significant reduction in the expression of vascular cell adhesion molecule-1 (*VCAM1*) in Cntrl 2 and Stea 1. Furthermore, we found members of the renin-angiotensin-system (RAS) differentially regulated in our model. For example,

Angiotensin converting enzyme 2 (*ACE2*) tended to be upregulated in the RNA-seq data, a non-significant trend that could be confirmed by qRT-PCR. In addition, we detected a reduction of alanyl aminopeptidase (*ANPEP*), which is also involved in the glutathione metabolism (reactive oxygen species (ROS)-regulation), in all three cell lines, albeit only significantly in Stea 1. The tendency of up- and down-regulation of the qRT-PCR data in Fig. 3B confirms the direction of regulation in the RNAseq data. Together, these findings strengthen the validity of our model, because MAFLD-associated pathways were differentially regulated upon OA. They further underline the importance of the investigated genes as their differential expression was independent of the genetic background.

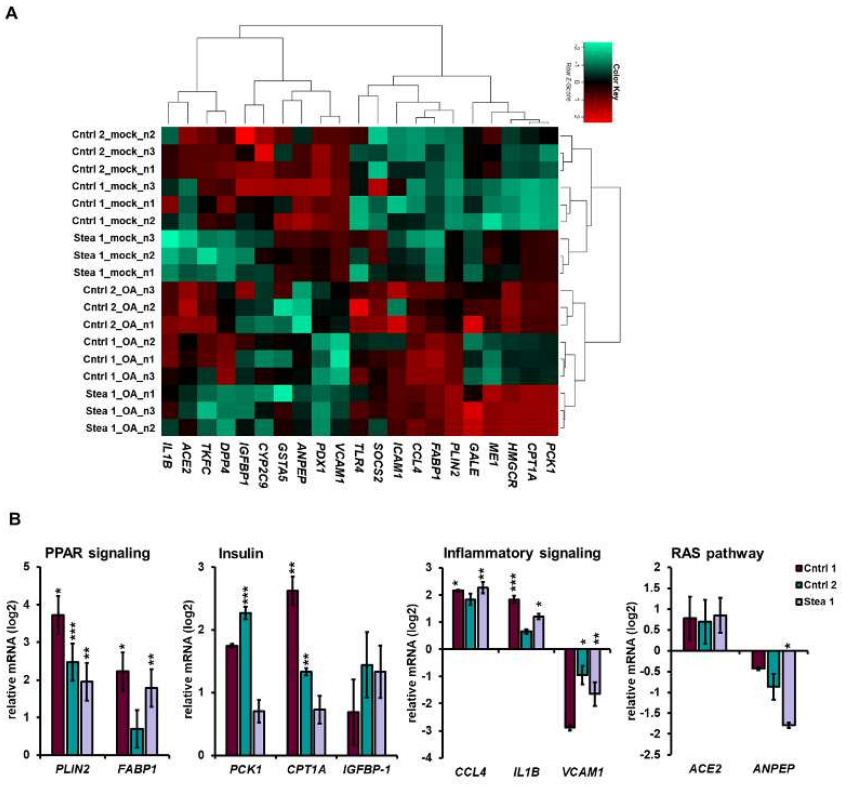

Fig. 3 OA-treatment induces differential gene expression. (A) Pearson's correlation heatmap analysis of the gene expression of members of OA-dysregulated

pathways like fatty acid metabolism (*PLIN2*, *FABP1*), metabolic pathways/ glutathione metabolism (*ANPEP, GSTA5*) and insulin resistance (*PCK1*, *CPT1A*, *IGFBP1*, *SERPINA7*, *PDX1*). **(B)** qRT-PCR analysis of the mRNA expression of *PLIN2*, *FABP1, PCK1*, *CPT1A*, *IGFBP1*, *CCL4*, *IL1B, VCAM1 ACE2*, and *ANPEP* relative to mock-treated HLCs from cell lines Cntrl 1, Cntrl 2 and Stea 1 normalized to mock-treated HLCs derived from each cell line as means of two or three biological replicates ± SE (n=2 or n=3), normalized to the housekeeping gene *RPLP0*. Two-tailed unpaired Student`s T-test was performed to calculate significances (*p < 0.05, **p < 0.01, ***p < 0.001).

Dipeptidyl peptidase 4 (DPP4) is secreted upon OA treatment

We analyzed the supernatant of OA-treated HLCs for released signaling proteins. Among others, we found a significant increase of DPP4, also known as Cluster of Differentiation 26 (CD26), upon OA-induction (Supp Fig. S4B/C). We confirmed this tendency of increase upon OA-treatment in Cntrl 1, Cntrl 2, and Stea 1 by ELISA (Fig. 4A) (0.95±0.11 ng/mL, 0.22±0.04 ng/mL, 2.51±0.27 ng/mL DPP4 under mock conditions and 3.94±0.38 ng/mL, 1.45±0.35 ng/mL, 5.53±0.02 ng/mL, under OA respectively).

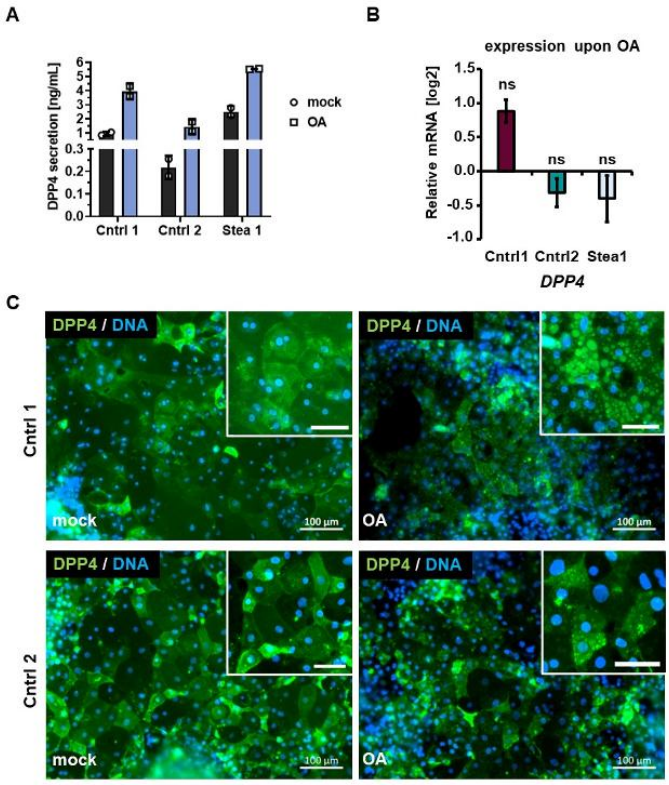

Fig. 4 DPP4 is secreted upon OA-treatment. (A) Secretion of Dipeptidyl peptidase (DPP4) upon OA-treatment measured by ELISA-detection, showing secreted DPP4 as the mean of two biological replicates (n=2 ±SD). **(B)** Gene expression of *DPP4* upon OA treatment relative to mock treatment in all cell lines, shown are means of three biological replicates, normalized to the housekeeping gene *RPLP0* (n=3 ±SE). Two-tailed unpaired Student`s T-test was performed to calculate significances (ns p> 0.05) between OA and mock treatment for each cell line. **(C)** Representative immunocytochemistry of DPP4 under mock and OA conditions in cell lines Cntrl 1 and Cntrl 2. Scale bars represent 100 µm and 50 µm in the zoom-in.

Interestingly, there was a greater increase of DPP4 secretion upon OA in cell lines derived from healthy individuals, compared to patient derived HLCs. DPP4 levels increased approximately 4.5- to 5-fold in Cntrl 1 and 2 while Stea 1 showed a DPP4

increase of 2-fold respectively. This indicates that the control cell lines are able to increase DPP4 secretion more strongly in response to OA. To gain insights into the mechanisms underlying upregulation of DPP4 upon OA-treatment, we analyzed the gene expression in the three cell lines, however we could not detect a significant change upon OA-induction (Fig. 4B). To elucidate the role of DPP4 in steatosis, we focused for further analyses on the Cntrl cell lines, because of the stronger induction of DPP4 secretion upon OA. Similar to the gene expression of *DPP4*, we did not detect a prominent change in the protein localization or amount upon OA (Fig. 4C).

Vildagliptin reduces DPP4 activity

Vildagliptin (VILDA) was tested in a phase-4 study (ID NCT01356381) to elucidate its potential use for treating steatosis patients(34). However, whether VILDA improves the hepatic phenotype directly or by incretin regulation, is yet to be elucidated. To shed light on its direct effects on hepatocytes, we induced the steatosis phenotype in our HLCs by a pre-treatment with OA for 48 h followed by incubation with 30 µM VILDA for a total of 5 days simultaneously with OA. We did not detect significant difference in *DPP4* expression on both the RNA and protein level upon the treatments in comparison to mock w/o VILDA (Fig. 5A-C), while we detected an expectedly strong increase for PLIN2 after OA induction in Cntrl 1 and 2 HLCs (Fig. 5B/C).

Considering the secretion of DPP4, we confirmed the previously detected increase of DPP4 upon OA w and w/o VILDA for both cell lines in comparison to the mock treatment. However, no significant difference upon VILDA treatment was detectable (Fig. 5D). Nevertheless, we detected a significant increase of DPP4 activity for both cell lines upon OA treatment which was significantly reduced when HLCs were treated with OA and VILDA together (Fig. 5 E). VILDA is capable of reducing DPP4 activity to

the level detected under mock conditions, with no significant difference between OA w VILDA and mock w/o VILDA. These findings confirm that VILDA mainly acts on DPP4 activity, and neither on its gene or protein expression, nor on its secretion.

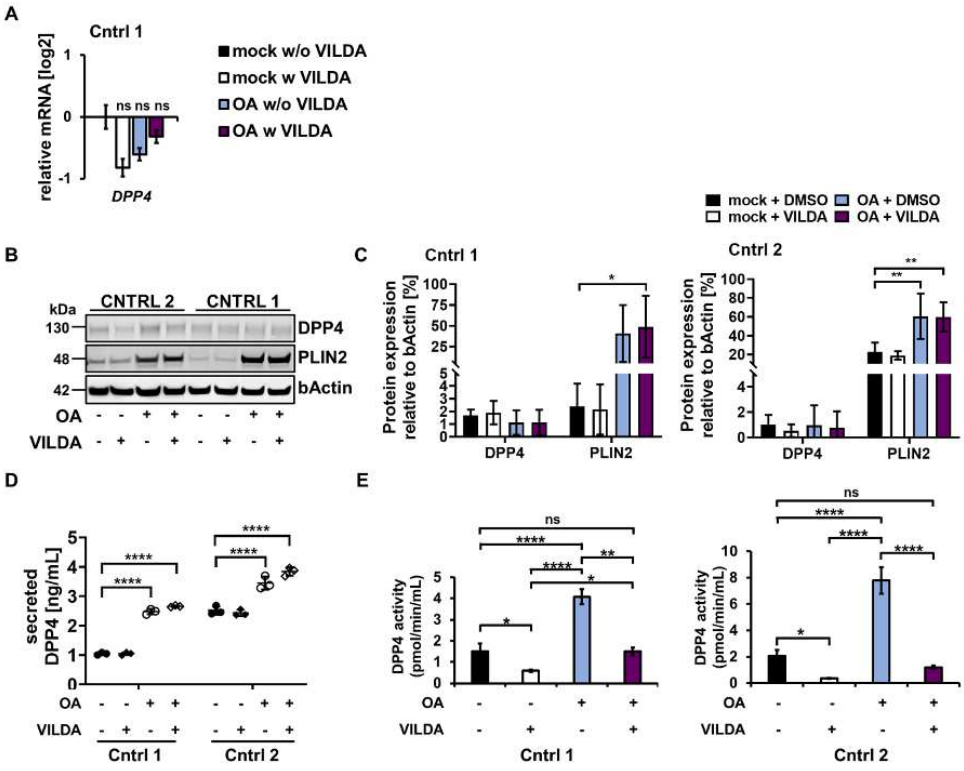

Fig. 5 Effects of VILDA on OA-induced HLCs. (A) Gene expression of *DPP4* in Cntrl 1 HLCs upon OA-treatment with (w) and without (w/o) 30 µM Vildagliptin (VILDA) for 5 days, in comparison to mock w/o VILDA, shown are means of three biological replicates, normalized to the housekeeping gene *RPLP0* (n=3 ±SE). Ordinary one-way ANOVA followed by Tukey's multiple comparisons was performed to calculate significances (ns p> 0.05). **(B)** Representative cropped WB of DPP4 and PLIN2 upon OA-treatment w and w/o VILDA. Uncropped full-length blots can be found in the supplementary Fig. S9. **(C)** Protein expression relative to bActin in comparison to mock w/o VILDA. Shown are means of three biological replicates (n=3 ± SD). Ordinary two-way ANOVA, followed by Tukey's multiple comparison test was performed to calculate significances (*p < 0.05, **p < 0.01). Uncropped full-length blots can be found in the

supplementary Fig. S9. **(D)** DPP4 secretion upon OA-treatment w and w/o VILDA. Shown are means of three biological replicates (n=3 ±SD). Ordinary two-way ANOVA, followed by Dunnet's multiple comparison test was performed to calculate significances (**p < 0.01, ***p < 0.001, ****p < 0.001). **(E)** DPP4 activity in HLCs upon OA-treatment w and w/o VILDA was analyzed by measuring the proteolytic activity over time. Ordinary one-way ANOVA and Tukey's multiple comparison test was performed to calculate significances (*p < 0.05, ****p < 0.001).

Inhibition of DPP4 activity might reduce inflammatory progression leading to the disease phenotype

To test whether VILDA further affects other genes involved in the steatosis phenotype, we analyzed the global gene expression upon OA w and w/o VILDA in cell line Cntrl 1. To gain first insights on potential effects of DPP4 inhibition, we selected Cntrl1 for in depth analysis by NGS which will give directions for the necessary follow up studies with other cell lines. First level dendrogram analysis revealed clustering according to mock- and OA-treatment, however not according to the VILDA treatment, indicating a stronger impact of OA on the gene expression in comparison to VILDA (Fig. S5A). To confirm the previously detected gene expression pattern in response to OA, we performed KEGG-associated pathway analysis of the gene expression upon OA w/o VILDA in comparison to mock w/o VILDA (Fig. S5B/C). Indeed, we found similar pathways to be differentially regulated upon OA w/o VILDA in comparison to the previous data, indicating that the solvent reagent had no impact on the OA-response (Fig. S5B/C).

In addition to the 14,118 genes expressed in common in all four conditions, we found exclusively expressed gene sets for every condition as indicated by Venn analysis (Fig. 6A). We found 91 and 339 exclusively expressed genes upon OA w VILDA and

mock w VILDA, respectively. 62 and 115 genes were exclusively expressed upon OA w/o VILDA and mock w/o VILDA treatment, respectively. KEGG- and Gene Ontologies (GO)- associated pathway analyses for the exclusively expressed genes upon the different conditions did not reveal characteristic profiles (Table S2), except for an exclusive expression of genes associated to KEGG pathways related to cancer after VILDA treatment (Table S2). In general, our findings underline a rather mild effect of VILDA compared to OA and for further analyses, we included both the exclusively and common but differentially expressed genes.

Next, we wanted to know, whether VILDA influences gene expression upon OA treatment and found 29 genes significantly up- and 31 genes significantly downregulated upon VILDA treatment (Fig. 6B). KEGG- pathway analysis revealed genes belonging to the inflammatory bowel disease pathway, asthma and Type 1 diabetes mellitus (T1DM) associated pathways significantly downregulated (Fig. 6C and Fig. S7A). Common downregulated genes of these pathways encode members of the Human leukocyte antigen II (HLAII) family, namely HLA-DQA1 and HLA-DMB, which are known to be ectopically expressed on hepatocytes upon hepatitis(35-37). Although the expression changes were small, we confirmed upregulation of *HLA-DMA*, *HLA-DMB* and *HLA-DRB1* upon OA-treatment and a tendency towards downregulation upon OA w VILDA (Fig. 6E). Interestingly, in contrast to the RNA-seq we found *HLA-DQA1* downregulated upon OA and a slight increase of expression upon OA w VILDA treatment (Fig. 6E). These data might indicate a potential association between DPP4 and HLAs in steatosis. However, experiments with more cell lines and prolonged treatment would be necessary for confirmation.

Genes associated with metabolic pathways, such as purine metabolism and fatty acid biosynthesis pathways were upregulated in OA w VILDA versus OA w/o VILDA (Fig.

6D and Fig. S7A). Interestingly, we found triokinase and FMN cyclase (*TKFC*), and 5'-nucleotidase, cytosolic II (*NT5C2*), both members of the purine metabolism, downregulated upon OA w/o VILDA in comparison to mock w/o VILDA, while VILDA treatment induced an upregulation, which might indicate a restoration of the pathway (Fig. 6F). Considering fatty acid metabolism, we detected O-acyltransferase 2 (*AGPAT2*) upregulated upon OA w/o VILDA treatment in comparison to mock w/o VILDA which was even reinforced upon OA w VILDA (Fig. 6F). We saw the same trend in gene expression of perilipin-3 (*PLIN3*) however, we did not detect differential protein expression (Fig. 6F-G). In contrast, considering another member of the perilipin family, namely PLIN2, we detected the same gene expression pattern, but differential protein expression (Fig. S6B, Fig. 6F). PLIN2 protein levels were upregulated upon OA, while PLIN3 protein levels were stable throughout the conditions. A reason might be, that PLIN3 belongs to the exchangeable PLINs, while PLIN2 is a constitutive protein, upregulated upon OA-treatment and unstable in the absence of LDs(38). PLIN3 is stable in the cytoplasm independently of LDs but is recruited to the lipid fractions(38). Nevertheless, considering the mRNA expression, our findings might indicate that DPP4 inhibition upon OA restores the hampered cellular energy homeostasis, however further studies are necessary to pinpoint the underlying mechanism.

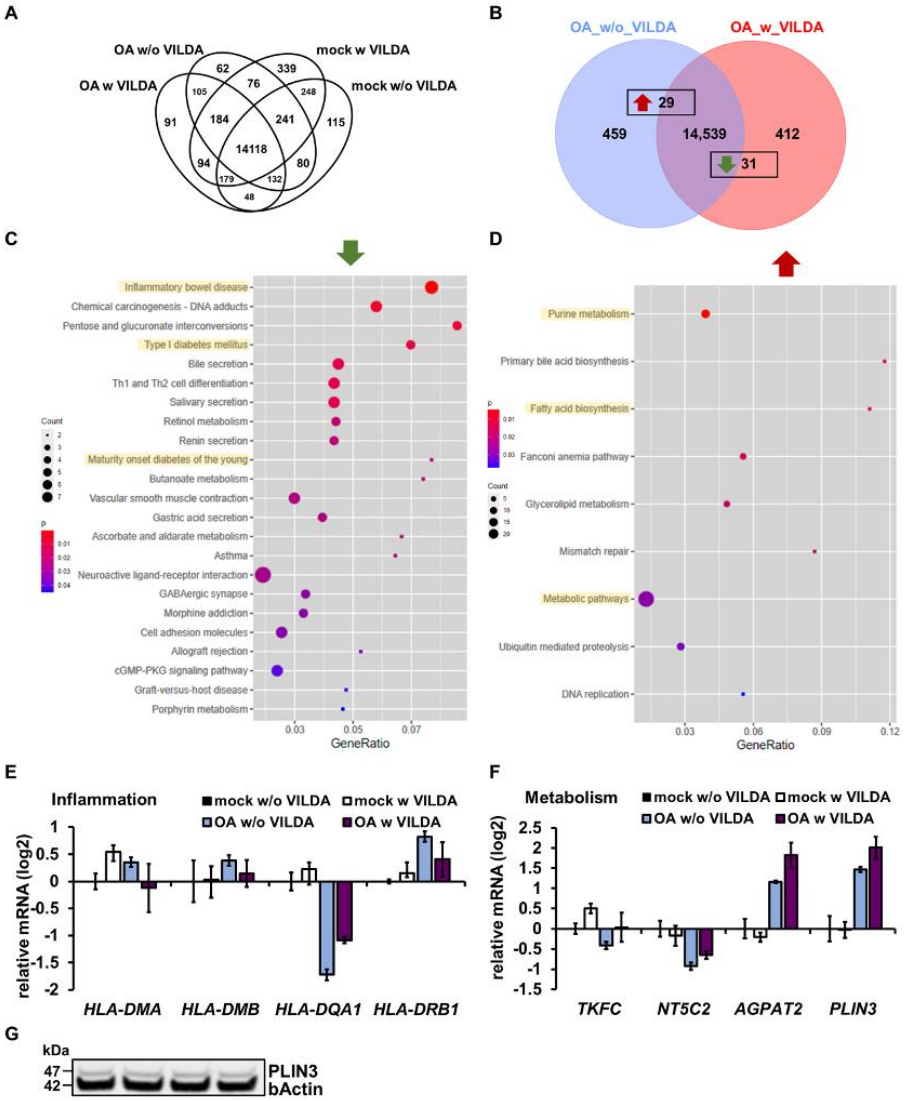

Fig. 6 VILDA effects on the global transcription of steatotic Cntrl 1 HLCs. (A) Venn diagram of expressed genes upon indicated treatments. **(B)** Venn diagram of the gene expression of OA treated HLCs w and w/o VILDA. **(C,D)** KEGG-associated pathways of significantly down- **(C)** and up- **(D)** regulated genes upon OA w VILDA treatment (complete gene lists in supplementary table S4). **(E,F)** Gene expression of inflammation-associated **(E)** and metabolism-associated **(F)** genes upon OA w and w/o VILDA treatment. **(G)** Cropped WB of Perilipin-3 (PLIN3) upon OA w and w/o VILDA

in comparison to housekeeping protein b-Actin. Uncropped full-length blots can be found in the supplementary Fig. S9.

To test whether VILDA affects the expression of steatosis-associated genes, we analyzed the expression of genes belonging to the PPAR and gluconeogenesis pathways, which were both relevant in our previous studies, via heatmaps and detected clustering according to each condition (Fig. S10, Fig. S11). In addition, we evaluated the steatosis gene set from the earlier global analysis. We could confirm the same trend of gene expression for Cntrl 1 upon OA (Fig. S6A), while we could not detect a significant difference when comparing OA w/o and w VILDA.

To gain insights into the overall VILDA effect, independent of the steatosis condition, we performed KEGG-pathway analysis of the genes differentially expressed under mock conditions. We found 47 genes significantly upregulated and 44 genes significantly downregulated upon mock w and w/o VILDA treatment (Fig. S8A). KEGG-associated pathway analysis revealed, among others, downregulated genes associated with inflammatory response pathways under mock conditions (Fig. S8B). Upregulated genes were involved in KEGG-associated pathways such as enhanced metabolism and insulin secretion, indicating beneficial effects for the compromised insulin pathway, since insulin resistance pathway was upregulated upon OA (Fig. S8C). Altogether, our findings support the hypothesis that DPP4 is involved not only in metabolic regulation via purine and fatty acid metabolism but furthermore affects inflammatory-associated pathways.

Discussion

Oleic acid feeding induces clinically relevant phenotype of steatosis

In this study, we generated induced pluripotent stem cell (iPSC)-derived steatotic hepatocyte-like cells (HLCs) from four individuals to elucidate the potential hepatocyte-specific contribution to the progression of MAFLD. Although iPSC-derived HLCs in general are not fully mature, we and others could show that they have considerable metabolic activity which makes them a valuable system to model MAFLD, reflecting the diverse genetic backgrounds of the donors(7, 8, 39-41). By stimulating HLCs with OA, we were able to induce lipid droplet formation in all four cell lines, as already shown in previous studies(7, 8). Although two of the cell lines were derived from steatosis patients, there was no disease-specific effect w or w/o OA detectable. This is specifically interesting, since our previous findings indeed indicated steatosis related gene expression patterns(9). Nevertheless, cell line-specific differences in the amount and size of the lipid droplets were observed. This is in line with our previously published data and the high divergence in individual symptoms and progression of MAFLD which are well-known difficulties in the clinic(7). They are due to genetic variations like single nucleotide polymorphisms (SNPs), epigenetic alterations and other co-morbidities that are associated with the disease(40, 42). Furthermore, considerable variability is typical for iPSC-derived data due to the individual genetic background and differences in differentiation efficiencies. Indeed, we excluded the patient derived cell line Stea 2 due to ambiguous clustering in the first level analysis.

Global transcriptomic analyses revealed MAFLD-associated pathways such as metabolism-associated and immune-modulating pathways differentially regulated in our model(43-45). A heatmap analysis of genes from these pathways, revealed clustering according to the treatment and independent of the genetic background. This underlines the importance of the involved genes for the disease. Although our model comprises only hepatocytes, the detected upregulation of cytokine-cytokine receptor

signaling, NF-kappa B and TNF signaling upon OA might indicate immune cell recruitment via inflammatory/ chemokine signaling. Recently, Yu et al demonstrated that hepatocyte-intrinsic changes contribute to the disease(44) while predisposition, environment, or other comorbidities might further regulate the pace of the progression towards fibrosis and cirrhosis. Comparing the gene expression profile detected in our HLCs with their single cell RNA-seq data from liver resections of NASH and HCC-patients, we found many pathways upregulated that are associated with a lower risk of NASH-HCC-transition, such as galactose catabolic processes, hexose metabolic processes, and glucose homeostasis.

Active Dipeptidyl peptidase 4 (DPP4) is secreted upon OA treatment

DPP4 is a serine protease with catalytic activity for various substrates(12) and considered a hepatokine, upregulated in metabolic liver disease and driver of inflammation(13). Similar to observations made in HepG2 cells(46), we could not detect elevated DPP4 on both the mRNA or protein level. However, we found elevated secretion and a drastic increase in the catalytic activity of DPP4 upon OA, in line with previously observed elevation in NAFLD/NASH patients(47, 48). As DPP4 is involved in various chronic and cancerous diseases throughout the human body, hepatocyte-specific secretion upon late-steatosis might indicate inflammatory signaling and a risk for the development of other comorbidities like cardiovascular and renal diseases(49).

VILDA interferes with DPP4 activity and regulates pathways related to inflammation and metabolism

As a first insight into the mechanism of action of DPP4, we inhibited its activity with VILDA- an FDA-approved T2DM medication. As a proof-of-principle, we found that VILDA interferes solely with DPP4 activity and not with the protein or mRNA level, as described in previous studies(50). In our study, as the first in this format, global

transcriptome analysis revealed clustering according to the OA- /mock treatment, but not according to VILDA treatment. This confirmed our expectation that OA treatment induced greater transcriptome changes than VILDA treatment. Nevertheless, we detected exclusively expressed genes for all four conditions. Although KEGG-associated pathway analysis did not identify characteristic profiles, we noticed that genes involved in the development of cancer were upregulated upon VILDA independently of steatosis. VILDA-associated safety concerns have already been addressed extensively and no significant overall cancer-association was found(51, 52). Considering the typical long-term or even life-long medication of T2DM, this should nevertheless be monitored carefully.

Furthermore, we found inflammation associated pathways such as Type 1 diabetes mellitus (T1DM), inflammatory bowel disease and asthma downregulated upon DPP4 inhibition. *HLA-DQA1* and *HLA-DMB* are common genes involved in all of them, and their expression was differentially regulated upon steatosis and additional DPP4 inhibition. HLA class II proteins are typically expressed on the surface of antigen presenting cells, however ectopic expression in hepatocytes upon disease has been shown(35, 37). In line with this, we found a tendency of elevated gene expression of *HLA-DMB*, *HLA-DMA* and *HLA-DRB1* upon OA, which are associated with NASH, hepatitis and cirrhosis(53, 54), and all decreased upon DPP4 inhibition. Since DPP4 activity affects (auto)-immune related diseases in a complex manner(55) this might provide a possible clue towards its role for steatosis/MAFLD progression. However, further studies are necessary to elucidate the role of DPP4 in the steatosis model.

To understand the role of DPP4 for the interplay between metabolism and inflammation, it is essential to determine, whether DPP4 is causal or correlative for late-steatosis. DPP4 was shown to be epigenetically regulated(56, 57). Indeed, we also found a slight,

albeit not significant demethylation upon OA treatment (not shown). This supports the speculation that early events of energy overload might change the methylation profiles of CpG islands in the DPP4 locus and enable DPP4 expression in hepatocytes at a rather early timepoint of disease progression.

The insulin resistance pathway was upregulated upon OA treatment, which matches with the well-known insulin resistance promoting effect of DPP4. In addition, genes involved in PPAR signaling and gluconeogenesis showed condition dependent gene expression patterns. Interestingly, we found genes involved in purine and fatty acid metabolism upregulated upon VILDA treatment. E.g. *AGPAT2,* which is involved in fatty acid metabolism, was upregulated upon DPP4 inhibition. Its deletion or mutation is associated with insulin resistance, diabetes and severe forms of metabolic syndrome in mice and humans(58-60). This could indicate a VILDA-mediated beneficial effect for the hampered metabolism due the energy overload during late-steatosis and underline the idea of a role for DPP4 in the interplay between metabolism and inflammation(16, 61).

Conclusions:

Taken together, we provide a human iPSC-derived model focusing on the hepatocyte-specific contribution to progression of steatosis. We could link DPP4 activity to the steatosis phenotype and show that its inhibition with Vildagliptin has effects on metabolism- and inflammation-associated gene expression during steatosis. Since we have performed global transcriptome analyses of the effects of VILDA with only one cell line, these can only provide first insights into possible effects, and more in depth analyses are needed. In the future, human DPP4-knockout HLCs, embedded in a multicellular liver model, could increase our understanding of the mechanisms of DPP4

through health and disease and help to further elucidate the interplay between the distinct cell types of the liver.

Abbreviations:

ACE2	Angiotensin converting enzyme 2
AFP	Alpha-Fetoprotein
AGPAT2	O-acyltransferase 2
ALB	Albumin
AMPK	Adenosine monophosphate-activated protein kinase
ANPEP	Alanyl Aminopeptidase
CCL4	C-C motif chemokine ligand 4
CD26	Cluster of differentiation 26
Cntrl	Control
CPT1A	Carnitine palmitoyltransferase I
CYP	Cytochrome P450
DE	Definitive endoderm
Dex	Dexamethasone
DPP4	Dipeptidyl peptidase 4
E-CAD	E Cadherin
ELISA	Enzyme-linked immunosorbent assay
FABP1	fatty acid binding protein 1
FDA	Food and drug administration (U.S.)
GOs	Gene ontologies
GSK-3	Glycogen synthase kinase 3
HE	Hepatic endoderm
HGF	Hepatocyte growth factor
HLAII	Human leukocyte antigen II
HLCs	Hepatocyte like cells
HNF4a	Hepatocyte nuclear factor 4alpha
ICC	Immunocytochemistry
IGFBP1	Insulin Like Growth Factor Binding Protein 1
igG	Immunoglobulin G
IL1B	Interleukin 1beta
iPSCs	induced pluripotent stem cells
KEGG	Kyoto Encyclopedia of Genes and Genomes
LD	Lipid droplet
MAFLD	Metabolic dysfunction-associated fatty liver disease
MASLD	Metabolic dysfunction-associated steatotic liver disease
NAFLD	Non-alcoholic fatty liver disease
NASH	Non-alcoholic steatohepatitis

NT5C2	5'-nucleotidase, cytosolic II
OA	Oleic acid
OCT4	octamer-binding transcription factor 4
OSM	Oncostatin M
P/S	Penicillin/Streptomycin
PCK1	Phosphoenolpyruvate Carboxykinase 1
PLIN2	Perilipin-2
PLIN3	Perilipin-3
PPAR	Peroxisome proliferator activated-receptor
qRT-PCR	Quantitative reverse transcription PCR
R.L.U.	Relative light units
RNA-seq	RNA sequencing
ROS	Reactive oxygen species
RPLP0	Ribosomal Protein Lateral Stalk Subunit P0
SNPs	single nucleotide polymorphisms
SOX	SRY-related HMG-box genes
Stea	Steatosis
T1DM	Type 1 diabetes mellitus
T2DM	Type 2 diabetes mellitus
TBS-T	Tris-buffered saline with Tween20
TKFC	triokinase and FMN cyclase
TNF	Tumor necrosis factor
VCAM1	Vascular cell adhesion molecule 1
VILDA	Vildagliptin

Declarations:

Ethics approval and consent to participate:

The use of iPS cell line Cntrl 1 was approved by the ethics committee of the medical faculty of Heinrich Heine University Düsseldorf under ethical approval number 5704 on the 01.03.2017. The title of the approved project is „Isolierung, Charakterisierung und Reprogrammierung von Stammzellen aus dem Urin". The use of iPS cell lines Cntrl 2, Stea 1 and Stea 2 was approved by the ethics committee of the medical faculty of Heinrich Heine University Düsseldorf under ethical approval number 5013 on the 09.07.2015. The title of the approved project is „Nutzung humaner embryonaler Stammzellen, fetaler humaner Stammzellen (MSC) sowie induzierter pluripotenter

Stammzellen zur Erforschung von Lebererkrankungen (NAFLD) und Hirnerkrankungen (Alzheimer)“. The patients or their guardian(s)/legally authorized representative(s)/next of kin provided written informed consent for participation in the study and/or the use of samples.

Availability of data and materials:

The data that support the findings of this study are available from the corresponding author upon reasonable request. NGS data will be provided on the GEO-server and/or on upon reasonable request upon acceptance. Additional files of produced sequencing data is provided in supplementary table S3 and S4.

Competing interests:

The authors declare no competing interests.

Funding:

C.L., N.G. and J.R. are funded by the Else Kröner-Fresenius-Stiftung – 2020_EKEA.64. J.A. acknowledges the medical faculty of Heinrich-Heine University Düsseldorf for part funding of this project

Acknowledgments:

C.L., N.G. and J.R. are funded by the Else Kröner-Fresenius-Stiftung – 2020_EKEA.64. J.A. acknowledges the medical faculty of Heinrich-Heine University Düsseldorf for part funding of this project. The authors declare that they have not use AI-generated work in this manuscript.

Authors contribution:

CL: Conceptualization, Data curation, Investigation, Methodology, Visualization, Writing–original draft, Writing–review and editing. WW: Data curation, Visualization, Writing–original draft, Writing–review and editing JR: Investigation, Methodology, JA: Conceptualization, Project administration, Resources, Supervision, Writing–original draft, Writing–review and editing. NG: Conceptualization, Formal Analysis, Funding acquisition, Investigation, Methodology, Project administration, Resources, Supervision, Visualization, Writing–original draft, Writing–review and editing

Authors information: Not applicable

References:

1. Angulo P. Obesity and nonalcoholic fatty liver disease. Nutr Rev 2007;65:S57-63.
2. Eslam M, Newsome PN, Sarin SK, Anstee QM, Targher G, Romero-Gomez M, Zelber-Sagi S, et al. A new definition for metabolic dysfunction-associated fatty liver disease: An international expert consensus statement. J Hepatol 2020;73:202-209.
3. Henry L, Paik J, Younossi ZM. Review article: the epidemiologic burden of non-alcoholic fatty liver disease across the world. Aliment Pharmacol Ther 2022;56:942-956.
4. Teng ML, Ng CH, Huang DQ, Chan KE, Tan DJ, Lim WH, Yang JD, et al. Global incidence and prevalence of nonalcoholic fatty liver disease. Clin Mol Hepatol 2023;29:S32-s42.
5. Barrera F, Uribe J, Olvares N, Huerta P, Cabrera D, Romero-Gómez M. The Janus of a disease: Diabetes and metabolic dysfunction-associated fatty liver disease. Ann Hepatol 2024;29:101501.
6. Zhao J, Liu L, Cao YY, Gao X, Targher G, Byrne CD, Sun DQ, et al. MAFLD as part of systemic metabolic dysregulation. Hepatol Int 2024.
7. Graffmann N, Ncube A, Martins S, Fiszl AR, Reuther P, Bohndorf M, Wruck W, et al. A stem cell based in vitro model of NAFLD enables the analysis of patient specific individual metabolic adaptations in response to a high fat diet and AdipoRon interference. Biol Open 2021;10.
8. Graffmann N, Ring S, Kawala MA, Wruck W, Ncube A, Trompeter HI, Adjaye J. Modeling Nonalcoholic Fatty Liver Disease with Human Pluripotent Stem Cell-Derived Immature Hepatocyte-Like Cells Reveals Activation of PLIN2 and Confirms Regulatory Functions of Peroxisome Proliferator-Activated Receptor Alpha. Stem Cells Dev 2016;25:1119-1133.
9. Wruck W, Kashofer K, Rehman S, Daskalaki A, Berg D, Gralka E, Jozefczuk J, et al. Multi-omic profiles of human non-alcoholic fatty liver disease tissue highlight heterogenic phenotypes. Sci Data 2015;2:150068.
10. Beygi M, Ahi S, Zolghadri S, Stanek A. Management of Metabolic-Associated Fatty Liver Disease/Metabolic Dysfunction-Associated Steatotic Liver Disease: From Medication Therapy to Nutritional Interventions. Nutrients 2024;16.
11. Lara-Romero C, Romero-Gómez M. Treatment Options and Continuity of Care in Metabolic-associated Fatty Liver Disease: A Multidisciplinary Approach. Eur Cardiol 2024;19:e06.
12. Mulvihill EE, Drucker DJ. Pharmacology, physiology, and mechanisms of action of dipeptidyl peptidase-4 inhibitors. Endocr Rev 2014;35:992-1019.
13. Trzaskalski NA, Fadzeyeva E, Mulvihill EE. Dipeptidyl Peptidase-4 at the Interface Between Inflammation and Metabolism. Clin Med Insights Endocrinol Diabetes 2020;13:1179551420912972.

14. de Meester I, Lambeir AM, Proost P, Scharpé S. Dipeptidyl peptidase IV substrates. An update on in vitro peptide hydrolysis by human DPPIV. Adv Exp Med Biol 2003;524:3-17.
15. Ahrén B, Landin-Olsson M, Jansson PA, Svensson M, Holmes D, Schweizer A. Inhibition of dipeptidyl peptidase-4 reduces glycemia, sustains insulin levels, and reduces glucagon levels in type 2 diabetes. J Clin Endocrinol Metab 2004;89:2078-2084.
16. Ghorpade DS, Ozcan L, Zheng Z, Nicoloro SM, Shen Y, Chen E, Bluher M, et al. Hepatocyte-secreted DPP4 in obesity promotes adipose inflammation and insulin resistance. Nature 2018;555:673-677.
17. Ohm B, Moneke I, Jungraithmayr W. Targeting cluster of differentiation 26 / dipeptidyl peptidase 4 (CD26/DPP4) in organ fibrosis. Br J Pharmacol 2023;180:2846-2861.
18. Hussain M, Majeed Babar MZ, Hussain MS, Akhtar L. Vildagliptin ameliorates biochemical, metabolic and fatty changes associated with non alcoholic fatty liver disease. Pak J Med Sci 2016;32:1396-1401.
19. Hendawy AS, El-Lakkany NM, Mantawy EM, Hammam OA, Botros SS, El-Demerdash E. Vildagliptin alleviates liver fibrosis in NASH diabetic rats via modulation of insulin resistance, oxidative stress, and inflammatory cascades. Life Sci 2022;304:120695.
20. Khalil R, Shata A, Abd El-Kader EM, Sharaf H, Abdo WS, Amin NA, Saber S. Vildagliptin, a DPP-4 inhibitor, attenuates carbon tetrachloride-induced liver fibrosis by targeting ERK1/2, p38alpha, and NF-kappaB signaling. Toxicol Appl Pharmacol 2020;407:115246.
21. Loerch C, Szepanowski L-P, Reiss J, Adjaye J, Graffmann N. Forskolin induces FXR expression and enhances maturation of iPSC-derived hepatocyte-like cells. Frontiers in Cell and Developmental Biology 2024;12.
22. Bohndorf M, Ncube A, Spitzhorn LS, Enczmann J, Wruck W, Adjaye J. Derivation and characterization of integration-free iPSC line ISRM-UM51 derived from SIX2-positive renal cells isolated from urine of an African male expressing the CYP2D6 *4/*17 variant which confers intermediate drug metabolizing activity. Stem Cell Res 2017;25:18-21.
23. Kawala MA, Bohndorf M, Graffmann N, Wruck W, Zatloukal K, Adjaye J. Characterization of iPSCs derived from dermal fibroblasts from a healthy 19year old female. Stem Cell Res 2016;17:597-599.
24. Kawala MA, Bohndorf M, Graffmann N, Wruck W, Zatloukal K, Adjaye J. Characterization of dermal fibroblast-derived iPSCs from a patient with high grade steatosis. Stem Cell Res 2016;17:568-571.
25. Graffmann N, Bohndorf M, Ncube A, Wruck W, Kashofer K, Zatloukal K, Adjaye J. Establishment and characterization of an iPSC line from a 58 years old high grade patient with nonalcoholic fatty liver disease (70% steatosis) with homozygous wildtype PNPLA3 genotype. Stem Cell Res 2018;31:131-134.
26. Kim D, Langmead B, Salzberg SL. HISAT: a fast spliced aligner with low memory requirements. Nat Methods 2015;12:357-360.
27. Kanehisa M, Furumichi M, Tanabe M, Sato Y, Morishima K. KEGG: new perspectives on genomes, pathways, diseases and drugs. Nucleic Acids Res 2017;45:D353-d361.
28. Falcon S, Gentleman R. Using GOstats to test gene lists for GO term association. Bioinformatics 2007;23:257-258.
29. Wickham H. ggplot2: Springer New York, NY, 2009.
30. Schneider CA, Rasband WS, Eliceiri KW. NIH Image to ImageJ: 25 years of image analysis. Nat Methods 2012;9:671-675.
31. Gentleman RC, Carey VJ, Bates DM, Bolstad B, Dettling M, Dudoit S, Ellis B, et al. Bioconductor: open software development for computational biology and bioinformatics. Genome Biol 2004;5:R80.
32. Wruck W, Boima V, Erichsen L, Thimm C, Koranteng T, Kwakyi E, Antwi S, et al. Urine-Based Detection of Biomarkers Indicative of Chronic Kidney Disease in a Patient Cohort from Ghana. J Pers Med 2022;13.

33. Warnes GR, Ben Bolker, Lodewijk Bonebakker, Robert Gentleman, Wolfgang Huber Andy Liaw, Thomas Lumley, Martin Maechler, et al. Gplots: Various R Programming Tools for Plotting Data. In; 2015.
34. Macauley M, Hollingsworth KG, Smith FE, Thelwall PE, Al-Mrabeh A, Schweizer A, Foley JE, et al. Effect of vildagliptin on hepatic steatosis. J Clin Endocrinol Metab 2015;100:1578-1585.
35. Lu JG, Ji P, French SW. The Major Histocompatibility Complex Class II–CD4 Immunologic Synapse in Alcoholic Hepatitis and Autoimmune Liver Pathology: The Role of Aberrant Major Histocompatibility Complex Class II in Hepatocytes. The American Journal of Pathology 2020;190:25-32.
36. Lu JG, Iyasu A, French B, Tillman B, French SW. Overexpression of MHCII by hepatocytes in alcoholic hepatitis (AH) compared to non-alcoholic steatohepatitis (NASH) and normal controls. Alcohol 2020;84:27-32.
37. Dezhbord M, Kim SH, Park S, Lee DR, Kim N, Won J, Lee AR, et al. Novel role of MHC class II transactivator in hepatitis B virus replication and viral counteraction. Clin Mol Hepatol 2024;30:539-560.
38. Wolins NE, Brasaemle DL, Bickel PE. A proposed model of fat packaging by exchangeable lipid droplet proteins. FEBS Lett 2006;580:5484-5491.
39. Sinton MC, Meseguer-Ripolles J, Lucendo-Villarin B, Wernig-Zorc S, Thomson JP, Carter RN, Lyall MJ, et al. A human pluripotent stem cell model for the analysis of metabolic dysfunction in hepatic steatosis. iScience 2021;24:101931.
40. Tilson SG, Morell CM, Lenaerts AS, Park SB, Hu Z, Jenkins B, Koulman A, et al. Modeling PNPLA3-Associated NAFLD Using Human-Induced Pluripotent Stem Cells. Hepatology 2021;74:2998-3017.
41. Lyall MJ, Cartier J, Thomson JP, Cameron K, Meseguer-Ripolles J, O'Duibhir E, Szkolnicka D, et al. Modelling non-alcoholic fatty liver disease in human hepatocyte-like cells. Philosophical Transactions of the Royal Society B: Biological Sciences 2018;373:20170362.
42. Metwally M, Eslam M, George J. Genetic and Epigenetic Associations of NAFLD: Focus on Clinical Decision Making. Current Hepatology Reports 2017;16:335-345.
43. Wruck W, Graffmann N, Kawala MA, Adjaye J. Concise Review: Current Status and Future Directions on Research Related to Nonalcoholic Fatty Liver Disease. Stem Cells 2017;35:89-96.
44. Yu Q, Zhang Y, Ni J, Shen Y, Hu W. Identification and analysis of significant genes in nonalcoholic steatohepatitis-hepatocellular carcinoma transformation: Bioinformatics analysis and machine learning approach. Molecular Immunology 2024;174:18-31.
45. Xiong Y, Shi X, Xiong X, Li S, Zhao H, Song H, Wang J, et al. A systematic review and meta-analysis of randomized controlled trials: effects of mediterranean diet and low-fat diet on liver enzymes and liver fat content of NAFLD. Food Funct 2024;15:8248-8257.
46. Miyazaki M, Kato M, Tanaka K, Tanaka M, Kohjima M, Nakamura K, Enjoji M, et al. Increased hepatic expression of dipeptidyl peptidase-4 in non-alcoholic fatty liver disease and its association with insulin resistance and glucose metabolism. Mol Med Rep 2012;5:729-733.
47. Barchetta I, Ceccarelli V, Cimini FA, Barone E, Sentinelli F, Coluzzi M, Chiappetta C, et al. Circulating dipeptidyl peptidase-4 is independently associated with the presence and severity of NAFLD/NASH in individuals with and without obesity and metabolic disease. J Endocrinol Invest 2021;44:979-988.
48. Barchetta I, Cimini FA, Dule S, Cavallo MG. Dipeptidyl Peptidase 4 (DPP4) as A Novel Adipokine: Role in Metabolism and Fat Homeostasis. Biomedicines 2022;10:2306.
49. Tomovic K, Lazarevic J, Kocic G, Deljanin-Ilic M, Anderluh M, Smelcerovic A. Mechanisms and pathways of anti-inflammatory activity of DPP-4 inhibitors in cardiovascular and renal protection. Med Res Rev 2019;39:404-422.
50. Mathieu C, Degrande E. Vildagliptin: a new oral treatment for type 2 diabetes mellitus. Vasc Health Risk Manag 2008;4:1349-1360.

51. Zhao M, Chen J, Yuan Y, Zou Z, Lai X, Rahmani DM, Wang F, et al. Dipeptidyl peptidase-4 inhibitors and cancer risk in patients with type 2 diabetes: a meta-analysis of randomized clinical trials. Sci Rep 2017;7:8273.
52. Kanazawa I, Tanaka KI, Notsu M, Tanaka S, Kiyohara N, Koike S, Yamane Y, et al. Long-term efficacy and safety of vildagliptin add-on therapy in type 2 diabetes mellitus with insulin treatment. Diabetes Res Clin Pract 2017;123:9-17.
53. Zhang J-j, Shen Y, Chen X-y, Jiang M-l, Yuan F-h, Xie S-l, Zhang J, et al. Integrative network-based analysis on multiple Gene Expression Omnibus datasets identifies novel immune molecular markers implicated in non-alcoholic steatohepatitis. Frontiers in Endocrinology 2023;14.
54. Lu YY, Chen QL, Guan Y, Guo ZZ, Zhang H, Zhang W, Hu YY, et al. Transcriptional profiling and co-expression network analysis identifies potential biomarkers to differentiate chronic hepatitis B and the caused cirrhosis. Mol Biosyst 2014;10:1117-1125.
55. Huang J, Liu X, Wei Y, Li X, Gao S, Dong L, Rao X, et al. Emerging Role of Dipeptidyl Peptidase-4 in Autoimmune Disease. Front Immunol 2022;13:830863.
56. Hyun J, Jung Y. DNA Methylation in Nonalcoholic Fatty Liver Disease. Int J Mol Sci 2020;21.
57. Saussenthaler S, Ouni M, Baumeier C, Schwerbel K, Gottmann P, Christmann S, Laeger T, et al. Epigenetic regulation of hepatic Dpp4 expression in response to dietary protein. J Nutr Biochem 2019;63:109-116.
58. Cortés VA, Curtis DE, Sukumaran S, Shao X, Parameswara V, Rashid S, Smith AR, et al. Molecular mechanisms of hepatic steatosis and insulin resistance in the AGPAT2-deficient mouse model of congenital generalized lipodystrophy. Cell Metab 2009;9:165-176.
59. Araújo-Vilar D, Santini F. Diagnosis and treatment of lipodystrophy: a step-by-step approach. J Endocrinol Invest 2019;42:61-73.
60. Agarwal AK, Tunison K, Horton JD, Garg A. Regulated regeneration of adipose tissue in lipodystrophic Agpat2-null mice partially ameliorates hepatic steatosis. iScience 2024;27:109517.
61. Baumeier C, Schluter L, Saussenthaler S, Laeger T, Rodiger M, Alaze SA, Fritsche L, et al. Elevated hepatic DPP4 activity promotes insulin resistance and non-alcoholic fatty liver disease. Mol Metab 2017;6:1254-1263.

5. Discussion

In 2023, liver diseases displayed a global health burden, causing 4% of all deaths worldwide (Devarbhavi et al., 2023). Liver diseases have several etiologies with prevalences varying from region to region. For example, infections still massively contribute to the global health burden, with the highest prevalence in south and east Asian countries and western Africa (Devarbhavi et al., 2023). In comparison, inherited disorders and auto-immune liver diseases are especially prevalent in Europe, USA and higher-income countries. AATD is an inherited monogenic disease, derived from different mutations in the *SERPINA1* gene locus. The severe Pi*ZZ genotype has a globally highly varying prevalence, however it is associated with increased risk for the development of fibrosis (36% of the patients) and cirrhosis (2-10% of the patients) (Blanco et al., 2017; Strnad et al., 2020). The severe liver phenotype manifests typically in infants or middle-aged adults, however the underlying mechanisms for this difference remain elusive (Katzer et al., 2021). Currently, the only treatment option is to slow down fibrotic processes and keep cirrhosis compensated (Ruiz et al., 2023).

In contrast, lifestyle-derived liver diseases such as alcohol-related and drug induced liver diseases are globally on the rise (Devarbhavi et al., 2023). Specifically, the incidences of liver diseases caused by excessive calorie intake and obesity (MAFLD) have drastically risen in the past 30 years, currently affecting one-third of the global population (Devarbhavi et al., 2023; Guo et al., 2025; Jiang et al., 2023). MAFLD is a multifactorial disease as other co-pathologies or SNPs are driving factors for the progression to the inflammatory state MASH and the development of fibrosis and cirrhosis. Although the numbers are controversial, a recent study found that 6.1% of MASH patients are likely to develop cirrhosis (Luthra & Sheth, 2025).

Varying symptoms and silent progression of liver diseases display an enormous challenge for the development of therapeutic and preventative measurements (Asrani et al., 2019; Huang et al., 2023; Jiang et al., 2023; Luthra & Sheth, 2025; Ruiz et al., 2023). Furthermore, animal models as well as low quality *in vitro* models display a bottleneck for the translation of results to clinical trials. To date, upon cirrhotic liver failure, liver transplantation is the only therapeutic option (Asrani et al., 2019; Huang et al., 2023; Jiang et al., 2023; Ruiz et al., 2023).

5.1. Patient-derived iPSCs for modeling monogenic and multifactorial diseases

AATD is an autosomal co-dominant inherited genetic disorder resulting from different mutations in the *SERPINA1* gene locus. The Pi*Z genotype describes a G→A missense mutation at the position rs28929474, leading to a glutamate-to-lysine substitution (Glu342Lys) and a misfolded version of the serine protease inhibitor AAT (Strnad et al., 2020). The homogenous Pi*Z genotype results in polymers which are retained within the hepatocytes, leading to an 85% reduction of AAT levels in the circulation (Fromme et al., 2025). This causes ER stress in the hepatocytes and can result in inflammation, fibrosis and cirrhosis. Additionally, the retained AAT causes limited protease inhibitor functions for tissues, which can result in a lung phenotype. The concrete pathomechanisms determining onset and progression of the liver phenotype are still elusive and there is no treatment available to cure cirrhosis. Hence, liver transplantation is the only therapeutic option upon decompensated cirrhosis (Ruiz et al., 2023). The heterogenous symptoms and variable onset of AATD implies environmental or genetic contributors to the disease phenotype. Nevertheless, the heterogeneity of available data complicates research and contributes to the poor understanding of the disease to date (Townsend et al., 2018). This is especially true for pediatric AATD patients, since there are only limited studies available and predictors of the disease progression and severe outcomes are yet to be fully understood (Lemke et al., 2024; Sveger, 1976).

Somatic cells of adult and pediatric AATD patients carrying the Pi*ZZ genotype were reprogrammed. The adult male and female patients were of white ethnicity, and 57 and 63 years old, respectively, while the pediatric male liver cirrhosis patient of unknown ethnicity was 11 years old. Urine was collected, representing an easy-approachable, non-invasive method to acquire somatic cells. A fraction of collected cells was rice-grain shaped and adherent on plastic and therefore called urine-derived renal progenitor cells (UdRPCs) (Rahman et al., 2018; Rahman et al., 2020). These cells were cultured and reprogrammed by episomal-based overexpression of the Yamanaka and Thomson transcription factors *KLF4*, *OCT3/4*, *C-MYC*, *SOX2*, *NANOG* and *LIN28*. Clones of potential iPS cells were thoroughly characterized to exclude the integration of the plasmid and confirm the genetic integrity and pluripotency of the generated cell lines. The established iPSC lines showed spontaneous differentiation to cells of the three germ layers endoderm, mesoderm and ectoderm. Global transcriptomic resemblance with embryonic stem cells (ESCs), showed a coefficient of 0.94 for ISRM-AATD-iPSC-1 and 2

and 0.9 for ISRM-AATD-iPSC-3, respectively. DNA fingerprinting and Pi*ZZ genotyping was performed and confirmed the patients' genetic background.

Generation of AATD iPSCs from pediatric patients with severe symptomatic, as described in this study, will advance the currently limited state-of-knowledge of AATD in children. Although in 2020 an AATD-iPSC repository has been established, from the 140 patients carrying the Pi*ZZ genotype, the youngest was 16 years old (Kaserman et al., 2020). Future studies using iPSCs derived from pediatric AATD patients may help to develop options for prevention and treatment. The establishment and thorough characterization of the AATD iPSC lines from adult and pediatric patients provide tools to analyze the underlying mechanisms of AATD onset, progression and disease development in a comparative manner. By registering them in the global hPSC registry, they provide a valuable source for other scientists (*hPSCreg – The Human Pluripotent Stem Cell Registry*, 2025). To analyze the liver phenotype, iPSCs may be differentiated to HLCs allowing comparative investigation of AATD patient-derived hepatic phenotypes.

Patient-derived iPSCs are also useful for the study of multifactorial diseases such as MAFLD. The complete genetic background of steatosis patient derived iPSCs ensures the inclusion of potential unknown driving factors. Studies using iPSCs derived from steatosis patients, differentiated to HLCs and treated with oleic acid might reveal a disease specific response (Graffmann et al., 2021) Such iPSCs from female and male steatosis patients have been established by the working group in the past (Graffmann et al., 2018a; Kawala et al., 2016).

5.2. Functional hepatocyte-like cells as platforms for the study of liver diseases

Although HLCs allow the study of hepatocyte-specific (patho-)mechanisms, their limited maturation restricts the use in basic research such as liver disease modeling. Beyond that, their application in translational approaches such as toxicological assessment, is restricted by limited functionality. Complex protocols involving multiple cell types, 3D spheres and organoids, or genetic engineering are promising methods to improve maturation (Rashidi et al., 2018; Touboul et al., 2010; Weber et al., 2023). Yet, these methods are cost and labor intensive challenging their application. In order to establish a cost- and time-efficient protocol for the differentiation of iPSCs to HLCs, an established protocol was re-evaluated and optimized

(Graffmann et al., 2016; Hay et al., 2008a; Hay et al., 2008b; Matz et al., 2017). This protocol relies on three main steps: DE induction i) by Wnt and TGFβ signaling, which is established by CHIR and activin A signaling. HE ii) is induced by DMSO treatment. HLC maturation is introduced by iii) stimulation with HGF, Ins, DEX and OSM for up to 15 days. Although the resulting HLCs showed typical hepatic gene expression, the enzyme activity of cytochrome P450 members was low, limiting their potential for drug testing and toxicity assays (Graffmann et al., 2021; Graffmann et al., 2016; Matz et al., 2017).

Re-evaluation of the protocol revealed several factors, which possibly influenced the outcome of the HLC quality. Firstly, the initial number of seeded cells needed to be adjusted for each cell line. In comparison to the initial protocol, the cell number was adjusted to 1.04 x10^5 iPSCs/cm^2, implying an increase of cells of almost 100%. The initial cell number is crucial for efficient differentiation, as the cells need to build a dense monolayer (approx. 80% confluency). This is important, because during the DE induction step a lot of cell death will occur due to high concentrations of activin A and CHIR99021 (Peaslee et al., 2021). After this initial wave of cell death, massive proliferation starts. If the cells are not dense enough when reaching the HE-stage, the cells might transit into an endoderm-derived epithelial cell-type, incapable of HLC maturation (Graffmann et al., 2018b). On the other hand, if the cell density is too high initially, DE induction might not be efficient. Therefore, it is important to carefully adjust the initial cell number for each cell line.
The HLC basal medium was changed from L15 to DMEM/F12 to improve the pH-balance under 5% CO_2 cell culture conditions. L15 medium is buffered by phosphate and amino acid-formulations, optimized for CO_2-free culture conditions, and not capable to optimally buffer the pH of the HLC medium under the used conditions (Leibovitz, 1963). In fact, during HLC cultivation with DMEM/F12 (with phenol-red) the color change of the medium was not as strong as observed when using L15 (with phenol-red), indicating less drastic pH-changes. Furthermore, the antibiotics used for all differentiation media were changed from penicillin-streptomycin to doxycycline. Doxycycline has been shown to reduce apoptosis after induction of high concentrations of activin A and promotes DE differentiation (Peaslee et al., 2021).

The main finding, however, was that regulation of cyclic adenosine monophosphate (cAMP) by forskolin induced the gene and protein expression of the nuclear farnesoid X receptor (FXR). Under physiological conditions, the receptor families FXR and pregnane X receptor (PXR) are activated by bile acids and were found to be essential for hepatocyte gene expression (Nell et

al., 2022). In the presented study, *FXR* gene expression was shown to be induced by the optimized HLC differentiation protocol including forskolin. Upon differentiation with the optimized HLC maturation medium, HLCs exhibited higher gene expression of *AFP*, *ALB*, *CYP3A4* and *FXR*. On the protein level AFP and ALB expression was drastically increased in comparison to the old protocol. Moreover, seemingly more cells expressed HNF4α and the epithelial marker e-cadherin (E-CAD). Conformingly, *ALB* and *AFP* gene expression and cytochrome P450 3A4 and 2D6 (CYP3A4, CYP2D6) activity and CYP3A4 inducibility was increased by forskolin induction, independent of the general protocol changes. These findings underlined the importance of FXR for HLC maturation and the importance of ongoing literature research and the constant re-evaluation of established protocols to stay up-to-date.

Conclusively, optimizing relatively small steps in the protocol increased the HLC quality significantly. Indeed, the established protocol provides a robust and simple tool for the generation of functional hiPSC-derived HLCs in a cost- and time-efficient manner.

5.3. Establishment of a relevant human iPSC-derived hepatic steatosis model

In the third study, both of the aforementioned approaches were applied in order to establish a relevant human iPSC-derived hepatic steatosis model. Functional HLCs derived from two steatosis patients and two healthy individuals were generated by using the aforementioned optimized differentiation protocol.

Successful differentiation of the four iPS cell lines to HLCs was shown by hepatic gene and protein expression as well as CYP3A4 and CYP2D6 enzyme activity. The steatosis phenotype was induced by OA treatment for 7 days. Although there were differences in the lipid droplet formation between the cell lines, these were independent of the disease background and seemed to be cell line specific. Hierarchical sample clustering based on the global gene expression profiles revealed clustering according to the treatment, based on the genetic background. However, for cell line Stea2, two of the replicates did not cluster according to the treatment. This observation indicated differences in gene expression response upon the treatment in comparison to the other iPSC lines, possibly caused by individual genetic variations. The findings recapitulate the variance of symptoms presented in MAFLD patients and underline the importance of the genetic background in iPSC-based research, especially for modeling multifactorial diseases (Bonder et al., 2021). To prevent misinterpretation due to the genetic background, this cell line was excluded for further analyses.

Previously published data indicated differential gene expression patterns upon steatosis induction, dependent on the healthy and diseased background (Graffmann et al., 2021). In contrast, in this study global transcriptomic analyses revealed clustering according to the individual genetic background, independent of the disease status. The findings underline again the importance of including more than one control cell line in the study to prevent bias caused by individual responses, independent of the disease context.

Upon OA treatment, global transcriptome analyses confirmed differential regulation of KEGG pathways, indicating potential hits on the progression axis from MAFLD to MASH. Pathways including insulin resistance, fatty acid metabolism and AMPK and PPAR signaling were upregulated and indicated earlier hits on the disease progression axis (Fang et al., 2022; Wruck & Adjaye, 2017). Genes belonging to glutathione metabolism and metabolic pathways were downregulated, indicating oxidative stress and dysregulated cell homeostasis, hallmarks of steatosis progression (Fang et al., 2022; Masarone et al., 2018). Additionally, pathways indicating inflammatory signaling such as inflammatory bowel disease, TNFα, NFkB and cytokine-cytokine signaling were upregulated and suggested early steps of steatohepatitis progression (Catrysse & van Loo, 2017; Fang et al., 2022; Heida et al., 2021; Vachliotis & Polyzos, 2023).
Conclusively, the established hepatic steatosis model was able to resemble the clinical phenotype of steatosis and likely showed early symptoms of steatohepatitis progression. This was probably accomplished by the relatively long exposure to OA, mimicking the typical gradual transition from steatosis to steatohepatitis.
The fact that the transcriptomic changes observed after 7 days of steatosis induction were derived from three individuals, underscores the relevance of the presented findings. As several hallmarks of hepatic steatosis and progression were observed, the data confirmed the hypothesis, that several hits promote the progression simultaneously (Tilg & Moschen, 2010). The presented model is able to recapitulate the complex pathology, on the transcriptomic level in hepatocytes, which is typically observed in patients. Thus, the model has proven its relevance for the study of the hepatocyte-specific contribution to MAFLD-MASH transition.

5.3.1. HLCs secrete active DPP4 upon steatosis

Because HLCs of three individuals showed enhanced expression of genes involved in cytokine-cytokine signaling pathways upon steatosis, factors, secreted to the cell culture supernatant were analyzed. Among others, DPP4 was upregulated upon steatosis in the control cell line. To test

whether the observed finding was cell line specific, hepatic DPP4 secretion upon steatosis induction was quantified in steatotic and non-steatotic HLCs derived from all four individuals. Indeed, enhanced secretion of DPP4 in HLCs upon steatosis induction was observed throughout the cell lines. Interestingly, there seemed to be a stronger increase of DPP4 secretion upon steatosis in the control cell lines in comparison to the patient-derived cell lines, which is why further studies focused on the control lines. Albeit the difference of DPP4 secretion, DPP4 gene and protein expression, as well as its location within the HLCs was not altered. Along with the enhanced secretion, enhanced DPP4 activity upon steatosis was observed, suggesting a potential role of hepatic DPP4 signaling under MAFLD condition.
This is in line with previous findings suggesting DPP4 as a potential target for drug development (Barchetta et al., 2021). DPP4 is a serine protease with multiple functions involved in the regulation of insulin signaling, inflammatory response and extracellular matrix modulation and was found enhanced in MAFLD patients (Barchetta et al., 2021; Baumeier et al., 2017b; Deacon, 2019; Lambeir et al., 2003; Niu et al., 2019; Ohm et al., 2023; Trzaskalski et al., 2020).

Considering the observed findings of DPP4 activity upon steatosis the question remains whether DPP4 is the cause or a correlation of steatosis. Indications point to a more causative role of DPP4, because its expression is indeed regulated by epigenetic changes. DPP4 shows glucose and steatosis induced downregulation of methylation and enhanced expression (Baumeier et al., 2017a; Saussenthaler et al., 2019). Confirming these findings, demethylation of DPP4 CpG islands was observed upon steatosis induction in the presented study, (unpublished). However, due to the rather late time points used in this study (7 days of OA induction), it was not possible to analyze at which time point DPP4 expression or secretion was regulated. Future studies are necessary to decipher the mechanisms of DPP4 expression upon steatosis induction in a time-dose-dependent analysis. Nevertheless, the presented findings integrated with previous studies indicate a potential modulating role of hepatic DPP4 for the progression from MAFLD to MASH, induced by steatosis.

Conclusively, enhanced hepatic DPP4 secretion in all three cell lines upon steatosis as well as elevated hepatic DPP4 activity confirmed the clinical evidence. In line with the complex and context dependent functions, the findings showed that upon steatosis, hepatocyte-specific DPP4 secretion and activity are increased.

5.3.2. Hepatic DPP4 activity modulates inflammatory- and metabolism-associated pathways during steatosis

In order to decipher the potential role of hepatic DPP4 during steatosis, its activity was diminished by vildagliptin, a potent DPP4 inhibitor (DPP4i). DPP4 inhibition is an established treatment option for T2DM as it prevents the degradation of the incretins GIP-1 and GLP-1 and thereby improves the postprandial insulin response and glycemic control (Ahrén et al., 2004; Ahrén et al., 2007; Azuma et al., 2008; Kanazawa et al., 2017). Besides the overall effects on the glucose and insulin metabolism, DPP4i have been shown to improve the liver lipid profile in NAFLD patients with and without T2DM (Hussain et al., 2016; Macauley et al., 2015). In line, vildagliptin has been shown to improve inflammatory response by interfering with inflammatory signaling (Khalil et al., 2020). Furthermore, it was found to increase insulin sensitivity and modulation of oxidative stress in rats (Hendawy et al., 2022).

After confirming successful inhibition of DPP4 activity upon steatosis by vildagliptin, the effects on the global gene expression of steatosis with or without vildagliptin were dissected in cell line Cntrl 1. In accordance with previous studies highlighting the role of DPP4 for hepatic insulin sensitivity, genes involved in KEGG pathways of insulin resistance were downregulated (Baumeier et al., 2017b). The findings underline the potential role of DPP4 for insulin resistance development in hepatocytes (Baumeier et al., 2017b; Hendawy et al., 2022). Furthermore, genes involved in pathways of inflammatory bowel disease, asthma, T1DM and maturity onset diabetes of the young were downregulated upon DPP4i. Since all of these pathways are inflammation-associated, this might be a confirmation of the previously observed improvements in rodent models, where vildagliptin modulated NFkB and TNFα pathways (Hendawy et al., 2022; Khalil et al., 2020). Interestingly, the majority of inflammation-associated pathways represented auto-immune pathways. Indeed, DPP4 is associated with auto-immune diseases and beneficial effects of DPP4i for inflammatory bowel disease and T1DM are discussed (Duan et al., 2017; Lambeir et al., 2003; Melo et al., 2021; Rahim et al., 2024). Nevertheless, the role of DPP4 and the effects of DPP4i for auto-immune diseases remain controversial. Considering inflammatory bowel disease, lower levels of DPP4 are associated with a more severe phenotype, while in T1DM higher DPP4 levels seem to be unfavorable (Iwabuchi et al., 2013; Mahmood et al., 2024; Melo et al., 2021). The results underline the complexity of DPP4 signaling and support a context-dependent role of the catalytic and non-catalytic function of DPP4 as introduced earlier (Barchetta et al., 2022; Varin et al., 2019). Future studies are necessary to dissect the exact consequence on auto-immune responses to

exclude potential adverse effects, considering that MAFLD progresses gradually and long-term treatment would probably be necessary.
Interestingly, a trend of downregulation of genes encoding major histocompatibility complex (MHC)-II proteins human leucocyte antigen (HLA) *HLA-DMA*, *HLA-DMB*, *HLA-DRB1* upon vildagliptin and steatosis condition was observed. Although expressional changes are not directly linked to inflammation or auto-immune diseases, specific haplotypes of HLA-DQ are associated with liver fibrosis and T1DM (Moustakas & Papadopoulos, 2002; Tan et al., 2020). The presented data indicate a modulation of insulin resistance and inflammation-associated pathways mediated by DPP4 activity.

Beyond the observed downregulation of insulin- and inflammation-associated pathways, DPP4i revealed upregulation of fatty acid and purine metabolism as well as metabolic pathways. Upon DPP4i, 1-acylglycerol-3-phosphate O-acyltransferase 2 (*AGPAT2*) and *PLIN3*, which are involved in lipogenesis, were upregulated as confirmed by qRT-PCR analysis. Furthermore, triokinase and FMN cyclase (*TKFC*) and 5'-nucleotidase, cytosolic-2 (*NT5C2*) showed upregulation upon vildagliptin treatment, indicating enhanced purine metabolism. While lipogenesis seems disadvantageous during steatosis, upregulation of lipogenic pathways in parallel with metabolic pathways and purine metabolism might indicate restoration of the cell homeostasis, implying beneficial effect for liver fat content (Hussain et al., 2016; Macauley et al., 2015).

The presented data indicate a role of hepatic DPP4 activity mediating inflammation-associated and metabolic pathways, in line with previous findings. (Trzaskalski et al., 2020). Findings indicated steatosis induced hepatic DPP4 secretion and activity, and highlighted its potential relevance for modulating inflammatory-associated and metabolic pathways. Conclusively, the study provided a first-in-this-format human iPSC-derived hepatic steatosis model, capable of recapitulating the clinical phenotype to study the hepatocyte-specific contribution in the context of MAFLD.

6. Conclusion and outlook

The aim of this dissertation was to contribute to the understanding of liver diseases by applying iPSC-technology. The first objective was to establish patient-derived iPSCs from adult and pediatric AATD patients, providing a platform for comparative studies considering the onset of the disease. By including an 11-year-old pediatric patient, our study aimed to provide a novel tool for studying AATD in children and closing the current gap of knowledge. The second objective was to optimize an established HLC differentiation protocol. Forskolin was found to significantly enhance the maturation by modulating FXR expression. The findings thereby provided novel evidence for the importance of FXR for HLC maturation. Furthermore, the optimized protocol provided a time- and cost-efficient protocol for the derivation of functional iPSC-derived HLCs, which helps to overcome well-known limitations in the field of hepatocyte modeling and improve the existing translational bottleneck of current models.
The third objective focused on applying the optimized protocol, yielding functional HLCs to decipher the hepatocyte-specific contribution to MAFLD progression. Steatosis was induced in HLCs derived from healthy and diseased individuals and the complex modulations of metabolism- and inflammation-associated pathways known from MAFLD-patients were successfully recapitulated. Next generation sequencing (NGS) confirmed metabolic changes as observed by upregulation of genes involved in the insulin resistance pathway and AMPK- and PPAR-signaling. Dysregulation of cell homeostasis by glutathione metabolism downregulation was observed. Indications of the potential progression from steatosis to steatohepatitis were observed as genes involved in inflammatory-associated pathways such as TNFα, NFkB and cytokine-cytokine signaling were upregulated. Additionally, DPP4 secretion and activity was enhanced in steatotic HLCs compared to untreated HLCs. After inhibition of DPP4 activity, inflammation-associated pathways tended to be downregulated, while metabolism-associated pathways showed a trend of upregulation. Thus, the findings indicated a beneficial effect of vildagliptin on steatotic hepatocytes, underlining the relevance of hepatic DPP4 activity for MAFLD modulation. As this study is the first-in-this-format, it provided a novel perspective on the complicated entanglements of DPP4 in a relevant human hepatic steatosis model.

The presented data offers great potential for future studies. Beyond using the generated iPSC-lines for the study of AATD, functional HLCs, showinginducible cytochrome P450 activity represent a valuable tool for liver research. Functional HLCs as generated in this study, facilitate recapitulation of the population diversity, are reproducible and time- and cost-efficiently

produced. Hence, they allow improvement of the current translational bottleneck of *in vitro* studies. Furthermore, functional HLCs may be applied for toxicological assays in order to reduce animal testing. Steatotic HLCs, which recapitulate the gradual progression from steatosis to steatohepatitis were shown to provide insights on the hepatocyte-specific contribution to MAFLD. The presented model offers a reproducible and relevant tool. In the future, it has the potential to incorporate additional aspects such as co-pathologies (e.g. insulin resistance, gut dysbiosis) or behaviors (e.g. alcohol consumption) by adjusting the experimental setting. To further dissect the concrete function of hepatic DPP4 in this context, future investigations including the genetic knockout of DPP4 might provide new insights. Beyond that it would be interesting to co-culture steatotic hepatocytes with liver-specific cell types, such as stellate cells to understand the effect of secreted active DPP4 in a more physiological environment.

7. References

Adeva-Andany, M. M., Pérez-Felpete, N., Fernández-Fernández, C., Donapetry-García, C., & Pazos-García, C. (2016). Liver glucose metabolism in humans. *Biosci Rep*, *36*(6). https://doi.org/10.1042/bsr20160385

Agarwal, S., Holton, K. L., & Lanza, R. (2008). Efficient Differentiation of Functional Hepatocytes from Human Embryonic Stem Cells. *Stem Cells*, *26*(5), 1117-1127. https://doi.org/10.1634/stemcells.2007-1102

Ahrén, B., Landin-Olsson, M., Jansson, P. A., Svensson, M., Holmes, D., & Schweizer, A. (2004). Inhibition of dipeptidyl peptidase-4 reduces glycemia, sustains insulin levels, and reduces glucagon levels in type 2 diabetes. *J Clin Endocrinol Metab*, *89*(5), 2078-2084. https://doi.org/10.1210/jc.2003-031907

Ahrén, B., Winzell, M. S., Wierup, N., Sundler, F., Burkey, B., & Hughes, T. E. (2007). DPP-4 inhibition improves glucose tolerance and increases insulin and GLP-1 responses to gastric glucose in association with normalized islet topography in mice with β-cell-specific overexpression of human islet amyloid polypeptide. *Regulatory Peptides*, *143*(1), 97-103. https://doi.org/https://doi.org/10.1016/j.regpep.2007.03.008

Ampuero, J., & Romero-Gomez, M. (2020). Stratification of patients in NASH clinical trials: A pitfall for trial success. *JHEP Reports*, *2*(5). https://doi.org/10.1016/j.jhepr.2020.100148

Anania, F. A., Dimick‐Santos, L., Mehta, R., Toerner, J., & Beitz, J. (2021). Nonalcoholic Steatohepatitis: Current Thinking From the Division of Hepatology and Nutrition at the Food and Drug Administration. *Hepatology*, *73*(5), 2023-2027. https://doi.org/10.1002/hep.31687

Andersen, J., Revah, O., Miura, Y., Thom, N., Amin, N. D., Kelley, K. W., Singh, M., Chen, X., Thete, M. V., Walczak, E. M., Vogel, H., Fan, H. C., & Paşca, S. P. (2020). Generation of Functional Human 3D Cortico-Motor Assembloids. *Cell*, *183*(7), 1913-1929.e1926. https://doi.org/10.1016/j.cell.2020.11.017

Angulo, P. (2007). Obesity and nonalcoholic fatty liver disease. *Nutr Rev*, *65*(6 Pt 2), S57-63. https://doi.org/10.1111/j.1753-4887.2007.tb00329.x

Araki, H., Miura, F., Watanabe, A., Morinaga, C., Kitaoka, F., Kitano, Y., Sakai, N., Shibata, Y., Terada, M., Goto, S., Yamanaka, S., Takahashi, M., & Ito, T. (2019). Base-Resolution Methylome of Retinal Pigment Epithelial Cells Used in the First Trial of Human Induced Pluripotent Stem Cell-Based Autologous Transplantation. *Stem Cell Reports*, *13*(4), 761-774. https://doi.org/10.1016/j.stemcr.2019.08.014

Arrieta-Bolaños, E., Hernández-Zaragoza, D. I., & Barquera, R. (2023). An HLA map of the world: A comparison of HLA frequencies in 200 worldwide populations reveals diverse patterns for class I and class II. *Front Genet*, *14*, 866407. https://doi.org/10.3389/fgene.2023.866407

Asrani, S. K., Devarbhavi, H., Eaton, J., & Kamath, P. S. (2019). Burden of liver diseases in the world. *J Hepatol*, *70*(1), 151-171. https://doi.org/10.1016/j.jhep.2018.09.014

Azuma, K., Rádiková, Z., Mancino, J., Toledo, F. G., Thomas, E., Kangani, C., Dalla Man, C., Cobelli, C., Holst, J. J., Deacon, C. F., He, Y., Ligueros-Saylan, M., Serra, D., Foley, J. E., & Kelley, D. E. (2008). Measurements of islet function and glucose metabolism with the dipeptidyl peptidase 4 inhibitor vildagliptin in patients with type 2 diabetes. *J Clin Endocrinol Metab*, *93*(2), 459-464. https://doi.org/10.1210/jc.2007-1369

Babaie, Y., Herwig, R., Greber, B., Brink, T. C., Wruck, W., Groth, D., Lehrach, H., Burdon, T., & Adjaye, J. (2007). Analysis of Oct4-dependent transcriptional networks regulating self-renewal and pluripotency in human embryonic stem cells. *Stem Cells*, *25*(2), 500-510. https://doi.org/10.1634/stemcells.2006-0426

Baggio, L. L., & Drucker, D. J. (2007). Biology of incretins: GLP-1 and GIP. *Gastroenterology*, *132*(6), 2131-2157. https://doi.org/10.1053/j.gastro.2007.03.054

Barchetta, I., Ceccarelli, V., Cimini, F. A., Barone, E., Sentinelli, F., Coluzzi, M., Chiappetta, C., Bertoccini, L., Tramutola, A., Labbadia, G., Di Cristofano, C., Silecchia, G., Leonetti, F., & Cavallo, M. G. (2021). Circulating dipeptidyl peptidase-4 is independently associated with the presence and severity of NAFLD/NASH in individuals with and without obesity and metabolic disease. *J Endocrinol Invest*, *44*(5), 979-988. https://doi.org/10.1007/s40618-020-01392-5

Barchetta, I., Cimini, F. A., Dule, S., & Cavallo, M. G. (2022). Dipeptidyl Peptidase 4 (DPP4) as A Novel Adipokine: Role in Metabolism and Fat Homeostasis. *Biomedicines*, *10*(9), 2306. https://www.mdpi.com/2227-9059/10/9/2306

Barrera, F., Uribe, J., Olvares, N., Huerta, P., Cabrera, D., & Romero-Gómez, M. (2024). The Janus of a disease: Diabetes and metabolic dysfunction-associated fatty liver disease. *Ann Hepatol*, *29*(4), 101501. https://doi.org/10.1016/j.aohep.2024.101501

Bataller, R., & Brenner, D. A. (2005). Liver fibrosis. *J Clin Invest*, *115*(2), 209-218. https://doi.org/10.1172/jci24282

Baumeier, C., Saussenthaler, S., Kammel, A., Jahnert, M., Schluter, L., Hesse, D., Canouil, M., Lobbens, S., Caiazzo, R., Raverdy, V., Pattou, F., Nilsson, E., Pihlajamaki, J., Ling, C., Froguel, P., Schurmann, A., & Schwenk, R. W. (2017a). Hepatic DPP4 DNA Methylation Associates With Fatty Liver. *Diabetes*, *66*(1), 25-35. https://doi.org/10.2337/db15-1716

Baumeier, C., Saussenthaler, S., Kammel, A., Jähnert, M., Schlüter, L., Hesse, D., Canouil, M., Lobbens, S., Caiazzo, R., Raverdy, V., Pattou, F., Nilsson, E., Pihlajamäki, J., Ling, C., Froguel, P., Schürmann, A., & Schwenk, R. W. (2016). Hepatic DPP4 DNA Methylation Associates With Fatty Liver. *Diabetes*, *66*(1), 25-35. https://doi.org/10.2337/db15-1716

Baumeier, C., Schluter, L., Saussenthaler, S., Laeger, T., Rodiger, M., Alaze, S. A., Fritsche, L., Haring, H. U., Stefan, N., Fritsche, A., Schwenk, R. W., & Schurmann, A. (2017b). Elevated hepatic DPP4 activity promotes insulin resistance and non-alcoholic fatty liver disease. *Mol Metab*, *6*(10), 1254-1263. https://doi.org/10.1016/j.molmet.2017.07.016

Baxter, M., Withey, S., Harrison, S., Segeritz, C.-P., Zhang, F., Atkinson-Dell, R., Rowe, C., Gerrard, D. T., Sison-Young, R., Jenkins, R., Henry, J., Berry, A. A., Mohamet, L., Best, M., Fenwick, S. W., Malik, H., Kitteringham, N. R., Goldring, C. E., Piper Hanley, K.,…Hanley, N. A. (2015). Phenotypic and functional analyses show stem cell-derived hepatocyte-like cells better mimic fetal rather than adult hepatocytes. *Journal of Hepatology*, *62*(3), 581-589. https://doi.org/10.1016/j.jhep.2014.10.016

Benda, C., Zhou, T., Wang, X., Tian, W., Grillari, J., Tse, H. F., Grillari-Voglauer, R., Pei, D., & Esteban, M. A. (2013). Urine as a source of stem cells. *Adv Biochem Eng Biotechnol*, *129*, 19-32. https://doi.org/10.1007/10_2012_157

Benhamouche, S., Decaens, T., Godard, C., Chambrey, R., Rickman, D. S., Moinard, C., Vasseur-Cognet, M., Kuo, C. J., Kahn, A., Perret, C., & Colnot, S. (2006). APC Tumor Supressor Gene is the Zonation Keeper of Mouse Liver. *Developmental Cell*, *10*(6), 759-770. https://doi.org/10.1016/j.devcel.2006.03.015

Bergqvist, C. J., Skoien, R., Horsfall, L., Clouston, A. D., Jonsson, J. R., & Powell, E. E. (2013). Awareness and opinions of non-alcoholic fatty liver disease by hospital specialists. *Intern Med J*, *43*(3), 247-253. https://doi.org/10.1111/j.1445-5994.2012.02848.x

Blanco, I., Bueno, P., Diego, I., Pérez-Holanda, S., Casas-Maldonado, F., Esquinas, C., & Miravitlles, M. (2017). Alpha-1 antitrypsin Pi*Z gene frequency and Pi*ZZ genotype numbers worldwide: an update. *Int J Chron Obstruct Pulmon Dis*, *12*, 561-569. https://doi.org/10.2147/copd.S125389

Bohndorf, M., Ncube, A., Spitzhorn, L.-S., Enczmann, J., Wruck, W., & Adjaye, J. (2017). Derivation and characterization of integration-free iPSC line ISRM-UM51 derived from SIX2-positive renal cells isolated from urine of an African male expressing the CYP2D6 *4/*17 variant which confers intermediate drug metabolizing activity. *Stem Cell Research*, *25*, 18-21. https://doi.org/https://doi.org/10.1016/j.scr.2017.10.004

Bonder, M. J., Smail, C., Gloudemans, M. J., Frésard, L., Jakubosky, D., D'Antonio, M., Li, X., Ferraro, N. M., Carcamo-Orive, I., Mirauta, B., Seaton, D. D., Cai, N., Vakili, D., Horta, D., Zhao, C., Zastrow, D. B., Bonner, D. E., Jan Bonder, M., Seaton, D.,…PhLi, P. S. c. (2021). Identification of rare and common regulatory variants in pluripotent cells using population-scale transcriptomics. *Nature Genetics*, *53*(3), 313-321. https://doi.org/10.1038/s41588-021-00800-7

Cai, J., Zhao, Y., Liu, Y., Ye, F., Song, Z., Qin, H., Meng, S., Chen, Y., Zhou, R., Song, X., Guo, Y., Ding, M., & Deng, H. (2007). Directed differentiation of human embryonic stem cells into functional hepatic cells†. *Hepatology*, *45*(5). https://journals.lww.com/hep/fulltext/2007/05000/directed_differentiation_of_human_embryonic_stem.18.aspx

Cameron, K., Tan, R., Schmidt-Heck, W., Campos, G., Lyall, M. J., Wang, Y., Lucendo-Villarin, B., Szkolnicka, D., Bates, N., Kimber, S. J., Hengstler, J. G., Godoy, P., Forbes, S. J., & Hay, D. C. (2015). Recombinant Laminins Drive the Differentiation and Self-Organization of hESC-Derived Hepatocytes. *Stem Cell Reports*, *5*(6), 1250-1262. https://doi.org/10.1016/j.stemcr.2015.10.016

Carlson, J. A., Rogers, B. B., Sifers, R. N., Finegold, M. J., Clift, S. M., DeMayo, F. J., Bullock, D. W., & Woo, S. L. (1989). Accumulation of PiZ alpha 1-antitrypsin causes liver damage in transgenic mice. *J Clin Invest*, *83*(4), 1183-1190. https://doi.org/10.1172/jci113999

Catrysse, L., & van Loo, G. (2017). Inflammation and the Metabolic Syndrome: The Tissue-Specific Functions of NF-κB. *Trends in Cell Biology*, *27*(6), 417-429. https://doi.org/https://doi.org/10.1016/j.tcb.2017.01.006

Cerneckis, J., Cai, H., & Shi, Y. (2024). Induced pluripotent stem cells (iPSCs): molecular mechanisms of induction and applications. *Signal Transduction and Targeted Therapy*, *9*(1), 112. https://doi.org/10.1038/s41392-024-01809-0

Charlton, M. R. (1996). Protein metabolism and liver disease. *Baillière's Clinical Endocrinology and Metabolism*, *10*(4), 617-635. https://doi.org/https://doi.org/10.1016/S0950-351X(96)80771-3

Chiang, J. (2014). Liver Physiology: Metabolism and Detoxification. In L. M. McManus & R. N. Mitchell (Eds.), *Pathobiology of Human Disease* (pp. 1770-1782). Academic Press. https://doi.org/https://doi.org/10.1016/B978-0-12-386456-7.04202-7

Chowdhury, S., & Ghosh, S. (2021). Stem Cells an Overview. In S. Chowdhury & S. Ghosh (Eds.), *Stem Cells : Biology and Therapeutics* (pp. 1-21). Springer Singapore. https://doi.org/10.1007/978-981-16-1638-9_1

Ciardullo, S., Muraca, E., Vergani, M., Invernizzi, P., & Perseghin, G. (2024). Advancements in pharmacological treatment of NAFLD/MASLD: a focus on metabolic and liver-targeted interventions. *Gastroenterology Report*, *12*. https://doi.org/10.1093/gastro/goae029

Clemente-Suárez, V. J., Beltrán-Velasco, A. I., Redondo-Flórez, L., Martín-Rodríguez, A., & Tornero-Aguilera, J. F. (2023). Global Impacts of Western Diet and Its Effects on Metabolism and Health: A Narrative Review. *Nutrients*, *15*(12). https://doi.org/10.3390/nu15122749

Collin de l'Hortet, A., Takeishi, K., Guzman-Lepe, J., Morita, K., Achreja, A., Popovic, B., Wang, Y., Handa, K., Mittal, A., Meurs, N., Zhu, Z., Weinberg, F., Salomon, M., Fox, I. J., Deng, C. X., Nagrath, D., & Soto-Gutierrez, A. (2019). Generation of Human Fatty

Livers Using Custom-Engineered Induced Pluripotent Stem Cells with Modifiable SIRT1 Metabolism. *Cell Metab*, *30*(2), 385-401.e389. https://doi.org/10.1016/j.cmet.2019.06.017

Davison, B. A., Harrison, S. A., Cotter, G., Alkhouri, N., Sanyal, A., Edwards, C., Colca, J. R., Iwashita, J., Koch, G. G., & Dittrich, H. C. (2020). Suboptimal reliability of liver biopsy evaluation has implications for randomized clinical trials. *J Hepatol*, *73*(6), 1322-1332. https://doi.org/10.1016/j.jhep.2020.06.025

Dawood, A. A., Ghobashy, Y. E., & Elgamal, A. A. (2018). The relationship between serum dipeptidyl peptidase-4 enzyme and nonalcoholic fatty liver disease in diabetic and nondiabetic patients. *The Egyptian Journal of Internal Medicine*, *30*(2), 49-53. https://doi.org/10.4103/ejim.ejim_34_17

Day, C. P., & James, O. F. (1998). Steatohepatitis: a tale of two "hits"? *Gastroenterology*, *114*(4), 842-845. https://doi.org/10.1016/s0016-5085(98)70599-2

de Serres, F., & Blanco, I. (2014). Role of alpha-1 antitrypsin in human health and disease. *J Intern Med*, *276*(4), 311-335. https://doi.org/10.1111/joim.12239

Deacon, C. F. (2019). Physiology and Pharmacology of DPP-4 in Glucose Homeostasis and the Treatment of Type 2 Diabetes. *Front Endocrinol (Lausanne)*, *10*, 80. https://doi.org/10.3389/fendo.2019.00080

Dempsey, J. L., Ioannou, G. N., & Carr, R. M. (2023). Mechanisms of Lipid Droplet Accumulation in Steatotic Liver Diseases. *Semin Liver Dis*, *43*(4), 367-382. https://doi.org/10.1055/a-2186-3557

Deng, K. Q., Huang, X., Lei, F., Zhang, X. J., Zhang, P., She, Z. G., Cai, J., Ji, Y. X., & Li, H. (2022). Role of hepatic lipid species in the progression of nonalcoholic fatty liver disease. *Am J Physiol Cell Physiol*, *323*(2), C630-c639. https://doi.org/10.1152/ajpcell.00123.2022

Devarbhavi, H., Asrani, S. K., Arab, J. P., Nartey, Y. A., Pose, E., & Kamath, P. S. (2023). Global burden of liver disease: 2023 update. *J Hepatol*, *79*(2), 516-537. https://doi.org/10.1016/j.jhep.2023.03.017

Duan, L., Rao, X., Braunstein, Z., Toomey, A. C., & Zhong, J. (2017). Role of Incretin Axis in Inflammatory Bowel Disease. *Front Immunol*, *8*, 1734. https://doi.org/10.3389/fimmu.2017.01734

Dutta, R. K., Jun, J., Du, K., & Diehl, A. M. (2023). Hedgehog Signaling: Implications in Liver Pathophysiology. *Semin Liver Dis*, *43*(4), 418-428. https://doi.org/10.1055/a-2187-3382

Ekstedt, M., Hagström, H., Nasr, P., Fredrikson, M., Stål, P., Kechagias, S., & Hultcrantz, R. (2015). Fibrosis stage is the strongest predictor for disease-specific mortality in NAFLD after up to 33 years of follow-up. *Hepatology*, *61*(5), 1547-1554. https://doi.org/10.1002/hep.27368

Escribá, R., Beksac, M., Bennaceur-Griscelli, A., Glover, J. C., Koskela, S., Latsoudis, H., Querol, S., & Alvarez-Palomo, B. (2024). Current Landscape of iPSC Haplobanks. *Stem Cell Rev Rep*, *20*(8), 2155-2164. https://doi.org/10.1007/s12015-024-10783-7

Eslam, M., Newsome, P. N., Sarin, S. K., Anstee, Q. M., Targher, G., Romero-Gomez, M., Zelber-Sagi, S., Wai-Sun Wong, V., Dufour, J. F., Schattenberg, J. M., Kawaguchi, T., Arrese, M., Valenti, L., Shiha, G., Tiribelli, C., Yki-Järvinen, H., Fan, J. G., Grønbæk, H., Yilmaz, Y.,…George, J. (2020). A new definition for metabolic dysfunction-associated fatty liver disease: An international expert consensus statement. *J Hepatol*, *73*(1), 202-209. https://doi.org/10.1016/j.jhep.2020.03.039

European Medicines Agency (EMA). (2024). *Medicines for human use under evaluation*. European Medicines Agency. Retrieved 04.01.2025 from https://www.ema.europa.eu/en/medicines/medicines-human-use-under-evaluation#monthly-lists-2024-64952

Evans, M. J., & Kaufman, M. H. (1981). Establishment in culture of pluripotential cells from mouse embryos. *Nature*, *292*(5819), 154-156. https://doi.org/10.1038/292154a0

Fang, C., Pan, J., Qu, N., Lei, Y., Han, J., Zhang, J., & Han, D. (2022). The AMPK pathway in fatty liver disease. *Front Physiol*, *13*, 970292. https://doi.org/10.3389/fphys.2022.970292

Febbraio, M. A., Reibe, S., Shalapour, S., Ooi, G. J., Watt, M. J., & Karin, M. (2019). Preclinical Models for Studying NASH-Driven HCC: How Useful Are They? *Cell Metab*, *29*(1), 18-26. https://doi.org/10.1016/j.cmet.2018.10.012

Friedman, S. L. (2008). Hepatic stellate cells: protean, multifunctional, and enigmatic cells of the liver. *Physiol Rev*, *88*(1), 125-172. https://doi.org/10.1152/physrev.00013.2007

Friedman, S. L., Neuschwander-Tetri, B. A., Rinella, M., & Sanyal, A. J. (2018). Mechanisms of NAFLD development and therapeutic strategies. *Nat Med*, *24*(7), 908-922. https://doi.org/10.1038/s41591-018-0104-9

Fromme, M., Klebingat, F., Ellis, P., & Strnad, P. (2025). Alpha-1 antitrypsin deficiency-associated liver disease: From understudied disorder to the poster child of genetic medicine. *Hepatol Commun*, *9*(5). https://doi.org/10.1097/hc9.0000000000000699

Gatzios, A., Rombaut, M., Buyl, K., De Kock, J., Rodrigues, R. M., Rogiers, V., Vanhaecke, T., & Boeckmans, J. (2022). From NAFLD to MAFLD: Aligning Translational In Vitro Research to Clinical Insights. *Biomedicines*, *10*(1). https://doi.org/10.3390/biomedicines10010161

Godoy, P., Widera, A., Schmidt-Heck, W., Campos, G., Meyer, C., Cadenas, C., Reif, R., Stober, R., Hammad, S., Putter, L., Gianmoena, K., Marchan, R., Ghallab, A., Edlund, K., Nussler, A., Thasler, W. E., Damm, G., Seehofer, D., Weiss, T. S.,…Hengstler, J. G. (2016). Gene network activity in cultivated primary hepatocytes is highly similar to diseased mammalian liver tissue. *Arch Toxicol*, *90*(10), 2513-2529. https://doi.org/10.1007/s00204-016-1761-4

Goel, C., Monga, S. P., & Nejak-Bowen, K. (2022). Role and Regulation of Wnt/β-Catenin in Hepatic Perivenous Zonation and Physiological Homeostasis. *Am J Pathol*, *192*(1), 4-17. https://doi.org/10.1016/j.ajpath.2021.09.007

Gofton, C., Upendran, Y., Zheng, M. H., & George, J. (2023). MAFLD: How is it different from NAFLD? *Clin Mol Hepatol*, *29*(Suppl), S17-s31. https://doi.org/10.3350/cmh.2022.0367

Gorrell, M. D., Gysbers, V., & McCaughan, G. W. (2001). CD26: a multifunctional integral membrane and secreted protein of activated lymphocytes. *Scand J Immunol*, *54*(3), 249-264. https://doi.org/10.1046/j.1365-3083.2001.00984.x

Graffmann, N., Bohndorf, M., Ncube, A., Wruck, W., Kashofer, K., Zatloukal, K., & Adjaye, J. (2018a). Establishment and characterization of an iPSC line from a 58 years old high grade patient with nonalcoholic fatty liver disease (70% steatosis) with homozygous wildtype PNPLA3 genotype. *Stem Cell Res*, *31*, 131-134. https://doi.org/10.1016/j.scr.2018.07.011

Graffmann, N., Ncube, A., Martins, S., Fiszl, A. R., Reuther, P., Bohndorf, M., Wruck, W., Beller, M., Czekelius, C., & Adjaye, J. (2021). A stem cell based in vitro model of NAFLD enables the analysis of patient specific individual metabolic adaptations in response to a high fat diet and AdipoRon interference. *Biol Open*, *10*(1). https://doi.org/10.1242/bio.054189

Graffmann, N., Ncube, A., Wruck, W., & Adjaye, J. (2018b). Cell fate decisions of human iPSC-derived bipotential hepatoblasts depend on cell density. *PLoS One*, *13*(7), e0200416. https://doi.org/10.1371/journal.pone.0200416

Graffmann, N., Ring, S., Kawala, M. A., Wruck, W., Ncube, A., Trompeter, H. I., & Adjaye, J. (2016). Modeling Nonalcoholic Fatty Liver Disease with Human Pluripotent Stem Cell-Derived Immature Hepatocyte-Like Cells Reveals Activation of PLIN2 and Confirms

Regulatory Functions of Peroxisome Proliferator-Activated Receptor Alpha. *Stem Cells Dev*, *25*(15), 1119-1133. https://doi.org/10.1089/scd.2015.0383

Graffmann, N., Scherer, B., & Adjaye, J. (2022). In vitro differentiation of pluripotent stem cells into hepatocyte like cells – Basic principles and current progress. *Stem Cell Research*, *61*, 102763. https://doi.org/https://doi.org/10.1016/j.scr.2022.102763

Greber, B., Lehrach, H., & Adjaye, J. (2007). Fibroblast growth factor 2 modulates transforming growth factor beta signaling in mouse embryonic fibroblasts and human ESCs (hESCs) to support hESC self-renewal. *Stem Cells*, *25*(2), 455-464. https://doi.org/10.1634/stemcells.2006-0476

Guo, Z., Wu, D., Mao, R., Yao, Z., Wu, Q., & Lv, W. (2025). Global burden of MAFLD, MAFLD related cirrhosis and MASH related liver cancer from 1990 to 2021. *Sci Rep*, *15*(1), 7083. https://doi.org/10.1038/s41598-025-91312-5

Gurdon, J. B., Elsdale, T. R., & Fischberg, M. (1958). Sexually Mature Individuals of Xenopus laevis from the Transplantation of Single Somatic Nuclei. *Nature*, *182*(4627), 64-65. https://doi.org/10.1038/182064a0

Gurevich, I., Burton, S. A., Munn, C., Ohshima, M., Goedland, M. E., Czysz, K., & Rajesh, D. (2020). iPSC-derived hepatocytes generated from NASH donors provide a valuable platform for disease modeling and drug discovery. *Biol Open*, *9*(12). https://doi.org/10.1242/bio.055087

Han, H.-S., Kang, G., Kim, J. S., Choi, B. H., & Koo, S.-H. (2016). Regulation of glucose metabolism from a liver-centric perspective. *Experimental & Molecular Medicine*, *48*(3), e218-e218. https://doi.org/10.1038/emm.2015.122

Harrison, S. A., Bedossa, P., Guy, C. D., Schattenberg, J. M., Loomba, R., Taub, R., Labriola, D., Moussa, S. E., Neff, G. W., Rinella, M. E., Anstee, Q. M., Abdelmalek, M. F., Younossi, Z., Baum, S. J., Francque, S., Charlton, M. R., Newsome, P. N., Lanthier, N., Schiefke, I.,…Ratziu, V. (2024). A Phase 3, Randomized, Controlled Trial of Resmetirom in NASH with Liver Fibrosis. *N Engl J Med*, *390*(6), 497-509. https://doi.org/10.1056/NEJMoa2309000

Hay, D. C., Fletcher, J., Payne, C., Terrace, J. D., Gallagher, R. C., Snoeys, J., Black, J. R., Wojtacha, D., Samuel, K., Hannoun, Z., Pryde, A., Filippi, C., Currie, I. S., Forbes, S. J., Ross, J. A., Newsome, P. N., & Iredale, J. P. (2008a). Highly efficient differentiation of hESCs to functional hepatic endoderm requires ActivinA and Wnt3a signaling. *Proc Natl Acad Sci U S A*, *105*(34), 12301-12306. https://doi.org/10.1073/pnas.0806522105

Hay, D. C., Zhao, D., Fletcher, J., Hewitt, Z. A., McLean, D., Urruticoechea-Uriguen, A., Black, J. R., Elcombe, C., Ross, J. A., Wolf, R., & Cui, W. (2008b). Efficient differentiation of hepatocytes from human embryonic stem cells exhibiting markers recapitulating liver development in vivo. *Stem Cells*, *26*(4), 894-902. https://doi.org/10.1634/stemcells.2007-0718

Heida, A., Gruben, N., Catrysse, L., Koehorst, M., Koster, M., Kloosterhuis, N. J., Gerding, A., Havinga, R., Bloks, V. W., Bongiovanni, L., Wolters, J. C., van Dijk, T., van Loo, G., de Bruin, A., Kuipers, F., Koonen, D. P. Y., & van de Sluis, B. (2021). The hepatocyte IKK:NF-κB axis promotes liver steatosis by stimulating de novo lipogenesis and cholesterol synthesis. *Mol Metab*, *54*, 101349. https://doi.org/10.1016/j.molmet.2021.101349

Hendawy, A. S., El-Lakkany, N. M., Mantawy, E. M., Hammam, O. A., Botros, S. S., & El-Demerdash, E. (2022). Vildagliptin alleviates liver fibrosis in NASH diabetic rats via modulation of insulin resistance, oxidative stress, and inflammatory cascades. *Life Sci*, *304*, 120695. https://doi.org/10.1016/j.lfs.2022.120695

Heydari, Z., Najimi, M., Mirzaei, H., Shpichka, A., Ruoss, M., Farzaneh, Z., Montazeri, L., Piryaei, A., Timashev, P., Gramignoli, R., Nussler, A., Baharvand, H., & Vosough, M.

(2020). Tissue Engineering in Liver Regenerative Medicine: Insights into Novel Translational Technologies. *Cells*, *9*(2). https://doi.org/10.3390/cells9020304

Hodson, L., Skeaff, C. M., & Fielding, B. A. (2008). Fatty acid composition of adipose tissue and blood in humans and its use as a biomarker of dietary intake. *Progress in Lipid Research*, *47*(5), 348-380. https://doi.org/https://doi.org/10.1016/j.plipres.2008.03.003

hPSCreg – The Human Pluripotent Stem Cell Registry. (2025). Retrieved May 15, 2025 from https://hpscreg.eu

Huang, C. Y., Nicholson, M. W., Wang, J. Y., Ting, C. Y., Tsai, M. H., Cheng, Y. C., Liu, C. L., Chan, D. Z. H., Lee, Y. C., Hsu, C. C., Hsu, Y. H., Yang, C. F., Chang, C. M. C., Ruan, S. C., Lin, P. J., Lin, J. H., Chen, L. L., Hsieh, M. L., Cheng, Y. Y.,…Hsieh, P. C. H. (2022). Population-based high-throughput toxicity screen of human iPSC-derived cardiomyocytes and neurons. *Cell Reports*, *39*(1). https://doi.org/10.1016/j.celrep.2022.110643

Huang, D. Q., Terrault, N. A., Tacke, F., Gluud, L. L., Arrese, M., Bugianesi, E., & Loomba, R. (2023). Global epidemiology of cirrhosis - aetiology, trends and predictions. *Nat Rev Gastroenterol Hepatol*, *20*(6), 388-398. https://doi.org/10.1038/s41575-023-00759-2

Huang, Y. Z., He, T., Cui, J., Jiang, Y. L., Zeng, J. F., Zhang, W. Q., & Xie, H. Q. (2022). Urine-Derived Stem Cells for Regenerative Medicine: Basic Biology, Applications, and Challenges. *Tissue Eng Part B Rev*, *28*(5), 978-994. https://doi.org/10.1089/ten.teb.2021.0142

Huang, Z., Iqbal, Z., Zhao, Z., Liu, J., Alabsi, A. M., Shabbir, M., Mahmood, A., Liang, Y., Li, W., & Deng, Z. (2024). Cellular crosstalk in the bone marrow niche. *J Transl Med*, *22*(1), 1096. https://doi.org/10.1186/s12967-024-05900-6

Huh, D., Hamilton, G. A., & Ingber, D. E. (2011). From 3D cell culture to organs-on-chips. *Trends Cell Biol*, *21*(12), 745-754. https://doi.org/10.1016/j.tcb.2011.09.005

Hussain, M., Majeed Babar, M. Z., Hussain, M. S., & Akhtar, L. (2016). Vildagliptin ameliorates biochemical, metabolic and fatty changes associated with non alcoholic fatty liver disease. *Pak J Med Sci*, *32*(6), 1396-1401. https://doi.org/10.12669/pjms.326.11133

Hyun, J., & Jung, Y. (2020). DNA Methylation in Nonalcoholic Fatty Liver Disease. *Int J Mol Sci*, *21*(21). https://doi.org/10.3390/ijms21218138

Idilman, I. S., Ozdeniz, I., & Karcaaltincaba, M. (2016). Hepatic Steatosis: Etiology, Patterns, and Quantification. *Semin Ultrasound CT MR*, *37*(6), 501-510. https://doi.org/10.1053/j.sult.2016.08.003

Inamura, M., Kawabata, K., Takayama, K., Tashiro, K., Sakurai, F., Katayama, K., Toyoda, M., Akutsu, H., Miyagawa, Y., Okita, H., Kiyokawa, N., Umezawa, A., Hayakawa, T., Furue, M. K., & Mizuguchi, H. (2011). Efficient Generation of Hepatoblasts From Human ES Cells and iPS Cells by Transient Overexpression of Homeobox Gene HEX. *Molecular Therapy*, *19*(2), 400-407. https://doi.org/https://doi.org/10.1038/mt.2010.241

Iwabuchi, A., Kamoda, T., Saito, M., Nozue, H., Izumi, I., Hirano, T., & Sumazaki, R. (2013). Serum dipeptidyl peptidase 4 activity in children with type 1 diabetes mellitus. *J Pediatr Endocrinol Metab*, *26*(11-12), 1093-1097. https://doi.org/10.1515/jpem-2013-0122

Jackson, E. B., & Brues, A. M. (1941). Studies on a Transplantable Embryoma of the Mouse. *Cancer Research*, *1*, 494-498.

Jiang, W., Mao, X., Liu, Z., Zhang, T., Jin, L., & Chen, X. (2023). Global Burden of Nonalcoholic Fatty Liver Disease, 1990 to 2019: Findings From the Global Burden of Disease Study 2019. *J Clin Gastroenterol*, *57*(6), 631-639. https://doi.org/10.1097/mcg.0000000000001739

Johnson, S. M., Bao, H., McMahon, C. E., Chen, Y., Burr, S. D., Anderson, A. M., Madeyski-Bengtson, K., Lindén, D., Han, X., & Liu, J. (2024). PNPLA3 is a triglyceride lipase

that mobilizes polyunsaturated fatty acids to facilitate hepatic secretion of large-sized very low-density lipoprotein. *Nature Communications*, *15*(1), 4847. https://doi.org/10.1038/s41467-024-49224-x

Jozefczuk, J., Kashofer, K., Ummanni, R., Henjes, F., Rehman, S., Geenen, S., Wruck, W., Regenbrecht, C., Daskalaki, A., Wierling, C., Turano, P., Bertini, I., Korf, U., Zatloukal, K., Westerhoff, H. V., Lehrach, H., & Adjaye, J. (2012). A Systems Biology Approach to Deciphering the Etiology of Steatosis Employing Patient-Derived Dermal Fibroblasts and iPS Cells. *Front Physiol*, *3*, 339. https://doi.org/10.3389/fphys.2012.00339

Jozefczuk, J., Prigione, A., Chavez, L., & Adjaye, J. (2011). Comparative analysis of human embryonic stem cell and induced pluripotent stem cell-derived hepatocyte-like cells reveals current drawbacks and possible strategies for improved differentiation. *Stem Cells Dev*, *20*(7), 1259-1275. https://doi.org/10.1089/scd.2010.0361

Kanazawa, I., Tanaka, K. I., Notsu, M., Tanaka, S., Kiyohara, N., Koike, S., Yamane, Y., Tada, Y., Sasaki, M., Yamauchi, M., & Sugimoto, T. (2017). Long-term efficacy and safety of vildagliptin add-on therapy in type 2 diabetes mellitus with insulin treatment. *Diabetes Res Clin Pract*, *123*, 9-17. https://doi.org/10.1016/j.diabres.2016.11.010

Kanel, G. C. (2009). Liver: anatomy, microscopic structure, and cell types. In T. Yamada (Ed.), *Atlas of Gastroenterology* (4 ed., pp. 615-622). Backwell Publishing Ltd.

Karagiannis, P., Takahashi, K., Saito, M., Yoshida, Y., Okita, K., Watanabe, A., Inoue, H., Yamashita, J. K., Todani, M., Nakagawa, M., Osawa, M., Yashiro, Y., Yamanaka, S., & Osafune, K. (2019). Induced Pluripotent Stem Cells and Their Use in Human Models of Disease and Development. *Physiol Rev*, *99*(1), 79-114. https://doi.org/10.1152/physrev.00039.2017

Kasai, F., Hirayama, N., Ozawa, M., Satoh, M., & Kohara, A. (2018). HuH-7 reference genome profile: complex karyotype composed of massive loss of heterozygosity. *Hum Cell*, *31*(3), 261-267. https://doi.org/10.1007/s13577-018-0212-3

Kaserman, J. E., Hurley, K., Dodge, M., Villacorta-Martin, C., Vedaie, M., Jean, J. C., Liberti, D. C., James, M. F., Higgins, M. I., Lee, N. J., Washko, G. R., San Jose Estepar, R., Teckman, J., Kotton, D. N., & Wilson, A. A. (2020). A Highly Phenotyped Open Access Repository of Alpha-1 Antitrypsin Deficiency Pluripotent Stem Cells. *Stem Cell Reports*, *15*(1), 242-255. https://doi.org/10.1016/j.stemcr.2020.06.006

Katzer, D., Ganschow, R., Strnad, P., & Hamesch, K. (2021). Pi*ZZ-related liver disease in children and adults—narrative review of the typical presentation and management of alpha-1 antitrypsin deficiency. *Digestive Medicine Research*.

Kawala, M. A., Bohndorf, M., Graffmann, N., Wruck, W., Zatloukal, K., & Adjaye, J. (2016). Characterization of dermal fibroblast-derived iPSCs from a patient with high grade steatosis. *Stem Cell Res*, *17*(3), 568-571. https://doi.org/10.1016/j.scr.2016.10.007

Khalil, R., Shata, A., Abd El-Kader, E. M., Sharaf, H., Abdo, W. S., Amin, N. A., & Saber, S. (2020). Vildagliptin, a DPP-4 inhibitor, attenuates carbon tetrachloride-induced liver fibrosis by targeting ERK1/2, p38alpha, and NF-kappaB signaling. *Toxicol Appl Pharmacol*, *407*, 115246. https://doi.org/10.1016/j.taap.2020.115246

Kim, S. U. (1973). Morphological development of neonatal mouse hippocampus cultured in vitro. *Experimental Neurology*, *41*(1), 150-162. https://doi.org/https://doi.org/10.1016/0014-4886(73)90186-6

Kirkeby, A., Main, H., & Carpenter, M. (2025). Pluripotent stem-cell-derived therapies in clinical trial: A 2025 update. *Cell Stem Cell*, *32*(1), 10-37. https://doi.org/https://doi.org/10.1016/j.stem.2024.12.005

Klemann, C., Wagner, L., Stephan, M., & von Hörsten, S. (2016). Cut to the chase: a review of CD26/dipeptidyl peptidase-4's (DPP4) entanglement in the immune system. *Clin Exp Immunol*, *185*(1), 1-21. https://doi.org/10.1111/cei.12781

Kobold, S., Guhr, A., Mah, N., Bultjer, N., Seltmann, S., Seiler Wulczyn, A. E. M., Stacey, G., Jie, H., Liu, W., Löser, P., & Kurtz, A. (2020). A Manually Curated Database on Clinical Studies Involving Cell Products Derived from Human Pluripotent Stem Cells. *Stem Cell Reports*, *15*(2), 546-555. https://doi.org/10.1016/j.stemcr.2020.06.014

Kolbe, E., Aleithe, S., Rennert, C., Spormann, L., Ott, F., Meierhofer, D., Gajowski, R., Stöpel, C., Hoehme, S., Kücken, M., Brusch, L., Seifert, M., von Schoenfels, W., Schafmayer, C., Brosch, M., Hofmann, U., Damm, G., Seehofer, D., Hampe, J.,…Matz-Soja, M. (2019). Mutual Zonated Interactions of Wnt and Hh Signaling Are Orchestrating the Metabolism of the Adult Liver in Mice and Human. *Cell Reports*, *29*(13), 4553-4567.e4557. https://doi.org/10.1016/j.celrep.2019.11.104

Kordes, C., Sawitza, I., Götze, S., & Häussinger, D. (2013). Hepatic stellate cells support hematopoiesis and are liver-resident mesenchymal stem cells. *Cell Physiol Biochem*, *31*(2-3), 290-304. https://doi.org/10.1159/000343368

Kordes, C., Sawitza, I., Götze, S., Herebian, D., & Häussinger, D. (2014). Hepatic stellate cells contribute to progenitor cells and liver regeneration. *J Clin Invest*, *124*(12), 5503-5515. https://doi.org/10.1172/jci74119

Kubo, A., Shinozaki, K., Shannon, J. M., Kouskoff, V., Kennedy, M., Woo, S., Fehling, H. J., & Keller, G. (2004). Development of definitive endoderm from embryonic stem cells in culture. *Development*, *131*(7), 1651-1662. https://doi.org/10.1242/dev.01044

Kuebler, B., Alvarez-Palomo, B., Aran, B., Castaño, J., Rodriguez, L., Raya, A., Querol Giner, S., & Veiga, A. (2023). Generation of a bank of clinical-grade, HLA-homozygous iPSC lines with high coverage of the Spanish population. *Stem Cell Res Ther*, *14*(1), 366. https://doi.org/10.1186/s13287-023-03576-1

Kumashiro, N., Erion, D. M., Zhang, D., Kahn, M., Beddow, S. A., Chu, X., Still, C. D., Gerhard, G. S., Han, X., Dziura, J., Petersen, K. F., Samuel, V. T., & Shulman, G. I. (2011). Cellular mechanism of insulin resistance in nonalcoholic fatty liver disease. *Proc Natl Acad Sci U S A*, *108*(39), 16381-16385. https://doi.org/10.1073/pnas.1113359108

Lambeir, A. M., Durinx, C., Scharpé, S., & De Meester, I. (2003). Dipeptidyl-peptidase IV from bench to bedside: an update on structural properties, functions, and clinical aspects of the enzyme DPP IV. *Crit Rev Clin Lab Sci*, *40*(3), 209-294. https://doi.org/10.1080/713609354

Lamers, D., Famulla, S., Wronkowitz, N., Hartwig, S., Lehr, S., Ouwens, D. M., Eckardt, K., Kaufman, J. M., Ryden, M., Müller, S., Hanisch, F. G., Ruige, J., Arner, P., Sell, H., & Eckel, J. (2011). Dipeptidyl peptidase 4 is a novel adipokine potentially linking obesity to the metabolic syndrome. *Diabetes*, *60*(7), 1917-1925. https://doi.org/10.2337/db10-1707

Lammert, E., Cleaver, O., & Melton, D. (2003). Role of endothelial cells in early pancreas and liver development. *Mechanisms of Development*, *120*(1), 59-64. https://doi.org/https://doi.org/10.1016/S0925-4773(02)00332-5

Lang, R., Liu, G., Shi, Y., Bharadwaj, S., Leng, X., Zhou, X., Liu, H., Atala, A., & Zhang, Y. (2013). Self-renewal and differentiation capacity of urine-derived stem cells after urine preservation for 24 hours. *PLoS One*, *8*(1), e53980. https://doi.org/10.1371/journal.pone.0053980

Lara-Romero, C., & Romero-Gómez, M. (2024). Treatment Options and Continuity of Care in Metabolic-associated Fatty Liver Disease: A Multidisciplinary Approach. *Eur Cardiol*, *19*, e06. https://doi.org/10.15420/ecr.2023.34

Leibovitz, A. (1963). The Growth and Maintenance of Tissue-Cell Culture in Free Gas Exchange with the Atmosphere. *American Journal of Epidemiology*, *78*(2), 173-180. https://doi.org/10.1093/oxfordjournals.aje.a120336

Lekkala, V. K. R., Shrestha, S., Al Qaryoute, A., Dhinoja, S., Acharya, P., Raheem, A., Jagadeeswaran, P., & Lee, M. Y. (2025). Enhanced Maturity and Functionality of Vascular Human Liver Organoids through 3D Bioprinting and Pillar Plate Culture. *ACS Biomater Sci Eng*, *11*(1), 506-517. https://doi.org/10.1021/acsbiomaterials.4c01658

Lemaigre, F. P. (2007). Embryology of the Liver and Intrahepatic Biliary Tract. In *Textbook of Hepatology* (pp. 65-71). https://doi.org/https://doi.org/10.1002/9780470691861.ch1i

Lemke, J., Weigert, A., Bagci, S., Born, M., Ganschow, R., & Katzer, D. (2024). Alpha-1-Antitrypsin Deficiency in Children—Unmet Needs Concerning the Liver Manifestation. *Children*, *11*(6), 694. https://www.mdpi.com/2227-9067/11/6/694

Limaye, P. B., Alarcón, G., Walls, A. L., Nalesnik, M. A., Michalopoulos, G. K., Demetris, A. J., & Ochoa, E. R. (2008). Expression of specific hepatocyte and cholangiocyte transcription factors in human liver disease and embryonic development. *Lab Invest*, *88*(8), 865-872. https://doi.org/10.1038/labinvest.2008.56

Loh, Y. H., Agarwal, S., Park, I. H., Urbach, A., Huo, H., Heffner, G. C., Kim, K., Miller, J. D., Ng, K., & Daley, G. Q. (2009). Generation of induced pluripotent stem cells from human blood. *Blood*, *113*(22), 5476-5479. https://doi.org/10.1182/blood-2009-02-204800

Lonardo, A., Leoni, S., Alswat, K. A., & Fouad, Y. (2020). History of Nonalcoholic Fatty Liver Disease. *International Journal of Molecular Sciences*, *21*(16), 5888. https://www.mdpi.com/1422-0067/21/16/5888

Loomba, R., Ratziu, V., & Harrison, S. A. (2022). Expert Panel Review to Compare FDA and EMA Guidance on Drug Development and Endpoints in Nonalcoholic Steatohepatitis. *Gastroenterology*, *162*(3), 680-688. https://doi.org/10.1053/j.gastro.2021.10.051

Lu, T. Y., Lin, B., Kim, J., Sullivan, M., Tobita, K., Salama, G., & Yang, L. (2013). Repopulation of decellularized mouse heart with human induced pluripotent stem cell-derived cardiovascular progenitor cells. *Nat Commun*, *4*, 2307. https://doi.org/10.1038/ncomms3307

Luthra, R., & Sheth, A. (2025). Understanding MASH: An Examination of Progression and Clinical Outcomes by Disease Severity in the TARGET-NASH Database. *Advances in Therapy*, *42*(2), 1165-1195. https://doi.org/10.1007/s12325-024-03085-4

Macauley, M., Hollingsworth, K. G., Smith, F. E., Thelwall, P. E., Al-Mrabeh, A., Schweizer, A., Foley, J. E., & Taylor, R. (2015). Effect of vildagliptin on hepatic steatosis. *J Clin Endocrinol Metab*, *100*(4), 1578-1585. https://doi.org/10.1210/jc.2014-3794

MacDonald, B. T., Tamai, K., & He, X. (2009). Wnt/beta-catenin signaling: components, mechanisms, and diseases. *Dev Cell*, *17*(1), 9-26. https://doi.org/10.1016/j.devcel.2009.06.016

Mahmood, T., Rahman, H., Jahan, S., Sultana, N., Hasan, M., Hasan, M. I., Shehab, M. A., Fariduddin, M., Salimullah, M., & Hasanat, M. A. (2024). Higher Serum Dipeptidyl Peptidase-4 Activity in Newly Diagnosed Young-Onset Type 2 Diabetes Mellitus. *Cureus*, *16*(10), e70968. https://doi.org/10.7759/cureus.70968

Marshall, L. J., Bailey, J., Cassotta, M., Herrmann, K., & Pistollato, F. (2023). Poor Translatability of Biomedical Research Using Animals - A Narrative Review. *Altern Lab Anim*, *51*(2), 102-135. https://doi.org/10.1177/02611929231157756

Martin, G. R., & Evans, M. J. (1975). Differentiation of clonal lines of teratocarcinoma cells: formation of embryoid bodies in vitro. *Proc Natl Acad Sci U S A*, *72*(4), 1441-1445. https://doi.org/10.1073/pnas.72.4.1441

Martini, T., Naef, F., & Tchorz, J. S. (2023). Spatiotemporal Metabolic Liver Zonation and Consequences on Pathophysiology. *Annu Rev Pathol*, *18*, 439-466. https://doi.org/10.1146/annurev-pathmechdis-031521-024831

Masarone, M., Rosato, V., Dallio, M., Gravina, A. G., Aglitti, A., Loguercio, C., Federico, A., & Persico, M. (2018). Role of Oxidative Stress in Pathophysiology of Nonalcoholic

Fatty Liver Disease. *Oxid Med Cell Longev*, *2018*, 9547613. https://doi.org/10.1155/2018/9547613

Matz, P., Wruck, W., Fauler, B., Herebian, D., Mielke, T., & Adjaye, J. (2017). Footprint-free human fetal foreskin derived iPSCs: A tool for modeling hepatogenesis associated gene regulatory networks. *Sci Rep*, *7*(1), 6294. https://doi.org/10.1038/s41598-017-06546-9

Melo, F. J., Pinto-Lopes, P., Estevinho, M. M., & Magro, F. (2021). The Role of Dipeptidyl Peptidase 4 as a Therapeutic Target and Serum Biomarker in Inflammatory Bowel Disease: A Systematic Review. *Inflamm Bowel Dis*, *27*(7), 1153-1165. https://doi.org/10.1093/ibd/izaa324

Metcalf, D. (1974). III. HEMATOPOIETIC STEM CELLS. *Blood*, *5*, 251.

Mills, R. J., & Hudson, J. E. (2020). There's No I in Team: Cellular Crosstalk Enhances In Vitro Cardiac Maturation. *Cell Stem Cell*, *26*(6), 799-801. https://doi.org/10.1016/j.stem.2020.05.009

Misumi, Y., Hayashi, Y., Arakawa, F., & Ikehara, Y. (1992). Molecular cloning and sequence analysis of human dipeptidyl peptidase IV, a serine proteinase on the cell surface. *Biochimica et Biophysica Acta (BBA) - Gene Structure and Expression*, *1131*(3), 333-336. https://doi.org/https://doi.org/10.1016/0167-4781(92)90036-Y

Mitani, H., Takimoto, M., Hughes, T. E., & Kimura, M. (2002). Dipeptidyl Peptidase IV Inhibition Improves Impaired Glucose Tolerance in High-Fat Diet-Fed Rats: Study Using a Fischer 344 Rat Substrain Deficient in Its Enzyme Activity. *Japanese Journal of Pharmacology*, *88*(4), 442-450. https://doi.org/https://doi.org/10.1254/jjp.88.442

Miyagawa, S., Kainuma, S., Kawamura, T., Suzuki, K., Ito, Y., Iseoka, H., Ito, E., Takeda, M., Sasai, M., Mochizuki-Oda, N., Shimamoto, T., Nitta, Y., Dohi, H., Watabe, T., Sakata, Y., Toda, K., & Sawa, Y. (2022). Case report: Transplantation of human induced pluripotent stem cell-derived cardiomyocyte patches for ischemic cardiomyopathy. *Front Cardiovasc Med*, *9*, 950829. https://doi.org/10.3389/fcvm.2022.950829

Moro, L. G., Guarnier, L. P., Azevedo, M. F., Fracasso, J. A. R., Lucio, M. A., Castro, M. V., Dias, M. L., Lívero, F., & Ribeiro-Paes, J. T. (2024). A Brief History of Cell Culture: From Harrison to Organs-on-a-Chip. *Cells*, *13*(24). https://doi.org/10.3390/cells13242068

Moustakas, A. K., & Papadopoulos, G. K. (2002). Molecular properties of HLA-DQ alleles conferring susceptibility to or protection from insulin-dependent diabetes mellitus: keys to the fate of islet beta-cells. *Am J Med Genet*, *115*(1), 37-47. https://doi.org/10.1002/ajmg.10342

Nell, P., Kattler, K., Feuerborn, D., Hellwig, B., Rieck, A., Salhab, A., Lepikhov, K., Gasparoni, G., Thomitzek, A., Belgasmi, K., Bluthgen, N., Morkel, M., Kuppers-Munther, B., Godoy, P., Hay, D. C., Cadenas, C., Marchan, R., Vartak, N., Edlund, K.,…Hengstler, J. G. (2022). Identification of an FXR-modulated liver-intestine hybrid state in iPSC-derived hepatocyte-like cells. *J Hepatol*, *77*(5), 1386-1398. https://doi.org/10.1016/j.jhep.2022.07.009

Nguyen-Lefebvre, A. T., & Horuzsko, A. (2015). Kupffer Cell Metabolism and Function. *J Enzymol Metab*, *1*(1).

Niu, L., Geyer, P. E., Wewer Albrechtsen, N. J., Gluud, L. L., Santos, A., Doll, S., Treit, P. V., Holst, J. J., Knop, F. K., Vilsboll, T., Junker, A., Sachs, S., Stemmer, K., Muller, T. D., Tschop, M. H., Hofmann, S. M., & Mann, M. (2019). Plasma proteome profiling discovers novel proteins associated with non-alcoholic fatty liver disease. *Mol Syst Biol*, *15*(3), e8793. https://doi.org/10.15252/msb.20188793

Nobel Assembly at Karolinska Insitutet. (2012). *The Nobel Prize in Physiology or Medicine 2012*. Nobel outreach 2025, press release. Retrieved 14 Feb 2025 from https://www.nobelprize.org/prizes/medicine/2012/press-release/

O'Connor, M. D. (2013). The 3R principle: advancing clinical application of human pluripotent stem cells. *Stem Cell Res Ther*, *4*(2), 21. https://doi.org/10.1186/scrt169

Ohm, B., Moneke, I., & Jungraithmayr, W. (2023). Targeting cluster of differentiation 26 / dipeptidyl peptidase 4 (CD26/DPP4) in organ fibrosis. *Br J Pharmacol*, *180*(22), 2846-2861. https://doi.org/10.1111/bph.15967

Paik, D. T., Chandy, M., & Wu, J. C. (2020). Patient and Disease–Specific Induced Pluripotent Stem Cells for Discovery of Personalized Cardiovascular Drugs and Therapeutics. *Pharmacological Reviews*, *72*(1), 320-342. https://doi.org/https://doi.org/10.1124/pr.116.013003

Panday, R., Monckton, C. P., & Khetani, S. R. (2022). The Role of Liver Zonation in Physiology, Regeneration, and Disease. *Semin Liver Dis*, *42*(1), 1-16. https://doi.org/10.1055/s-0041-1742279

Park, J., Zhao, Y., Zhang, F., Zhang, S., Kwong, A. C., Zhang, Y., Hoffmann, H. H., Bushweller, L., Wu, X., Ashbrook, A. W., Stefanovic, B., Chen, S., Branch, A. D., Mason, C. E., Jung, J. U., Rice, C. M., & Wu, X. (2023). IL-6/STAT3 axis dictates the PNPLA3-mediated susceptibility to non-alcoholic fatty liver disease. *J Hepatol*, *78*(1), 45-56. https://doi.org/10.1016/j.jhep.2022.08.022

Park, S., Song, J., Baek, I. J., Jang, K. Y., Han, C. Y., Jun, D. W., Kim, P. K., Raught, B., & Jin, E. J. (2021). Loss of Acot12 contributes to NAFLD independent of lipolysis of adipose tissue. *Exp Mol Med*, *53*(7), 1159-1169. https://doi.org/10.1038/s12276-021-00648-1

Paulusma, C. C., Lamers, W. H., Broer, S., & van de Graaf, S. F. J. (2022). Amino acid metabolism, transport and signalling in the liver revisited. *Biochemical Pharmacology*, *201*, 115074. https://doi.org/https://doi.org/10.1016/j.bcp.2022.115074

Peaslee, C., Esteva-Font, C., Su, T., Munoz-Howell, A., Duwaerts, C. C., Liu, Z., Rao, S., Liu, K., Medina, M., Sneddon, J. B., Maher, J. J., & Mattis, A. N. (2021). Doxycycline Significantly Enhances Induction of Induced Pluripotent Stem Cells to Endoderm by Enhancing Survival Through Protein Kinase B Phosphorylation. *Hepatology*, *74*(4), 2102-2117. https://doi.org/10.1002/hep.31898

Pipitone, R. M., Ciccioli, C., Infantino, G., La Mantia, C., Parisi, S., Tulone, A., Pennisi, G., Grimaudo, S., & Petta, S. (2023). MAFLD: a multisystem disease. *Ther Adv Endocrinol Metab*, *14*, 20420188221145549. https://doi.org/10.1177/20420188221145549

Pranty, A. I., Wruck, W., & Adjaye, J. (2023). Free Bilirubin Induces Neuro-Inflammation in an Induced Pluripotent Stem Cell-Derived Cortical Organoid Model of Crigler-Najjar Syndrome. *Cells*, *12*(18). https://doi.org/10.3390/cells12182277

Rahim, K., Shan, M., Ul Haq, I., Nawaz, M. N., Maryam, S., Alturki, M. S., Al Khzem, A. H., Metwally, K., Cavalu, S., Alqifari, S. F., & Yahya, G. (2024). Revolutionizing Treatment Strategies for Autoimmune and Inflammatory Disorders: The Impact of Dipeptidyl-Peptidase 4 Inhibitors. *J Inflamm Res*, *17*, 1897-1917. https://doi.org/10.2147/jir.S442106

Rahman, M. S., Spitzhorn, L.-S., Wruck, W., Hagenbeck, C., Balan, P., Graffmann, N., Bohndorf, M., Ncube, A., Guillot, P. V., Fehm, T., & Adjaye, J. (2018). The presence of human mesenchymal stem cells of renal origin in amniotic fluid increases with gestational time. *Stem Cell Research & Therapy*, *9*(1), 113. https://doi.org/10.1186/s13287-018-0864-7

Rahman, M. S., Wruck, W., Spitzhorn, L.-S., Nguyen, L., Bohndorf, M., Martins, S., Asar, F., Ncube, A., Erichsen, L., Graffmann, N., & Adjaye, J. (2020). The FGF, TGFβ and WNT axis Modulate Self-renewal of Human SIX2+ Urine Derived Renal Progenitor Cells. *Scientific Reports*, *10*(1), 739. https://doi.org/10.1038/s41598-020-57723-2

Ramos, M. J., Bandiera, L., Menolascina, F., & Fallowfield, J. A. (2022). In vitro models for non-alcoholic fatty liver disease: Emerging platforms and their applications. *iScience*, *25*(1), 103549. https://doi.org/10.1016/j.isci.2021.103549

Rashidi, H., Luu, N. T., Alwahsh, S. M., Ginai, M., Alhaque, S., Dong, H., Tomaz, R. A., Vernay, B., Vigneswara, V., Hallett, J. M., Chandrashekran, A., Dhawan, A., Vallier, L., Bradley, M., Callanan, A., Forbes, S. J., Newsome, P. N., & Hay, D. C. (2018). 3D human liver tissue from pluripotent stem cells displays stable phenotype in vitro and supports compromised liver function in vivo. *Arch Toxicol*, *92*(10), 3117-3129. https://doi.org/10.1007/s00204-018-2280-2

Reinhardt, P., Schmid, B., Burbulla, L. F., Schöndorf, D. C., Wagner, L., Glatza, M., Höing, S., Hargus, G., Heck, S. A., Dhingra, A., Wu, G., Müller, S., Brockmann, K., Kluba, T., Maisel, M., Krüger, R., Berg, D., Tsytsyura, Y., Thiel, C. S.,…Sterneckert, J. (2013). Genetic correction of a LRRK2 mutation in human iPSCs links parkinsonian neurodegeneration to ERK-dependent changes in gene expression. *Cell Stem Cell*, *12*(3), 354-367. https://doi.org/10.1016/j.stem.2013.01.008

Reinke, H., & Asher, G. (2016). Circadian Clock Control of Liver Metabolic Functions. *Gastroenterology*, *150*(3), 574-580. https://doi.org/10.1053/j.gastro.2015.11.043

Riazi, K., Azhari, H., Charette, J. H., Underwood, F. E., King, J. A., Afshar, E. E., Swain, M. G., Congly, S. E., Kaplan, G. G., & Shaheen, A.-A. (2022). The prevalence and incidence of NAFLD worldwide: a systematic review and meta-analysis. *The Lancet Gastroenterology & Hepatology*, *7*(9), 851-861. https://doi.org/https://doi.org/10.1016/S2468-1253(22)00165-0

Ricchi, M., Odoardi, M. R., Carulli, L., Anzivino, C., Ballestri, S., Pinetti, A., Fantoni, L. I., Marra, F., Bertolotti, M., Banni, S., Lonardo, A., Carulli, N., & Loria, P. (2009). Differential effect of oleic and palmitic acid on lipid accumulation and apoptosis in cultured hepatocytes. *Journal of Gastroenterology and Hepatology*, *24*(5), 830-840. https://doi.org/https://doi.org/10.1111/j.1440-1746.2008.05733.x

Romeo, S., Kozlitina, J., Xing, C., Pertsemlidis, A., Cox, D., Pennacchio, L. A., Boerwinkle, E., Cohen, J. C., & Hobbs, H. H. (2008). Genetic variation in PNPLA3 confers susceptibility to nonalcoholic fatty liver disease. *Nature Genetics*, *40*(12), 1461-1465. https://doi.org/10.1038/ng.257

Rui, L. (2014). Energy metabolism in the liver. *Compr Physiol*, *4*(1), 177-197. https://doi.org/10.1002/cphy.c130024

Ruiz, M., Lacaille, F., Schrader, C., Pons, M., Socha, P., Krag, A., Sturm, E., Bouchecareilh, M., & Strnad, P. (2023). Pediatric and Adult Liver Disease in Alpha-1 Antitrypsin Deficiency. *Semin Liver Dis*, *43*(3), 258-266. https://doi.org/10.1055/a-2122-7674

Sahoo, S., Mishra, A., Diehl, A. M., & Jolly, M. K. (2022). Dynamics of hepatocyte-cholangiocyte cell-fate decisions during liver development and regeneration. *iScience*, *25*(9), 104955. https://doi.org/10.1016/j.isci.2022.104955

Sanders, F. W. B., Acharjee, A., Walker, C., Marney, L., Roberts, L. D., Imamura, F., Jenkins, B., Case, J., Ray, S., Virtue, S., Vidal-Puig, A., Kuh, D., Hardy, R., Allison, M., Forouhi, N., Murray, A. J., Wareham, N., Vacca, M., Koulman, A., & Griffin, J. L. (2018). Hepatic steatosis risk is partly driven by increased de novo lipogenesis following carbohydrate consumption. *Genome Biology*, *19*(1), 79. https://doi.org/10.1186/s13059-018-1439-8

Saussenthaler, S., Ouni, M., Baumeier, C., Schwerbel, K., Gottmann, P., Christmann, S., Laeger, T., & Schurmann, A. (2019). Epigenetic regulation of hepatic Dpp4 expression in response to dietary protein. *J Nutr Biochem*, *63*, 109-116. https://doi.org/10.1016/j.jnutbio.2018.09.025

Schlaeger, T. M., Daheron, L., Brickler, T. R., Entwisle, S., Chan, K., Cianci, A., DeVine, A., Ettenger, A., Fitzgerald, K., Godfrey, M., Gupta, D., McPherson, J., Malwadkar, P.,

Gupta, M., Bell, B., Doi, A., Jung, N., Li, X., Lynes, M. S.,…Daley, G. Q. (2015). A comparison of non-integrating reprogramming methods. *Nature Biotechnology*, *33*(1), 58-63. https://doi.org/10.1038/nbt.3070

Schwank, G., Koo, B. K., Sasselli, V., Dekkers, J. F., Heo, I., Demircan, T., Sasaki, N., Boymans, S., Cuppen, E., van der Ent, C. K., Nieuwenhuis, E. E., Beekman, J. M., & Clevers, H. (2013). Functional repair of CFTR by CRISPR/Cas9 in intestinal stem cell organoids of cystic fibrosis patients. *Cell Stem Cell*, *13*(6), 653-658. https://doi.org/10.1016/j.stem.2013.11.002

Schweitzer, J. S., Song, B., Herrington, T. M., Park, T.-Y., Lee, N., Ko, S., Jeon, J., Cha, Y., Kim, K., Li, Q., Henchcliffe, C., Kaplitt, M., Neff, C., Rapalino, O., Seo, H., Lee, I.-H., Kim, J., Kim, T., Petsko, G. A.,…Kim, K.-S. (2020). Personalized iPSC-Derived Dopamine Progenitor Cells for Parkinson's Disease. *New England Journal of Medicine*, *382*(20), 1926-1932. https://doi.org/doi:10.1056/NEJMoa1915872

Scorletti, E., Saiman, Y., Jeon, S., Schneider, C. V., Buyco, D. G., Lin, C., Himes, B. E., Mesaros, C. A., Vujkovic, M., Creasy, K. T., Furth, E. E., Billheimer, J. T., Hand, N. J., Kaplan, D. E., Chang, K.-M., Tsao, P. S., Lynch, J. A., Dempsey, J. L., Harkin, J.,…Carr, R. M. (2024). A missense variant in human perilipin 2 (PLIN2 Ser251Pro) reduces hepatic steatosis in mice. *JHEP Reports*, *6*(1), 100902. https://doi.org/https://doi.org/10.1016/j.jhepr.2023.100902

Seino, Y., Fukushima, M., & Yabe, D. (2010). GIP and GLP-1, the two incretin hormones: Similarities and differences. *J Diabetes Investig*, *1*(1-2), 8-23. https://doi.org/10.1111/j.2040-1124.2010.00022.x

Seki, T., Yuasa, S., Oda, M., Egashira, T., Yae, K., Kusumoto, D., Nakata, H., Tohyama, S., Hashimoto, H., Kodaira, M., Okada, Y., Seimiya, H., Fusaki, N., Hasegawa, M., & Fukuda, K. (2010). Generation of induced pluripotent stem cells from human terminally differentiated circulating T cells. *Cell Stem Cell*, *7*(1), 11-14. https://doi.org/10.1016/j.stem.2010.06.003

Seltmann, S., Lekschas, F., Müller, R., Stachelscheid, H., Bittner, M.-S., Zhang, W., Kidane, L., Seriola, A., Veiga, A., Stacey, G., & Kurtz, A. (2015). hPSCreg—the human pluripotent stem cell registry. *Nucleic Acids Research*, *44*(D1), D757-D763. https://doi.org/10.1093/nar/gkv963

Sifers, R. N., Carlson, J. A., Clift, S. M., DeMayo, F. J., Bullock, D. W., & Woo, S. L. (1987). Tissue specific expression of the human alpha-1-antitrypsin gene in transgenic mice. *Nucleic Acids Res*, *15*(4), 1459-1475. https://doi.org/10.1093/nar/15.4.1459

Simon, D., Aden, D. P., & Knowles, B. B. (1982). Chromosomes of human hepatoma cell lines. *International Journal of Cancer*, *30*(1), 27-33. https://doi.org/https://doi.org/10.1002/ijc.2910300106

Singh, S., & Watt, K. D. (2012). Long-term medical management of the liver transplant recipient: what the primary care physician needs to know. *Mayo Clin Proc*, *87*(8), 779-790. https://doi.org/10.1016/j.mayocp.2012.02.021

Sinton, M. C., Meseguer-Ripolles, J., Lucendo-Villarin, B., Drake, A. J., & Hay, D. C. (2021). Modeling human hepatic steatosis in pluripotent stem cell-derived hepatocytes. *STAR Protocols*, *2*(2), 100493. https://doi.org/https://doi.org/10.1016/j.xpro.2021.100493

Stevens, L. C., & Little, C. C. (1954). Spontaneous Testicular Teratomas in an Inbred Strain of Mice. *Proc Natl Acad Sci U S A*, *40*(11), 1080-1087. https://doi.org/10.1073/pnas.40.11.1080

Stoller JK, Hupertz V, & LS, A. (2006, updated 2023). Alpha-1 Antitrypsin Deficiency. In Adam MP, Feldman J, & M. G. e. al. (Eds.), *GeneReviews*. University of Washington, Seattle. **https://www.ncbi.nlm.nih.gov/books/NBK1519/ ;** *accessed 2025, April 29*

Striedter, G. F. (2022). *Models in Biology: history, philosophy an practical concerns*. The MIT Press.

Strnad, P., McElvaney, N. G., & Lomas, D. A. (2020). Alpha(1)-Antitrypsin Deficiency. *N Engl J Med*, *382*(15), 1443-1455. https://doi.org/10.1056/NEJMra1910234

Sumi, T., Tsuneyoshi, N., Nakatsuji, N., & Suemori, H. (2008). Defining early lineage specification of human embryonic stem cells by the orchestrated balance of canonical Wnt/β-catenin, Activin/Nodal and BMP signaling. *Development*, *135*(17), 2969-2979. https://doi.org/10.1242/dev.021121

Sveger, T. (1976). Liver disease in alpha1-antitrypsin deficiency detected by screening of 200,000 infants. *N Engl J Med*, *294*(24), 1316-1321. https://doi.org/10.1056/nejm197606102942404

Szepanowski, L. P., Wruck, W., Kapr, J., Rossi, A., Fritsche, E., Krutmann, J., & Adjaye, J. (2024). Cockayne Syndrome Patient iPSC-Derived Brain Organoids and Neurospheres Show Early Transcriptional Dysregulation of Biological Processes Associated with Brain Development and Metabolism. *Cells*, *13*(7). https://doi.org/10.3390/cells13070591

Tabibian, J. H., Masyuk, A. I., Masyuk, T. V., O'Hara, S. P., & LaRusso, N. F. (2013). Physiology of cholangiocytes. *Compr Physiol*, *3*(1), 541-565. https://doi.org/10.1002/cphy.c120019

Tachmatzidi, E. C., Galanopoulou, O., & Talianidis, I. (2021). Transcription Control of Liver Development. *Cells*, *10*(8). https://doi.org/10.3390/cells10082026

Takahashi, K., Tanabe, K., Ohnuki, M., Narita, M., Ichisaka, T., Tomoda, K., & Yamanaka, S. (2007). Induction of Pluripotent Stem Cells from Adult Human Fibroblasts by Defined Factors. *Cell*, *131*(5), 861-872. https://doi.org/10.1016/j.cell.2007.11.019

Takahashi, K., & Yamanaka, S. (2006). Induction of Pluripotent Stem Cells from Mouse Embryonic and Adult Fibroblast Cultures by Defined Factors. *Cell*, *126*(4), 663-676. https://doi.org/https://doi.org/10.1016/j.cell.2006.07.024

Takebe, T., Zhang, R. R., Koike, H., Kimura, M., Yoshizawa, E., Enomura, M., Koike, N., Sekine, K., & Taniguchi, H. (2014). Generation of a vascularized and functional human liver from an iPSC-derived organ bud transplant. *Nat Protoc*, *9*(2), 396-409. https://doi.org/10.1038/nprot.2014.020

Tan, H. L., Zain, S. M., Eng, H. S., Mohamed, Z., Mahadeva, S., Chan, W. K., Lau, P. C., Basu, R. C., & Mohamed, R. (2020). Allele HLA-DQB1*06 reduces fibrosis score in patients with non-alcoholic fatty liver disease. *Hepatol Res*, *50*(8), 947-954. https://doi.org/10.1111/hepr.13525

Teng, M. L., Ng, C. H., Huang, D. Q., Chan, K. E., Tan, D. J., Lim, W. H., Yang, J. D., Tan, E., & Muthiah, M. D. (2023). Global incidence and prevalence of nonalcoholic fatty liver disease. *Clin Mol Hepatol*, *29*(Suppl), S32-s42. https://doi.org/10.3350/cmh.2022.0365

Thomson, J. A., Itskovitz-Eldor, J., Shapiro, S. S., Waknitz, M. A., Swiergiel, J. J., Marshall, V. S., & Jones, J. M. (1998). Embryonic stem cell lines derived from human blastocysts. *Science*, *282*(5391), 1145-1147. https://doi.org/10.1126/science.282.5391.1145

Tilg, H., & Moschen, A. R. (2010). Evolution of inflammation in nonalcoholic fatty liver disease: the multiple parallel hits hypothesis. *Hepatology*, *52*(5), 1836-1846. https://doi.org/10.1002/hep.24001

Till, J. E., & McCulloch, E. A. (1961). A direct measurement of the radiation sensitivity of normal mouse bone marrow cells. *Radiat Res*, *14*, 213-222.

Tilson, S. G., Morell, C. M., Lenaerts, A. S., Park, S. B., Hu, Z., Jenkins, B., Koulman, A., Liang, T. J., & Vallier, L. (2021). Modeling PNPLA3-Associated NAFLD Using Human-Induced Pluripotent Stem Cells. *Hepatology*, *74*(6), 2998-3017. https://doi.org/10.1002/hep.32063

Tincopa, M. A., Anstee, Q. M., & Loomba, R. (2024). New and emerging treatments for metabolic dysfunction-associated steatohepatitis. *Cell Metabolism*, *36*(5), 912-926. https://doi.org/10.1016/j.cmet.2024.03.011

Tomaz, R. A., Zacharis, E. D., Bachinger, F., Wurmser, A., Yamamoto, D., Petrus-Reurer, S., Morell, C. M., Dziedzicka, D., Wesley, B. T., Geti, I., Segeritz, C. P., de Brito, M. C., Chhatriwala, M., Ortmann, D., Saeb-Parsy, K., & Vallier, L. (2022). Generation of functional hepatocytes by forward programming with nuclear receptors. *Elife*, *11*. https://doi.org/10.7554/eLife.71591

Tonk, C. H., Witzler, M., Schulze, M., & Tobiasch, E. (2020). Mesenchymal Stem Cells. In B. Brand-Saberi (Ed.), *Essential Current Concepts in Stem Cell Biology* (pp. 21-39). Springer International Publishing. https://doi.org/10.1007/978-3-030-33923-4_2

Touboul, T., Hannan, N. R., Corbineau, S., Martinez, A., Martinet, C., Branchereau, S., Mainot, S., Strick-Marchand, H., Pedersen, R., Di Santo, J., Weber, A., & Vallier, L. (2010). Generation of functional hepatocytes from human embryonic stem cells under chemically defined conditions that recapitulate liver development. *Hepatology*, *51*(5), 1754-1765. https://doi.org/10.1002/hep.23506

Townsend, S. A., Edgar, R. G., Ellis, P. R., Kantas, D., Newsome, P. N., & Turner, A. M. (2018). Systematic review: the natural history of alpha-1 antitrypsin deficiency, and associated liver disease. *Aliment Pharmacol Ther*, *47*(7), 877-885. https://doi.org/10.1111/apt.14537

Trefts, E., Gannon, M., & Wasserman, D. H. (2017). The liver. *Curr Biol*, *27*(21), R1147-r1151. https://doi.org/10.1016/j.cub.2017.09.019

Trzaskalski, N. A., Fadzeyeva, E., & Mulvihill, E. E. (2020). Dipeptidyl Peptidase-4 at the Interface Between Inflammation and Metabolism. *Clin Med Insights Endocrinol Diabetes*, *13*, 1179551420912972. https://doi.org/10.1177/1179551420912972

Tuffs, A. (2001). Germany debates embryonic stem cell research. *Bmj*, *323*(7303), 8.

U.S. Food and Drug Administration. (2018). Noncirrhotic Nonalcoholic Steatohepatitis With Liver Fibrosis: Developing Drugs for Treatment (Guidance for Industry – Draft Guidance). In.

Vacca, M., Kamzolas, I., Harder, L. M., Oakley, F., Trautwein, C., Hatting, M., Ross, T., Bernardo, B., Oldenburger, A., Hjuler, S. T., Ksiazek, I., Lindén, D., Schuppan, D., Rodriguez-Cuenca, S., Tonini, M. M., Castañeda, T. R., Kannt, A., Rodrigues, C. M. P., Cockell, S.,…Vidal-Puig, A. (2024). An unbiased ranking of murine dietary models based on their proximity to human metabolic dysfunction-associated steatotic liver disease (MASLD). *Nat Metab*, *6*(6), 1178-1196. https://doi.org/10.1038/s42255-024-01043-6

Vachliotis, I. D., & Polyzos, S. A. (2023). The Role of Tumor Necrosis Factor-Alpha in the Pathogenesis and Treatment of Nonalcoholic Fatty Liver Disease. *Curr Obes Rep*, *12*(3), 191-206. https://doi.org/10.1007/s13679-023-00519-y

Varghese, D. S., Alawathugoda, T. T., Sheikh, M. A., Challagandla, A. K., Emerald, B. S., & Ansari, S. A. (2022). Developmental modeling of hepatogenesis using obese iPSCs-hepatocyte differentiation uncovers pathological features. *Cell Death Dis*, *13*(8), 670. https://doi.org/10.1038/s41419-022-05125-9

Varin, E. M., Mulvihill, E. E., Beaudry, J. L., Pujadas, G., Fuchs, S., Tanti, J. F., Fazio, S., Kaur, K., Cao, X., Baggio, L. L., Matthews, D., Campbell, J. E., & Drucker, D. J. (2019). Circulating Levels of Soluble Dipeptidyl Peptidase-4 Are Dissociated from Inflammation and Induced by Enzymatic DPP4 Inhibition. *Cell Metab*, *29*(2), 320-334.e325. https://doi.org/10.1016/j.cmet.2018.10.001

Vazin, T., & Freed, W. J. (2010). Human embryonic stem cells: derivation, culture, and differentiation: a review. *Restor Neurol Neurosci*, *28*(4), 589-603. https://doi.org/10.3233/rnn-2010-0543

Vergara Nieto Á, A., Diaz, A. H., Hernández, M., & Sagredo, D. (2025). A Narrative Review about Metabolic Pathways, Molecular Mechanisms and Clinical Implications of Intermittent Fasting as Autophagy Promotor. *Curr Nutr Rep*, *14*(1), 78. https://doi.org/10.1007/s13668-025-00666-9

Volpato, V., & Webber, C. (2020). Addressing variability in iPSC-derived models of human disease: guidelines to promote reproducibility. *Dis Model Mech*, *13*(1). https://doi.org/10.1242/dmm.042317

W. M. S. Russell, R. L. B. (1960). The Principles of Humane Experimental Technique. *Medical Journal of Australia*, *1*(13), 500-500. https://doi.org/https://doi.org/10.5694/j.1326-5377.1960.tb73127.x

Wang, S., Du, Y., Zhang, B., Meng, G., Liu, Z., Liew, S. Y., Liang, R., Zhang, Z., Cai, X., Wu, S., Gao, W., Zhuang, D., Zou, J., Huang, H., Wang, M., Wang, X., Wang, X., Liang, T., Liu, T.,…Shen, Z. (2024). Transplantation of chemically induced pluripotent stem-cell-derived islets under abdominal anterior rectus sheath in a type 1 diabetes patient. *Cell*, *187*(22), 6152-6164.e6118. https://doi.org/https://doi.org/10.1016/j.cell.2024.09.004

Wang, X., Ke, J., Zhu, Y.-j., Cao, B., Yin, R.-l., Wang, Y., Wei, L.-l., Zhang, L.-j., Yang, L.-y., & Zhao, D. (2021). Dipeptidyl peptidase-4 (DPP4) inhibitor sitagliptin alleviates liver inflammation of diabetic mice by acting as a ROS scavenger and inhibiting the NFκB pathway. *Cell Death Discovery*, *7*(1), 236. https://doi.org/10.1038/s41420-021-00625-7

Weber, J., Linti, C., Lörch, C., Weber, M., Andt, M., Schlensak, C., Wendel, H. P., Doser, M., & Avci-Adali, M. (2023). Combination of melt-electrospun poly-ε-caprolactone scaffolds and hepatocyte-like cells from footprint-free hiPSCs to create 3D biohybrid constructs for liver tissue engineering. *Scientific Reports*, *13*(1), 22174. https://doi.org/10.1038/s41598-023-49117-x

Wicinski, M., Gorski, K., Wodkiewicz, E., Walczak, M., Nowaczewska, M., & Malinowski, B. (2020). Vasculoprotective Effects of Vildagliptin. Focus on Atherogenesis. *Int J Mol Sci*, *21*(7). https://doi.org/10.3390/ijms21072275

Wisse, E. (1970). An electron microscopic study of the fenestrated endothelial lining of rat liver sinusoids. *Journal of Ultrastructure Research*, *31*(1), 125-150. https://doi.org/https://doi.org/10.1016/S0022-5320(70)90150-4

Wronkowitz, N., Görgens, S. W., Romacho, T., Villalobos, L. A., Sánchez-Ferrer, C. F., Peiró, C., Sell, H., & Eckel, J. (2014). Soluble DPP4 induces inflammation and proliferation of human smooth muscle cells via protease-activated receptor 2. *Biochim Biophys Acta*, *1842*(9), 1613-1621. https://doi.org/10.1016/j.bbadis.2014.06.004

Wruck, W., & Adjaye, J. (2017). Meta-analysis reveals up-regulation of cholesterol processes in non-alcoholic and down-regulation in alcoholic fatty liver disease. *World J Hepatol*, *9*(8), 443-454. https://doi.org/10.4254/wjh.v9.i8.443

Wruck, W., Kashofer, K., Rehman, S., Daskalaki, A., Berg, D., Gralka, E., Jozefczuk, J., Drews, K., Pandey, V., Regenbrecht, C., Wierling, C., Turano, P., Korf, U., Zatloukal, K., Lehrach, H., Westerhoff, H. V., & Adjaye, J. (2015). Multi-omic profiles of human non-alcoholic fatty liver disease tissue highlight heterogenic phenotypes. *Sci Data*, *2*, 150068. https://doi.org/10.1038/sdata.2015.68

Xue, C., & Greene, E. C. (2021). DNA Repair Pathway Choices in CRISPR-Cas9-Mediated Genome Editing. *Trends Genet*, *37*(7), 639-656. https://doi.org/10.1016/j.tig.2021.02.008

Xue, F., & Wei, L. (2024). THR-β Agonist for Nonalcoholic Steatohepatitis Treatment: Challenges of a Promising Drug. *J Clin Transl Hepatol*, *12*(8), 755-757. https://doi.org/10.14218/jcth.2024.00100

Yoshida, S., Kato, T. M., Sato, Y., Umekage, M., Ichisaka, T., Tsukahara, M., Takasu, N., & Yamanaka, S. (2023). A clinical-grade HLA haplobank of human induced pluripotent

stem cells matching approximately 40% of the Japanese population. *Med*, *4*(1), 51-66.e10. https://doi.org/10.1016/j.medj.2022.10.003

Yu, J., Chau, K. F., Vodyanik, M. A., Jiang, J., & Jiang, Y. (2011). Efficient feeder-free episomal reprogramming with small molecules. *PLoS One*, *6*(3), e17557. https://doi.org/10.1371/journal.pone.0017557

Yu, J., & Thomson, J. A. (2014). Chapter 30 - Induced Pluripotent Stem Cells. In R. Lanza, R. Langer, & J. Vacanti (Eds.), *Principles of Tissue Engineering (Fourth Edition)* (pp. 581-594). Academic Press. https://doi.org/https://doi.org/10.1016/B978-0-12-398358-9.00030-6

Yu, J., Vodyanik, M. A., Smuga-Otto, K., Antosiewicz-Bourget, J., Frane, J. L., Tian, S., Nie, J., Jonsdottir, G. A., Ruotti, V., Stewart, R., Slukvin, II, & Thomson, J. A. (2007). Induced pluripotent stem cell lines derived from human somatic cells. *Science*, *318*(5858), 1917-1920. https://doi.org/10.1126/science.1151526

Yu, Q., Zhang, Y., Ni, J., Shen, Y., & Hu, W. (2024). Identification and analysis of significant genes in nonalcoholic steatohepatitis-hepatocellular carcinoma transformation: Bioinformatics analysis and machine learning approach. *Molecular Immunology*, *174*, 18-31. https://doi.org/https://doi.org/10.1016/j.molimm.2024.07.015

Yuan, Y., Cotton, K., Samarasekera, D., & Khetani, S. R. (2023). Engineered Platforms for Maturing Pluripotent Stem Cell-Derived Liver Cells for Disease Modeling. *Cell Mol Gastroenterol Hepatol*, *15*(5), 1147-1160. https://doi.org/10.1016/j.jcmgh.2023.01.013

Yusoff, N. A., Abd Hamid, Z., Budin, S. B., & Taib, I. S. (2025). Hematopoietic stem cell discovery: unveiling the historical and future perspective of colony-forming units assay. *PeerJ*, *13*, e18854. https://doi.org/10.7717/peerj.18854

Zakrzewski, W., Dobrzynski, M., Szymonowicz, M., & Rybak, Z. (2019). Stem cells: past, present, and future. *Stem Cell Res Ther*, *10*(1), 68. https://doi.org/10.1186/s13287-019-1165-5

Zhao, Z., Cui, T., Wei, F., Zhou, Z., Sun, Y., Gao, C., Xu, X., & Zhang, H. (2024). Wnt/β-Catenin signaling pathway in hepatocellular carcinoma: pathogenic role and therapeutic target. *Front Oncol*, *14*, 1367364. https://doi.org/10.3389/fonc.2024.1367364

8. Addendum

8.1. Oral presentations

Christiane Loerch, Wasco Wruck, Julian Reiss, James Adjaye, Nina Graffmann. **DPP4 inhibition affects metabolism and inflammation associated pathways in hiPSC-derived steatotic HLCs.** 8th Annual Symposium, London Stem Cell Network, London, United Kingdom, 2025

Christiane Loerch, Martina Bohndorf, Wasco Wruck, James Adjaye, Nina Graffmann. **PPAR and DPP4 are potential drugable targets for NAFLD - revealed with an iPSC-derived HLC model.** 14th internal Meeting, Stem Cell Network North Rhine-Westphalia, Bonn, Germany, 2024

Christiane Loerch, Martina Bohndorf, Wasco Wruck, James Adjaye, Nina Graffmann. **Analysing the inflammatory response upon non-alcoholic fatty liver induction in an iPSC-based liver model.** 11th GSCN non-PI meeting, German Stem Cell Network, Ulm, Germany, 2023

8.1. Poster presentations

Christiane Loerch, Martina Bohndorf, Wasco Wruck, James Adjaye, Nina Graffmann. **PPAR and DPP4 are potential drugable targets for NAFLD - revealed with an iPSC-derived HLC model.** Annual Meeting, International Society for Stem Cell Research, Hamburg, Germany 2024

Christiane Loerch, Martina Bohndorf, Wasco Wruck, James Adjaye, Nina Graffmann. **PPAR and DPP4 are potential drugable targets for NAFLD - revealed with an iPSC-derived HLC model.** 14th internal Meeting, Stem Cell Network North Rhine-Westphalia, Bonn Germany, 2024

Christiane Loerch, Martina Bohndorf, Wasco Wruck, James Adjaye, Nina Graffmann. **Analysing the inflammatory response upon non-alcoholic fatty liver induction in an iPSC-based liver model.** 11th GSCN conference, German Stem Cell Network, Ulm, Germany, 2023

Christiane Loerch, Martina Bohndorf, Wasco Wruck, James Adjaye, Nina Graffmann. **Modeling non-alcoholic fatty liver disease with iPSC-derived HLCs and HepaRG cells.** 11th International Meeting, Stem Cell Network North Rhine-Westphalia, Aachen, Germany 2022

Christiane Loerch, Martina Bohndorf, Wasco Wruck, James Adjaye, Nina Graffmann. **Epigenetic changes in non-alcoholic fatty liver disease - modelled with iPSC-derived hepatocyte like cells.** 10th GSCN conference, German Stem Cell Network, Muenster, Germany 2022

Christiane Lörch, Martina Bohndorf, Wasco Wruck, James Adjaye, Nina Graffmann. **Epigenetic changes in non-alcoholic fatty liver disease - modelled with iPSC-derived hepatocyte like cells.** 13th Internal Meeting, Stem Cell Network North Rhine-Westphalia, Herne, Germany 2022

8.2. Additional scientific publications

8.2.1. Investigating BPDE-induced embryonic toxicity employing hiPSC-based models

Vanessa Cristina Meira de Amorim, Leon Szepanowski, Alessia Lofrano, **Christiane Loerch**, Wasco Wruck, Nina Graffmann, James Adjaye

BioRxiv, Article number 2024.12.16.628678

Abstract:

Benzo[a]pyrene diol epoxide (BPDE) is a metabolite of the environmental contaminant Benzo[a]pyrene- a byproduct of incomplete combustion of organic matter. BPDE reacts with DNA to form BPDE-DNA bulky adducts which if not removed can lead to mutations due to DNA base-pair substitutions. While the effects of BPDE on somatic cells are fairly well described, its effects on early human development are currently unknown. In this study, we investigated for the first time the effect of BPDE on human induced pluripotent stem cells (hiPSCs) and their differentiated neuroprogenitor cells (NPCs) as a model for early embryonic development. Furthermore, we compared hiPSCs and NPCs derived from cells of patients suffering from Nijmegen Breakage Syndrome (NBS), which is a chromosomal instability disorder characterized by defective DNA repair and increased risk of malignancies. Transcriptome analysis, coupled with protein content analysis employing immunostaining and Western blots, revealed that hiPSCs are more sensitive to BPDE exposure when compared to NPCs with an enhanced expression of several genes associated with p53-mediated DNA damage response, including DNA repair by lesion bypass, cell cycle checkpoints and extrinsic apoptosis. We also identified that cells from NBS patients showed less apoptotic response and a distinct p53 response than their healthy counterparts. This iPSC-based study enhances our meagre knowledge of the effects of BPDE on early human development in both healthy individuals and NBS patients. Furthermore, our model conforms with the 3Rs principle.

Author contribution (5%) of C.L. included:

- Conduction of experiments (qRT-PCR)

Status: Under Review at Archives of Toxicology to be published as open access article under the CC BY-NC-ND license. Currently available as preprint on BioRxiv.
DOI: 10.1101/2024.12.16.628678

Investigating BPDE-induced embryonic toxicity employing hiPSC-based models

Vanessa Cristina Meira de Amorim[1], Leon Szepanowski[1,2], Alessia Lofrano[1], Christiane Loerch[1], Wasco Wruck[1] Nina Graffmann*[1] and James Adjaye*[1,3]

[1] Institute for Stem Cell Research and Regenerative Medicine, Medical Faculty and University Hospital Düsseldorf, Heinrich-Heine University Düsseldorf, Düsseldorf, 40225, Germany
[2]Department of Ophthalmology, University Hospital Duesseldorf, Duesseldorf, Germany
[3] University College London (UCL) –EGA Institute for Women's Health, Zayed Centre for Research into Rare Diseases in Children (ZCR). 20 Guilford Street, London WC1N 1DZ

*Correspondence: James.Adjaye@med.uni-duesseldorf.de; Nina.graffmann@med.uni-duesseldorf.de

Abstract

Benzo[a]pyrene diol epoxide (BPDE) is a metabolite of the environmental contaminant Benzo[a]pyrene- a byproduct of incomplete combustion of organic matter. BPDE reacts with DNA to form BPDE-DNA bulky adducts which if not removed can lead to mutations due to DNA base-pair substitutions. While the effects of BPDE on somatic cells are fairly well described, its effects on early human development are currently unknown. In this study, we investigated for the first time the effect of BPDE on human induced pluripotent stem cells (hiPSCs) and their differentiated neuroprogenitor cells (NPCs) as a model for early embryonic development. Furthermore, we compared hiPSCs and NPCs derived from cells of patients suffering from Nijmegen Breakage Syndrome (NBS), which is a chromosomal instability disorder characterized by defective DNA repair and increased risk of malignancies. Transcriptome analysis, coupled with protein content analysis employing immunostaining and Western blots, revealed that hiPSCs are more sensitive to BPDE exposure when compared to NPCs with an enhanced expression of several genes associated with p53-mediated DNA damage response, including DNA repair by lesion bypass, cell cycle checkpoints and extrinsic apoptosis. We also identified that cells from NBS patients showed less apoptotic response and a distinct p53 response than their healthy counterparts. This iPSC-based study enhances our meagre knowledge of the effects of BPDE on early human development in both healthy individuals and NBS patients. Furthermore, our model conforms with the 3Rs principle.

Key words

Nijmegen Breakage Syndrome (NBS), benzo[a]pyrene diol epoxide (BPDE), developmental toxicology, DNA damage response, induced pluripotent stem cells, neuroprogenitor cells

1. Introduction

There is currently a worldwide endeavor to minimize and even replace animal experimentation. There are numerous problems associated with animal experimentation which include ethical issues, the high costs of animal experiments and difficulties in recapitulating specific human pathologies. The pharmaceutical and chemical industries contend with a failure rate of up to 90% in translating animal effects to human subjects (1,2).

Developmental toxicity testing aims to identify substances that can cause disturbances during embryo-fetal development. Currently, the gold standard are animal-based assays which are time consuming, expensive and do not always reliably translate to human physiology (3). Besides developmental toxicological evaluation, the identification and investigation of the effects of DNA-damaging agents (genotoxins) is of high importance. While DNA-repair mechanisms remain mostly conserved among mammals, there are marked differences on the efficiency of such repair processes between distinct species (4). Tests *in vitro* with a high sensitivity are also part of the standard battery of tests used for genotoxic assessment in human pharmaceuticals (5), but their specificity is often unsatisfactory (6,7).

A promising alternative for animal experimentation is the use of human pluripotent stem cells (hiPSCs) and their differentiated progeny as *in vitro* substitutes. In 2023, the U.S. Congress approved the FDA Modernization Act 2.0, stating that drug developers can now propose alternative methods, including the use of hiPSC-derived models, for the assessment of drug safety during the pre-clinical phase instead of mandating the use of animal models (8). hiPSC-based models are particularly interesting alternatives for developmental toxicology testing since they can mimic the developing embryo and parts of organ development (9).

Furthermore, hiPSCs are advantageous for modeling specific diseases, particularly genetic disorders. One example is Nijmegen Breakage Syndrome (NBS), a chromosomal instability disorder, characterized by an impaired immune system, microcephaly, growth retardation, premature aging, and increased susceptibility to malignancies (10). It is caused by a mutation within the NBS gene that codes for the protein Nibrin (NBN), which is part of the MRN complex together with Meiotic recombination 11 (MRE11) and RAD50 Double Strand Break Repair Protein (RAD50). This complex is involved in DNA damage signaling and repair, particularly of DNA double-strand breaks, a pathway that is severely impaired in NBS patients. Due to this deficiency in DNA repair, NBS patients have marked chromosomal instability, developing breakages and chromosomal rearrangements (11). That in turn leads to the development of malignancies, with over 40% of NBS patients developing one by the age of 20, predominantly hematological cancers (10).

Benzo[a]pyrene (B[a]p) is a polycyclic aromatic hydrocarbon and environmental contaminant formed during incomplete combustion of organic matter, such as exhaust fumes and cigarette smoke. B[a]p is metabolized in the body into benzo[a]pyrene diol epoxide, or BPDE, a potent mutagen and carcinogen. BPDE forms bulky DNA adducts by binding to the N2 atom of guanine (dG-N2-BPDE adduct) which, if not removed by nucleotide excision repair (NER), can lead to base-pair substitution mutations via trans-lesion DNA synthesis (TLS) (12) resulting in tumorigenesis (13). B[a]p is lipophilic and can cross the placenta to reach the developing fetus. The placenta can metabolize B[a]p into BPDE, and the fetuses themselves are metabolically capable, which can lead to fetal genotoxic exposure (14–16). Furthermore, BPDE-DNA adducts are detectable in the sperm (17) and ovarian cells (18) of cigarette smokers, and these DNA modifications can be paternally transmitted through the spermatozoa to the embryo (19). The potential issues that could arise from the presence of BPDE adducts on pre-implantation embryos and fetuses, are currently unknown. The undifferentiated pluripotent stem cells represent the pre-gastrulation stage whilst the differentiated neural progenitor cell gastrulation towards ectoderm.

Our work is the first to perform a comparative analysis of the response to BPDE exposure in pluripotent stem cells and their differentiated neural progenitor cell (NPC) progeny, using both healthy cells and those with an NBS mutation. We show here for the first time that low doses of BPDE do not interfere with the maintenance of the pluripotent state. However, it has distinct impacts on p53-associated stress responses such as DNA-damage repair and apoptosis in iPSCs and NPCs.

2. Methods and materials

2.1. Stem Cell Cultivation

Two hiPSC lines from healthy individuals, UM51 and iPSC-12, and one hiPSC line from an individual suffering from NBS, NBS8, were used in this study (Supplementary Table 1). hiPSCs were cultivated on plates coated with Matrigel (Corning) and fed with mTeSR plus™ medium (StemCell Technologies). Cell passaging was done every 5-6 days with ReLeSR™ (Stem Cell Technologies) according to the manufacturer's instructions. UM51 (20) and NBS8 (21) were generated under the ethical approval of the Ethikkommission der Medizinischen Fakultät der Heinrich-Heine-Universität Düsseldorf. iPSC-12 is a commercially available iPSC line from Cell Applications Inc. (https://www.cellapplications.com/).

Neural Progenitor Cell Differentiation

For NPC differentiation, hiPSCs were cultivated until 75-90% confluence. The cells were dissociated into single cells with accutase (Sigma-Aldrich) and plated in a 96-well U-bottom, low attachment plate (Thermo Scientific) with 100µL mTeSR Plus™ supplemented with 10 µM ROCK inhibitor (Y-27632, Sigma-Aldrich) in a density of 10^4 cells/well. The cells were incubated at 37°C with 5% CO2 for 24 hours, after which 50 µl of the medium was aspirated and replaced by 100 µl of neural induction medium (NiM, consisting of 47% DMEM/F12 (Gibco), 47% Neurobasal Medium™ (Gibco), 2% B27™ w/o retinoic acid (Gibco), 1% N2 (Gibco), 1% GlutaMAX™ (Gibco), 1% MEM non-essential amino acids (NEEA) (Gibco) and 1% Penicillin/Streptomycin (Gibco). In the following 5 days, 100 µl of medium was replaced daily with fresh NIM supplemented with 10 µM SB-431542 (Tocris), 500 nM LDN-193189 (Merck) and, until day 3, 10 µM ROCK inhibitor. The resultant neurospheres were seeded in Growth Factor Reduced Matrigel® (Corning) coated 6-well plates and fed daily with Neural Differentiation Medium (NDM, consisting of 95% Neurobasal Medium™ (Gibco), 2% B27™ w/o retinoic acid (Gibco), 1% N2 (Gibco), 1% GlutaMAX™ (Gibco), and 1% Penicillin/Streptomycin (Gibco) supplemented with 20 ng/ml epidermal growth factor (EGF) and 20 ng/ml fibroblast growth factor 2 (FGF2). On day 18, neural rosettes were selected with STEMdiff™ Neural Rosette Selection Reagent (Stem Cell Technologies) as per the manufacturer's recommendation. The rosettes were then incubated with accutase for 30 min at 37°C and the resulting cell aggregates were seeded at a density of 1:4 on Growth Factor Reduced Matrigel® (Corning) coated 6-well plates for expansion and fed daily with NDM supplemented with 20 ng/ml EGF and 20 ng/ml FGF2. For passaging, the NPCs were incubated with accutase for 5 min at 37°C and the resulting aggregates were seeded at a density of 1:4 on Growth Factor Reduced Matrigel® (Corning) coated 6-well plates every 5-6 days.

2.2. BPDE treatment

BPDE (Santa Cruz Biotechnology) was dissolved in DMSO (Sigma-Aldrich) at a concentration of 40mM and the aliquots were stored at -80°C for up to six months. For treatment of hiPSCs and NPCs cells were cultured until 60-70% confluent, and then medium replaced with fresh medium containing BPDE (25nM or 75nM) or vehicle control (0.02% DMSO) for 24h. Thereafter, medium was discarded, and cells processed for analysis.

2.3. Resazurin reduction assay

A 0.15 mg/ml stock solution of resazurin (Sigma-Aldrich) was prepared by dissolving 5mg of resazurin in 50mL of sterile PBS and kept at 4°C until use. Cells were cultivated in triplicates

on a 96-well plate and continuously exposed to BPDE in concentrations ranging from 10nM to 21µM for 22h, when 10µL medium supplemented with resazurin stock solution was added to the culture in a 1:10 dilution. The plates were returned to 37°C and incubated for a further 2h. Living cells convert resazurin into resofurin, a fluorescent compound, and fluorescence was measured using a microplate fluorimeter (Eppendorf PlateReader AF2200) equipped with a filter set of 560nm excitation and 590nm emission. Measurements of cell cultures treated with increasing doses of BPDE and normalized according to the manufacturer's protocol were imported into the R environment (22). The packages dr4pl (23) and ggplot2 (24) were employed to use a logistic model for curve-fitting, plotting the curve, and calculating the IC50 and additionally IC80 and IC90.

2.4. Immunocytochemistry

Cells were fixed with 4% paraformaldehyde (PFA) for 15 minutes. For staining of intracellular proteins, the cells were permeabilized with 0.5% Triton-x-100/DPBS for 10 min and then washed 2x with DPBS. Cells were then incubated with blocking buffer containing 3% bovine serum albumin (BSA, Sigma-Aldrich)/DPBS for 1h at RT. After the blocking period, cells were incubated with primary antibody diluted in blocking buffer overnight at 4°C with shaking. In the morning the cells were then washed 3x/5min with DPBS, then further incubated with a secondary antibody solution diluted in blocking buffer, supplemented with the nuclear stain Hoechst 33258 (Thermo Fisher) for 2h RT (antibodies are listed in Supplementary Table 2. Pictures were taken using a Zeiss LSM 700 microscope and analyzed using the software Zen Blue 2.5. When applicable, cells were counted manually using the program image J (ver. 1.54) and ratios of treated conditions and control were calculated using Microsoft Excel, as were standard deviations (SD). Ratios and SD were visualized as bar graphs. Statistical significance was measured using 2-way ANOVA and Tukey's multiple comparison test using GraphPad Prism 8. P values ≤ 0.05 were considered statistically significant.

2.5. Propidium Iodide (PI) staining and cell cycle FACS analysis

hiPSCs were treated with BPDE for 24h. Thereafter, cells were harvested using accutase (Sigma-Aldritch) and centrifuged at 500xg for 5min at 4°C. 10^5 cells were transferred to FACS tubes (Corning), washed with 1ml of PBS and centrifuged as stated above. The supernatant was discarded, and the cells were incubated for 1h in 25µl of staining solution composed of 0.1% sodium citrate, 0.1% Triton-x-100 and 50mg/L of propidium iodide (PI) (Invitrogen), diluted in distilled water. Cell cycle measurements were carried out on a CytoFlex BA26183 from Beckman Coulter and analysed with CytExpert 2.3. Statistical significance was measured using 2-way ANOVA and Tukey's multiple comparison test using GraphPad Prism 8. P values ≤ 0.05 were considered statistically significant.

2.6. Reverse Transcripion and real time PCR

TRIzol® was used to extract RNA from treated and non-treated hiPSCs and NPCs. Total RNA was extracted using the Direct-zol™ RNA MiniPrep kit (Zymo Research) according to the manufacturer's instructions. To avoid DNA contamination, a 30 min treatment with DNase was applied. The isolated RNA was transcribed into cDNA using the Reverse Transcription TaqMan® Kit (Applied Biosystems) following the manufacturer's instructions. The real time PCR was performed with Power SYBR® Green (Applied biosystems) on a ViiA7 machine (Applied biosystems). Mean values were normalized to the housekeeping gene *RPLP0* and the cycle threshold (CT) for each sample was determined with the ViiA7 Software v1.2 from Applied Biosystems. Fold-change values are depicted as mean values with 95% confidence interval. Statistical significance was measured using 2-way ANOVA and Tukey's multiple comparison test using GraphPad Prism 8. P values ≤ 0.05 were considered statistically significant. Primer sequences used are listed in Supplementary Table 3.

2.7. 5-ethynyl-2'-deoxyuridine (EdU) incorporation assay

hiPSCs were treated for 24h with BPDE. EdU incorporation and the fluorescence staining for incorporated EdU was performed using the Click-iT™ EdU Cell Proliferation Kit for Imaging, Alexa Fluor™ 488 dye (Invitrogen), as instructed by the manufacturer. Hoechst 33258 was used for DNA staining. Pictures were taken using a Zeiss LMS 700 and analyzed using the software Zen Blue 2.5. EdU+ cells were counted manually using the program image J (ver. 1.54) and ratios of treated conditions and control were calculated using Microsoft Excel 2010, as were standard deviations (SD). Ratios and SD were visualized as bar graphs. Statistical significance was measured using 2*way ANOVA and Turkey's multiple comparison test using GraphPad Prism 8. P values ≤ 0.05 were considered statistically significant.

2.8. Analysis of Gene Expression Data

Total RNA was extracted using the Direct-zol™ RNA MiniPrep kit (Zymo Research) according to the manufacturer's instructions from iPSCs UM51, iPSC-12 and NBS8, in CTRL conditions and after 24h treatment with 75nM BPDE. RNA was sent for analysis at the Biomedizinisches Forschungszentrum (BMFZ) facility at Heinrich-Heine University, Duesseldorf. Affymetrix CEL files were imported into the R/Bioconductor (22) environment,background-corrected, and normalized using the Robust Multi-array Average (RMA) method from the package oligo (25). Genes were considered expressed when their detection p-values - calculated as described in Graffmann et al. (26) - were below a threshold of 0.05. Using these expressed genes, expression was dissected with Venn diagrams employing the R package "VennDiagram" (27). Tables of Pearson correlation coefficients were generated using the R-built-in method "cor".

Hierarchical clustering dendrograms were generated with the method “hclust” using Pearson correlation as similarity measure and “complete linkage” as cluster agglomeration method. The “heatmap.2” function from the “gplots” package (28) was applied either with Pearson correlation as similarity measure and color scaling per gene or with Euclidean distance as distance measure and color scaling over the whole heatmap. Genes from the intersection of the venn diagrams, i.e., expressed in both conditions were further filtered for up-regulation by a ratio > 1.5 and down-regulation by a ratio < 0.67. When there were replicates, a threshold of 0.05 for the p-value of the differential expression test from the Bioconductor “limma” package (29) was added to the filter criteria.

2.9. Analysis of Pathways and Gene Ontologies (GOs)

Differentially up- and down-regulated genes with fold changes of 1.5 or 0.6 and P-value 0,05 were subjected to GO analysis via the Bioconductor package “GOstats” **(30)**. KEGG pathways and genes associated with them were downloaded from the KEGG database **(31)** and over-represented KEGG pathways were calculated for up- and down-regulated genes employing the R-built-in hypergeometric test. The enrichment analysis tool Metascape **(32)** was used to compare input gene lists extracted from the microarray data to thousands of available gene sets defined by their involvement in biological processes, protein localization, enzymatic function, pathways among other features.

2.10. Western Blotting

RIPA buffer (Sigma-Aldrich), with added protease and phosphatase inhibitors (Roche,), was used to extract the total protein from hiPSCs and NPCs. Protein concentration was measured with the Pierce™ BCA Protein Assay Kit (Thermo Fisher). 20μg of protein was run through a 4%-12% SDS-PAGE gel (NuPAGE, Thermo Fisher) and transferred to a 0.45 μm nitrocellulose membrane (GE Healthcare) using wet blotting. The membrane was blocked with 5% milk in TBST (20mM Tris, 150nM NaCl and 0,05% Tween 20) for 1h and stained for primary antibody in 4°C overnight, under constant agitation. The membranes were subsequently washed three times with TBST and stained for secondary antibody for two hours RT. Details of the antibodies used can be seen in Supplementary Table 2. Anti ß-actin and anti-RPLP0 were used as housekeepers. Protein bands were detected with Pierce™ ECL Western Blotting Substrate. Signaling was visualized using FusionCapt Advance FX7 and band intensities were quantified in the software Fusion Capt Advance (PeqLab) using rolling ball background correction.

3. Results

3.1. 24h of BPDE exposure does not impact hiPSC pluripotency.

In this study, we aimed at elucidating the effects of the genotoxin BPDE on iPSCs and see if iPSCs derived from an NBS patient (NBS8) react differently towards BPDE- induced DNA damage than wild type (WT) control cells (UM51, iPSC-12). To test for BPDE effects on the cellular stress response, we selected a suitable BPDE dosage scheme that assures cellular viability of more than 80% and does not interfere with pluripotency. Therefore, we treated all three hiPSC lines for 24h with distinct doses of BPDE and measured viability via resazurin assay. From this, we selected 25nM and 75nM as the IC10 and IC20, respectively, which were used for all further experiments. (Supplementary figure 1).

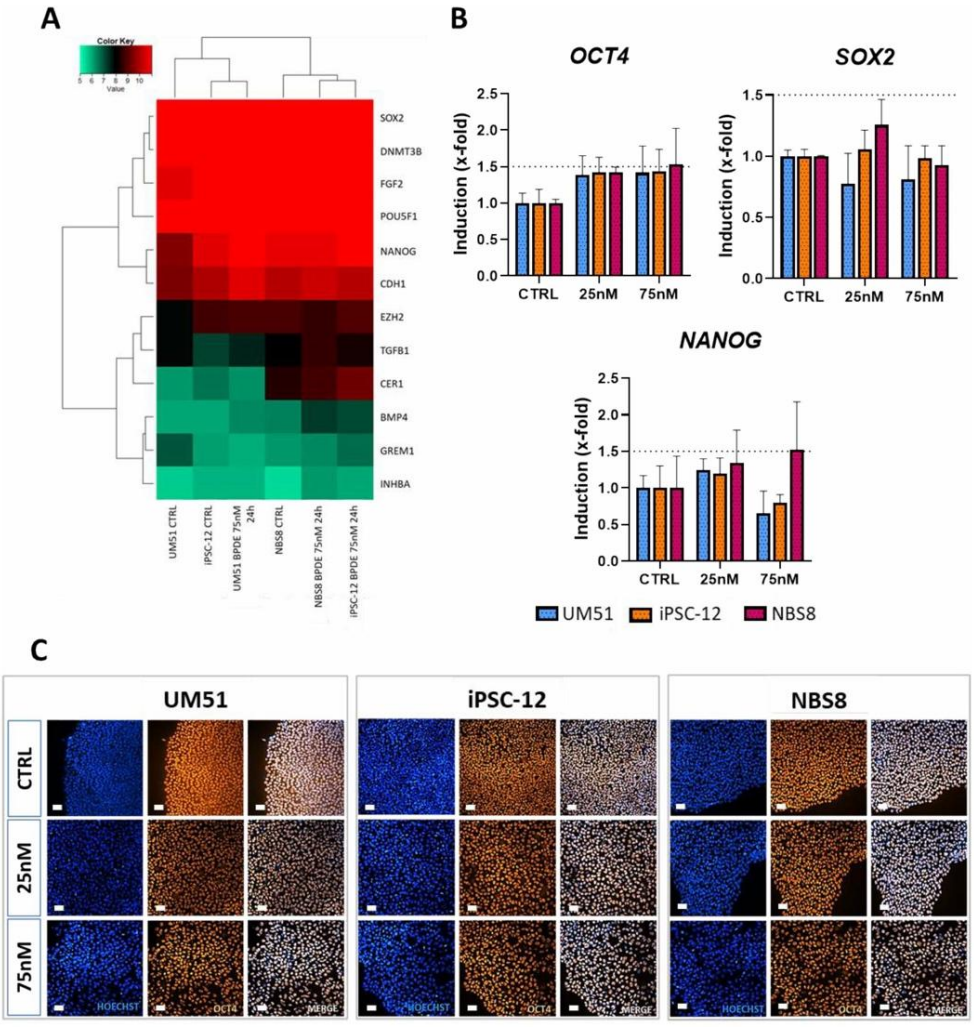

Figure 1: 24h of BPDE exposure does not negatively impact pluripotency.

WT and NBS8 hiPSCs were treated with 25nM and 75nM BPDE for 24h. RNA was extracted for microarray analysis or cells were fixed for immunocytochemistry. **(A)** Euclidean heatmap made with data extracted from the microarray analysis represents relative expression of key genes associated with pluripotency maintenance after 24h of 75nM BPDE exposure. **(B)** BPDE treatment did not alter *OCT4*, *SOX2* and *NANOG* transcription as confirmed via qRT-PCR (N=3. Error bar depicts 95% confidence interval. Scale bar 50µm. Dashed lines mark 1.5-fold.) **(C)** nor did it alter OCT4 expression as seen on immunocytochemistry.

The hiPSC lines UM51, iPSC-12, and NBS8 were exposed to 25 or 75nM BPDE for 24h or kept in control conditions, then subjected to microarray analysis. To investigate whether BPDE exposure had an effect on pluripotency, microarray data was used to generate a heatmap of twelve genes which are key in the regulation of pluripotency (Figure 1A). Genes such as POU Class 5 Homeobox 1 (*POU5F1*), SRY-Box Transcription Factor 2 (*SOX2*) and *NANOG,* key players orchestrating the maintenance of pluripotency, remained highly expressed after treatment, while genes involved in hiPSC differentiation like Gremlin 1 (*GREM1*) and bone morphogenetic protein 4 (*BMP4*) had a low expression. qRT-PCR for *POU5F1* (*OCT4*), *SOX2* and *NANOG* confirmed the microarray data (Figure 1B) and immunocytochemistry for OCT4 also revealed no difference in expression after BPDE treatment (Figure 1C).

3.2. BPDE exposure enhances gene expression of cell cycle arrest related genes, but does not impact cell cycle

As the integrity of the whole organism depends on the ability of stem cells to safely replace lost cells with their progeny, it is mandatory that stem cells keep their genome intact in order to avoid growth of malignantly transformed cells (33). Thus, they need to protect their genome by enhanced repair activity and if this is not possible, they usually die through apoptosis (34).

To see if these pathways are differentially regulated in healthy and diseased cells, we first investigated if the cell cycle was affected by BPDE as cell cycle arrest is necessary to give the cells enough time for DNA repair.

To investigate the transcriptional changes induced by BPDE exposure regardless of the mutation, we pooled the microarray results of all samples into control and BPDE treated (Supplementary figure 2A). We also investigated the transcriptional downstream effects of the mutation, both in the absence of stimulus and after BPDE treatment, comparing the WT and NBS8 lines in control conditions (Supplementary figure 2B) and after genotoxic exposure (Supplementary figure 2C). We performed Gene Ontologies (GO), KEGG pathway, as well as Metascape analyses (Supplementary figures 3 to 6).

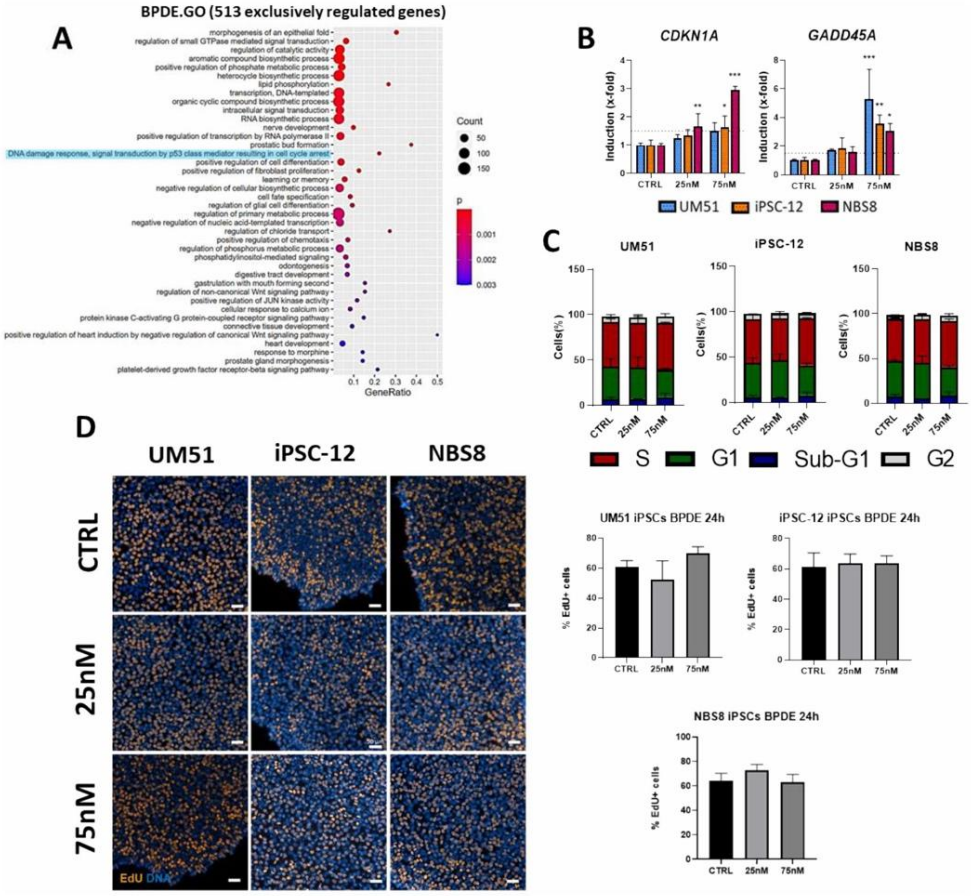

Figure 2: BPDE exposure enhances gene expression of cell cycle arrest related genes, but does not influence cell cycle. hiPSCs were treated for 24h with 25 or 75 nM BPDE **(A)** GO-Analysis for 513 genes exclusively expressed in all 3 cell lines after BPDE exposure in hiPSCs. The relevant DNA-damage cluster is highlighted in blue. **(B)** qRT-PCR for *CDKN1A* and *GADD45A*. Error bar depicts 95% confidence interval. N=3, *p<0.05, ** = p<0.01, *** = p<0.001. Dashed lines mark 1.5-fold. **(C)** Cell cycle distribution was analyzed via propidium iodide staining measured by FACS and presented here in percentage as bar graphs. N=3, mean +/- standard deviation. **(D)** Representative images of EdU staining of hiPSCs after CTRL, 25nM and 75nM treatment and bar graphs representing the percentage of EdU positive cells on each cell line compared to Hoechst after 24h treatment. N=3, mean +/- standard deviation. Scale bar 50µm.

Gene ontology analysis of 513 genes exclusively expressed after BPDE treatment (Figure 2A) revealed, amongst others, the cluster “DNA damage response, signal transduction by p53 class mediator resulting in cell cycle arrest” with four regulated genes: cyclin dependent kinase inhibitor 1A (*CDKN1A*); Mucin1 (*MUC1*); polo like kinase 2 (*PLK2*) and proline rich acidic protein 1 (*PRAP1*). qRT-PCR for *CDKN1A* and Growth arrest and DNA damage inducible alpha (*GADD45A*), another p53-inducible DNA damage and cell cycle arrest associated gene, revealed that all three cell lines exhibited upregulated expression levels (mean > 3-fold) of

GADD45A after exposure to 75nM BPDE, while there was no regulation after treatment with 25nM BPDE. *CDKN1A* was upregulated intensely in NBS8 (mean 1.6-fold at 25nM and 2.9-fold at 75nM) and slightly in iPSC-12 (mean 1.6-fold at 75nM) (Figure 2B). However, a cell cycle analysis using propidium iodide staining and flow cytometry showed that cell cycle distribution on all three lines was unaffected after BPDE exposure (Figure 2C). This result was supported by EdU staining, which confirmed that BPDE exposure had no effect on the percentage of cells in S phase (Figure 2D).

3.3. BPDE treatment enhances expression of targets related to the extrinsic apoptotic pathway in hiPSCs

As we observed that the expression of genes related to cell cycle arrest was enhanced by BPDE while there was no actual cell cycle arrest detectable, we aimed to investigate if BPDE influences apoptosis in hiPSCs.

The GOs extracted from the 254 genes upregulated after BPDE treatment revealed several clusters related to both positive and negative regulation of cell death (Figure 3A). Notably, several genes related to the extrinsic apoptotic signaling pathway were upregulated including all four known receptors for TNF-related apoptosis-inducing ligand (TRAIL): TNF Receptor Superfamily Member 10A (*TNFRSF10A*), *TNFRSF10B*, *TNFRSF10C* and *TNFRSF10D.* qRT-PCR for *TNFRSF10A* (Figure 3B) confirmed its upregulation in all three lines (mean > 1.7-fold), while the expression of the intrinsic apoptosis genes BCL2 associated X, apoptosis regulator (*BAX*) and Bcl-2-binding component 3 (*BBC3*) remained unchanged (Figure 3B).

Both the extrinsic and intrinsic apoptotic pathways depend on Caspases to induce cell death, therefore an executioner Caspase essential in both pathways- Caspase 3 (*CASP3*), was investigated. *CASP3* expression increased (mean > 1.7-fold) after BPDE treatment in both WT cell lines, but not in NBS8 (Figure 3B). Caspase 3 protein expression was unchanged in all three lines, but the expression of cleaved Caspase 3, the active form of Caspase 3, was enhanced particularly in the WT lines and far less in NBS8 (Figure 3F).

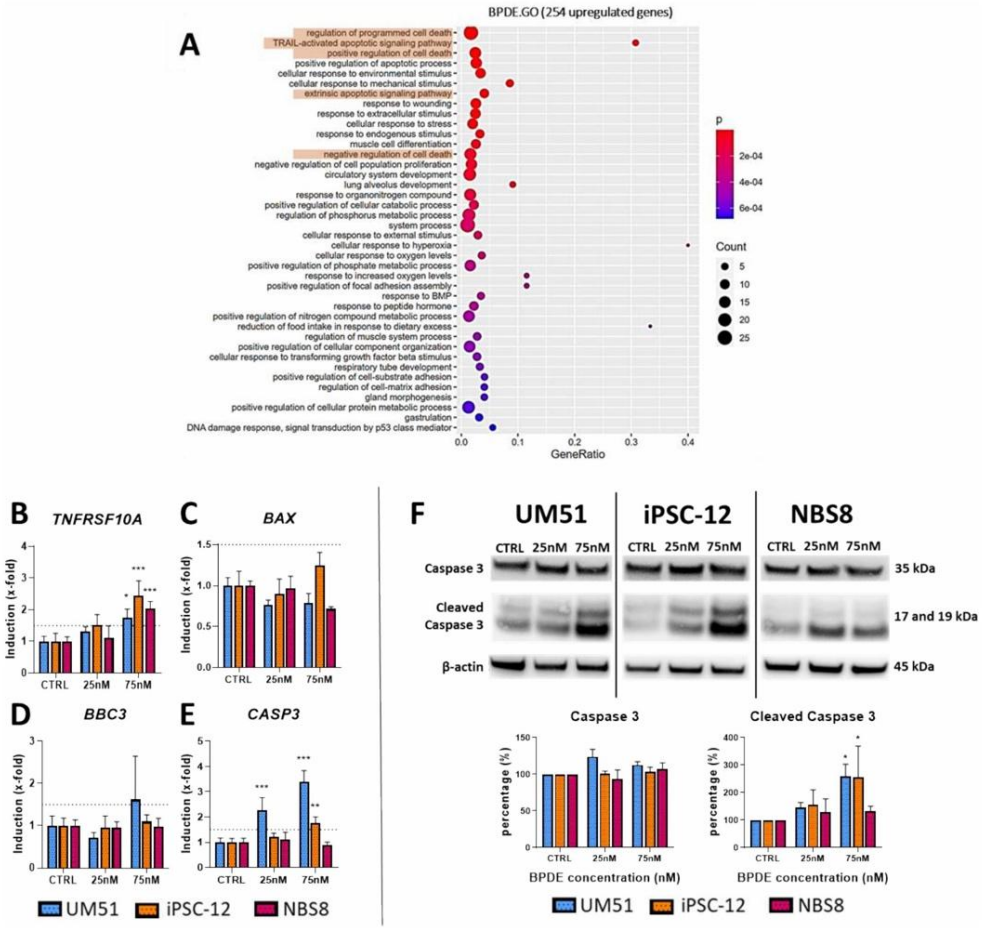

Figure 3: BPDE exposure differentially regulates apoptotic markers on WT and NBS8 hiPSCs. hiPSCs were treated with 25nM and 75nM of BPDE for 24h. RNA was extracted for microarray analysis and qRT-PCR. **(A)** Gene ontology analysis was performed for 254 genes upregulated in hiPSCs after BPDE treatment. Apoptosis related clusters are highlighted in orange. **(B, C, D, E)** qRT-PCR for *TNFRSF10A, BAX, BBC3*, and *CASP3*. Error bar depicts 95% confidence interval. N=3, *p<0.05, ** = p<0.01, *** = p<0.001. Dashed lines mark 1.5-fold. **(F)** Western blot for Caspase 3 and cleaved Caspase 3. β-actin was used as loading control. N=2, mean +/- standard deviation shown, *p<0.05.

3.54 BPDE differentially regulates DNA damage response genes in WT and NBS8 hiPSCs

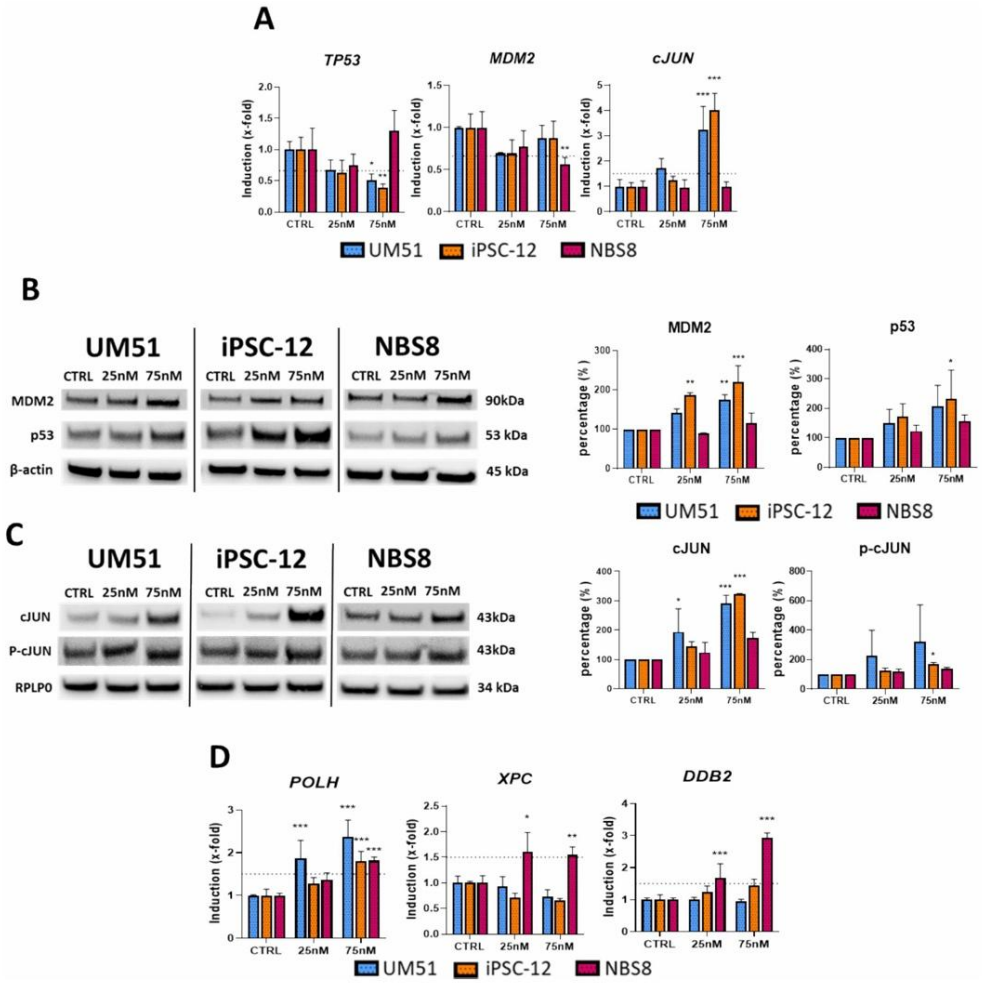

Figure 4: BPDE differentially regulates the DNA damage response in WT and NBS8 hiPSCs. hiPSCs were exposed to 25nM and 75nM of BPDE for 24h. **(A)** qRT-PCR for *TP53*, *MDM2* and *cJUN*. Error bar depicts 95% confidence interval. N=3, *p<0.05, ** = p<0.01. *** = p<0.001. Dashed lines mark 0.6 -fold (*TP53, MDM2*) and1.5-fold (*cJUN*). **(B and C)** Western blot for MDM2, p53, cJUN and p-cJUN. B-actin or RPLP0 were used as loading controls. N=2, mean +/- standard deviation shown, * = p<0.05, ** = p<0.01, *** = p<0.001. **(D)** qRT-PCR for *POLH*, *XPC* and *DDB2*. Error bar depicts 95% confidence interval. N=3, *p<0.05, ** = p<0.01, *** = p<0.001. Dashed lines mark 1.5-fold.

The enrichment analysis tool- Metascape, was used to compare the input gene list of the common 254 upregulated genes in all 3 cell lines after BPDE exposure. Two of the top non-redundant enrichment clusters were related to the p53 signaling pathway with 26 upregulated genes (Supplementary figure 3B). Among them were three known regulators of p53 signaling,

cJUN, MDM2 and protein Phosphatase, Mg^{2+}/Mn^{2+} Dependent 1D (*PPM1D*), as well as other genes involved in p53-mediated DNA damage response such as *GADD45A*, Sestrin 1 (*SESN1*), *POLH*, BTG Anti-Proliferation Factor 2 (*BTG2*) and Stratifin (*SFN*).

As p53 is an important factor in the regulation of pluripotency and differentiation (35), we aimed to investigate the influence of BPDE exposure on p53 and its effectors in our model. Interestingly, qRT-PCR revealed that *TP53* was significantly downregulated (mean < 0.5-fold) in both WT lines after treatment with 75nM BPDE (Figure 4A), whilst the expression p53 protein was increased in both healthy controls albeit only significantly in iPSC-12 hiPSCs (Figure 4B). Both gene and protein expression remained unchanged in NBS8 (Figure 4A and 4B). Two targets related to p53 regulation, *MDM2* and *cJUN*, were measured in an attempt to clarify the differences in the expression of *TP53* and p53 between WT and NBS8 cells after BPDE treatment. *MDM2* gene expression was downregulated (mean 0.56 -fold) exclusively in NBS8 (Figure 4A), while its protein levels were increased only in the WT cells (Figure 4B). A similar pattern was observed with cJUN. The mRNA levels (mean > 3.2 -fold) and protein expression were both increased in WT cells after treatment, but unchanged in NBS8 (Figure 4A and 4C). Since the activity of cJUN is stimulated by its phosphorylation at serines 63/73, the protein levels of serine 73 p-cJUN were also measured, this revealed increased expression in the iPSC-12 cells (Figure 4C). Next, we evaluated the mRNA expression of four upstream components of the p53 signaling cascade, *ATR*, *ATM,* and their respective downstream effectors, *CHEK1* and *CHEK2* (Supplementary figure 7). BPDE exposure did not affect the expression of *ATM*, *CHEK1* or *CHEK2* however, it upregulated the expression of ATR (mean 7.1 -fold) in the NBS8 cell line (Supplementary figure 7A). p53 is involved in NER, regulating the expression of targets such as XPC and DDB2, and it has also been implicated in the transcriptional regulation of trans-lesion synthesis DNA polymerases in reaction to DNA damage (173). After BPDE exposure, gene expression of the trans-lesion synthesis DNA polymerase *POLH* was upregulated (mean > 1.8-fold) in all three cell lines (Figure 4D). Interestingly, *XPC* and *DDB2* were upregulated exclusively in NBS8, and in both tested concentrations. *XPC* was upregulated by 1.5-fold in both concentrations, whilst the regulation of *DDB2* increased in a dose-dependent manner; 1.6-fold at 25nM and 3-fold at 75nM (Figure 4D).

3.5. Responses to BPDE exposure is different in neural progenitor cells compared to their undifferentiated hiPSC parental lines

We next wanted to see, if BDPE has any influence on the early steps of neuro-development. As such, iPSCs were differentiated into NPCs and treated with 25nM or 75nM of BPDE for 24h. Immunostaining-based detection of expression of the NPC markers SOX2, SOX1 and Nestin, and the proliferation marker Ki67, was unchanged after BPDE treatment, and also for the neuron marker TUJ1 (Supplementary figure 8A). Likewise, gene expression levels of the

NPC markers *SOX2*, *SOX1* and *PAX6* remained stable after genotoxic exposure (Supplementary figure 8B). Thus, BPDE treatment did not impair differentiation towards NPCs. However, they reacted less sensitive in terms of apoptosis and DNA damage marker expression than their undifferentiated counterparts.

The expression of *TNFRSF10A* and *CASP3* were upregulated in hiPSCs after BPDE treatment (Figure 3B and 3E), unlike in NPCs. The intrinsic apoptotic markers *BBC3* and *BAX* remained unchanged in both cell types (Figure 5A to 5D). The protein expression of Caspase 3, as well as that of its active form cleaved Caspase 3, remained mostly unchanged in NPCs after BPDE treatment, with only a slight upregulation (1.5-fold) of cleaved caspase 3 seen on iPSC-12 NPCs (Figure 5E). These results suggest that hiPSCs showed a lower resistance to BPDE cytotoxicity after 24h of exposure than their differentiated NPCs.

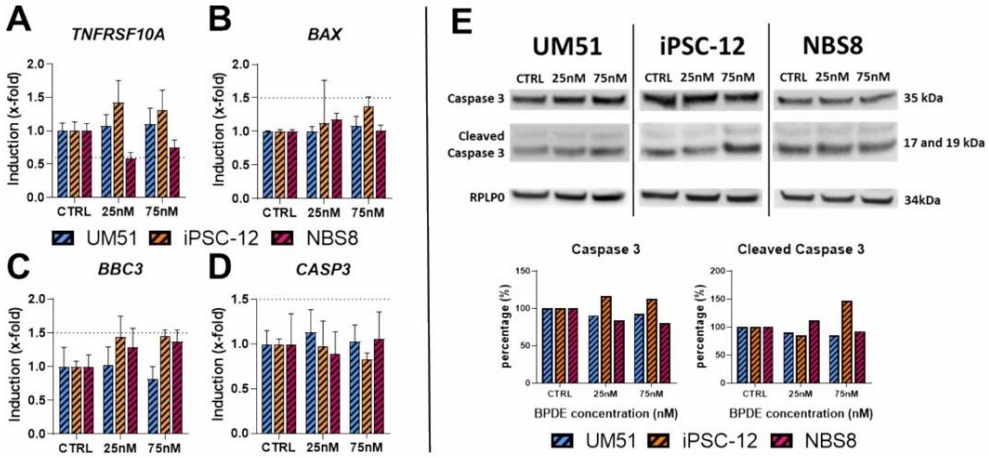

Figure 5: 24h BPDE exposure does not influence expression of key apoptotic markers on NPCs. NPCs were treated with 25nM and 75nM of BPDE for 24h, then RNA was extracted for qRT-PCR and protein was extracted for western blot. qRT-PCR for **(A)** *TNFRSF10A*, **(B)** *BAX*, **(C)** *BBC3* and **(D)** *CASP3*. N=3. Error bar depicts 95% confidence interval. **(E)** Western blot and quantification for caspase 3 and cleaved caspase 3. N=1, RPLP0 was used for loading control.

Gene expression levels of the p53-inducible cell cycle regulators *CDKN1A* and *GADD45A* was unchanged in NPCs, with the exception of iPSC-12 NPCs, which showed a slight upregulation (1.8-fold) of both markers at 75nM (Figure 6A and 6B). With the intent to analyze the p53-mediated DNA damage response, the gene and protein expression of p53 was measured, as well as that of the p53 regulators MDM2 and cJUN. *TP53* and *MDM2* gene expression remained constant after BPDE treatment in NPCs in all lines, as did *cJUN* (Figure 6C to 6E). Investigation of the protein expression of MDM2 in NPCs after BPDE exposure revealed a similar pattern to that observed in hiPSCs, with the expression being enhanced in WT NPCs

after treatment, but unchanged in NBS8 NPCs. Interestingly, p53 protein expression was enhanced only in iPSC-12 NPCs after genotoxic exposure, while the protein expression of cJUN was unchanged in all three NPC cell lines (Figure 6F).

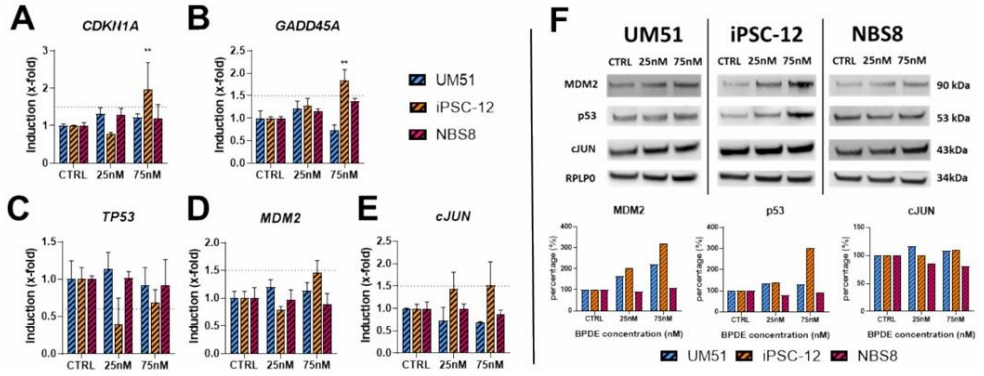

Figure 6: BPDE exposure of NPCs differentially regulates targets related to cell cycle control and p53 modulation when compared to hiPSCs. NPCs were treated with 25nM or 75nM of BPDE for 24h, then RNA was harvested for qRT-PCR and protein was harvested for western blot. qRT-PCR for **(A)** *CDKN1A*, **(B)** *GADD45A*, **(C)** *TP53* **(D)** *MDM2* and **(E)** *cJUN*. N=3, *p<0.05, **p<0.01. Error bar depict 95% confidence interval. Dashed lines mark 1.5- and 0.6-fold. **(F)** Western blot and quantification for MDM2, p53, and cJUN. N=1. RPLP0 was used as loading control.

While *ATM*, *CHEK1,* and *CHEK2* maintained a stable gene expression in both hiPSCs and NPCs after BPDE treatment, the upregulation of *ATR* which was noted in NBS8 hiPSCs after exposure to both 25nM and 75nM BPDE (1.6- fold and 7.1-fold respectively) was not observed in their differentiated NPC progeny (Supplementary figure 9A to 9D).

Lastly, gene expression of three p53-inducible genes related to bulky DNA-adduct repair, *POLH*, *XPC* and *DDB2*, was investigated. *XPC* and *DDB2* were upregulated in NBS8 hiPSCs in both concentrations tested (Figure 4D), but in NPCs *XPC* expression was unchanged after BPDE exposure (Supplementary figure 9F) and *DDB2* was only upregulated at 75nM (1.5-fold) and less than in their hiPSC counterparts (3-fold) (Supplementary figure 9E). In hiPSCs, the expression of *POLH* was upregulated in all three cell lines after BPDE treatment (Figure 5D), which was not seen in NPCs (Supplementary figure 9G).

These results are summarized in Table 1 and Table 2. An observation from the summary is that NBS8 cells, in particular NBS8 hiPSCs, present a distinct DNA damage response upon BPDE exposure than their WT counterparts. For example, NBS8 hiPSCs upregulate mRNA expression of *XPC* and DDB2, genes involved in NER, while showing a lower upregulation of targets involved in the apoptotic response such as cleaved Caspase 3. Secondly, the different cell types have distinct responses to BPDE exposure. hiPSCs have generally a more robust DNA damage response, with the regulation of several targets related to cell cycle checkpoint,

apoptosis, and DNA damage repair, while NPCs had a more moderate response, with few regulated targets.

Table 1: Summary table of results from the set of genes investigated through qRT-PCR after BPDE exposure. Cells were exposed to BPDE in the concentrations of 25nM and 75nM for 24h. Their RNA was extracted and used for qRT-PCR. The table summarizes the results obtained from the investigation of known BPDE targets as seen on the literature and those that were identified as BPDE targets through microarray analysis of BPDE exposed hiPSCs. Empty cells indicate no change in expression. One and two crosses indicate over 1.5x -fold or over 2x -fold increase in expression compared to control, respectively. The minus sign indicates a downregulation of at least less than 0.6x -fold.

Symbols key							
+++	>2.0x -fold						
+	>1.5x -fold		iPSCs			NPCs	
-	< 0.6x -fold	UM51	iPSC-12	NBS8	UM51	iPSC-12	NBS8
ATM							
ATR				+++			
BAX							
BBC3							
CASP3		+++	+				
CDKN1A			+	+++			
CHEK1							
CHEK2							
cJUN		+++	+++			+	
DDB2				+++			+
GADD45A		+++	+++	+++		+	
MDM2				-			
POLH		+++	+	+			
TNFRSF10A		+	+++	+		+	
TP53		-	-				
XPC				+			

Table 2: Summary table of results from the set of proteins investigated after BPDE exposure. Cells were exposed to BPDE in the concentrations of 25nM and 75nM for 24h. Then, their protein was extracted and used for western blot. The table summarizes the results obtained from the investigation of proteins related to the DNA damage response. Empty cells indicate no change in expression. One and two crosses indicate over 150% or over 200%

increase in protein expression compared to control, respectively. Blocked cells indicates that the target was not investigated.

Symbols key		iPSCs			NPCs		
+++	>200% increase						
+	>150% increase	UM51	iPSC-12	NBS8	UM51	iPSC-12	NBS8
p53		+++	+++			+	
cJUN		+++	+++	+			
P-cJUN		+++	+++				
Caspase 3							
Cleaved Caspase 3		+++	+++	+			
MDM2		+++	+++		+++	+++	

4. Discussion

To elucidate the effects of BPDE on undifferentiated hiPSCs at the transcriptional level, we performed for the first time a whole-genome transcriptome analysis of WT hiPSCs exposed to BPDE, which we compared to NBS patient-derived iPSCs that have a defect in the DNA repair mechanism.

Pluripotent stem cells have highly efficient DNA repair systems (36–38), but in case of failure to repair DNA lesions they will either rapidly undergo apoptosis (34) or suffer a p53-mediated loss of pluripotency by repressing the transcription factors *OCT4* and *NANOG*, and activating genes associated with differentiation (39,40). Our results show that 24h of BPDE exposure on hiPSCs affected neither the expression of *OCT4* and *NANOG*, nor that of targets associated with triggering differentiation such as *BMP4* or *GREM1* (Figure 1A and 1B). The nuclear expression of OCT4 also remained stable (Figure 1C). In line with data from Momcilovic et al, who studied the effects of γ-irradiation in hiPSCs (42), this suggests that our cells retained pluripotency for at least 24h after BPDE exposure.

BPDE treatment has been documented to induce cell cycle disruption in somatic cells, dependent on the treatment dose, the cell type, and the phase in the cell cycle that the cells were in at the start of treatment (41–43).

The GOs of hiPSC exposed to BPDE revealed an upregulated cluster related to DNA damage-induced cell cycle arrest. *GADD45A*, which is known to stimulate cell cycle arrest upon genotoxic exposure (44,45) was upregulated in all cell lines after treatment (Figure 2B). However, cell cycle analysis via flow cytometry for PI and EdU incorporation assays indicated

that hiPSCs had no change in their cell cycle distribution after BPDE exposure (Figure 2C and 2D). This could be related to the timepoint of the analysis, since it has been shown that hiPSCs exposed to γ-irradiation show cell cycle arrest at the G2/M phase in the first 9h after exposure, but after 24h their cell cycle distribution returns to the same pattern as non-irradiated controls (37). Interestingly, *CDKN1A*, a p53-associated cell cycle regulator (46), was up-regulated only in the NBS8 cell line after BPDE exposure (Figure 2A), lending support to reports of perturbed cell cycle arrest signaling after genotoxic exposure in NBN-impaired cells (47–49).

Bioinformatic analysis of hiPSC exposed to BPDE revealed upregulated clusters related to the p53 signalling pathway (Supplementary Figure 3B). Investigation of the gene and protein expression of p53, MDM2 and cJUN, as well as Ser73 phospho-cJUN, revealed a general pattern of upregulation of these targets in WT hiPSC and little or no regulation in NBS8 cells (Figure 4).

Although *TP53* gene expression was downregulated in WT hiPSCs after BPDE exposure, p53 protein expression was increased in these cells, while NBS8 hiPSCs showed no *TP53* or p53 regulation (Figure 4A). Interestingly, dysregulation of p53 function upon DNA damage is a defining aspect of NBS. It is known that NBS fibroblasts exposed to ionizing radiation have a delayed and reduced p53-mediated response to DNA damage (51). We made a similar observation for NBS fibroblasts and NBS iPSC-derived cerebral organoids exposed to bleomycin in earlier studies (50,51). This effect does not seem to be related to MDM2 mediated p53 degradation, as MDM2 protein expression was significantly increased only in WT hiPSCs after BPDE treatment but not in NBS8 hiPSC (Figure 4A and 4B).

The upregulation of cJUN and Ser73 p-cJUN in BPDE treated WT hiPSCs (Figure 4A and 4C) could help explain the downregulation of *TP53* and the low or no upregulation of *CDKN1A* mRNA levels seen in the cells and hint at a protective effect being elicited. cJUN has a variety of roles during the DNA damage response, repressing p53 mRNA expression to allow for cell cycle progression and proliferation (52), and playing a role in genotoxic resistance and activation of DNA damage repair (53–55). It is interesting to note that the phosphorylation of cJUN at Ser63/73 seems to be essential for its protective role against DNA damaging agents (54,55). However, cJUN has also been linked to cellular stress induced apoptosis, which seems to occur through the sustained upregulation of cJUN levels and, at least in some cell types, enhanced extrinsic apoptotic signalling (56,57). Thus, a possible pro-apoptotic effect through the extrinsic apoptotic pathway cannot be discarded.

Indeed, GO analysis of genes which were upregulated after BPDE exposure on hiPSCs revealed several clusters associated with positive and negative regulation of apoptosis (Figure 3A). Curiously, while reports of BPDE exposure on somatic cells reported the upregulation of the intrinsic apoptotic pathway, and genes such as *BAX* and *BBC3* (58–60), hiPSCs showed a distinct upregulation of the extrinsic apoptotic pathway, confirmed through qRT-PCR (Figure

3A to 3C). It was also observed that, although the gene expression of *TNFRSF10A* was upregulated in all three cell lines, the expression of the executioner *CASP3* was only upregulated in WT cells (Figure 3D), and the same was observed for the protein expression of cleaved Caspase 3, the active form of the Caspase 3 protein (Figure 3E). NBN-impaired cells have been reported as having deficient apoptosis regulation (47,50). This translates into a delayed genotoxic exposure response that leads to deficient activation of the apoptotic pathway after DNA damage (47–49).

In line with this, our data confirm previously reported delays in the activation of the DNA repair machinery in NBN-deficient hiPSCs after BPDE treatment (47–49), as we could only observe up-regulation of X*PC* and *DDB2* in these cells but not in the WT cells (Figure 4B and 4C). *POLH* expression, however, was upregulated in all three hiPSC lines (Figure 4A). *POLH* is involved in the error-prone bypass of BPDE-adducts (61,62) and induction of *POLH* by BPDE has been implicated in enhanced cell survival, but at the expense of a higher number of genomic mutations (41,58). This adaptative reaction is particularly worth of further study since mutations that occur during early embryogenesis can contribute to cancer development later in life (63).

5. Conclusion

To the best of our knowledge, this is the first time the effects of BPDE exposure have been investigated on an hiPSCs model and the first comparison made between the effects of BPDE on pluripotent stem cells and differentiated NPCs. This mimics pre-gastrulation and differentiation towards the ectoderm lineage of early human development.

We showed that hiPSC and NPCs harbouring an NBS mutation reacted differently to BPDE treatment compared to WT cells, showing less apoptotic response and no increase in the expression of p53 and MDM2. Our data also emphasizes the differences in the DNA damage response between hiPSCS and NPCs, with the former presenting a robust response compared to NPCs, enhancing the mRNA and/or protein expression of several targets related to DNA damage response, apoptosis and cell cycle checkpoints. Furthermore, our model conforms with the 3Rs principle.

Supplementary Materials:

Supplementary figure 1: Dose-response curve of BPDE-treated hiPSCs.

Supplementary figure 2: Venn Diagrams of differentially regulated genes extracted from microarray analysis.

Supplementary figure 3: Metascape analysis of differentially regulated genes extracted from microarray analysis.

Supplementary figure 4: GO and KEGG pathways of differentially regulated genes extracted from microarray analysis.

Supplementary figure 5: In control conditions, NBS8 hiPSCs have enhanced cancer related KEGG pathways compared to WT hiPSCs.

Supplementary figure 6: BPDE treatment enhances cancer-related GO clusters and KEGG pathways in NBS8 hiPSCs.

Supplementary figure 7: BPDE differentially regulates the gene expression of DNA damage response gene *ATR* between WT and mutant hiPSCs.

Supplementary figure 8: 24h BPDE exposure on NPCs does not affect expression of key NPC markers.

Supplementary figure 9: BPDE exposure differentially regulates gene targets related to DNA damage response and repair in NPCs when compared to hiPSCs.

Supplementary table 1: Cell lines used in this work.

Supplementary table 2: Antibodies and dilutions used on immunocytochemistry (ICC) and Western blot.

Supplementary table 3: Primer sequences used in this work.

Funding

J.A. acknowledges the medical faculty of Heinrich Heine University and the Deutsche Forschungsgemeinschaft (DFG, German Research Foundation) - 417677437/GRK2578 for the financial support.

Institutional Review Board Statement

The study was conducted according to the guidelines by the Ethics Committee of the medical faculty of Heinrich-Heine University, Germany (protocol code: 5704).

Data availability statement

All microarray data will be available at NCBI GEO server once the manuscript is accepted.

Conflicts of Interest

The authors declare no conflict of interest.

References

1. Van Norman GA. Limitations of Animal Studies for Predicting Toxicity in Clinical Trials. JACC Basic Transl Sci. 2019 Nov;4(7):845–54.

2. Van Norman GA. Limitations of Animal Studies for Predicting Toxicity in Clinical Trials. JACC Basic Transl Sci. 2020 Apr;5(4):387–97.

3. Luconi M, Sogorb MA, Markert UR, Benfenati E, May T, Wolbank S, et al. Human-Based New Approach Methodologies in Developmental Toxicity Testing: A Step Ahead from the State of the Art with a Feto–Placental Organ-on-Chip Platform. Int J Environ Res Public Health. 2022 Nov 28;19(23):15828.

4. MacRae SL, Croken MM, Calder RB, Aliper A, Milholland B, White RR, et al. DNA repair in species with extreme lifespan differences. Aging. 2015 Dec 30;7(12):1171–82.

5. Galloway SM. International regulatory requirements for genotoxicity testing for pharmaceuticals used in human medicine, and their impurities and metabolites. Environ Mol Mutagen. 2017 Jun;58(5):296–324.

6. Kirkland D, Aardema M, Henderson L, Müller L. Evaluation of the ability of a battery of three in vitro genotoxicity tests to discriminate rodent carcinogens and non-carcinogens. Mutat Res Toxicol Environ Mutagen. 2005 Jul;584(1–2):1–256.

7. Kirkland D, Aardema M, Müller L, Hayashi M. Evaluation of the ability of a battery of three in vitro genotoxicity tests to discriminate rodent carcinogens and non-carcinogens. Mutat Res Toxicol Environ Mutagen. 2006 Sep;608(1):29–42.

8. Zushin PJH, Mukherjee S, Wu JC. FDA Modernization Act 2.0: transitioning beyond animal models with human cells, organoids, and AI/ML-based approaches. J Clin Invest. 2023 Nov 1;133(21):e175824.

9. Weatherbee BAT, Gantner CW, Iwamoto-Stohl LK, Daza RM, Hamazaki N, Shendure J, et al. Pluripotent stem cell-derived model of the post-implantation human embryo. Nature. 2023 Oct 19;622(7983):584–93.

10. Chrzanowska KH, Gregorek H, Digweed M. Nijmegen breakage syndrome (NBS). 2012;

11. Włodarczyk M, Lejman M. Chromosomal instability associated with adverse outcome: a case report of patient with Nijmegen breakage syndrome and rapidly developed T-NHL with complex karyotype. Mol Cytogenet. 2020 Dec;13(1):35.

12. Eisenstadt Eri, Warren AJ, Porter J, Atkins D, MILLERt JH. Carcinogenic epoxides of benzo[alpyrene and cyclopenta[cd]pyrene induce base substitutions via specific transversions. Proc Natl Acad Sci USA. 1982;

13. Melendez-Colon VJ, Luch A, Seidel A, Baird WM. Cancer initiation by polycyclic aromatic hydrocarbons results from formation of stable DNA adducts rather than apurinic sites. Carcinogenesis. 1999 Oct;20(10):1885–91.

14. Filler R, Lewt KJ. Developmental onset of mixed-function oxidase activity in preimplantation mouse embryos. Dev Biol. 1981;

15. Rouet P, Dansette PM, Weston A, Frayssinet C. Metabolism of benzo[a]pyrene by mouse brain microsomes during perinatal development. Chem Biol Interact. 1984 Jan;48(1):115–9.

16. Arnould J, Verhoest P, Bach V, Libert J, Belegaud J. Detection of benzo[a]pyrene-DNA adducts in human placenta and umbilical cord blood. Hum Exp Toxicol. 1997 Dec;16(12):716–21.

17. Zenzes MT. Detection of benzo(a)pyrene diol epoxide– DNA adducts in sperm of men exposed to cigarette smoke. 1999;72(2).

18. Zenzes M. Immunodetection of benzo[a]pyrene adducts in ovarian cells of women exposed to cigarette smoke. Mol Hum Reprod. 1998 Feb 1;4(2):159–65.

19. Zenzes MT. Detection of benzo[a]pyrene diol epoxide-DNA adducts in embryos from smoking couples: evidence for transmission by spermatozoa. Mol Hum Reprod. 1999 Feb 1;5(2):125–31.

20. Bohndorf M, Ncube A, Spitzhorn LS, Enczmann J, Wruck W, Adjaye J. Derivation and characterization of integration-free iPSC line ISRM-UM51 derived from SIX2-positive renal cells isolated from urine of an African male expressing the CYP2D6 *4/*17 variant which confers intermediate drug metabolizing activity. Stem Cell Res. 2017 Dec;25:18–21.

21. Mlody B, Adjaye J. Generation of iPSC lines from a Nijmegen Breakage Syndrome patient. Stem Cell Res. 2015;4.

22. Ihaka R, Gentleman R. R: A Language for Data Analysis and Graphics. 2024;

23. An H, Landis J T, Bailey A G, Marron J S, Dittmer D P. dr4pl: A Stable Convergence Algorithm for the 4 Parameter Logistic Model. R J. 2019;11(2):171.

24. Wickham H. ggplot2: Elegant Graphics for Data Analysis [Internet]. New York, NY: Springer New York; 2009 [cited 2024 May 15]. Available from: https://link.springer.com/10.1007/978-0-387-98141-3

25. Carvalho BS, Irizarry RA. A framework for oligonucleotide microarray preprocessing. Bioinformatics. 2010 Oct 1;26(19):2363–7.

26. Graffmann N, Ring S, Kawala MA, Wruck W, Ncube A, Trompeter HI, et al. Modeling Nonalcoholic Fatty Liver Disease with Human Pluripotent Stem Cell-Derived Immature Hepatocyte-Like Cells Reveals Activation of PLIN2 and Confirms Regulatory Functions of Peroxisome Proliferator-Activated Receptor Alpha. Stem Cells Dev. 2016 Aug;25(15):1119–33.

27. Chen H, Boutros PC. VennDiagram: a package for the generation of highly-customizable Venn and Euler diagrams in R. BMC Bioinformatics. 2011 Dec;12(1):35.

28. Warnes GR, Bolker B, Bonebakker L, Gentleman R, Huber W, Liaw A, et al. gplots: Various R Programming Tools for Plotting Data [Internet]. 2005 [cited 2024 Sep 4]. p. 3.1.3.1. Available from: https://CRAN.R-project.org/package=gplots

29. Smyth GK. Linear Models and Empirical Bayes Methods for Assessing Differential Expression in Microarray Experiments. Stat Appl Genet Mol Biol. 2004 Jan 12;3(1):1–25.

30. Falcon S, Gentleman R. Using GOstats to test gene lists for GO term association. Bioinformatics. 2007 Jan 15;23(2):257–8.

31. Kanehisa M, Furumichi M, Tanabe M, Sato Y, Morishima K. KEGG: new perspectives on genomes, pathways, diseases and drugs. Nucleic Acids Res. 2017 Jan 4;45(D1):D353–61.

32. Zhou Y, Zhou B, Pache L, Chang M, Khodabakhshi AH, Tanaseichuk O, et al. Metascape provides a biologist-oriented resource for the analysis of systems-level datasets. Nat Commun. 2019 Apr 3;10(1):1523.

33. Vitale I, Manic G, De Maria R, Kroemer G, Galluzzi L. DNA Damage in Stem Cells. Mol Cell. 2017 May;66(3):306–19.

34. Dumitru R, Gama V, Fagan BM, Bower JJ, Swahari V, Pevny LH, et al. Human Embryonic Stem Cells Have Constitutively Active Bax at the Golgi and Are Primed to Undergo Rapid Apoptosis. Mol Cell. 2012 Jun;46(5):573–83.

35. Ayaz G, Yan H, Malik N, Huang J. An Updated View of the Roles of p53 in Embryonic Stem Cells. Stem Cells. 2022 Oct 21;40(10):883–91.

36. Maynard S, Swistowska AM, Lee JW, Liu Y, Liu ST, Da Cruz AB, et al. Human Embryonic Stem Cells Have Enhanced Repair of Multiple Forms of DNA Damage. Stem Cells. 2008 Sep 1;26(9):2266–74.

37. Momcilovic O, Knobloch L, Fornsaglio J, Varum S, Easley C, Schatten G. DNA Damage Responses in Human Induced Pluripotent Stem Cells and Embryonic Stem Cells. Capogrossi MC, editor. PLoS ONE. 2010 Oct 15;5(10):e13410.

38. Liedtke S, Biebernick S, Radke TF, Stapelkamp D, Coenen C, Zaehres H, et al. DNA Damage Response in Neonatal and Adult Stromal Cells Compared With Induced Pluripotent Stem Cells: DNA Damage Defense in iPSCs Versus Stromal Cells. STEM CELLS Transl Med. 2015 Jun;4(6):576–89.

39. Lin T, Chao C, Saito S, Mazur SJ, Murphy ME, Appella E, et al. p53 induces differentiation of mouse embryonic stem cells by suppressing Nanog expression. Nat Cell Biol. 2005 Feb;7(2):165–71.

40. Li M, He Y, Dubois W, Wu X, Shi J, Huang J. Distinct Regulatory Mechanisms and Functions for p53-Activated and p53-Repressed DNA Damage Response Genes in Embryonic Stem Cells. Mol Cell. 2012 Apr;46(1):30–42.

41. Christmann M, Boisseau C, Kitzinger R, Berac C, Allmann S, Sommer T, et al. Adaptive upregulation of DNA repair genes following benzo(a)pyrene diol epoxide protects against cell death at the expense of mutations. Nucleic Acids Res. 2016 Dec 15;44(22):10727–43.

42. Jeffy BD, Chen EJ, Gudas JM, Romagnolo DF. Disruption of Cell Cycle Kinetics by Benzo[a]pyrene: Inverse Expression Patterns of BRCA-1 and p53 in MCF-7 Cells Arrested in S and G2. Neoplasia. 2000 Sep;2(5):460–70.

43. Hamouchene H, Arlt VM, Giddings I, Phillips DH. Influence of cell cycle on responses of MCF-7 cells to benzo[a]pyrene. BMC Genomics. 2011 Dec;12(1):333.

44. Wang XW, Zhan Q, Coursen JD, Khan MA, Kontny HU, Yu L, et al. GADD45 induction of a G_2/M cell cycle checkpoint. Proc Natl Acad Sci. 1999 Mar 30;96(7):3706–11.

45. Jin S, Tong T, Fan W, Fan F, Antinore MJ, Zhu X, et al. GADD45-induced cell cycle G2-M arrest associates with altered subcellular distribution of cyclin B1 and is independent of p38 kinase activity. Oncogene. 2002 Dec 12;21(57):8696–704.

46. Smith ML, Ford JM, Hollander MC, Bortnick RA, Amundson SA, Seo YR, et al. p53-Mediated DNA Repair Responses to UV Radiation: Studies of Mouse Cells Lacking *p53* , *p21* , and/or *gadd45* Genes. Mol Cell Biol. 2000 May 1;20(10):3705–14.

47. Halevy T, Akov S, Bohndorf M, Mlody B, Adjaye J, Benvenisty N, et al. Chromosomal Instability and Molecular Defects in Induced Pluripotent Stem Cells from Nijmegen Breakage Syndrome Patients. Cell Rep. 2016 Aug;16(9):2499–511.

48. Jongmans W, Vuillaume M, Chrzanowska K, Smeets D, Sperling K, Hall J. Nijmegen Breakage Syndrome Cells Fail To Induce the p53-Mediated DNA Damage Response following Exposure to Ionizing Radiation. Mol Cell Biol. 1997 Sep 1;17(9):5016–22.

49. Buscemi G, Savio C, Zannini L, Miccichè F, Masnada D, Nakanishi M, et al. Chk2 Activation Dependence on Nbs1 after DNA Damage. Mol Cell Biol. 2001 Aug 1;21(15):5214–22.

50. Mlody B, Wruck W, Martins S, Sperling K, Adjaye J. Nijmegen Breakage Syndrome fibroblasts and iPSCs: cellular models for uncovering disease-associated signaling pathways and establishing a screening platform for anti-oxidants. Sci Rep. 2017 Aug 8;7(1):7516.

51. Martins S, Erichsen L, Datsi A, Wruck W, Goering W, Chatzantonaki E, et al. Impaired p53-Mediated DNA Damage Response Contributes to Microcephaly in Nijmegen Breakage Syndrome Patient-Derived Cerebral Organoids. Cells. 2022 Feb 25;11(5):802.

52. Schreiber M, Kolbus A, Piu F, Szabowski A, Mohle-Steinlein U, Tian J, et al. Control of cell cycle progression by c-Jun is p53 dependent. Genes Dev. 1999 Mar 1;13(5):607–19.

53. Xia Y, Yang W, Bu W, Ji H, Zhao X, Zheng Y, et al. Differential Regulation of c-Jun Protein Plays an Instrumental Role in Chemoresistance of Cancer Cells. J Biol Chem. 2013 Jul;288(27):19321–9.

54. Wisdom R. c-Jun regulates cell cycle progression and apoptosis by distinct mechanisms. EMBO J. 1999 Jan 4;18(1):188–97.

55. Potapova O, Basu S, Mercola D, Holbrook NJ. Protective Role for c-Jun in the Cellular Response to DNA Damage. J Biol Chem. 2001 Jul;276(30):28546–53.

56. Kasibhatla S, Brunner T, Genestier L, Echeverri F, Mahboubi A, Green DR. DNA Damaging Agents Induce Expression of Fas Ligand and Subsequent Apoptosis in T Lymphocytes via the Activation of NF-□B and AP-. Mol Cell.

57. Roos WP, Kaina B. DNA damage-induced cell death: From specific DNA lesions to the DNA damage response and apoptosis. Cancer Lett. 2013 May;332(2):237–48.

58. Piberger AL, Krüger CT, Strauch BM, Schneider B, Hartwig A. BPDE-induced genotoxicity: relationship between DNA adducts, mutagenicity in the in vitro PIG-A assay, and the transcriptional response to DNA damage in TK6 cells. Arch Toxicol. 2018 Jan;92(1):541–51.

59. Souza T, Jennen D, van Delft J, van Herwijnen M, Kyrtoupolos S, Kleinjans J. New insights into BaP-induced toxicity: role of major metabolites in transcriptomics and contribution to hepatocarcinogenesis. Arch Toxicol. 2016 Jun;90(6):1449–58.

60. Hockley SL, Arlt VM, Brewer D, te Poele R, Workman P, Giddings I, et al. AHR- and DNA-Damage-Mediated Gene Expression Responses Induced by Benzo[a]pyrene in Human Cell Lines. Chem Res Toxicol. 2007 Dec 1;20(12):1797–810.

61. Zhang Y, Wu X, Guo D, Rechkoblit O, Geacintov NE, Wang Z. Two-step error-prone bypass of the (+)- and (−)-trans-anti-BPDE-N2-dG adducts by human DNA polymerases eta and kappa. Mutat Res. 2002;

62. Chiapperino D, Kroth H, Kramarczuk IH, Sayer JM, Masutani C, Hanaoka F, et al. Preferential Misincorporation of Purine Nucleotides by Human DNA Polymerase η Opposite Benzo[a]pyrene 7,8-Diol 9,10-Epoxide Deoxyguanosine Adducts. J Biol Chem. 2002 Apr;277(14):11765–71.

63. Pareja F, Ptashkin RN, Brown DN, Derakhshan F, Selenica P, Da Silva EM, et al. Cancer-Causative Mutations Occurring in Early Embryogenesis. Cancer Discov. 2022 Apr 1;12(4):949–57.

8.3. Statutory declaration

Ich, Christiane Lörch, versichere an Eides Statt, dass die Dissertation von mir selbständig und ohne unzulässige fremde Hilfe unter Beachtung der „Grundsätze zur Sicherung guter wissenschaftlicher Praxis an der Heinrich-Heine-Universität Düsseldorf“ erstellt worden ist.
Diese Arbeit wurde noch nicht in gleicher oder ähnlicher Form bei einer Prüfungsstelle eingereicht und ist ebenso nicht veröffentlicht worden. Die Dissertation wurde ebenfalls nicht, auch nicht auszugsweise, in einer anderen Prüfung oder als Studienleistung verwendet.

Ort, Datum: ..... Unterschrift: .....

Christiane Lörch